

A PROCESS FOR THE DETERPENATION OF ESSENTIAL OILS BY  
EXTRACTION/ADSORPTION/DESORPTION USING  
SUPERCRITICAL CARBON DIOXIDE

by

**Orli A.ESKİNAZİ**

BS. in Ch.E., Boğaziçi University, 1991

Submitted to the Institute for Graduate Studies in  
Science and Engineering in partial fulfillment of  
the requirements for the degree of

Doctor

of

Philosophy

Bogazici University Library



39001100371007

Boğaziçi University

1999

## ACKNOWLEDGMENTS

I would like to express my sincere gratitude and regards to my thesis supervisors Prof. Dr. Öner Hortaçsu and Assoc. Prof. Dr. Uğur Akman for their continuous support, relentless guidance and encouragement which gave me self-confidence and stamina to complete this study.

I am grateful to Prof. Dr. Ayla Çalıklı, Prof. Dr. Esen Bolat and Assoc. Prof. Dr. Kutlu Ülgen for their kind interest in this project.

I would like to thank Prof. Dr. İlsen Önsan for letting me use the Flowsorb 2300 unit and Assoc. Prof. Dr. Nilgün Akın for assisting me.

I sincerely would like to express my gratitude to Department's Technician Bilgi Dedeoğlu, who was always ready to help me regardless of how demanding the job was. I would also like to thank Vice-Technician Nurettin Bektaş for his enthusiastic help. I would like to extend my special thanks to Mr. Hüseyin Erdoğan for his valuable contributions on GC/MS analysis of samples and Mr. Namık Mumcuoğlu from Altes Ltd. Şti for providing the origanum oil for this work.

Financial support provided by the Turkish State Planing Organization (DPT) via projects 95K120320 and 98K120870 and Fahir İlkel Memorial Doctoral Scholarship granted by the Boğaziçi University Foundation, and the administrative support of the Boğaziçi University Research Fund on these projects are gratefully acknowledged.

This thesis is dedicated to the beloved members of my family. From the beginning of this work my father has given his endless assistance. Also, I cannot repay my mother who worked very hard to help my absence from home pass by less noticed. However, I must express that without my husband's endless tolerance and help, there would not be an end to this thesis. To my son...

## ABSTRACT

The main purpose of this study was to establish a supercritical-fluid-aided process in order to enhance the quality of essential-oils products through the removal of the monoterpene (MT) hydrocarbons. The example oil chosen for this study among the hundreds of essential oils is origanum oil (*Origanum Munituflorum*). A new process arrangement constituted by a dense-CO<sub>2</sub> extraction coupled with continuous adsorption/desorption process has been developed, and is suggested for the fractionation and successful deterpenation of this essential oil.

During the different forms of operations and procedures implemented, the non-monoterpene (NMT) cut having the essential odor and properties of the origanum oil, was intended to be separated from the unstable MT fraction of the oil. Experiments were conducted to investigate the influences of extraction pressure, adsorbent quantity and type, desorption pressure, and origanum-oil/CO<sub>2</sub> feed composition on the selectivity of the fractionation process. These factors affecting the product quality are discussed and the process performance is analyzed in terms of the relative-distribution ratios of the twelve major components in origanum oil, the MT and NMT fractions of the oil collected during sampling, and the separation factor the value of which indicates the degree of fractionation. Based on these experimental results, enhanced fractionation of the oil is obtained via adsorption on activated carbon at 40°C/7.5 MPa and desorption at 40°C with step-wise pressure increase method: first at 8.0 MPa to recover the MT components and then, at 14.5 MPa to collect the NMT constituents. This process scheme, in which the mixing cell situated before the adsorber acts as a phase separation chamber, is more successful in deterpenating origanum oil since the mixing cell adds an extra degree of flexibility to the system through providing an additional separation between the more soluble components in CO<sub>2</sub> and the hard-to-extract substances by CO<sub>2</sub> of this oil, i.e., between the MT and NMT hydrocarbons. Furthermore, compared to silanized silica gel, activated carbon was found to be a more promising adsorbent in fractionating and producing an origanum-oil product almost free of its MT constituents.

## ÖZET

Çalışmanın ana amacı içerdikleri monoterpen (MT) hidrokarbonları ayırarak uçucu yağların ürün özelliklerini iyileştirmek için kritik nokta ötesi akışkan içeren bir süreç oluşturmaktır. Çalışmada uçucu yağ olarak bir kekik yağı (*Origanum Munituflorum*) kullanılmıştır. Bu amaçla, sürekli akımda yağın CO<sub>2</sub> özütlenmesine bağlı olarak, yüzey tutma/yüzey bırakma işlemleri içeren bir süreç geliştirilmiştir ve uçucu yağların monoterpenleri, monoterpen olmayan (NMT) bileşenlerinden ayrılmıştır.

Uygulanan farklı işlem ve yöntemlerle kekik yağının kendine has koku ve özelliklerini içeren NMT maddeleri, yağın kararlı olmayan ve kolay bozulabilen MT bileşenlerinden ayrılması amaçlanmıştır. Geliştirilen ayırma işleminde özütleme basıncı, yüzey tutucunun türü ve miktarı, yüzey bırakma basıncı ile besleme akımındaki yağ/CO<sub>2</sub> oranının geliştirilen ayırma sürecinin seçiciliği üzerindeki etkileri deneysel olarak incelenmiştir. Bu değişkenlerin MT ve NMT bileşen türleri arasındaki ayırma işleminin etkinliği ve ürün özellikleri, yağdaki oniki temel bileşenin evreler arasındaki dağılımları ve belirlenen ayırma katsayısı değerleri üzerindeki etkileri olarak incelenmiştir. Deneysel sonuçlar en etkin ayırmanın aktif karbon üzerinde 40°C/7.5 MPa şartlarında yüzey tutunma ve 40°C'de basamaklı olarak önce 8.0 MPa'da MT bileşenlerinin eldesi ve sonra da 14.5 MPa'da NMT bileşenlerinin yüzeyden ayrılması ile elde edilebileceğini göstermiştir. Önerilen süreçte yüzey tutma aşamasından önce yerleştirilmiş olan evre ayırma kabı işlevli karıştırma hücresi sürece ek bir esneklik getirmekte ve CO<sub>2</sub> içinde kolayca çözülebilen bileşenleri ile CO<sub>2</sub> tarafından özütlenmesi zor olan bileşenleri arasındaki (MT ve NMT) ayrılmaya ek bir aşama oluşturmaktadır. Bu çalışmada aktif karbonun silanize silika jel'e göre kekik yağı MT'lerinin ayrılmasında yüzey tutucu madde olarak daha etkin olduğu belirlenmiştir.

## TABLE OF CONTENTS

	Page
ACKNOWLEDGMENTS	iii
ABSTRACT	iv
ÖZET	v
LIST OF FIGURES	x
LIST OF TABLES	xviii
LIST OF SYMBOLS	xxi
1. INTRODUCTION	1
2. BACKGROUND	4
2.1. Basic Concepts	4
2.2. Overview of the Previous Extraction and Fractionation Studies	15
2.2.1. Supercritical Fluid Extraction Applications	16
2.2.2. Supercritical Fluid Fractionation Applications	19
3. BASIC FACTS, INTENTIONS AND PROCEDURES	28
3.1. Key Components of Origanum Oil	29
3.2. Intentions and Procedures	32
4. EXPERIMENTAL WORK	39
4.1. Materials Used	39
4.2. Experimental Set-up	40
4.3. Experimental Procedure	47
4.3.1. Preparing the System before Starting an Experiment	49
4.3.2. Experimental Procedure for Dense-CO <sub>2</sub> Extraction	50
4.3.3. Experimental Procedure for Supercritical-CO <sub>2</sub> Adsorption Following Dense-Gas Extraction	53
4.3.4. Experimental Procedure for Supercritical-CO <sub>2</sub> Desorption Following the Origanum-oil/CO <sub>2</sub> Adsorption Coupled with Dense-Gas Extraction	57
4.3.5. Cleaning of the Equipment between Experiments	60
4.4. Experimental Program for Fractionating Origanum Oil	62

	Page
4.5. Analysis of Origanum Oil Fractions by Gas Chromatography	65
4.6. Characterization of Activated Carbon and Silica Gel Adsorbents	66
4.6.1. Total Surface Area Measurement	67
4.6.2. Total Pore Volume Measurement	68
5. RESULTS AND DISCUSSION	69
5.1. Relative-Distribution Coefficients and Separation Factor	69
5.2. Fractionation of Origanum Oil by Supercritical-CO <sub>2</sub> Extraction	71
5.2.1. Supercritical-CO <sub>2</sub> Extraction at 40°C/7.5 MPa	71
5.2.2. Supercritical-CO <sub>2</sub> Extraction at 40°C/10.0 MPa	78
5.3. Fractionation of Origanum Oil by Supercritical-CO <sub>2</sub> Adsorption Following Dense-Gas Extraction at 40°C/7.5 MPa Using Activated Carbon Adsorbent	83
5.3.1. Supercritical-CO <sub>2</sub> Adsorption Following Dense-Gas Extraction on Two Grams Activated Carbon	84
5.3.2. Supercritical-CO <sub>2</sub> Adsorption Following Dense-Gas Extraction on Eight Grams Activated Carbon	90
5.4. Supercritical-CO <sub>2</sub> Desorption Following Origanum-oil/CO <sub>2</sub> Adsorption on Activated Carbon Coupled with Dense-Gas Extraction at 40°C	97
5.4.1. Supercritical-CO <sub>2</sub> Desorption at 14.5 MPa	98
5.4.2. Supercritical-CO <sub>2</sub> Desorption with Step-wise Pressure Increase	102
5.5. Fractionation of Origanum Oil by Supercritical-CO <sub>2</sub> Adsorption Following Dense-Gas Extraction at 40°C/7.5 MPa Using Silica Gel Adsorbent	114
5.5.1. Supercritical-CO <sub>2</sub> Adsorption Following Dense-Gas Extraction on Eight Grams Silica Gel	115
5.5.2. Supercritical-CO <sub>2</sub> Adsorption Following Dense-Gas Extraction on 15 Grams Silica Gel	123

	Page
5.6. Supercritical-CO <sub>2</sub> Desorption Following the Origanum-oil/CO <sub>2</sub> Adsorption on Silica Gel Coupled with Dense-Gas Extraction at 40°C/14.5 MPa	128
5.6.1. Supercritical-CO <sub>2</sub> Desorption from Eight Grams Silica Gel	128
5.6.2. Supercritical-CO <sub>2</sub> Desorption from 15 Grams Silica Gel	132
5.7. Effect of Origanum-oil/CO <sub>2</sub> Mixture Composition on the Fractionation of Origanum Oil at 40°C Using Activated Carbon	136
5.7.1. Supercritical-CO <sub>2</sub> Adsorption Following Dense-Gas Extraction at 10.0 MPa	137
5.7.2. Supercritical-CO <sub>2</sub> Desorption at 40°C/14.5 MPa Following the Origanum-oil/CO <sub>2</sub> Adsorption on Activated Carbon at 40°C/10.0 MPa	142
5.8. Pure Supercritical-CO <sub>2</sub> Adsorption on Activated Carbon at 40°C	146
6. CONCLUSIONS AND RECOMMENDATIONS	149
6.1. Conclusions	149
6.2. Recommendations for Further Work	153
APPENDIX A: Testing the System with Toluene/CO <sub>2</sub> Binary Mixture	155
APPENDIX B: Analytical Conditions Used on the GC/MS	173
APPENDIX C: Properties and Structures of Origanum-oil Components	174
APPENDIX D: Relative-distribution Ratios of the Key Components in Origanum Oil Calculated for Each Experiment Performed	178
APPENDIX E: Chromatogram and the GC/MS Results of the Original Origanum Oil	195
APPENDIX F: Chromatogram and the GC/MS Results of the Samples Collected at Different Time Intervals during Supercritical-CO <sub>2</sub> Extraction at 40°C/7.5 MPa	199
APPENDIX G: Chromatogram and the GC/MS Results of the Samples Collected at Different Time Intervals during Supercritical-CO <sub>2</sub> Adsorption (Following Dense-Gas Extraction) at 40°C/7.5 MPa on Eight Grams Activated Carbon	208

APPENDIX H: Chromatogram and the GC/MS Results of the Samples Collected at Different Time Intervals during Supercritical- CO <sub>2</sub> Desorption from Eight Grams Activated Carbon at 40°C using the Step-wise Pressure Increase Method	215
APPENDIX I: Chromatogram and the GC/MS Results of the Samples Collected at Different Time Intervals during Supercritical- CO <sub>2</sub> Adsorption (Following Dense-Gas Extraction) at 40°C/7.5 MPa on 15 Grams Silica Gel	222
APPENDIX J: Chromatogram and the GC/MS Results of the Samples Collected at Different Time Intervals during Supercritical- CO <sub>2</sub> Desorption from 15 Grams Silica Gel at 40°C/14.5 MPa	229
REFERENCES	236

## LIST OF FIGURES

	Page	
FIGURE 2.1.1	Typical pressure-temperature phase diagram for a pure material.	6
FIGURE 2.1.2	Variation of the reduced density of a pure component.	8
FIGURE 2.1.3	Solubility of benzoic acid in CO <sub>2</sub> .	9
FIGURE 2.1.4	Solubility of 2,3-dimethylnaphthalene in CO <sub>2</sub> .	10
FIGURE 2.1.5	Solubility isotherms of typical essential-oil components in dense CO <sub>2</sub> at 40°C.	12
FIGURE 2.1.6	Solubility isobars of limonene and carvone, as functions of temperature and density of dense CO <sub>2</sub> at 80 bar.	14
FIGURE 2.2.1.1	Physical states of CO <sub>2</sub> at various temperatures and pressures, illustrating regions useful for essential-oil applications.	16
FIGURE 2.2.1.2	Flow diagram of a pilot-scale supercritical fluid extraction system.	17
FIGURE 2.2.1.3	Schematic representation of the experimental apparatus used in studying supercritical-CO <sub>2</sub> extraction of marjoram-leaf oil.	18
FIGURE 2.2.2.1	Supercritical fractionation apparatus.	20
FIGURE 2.2.2.2	Semibatch fractionation apparatus.	21
FIGURE 2.2.2.3	Continuous fractionation apparatus.	22
FIGURE 2.2.2.4	Schematic diagram of the desorption apparatus.	24

	Page
FIGURE 2.2.2.5 Schematic representation of the PSA apparatus.	25
FIGURE 2.2.2.6 Experimental apparatus for the adsorption of supercritical mixtures.	26
FIGURE 3.1.1 Distribution of origanum oil ( <i>Origanum Munituflorum</i> ) key components.	31
FIGURE 3.2.1 Supercritical-CO <sub>2</sub> extraction (or supercritical-CO <sub>2</sub> adsorption following dense-gas extraction) experiments at 40°C/7.5 MPa.	33
FIGURE 3.2.2 Supercritical-CO <sub>2</sub> extraction (or supercritical-CO <sub>2</sub> adsorption following dense-gas extraction) experiments at 40°C/10.0 MPa.	35
FIGURE 3.2.3 Desorption with pure supercritical CO <sub>2</sub> .	36
FIGURE 4.2.1 Experimental set-up for fractionating origanum oil.	41
FIGURE 4.2.2 Solvent entry zone.	42
FIGURE 4.2.3 Constant temperature zone.	44
FIGURE 4.2.4 Sampling zone.	48
FIGURE 5.2.1.1 Relative-distribution ratios of origanum-oil components in extraction experiment at 40°C/7.5 MPa.	72
FIGURE 5.2.1.2 Relative-distribution ratios of MT and NMT cuts in extraction experiment at 40°C/7.5 MPa.	74
FIGURE 5.2.1.3 Separation factor in extraction experiment at 40°C/7.5 MPa.	74
FIGURE 5.2.1.4 Liquid phase relative-distribution ratios of residual-oil components in 40°C/7.5 MPa extraction experiment.	77

FIGURE 5.2.2.1	Relative-distribution ratios of origanum-oil components in extraction experiment at 40°C/10.0 MPa.	79
FIGURE 5.2.2.2	Pressure-dependence of the relative-distribution ratios of MT and NMT cuts in extraction experiments at 40°C/7.5 MPa and 40°C/10.0 MPa.	82
FIGURE 5.2.2.3	Pressure-dependence of the separation factor in extraction experiments at 40°C/7.5 MPa and 40°C/10.0 MPa.	82
FIGURE 5.3.1.1	Relative-distribution ratios of origanum-oil components in adsorption experiment at 40°C/7.5 MPa using two grams activated carbon.	85
FIGURE 5.3.1.2	Relative-distribution ratios of MT and NMT cuts at 40°C/7.5 MPa in extraction run, and adsorption on two grams activated carbon run.	86
FIGURE 5.3.1.3	Separation factor at 40°C/7.5 MPa conditions in extraction run, and adsorption on two grams activated carbon run.	86
FIGURE 5.3.1.4	Composition of the ethanol-extracted activated-carbon residue and of the last sample taken during the adsorption run at 40°C/7.5 MPa using two grams activated carbon.	88
FIGURE 5.3.1.5	Ratio of the area counts of the MT and NMT cuts in the sample to that in the original origanum oil in adsorption run at 40°C/7.5 MPa using two grams activated carbon.	89
FIGURE 5.3.2.1	Relative-distribution ratios of origanum-oil components in adsorption experiment at 40°C/7.5 MPa using eight grams activated carbon (replicate runs).	91

FIGURE 5.3.2.2	Evolution of the relative-distribution ratios of individual components in adsorption run at 40°C/7.5 MPa using eight grams activated carbon.	95
FIGURE 5.3.2.3	Relative-distribution ratios of MT and NMT cuts at 40°C/7.5 MPa in extraction run, and adsorption on two and eight grams activated carbon runs.	96
FIGURE 5.3.2.4	Separation factor at 40°C/7.5 MPa in extraction run, and adsorption on two and eight grams activated carbon runs.	96
FIGURE 5.4.1.1	Relative-distribution ratios of organum-oil components at 40°C using eight grams activated carbon during adsorption at 7.5 MPa, and desorption at 14.5 MPa.	99
FIGURE 5.4.1.2	Relative-distribution ratios of individual components in the adsorbed (7.5 MPa) and desorbed (14.5 MPa) fractions and of the ethanol-extracted activated-carbon residue, using eight grams activated carbon.	101
FIGURE 5.4.2.1	Relative-distribution ratios of organum-oil components in desorption experiment at 40°C with step-wise pressure increase from 8.0 to 14.5 MPa (replicate runs).	104
FIGURE 5.4.2.2	Area count results of organum-oil components in desorption experiment at 40°C with step-wise pressure increase from 8.0 to 14.5 MPa, and with constant-pressure at 14.5 MPa.	105
FIGURE 5.4.2.3	Relative-distribution ratios of organum-oil components in desorption experiment at 40°C with step-wise pressure increase from 8.0 to 14.5 MPa, and with constant-pressure at 14.5 MPa.	106

- FIGURE 5.4.2.4 Pressure-dependence of the relative-distribution ratios of MT and NMT cuts in desorption run at 40°C with step-wise pressure increase from 8.0 to 14.5 MPa, and with constant-pressure at 14.5 MPa. 110
- FIGURE 5.4.2.5 Pressure-dependence of the separation factor in desorption run at 40°C with step-wise pressure increase from 8.0 to 14.5 MPa, and with constant-pressure at 14.5 MPa. 110
- FIGURE 5.4.2.6 Normalized area counts of individual components in the desorption run at the end of 40°C/8.0 MPa step, 40°C/14.5 MPa step and in the ethanol-extracted activated-carbon residue. 112
- FIGURE 5.5.1.1 Relative-distribution ratios of origanum-oil components in adsorption experiment at 40°C/7.5 MPa using eight grams adsorbent (activated carbon and silica gel). 116
- FIGURE 5.5.1.2 Time dependence of the normalized area count of individual components in adsorption runs at 40°C/7.5 MPa (activated carbon and silica gel). 118
- FIGURE 5.5.1.3 Time dependence of the normalized area count of MT and NMT cuts in adsorption runs at 40°C/7.5 MPa (activated carbon and silica gel). 119
- FIGURE 5.5.1.4 Relative-distribution ratios of MT and NMT cuts at 40°C/7.5 MPa during extraction run, and adsorption on eight grams sorbent (activated carbon and silica gel) runs. 119

	Page
FIGURE 5.5.1.5 Ratio of the area counts of the MT and NMT cuts in the sample to that in the original oil at 40°C/7.5 MPa during extraction run, and adsorption on eight grams sorbent (activated carbon and silica gel) runs.	122
FIGURE 5.5.1.6 Separation factor at 40°C/7.5 MPa during extraction run, and adsorption on eight grams sorbent (activated carbon and silica gel) runs.	122
FIGURE 5.5.2.1 Relative-distribution ratios of organum-oil components in adsorption experiment at 40°C/7.5 MPa using 15 grams silica gel adsorbent.	125
FIGURE 5.5.2.2 Relative-distribution ratios of MT and NMT cuts in adsorption experiments at 40°C/7.5 MPa (eight grams activated carbon, eight grams silica gel and 15 grams silica gel).	127
FIGURE 5.5.2.3 Separation factor in adsorption runs at 40°C/7.5 MPa (eight grams activated carbon, eight grams silica gel and 15 grams silica gel).	127
FIGURE 5.6.1.1 Relative-distribution ratios of organum-oil components at 40°C using eight grams silica gel adsorbent (adsorption at 7.5 MPa, and desorption at 14.5 MPa).	129
FIGURE 5.6.1.2 Normalized area counts of individual components at the end of the adsorption and desorption runs using eight grams silica gel adsorbent.	131
FIGURE 5.6.1.3 Normalized area counts of the MT and NMT cuts at the end of the adsorption and desorption runs using eight grams silica gel adsorbent.	131

FIGURE 5.6.2.1	Relative-distribution ratios of origanum-oil components at 40°C using 15 grams silica gel adsorbent (adsorption at 7.5 MPa and desorption at 14.5 MPa).	133
FIGURE 5.6.2.2	Normalized area counts of individual components at the end of the adsorption and desorption runs using 15 grams silica gel adsorbent.	135
FIGURE 5.6.2.3	Normalized area counts of the MT and NMT cuts at the end of the adsorption and desorption runs using 15 grams silica gel adsorbent.	135
FIGURE 5.7.1.1	Relative-distribution ratios of origanum-oil components in adsorption experiments at 40°C/7.5 MPa and 40°C/10.0 MPa using eight grams activated carbon.	138
FIGURE 5.7.1.2	Pressure dependence of the relative-distribution ratios of MT and NMT cuts in adsorption runs at 40°C/7.5 MPa and 40°C/10.0 MPa using eight grams activated carbon.	140
FIGURE 5.7.1.3	Pressure dependence of the separation factor in adsorption runs at 40°C/7.5 MPa and 40°C/10.0 MPa using eight grams activated carbon.	140
FIGURE 5.7.2.1	Relative-distribution ratios of origanum-oil components at 40°C using eight grams activated carbon (adsorption at 10.0 MPa, and desorption at 14.5 MPa).	143
FIGURE 5.7.2.2	Effect of feed composition on normalized area counts of key components in the adsorbed and desorbed fractions and in the ethanol-extracted activated-carbon residue.	144

	Page	
FIGURE A.1.1	Experimental set-up used in studying toluene/CO <sub>2</sub> binary mixture.	156
FIGURE A.1.2	Calibration curve of toluene/ethanol mixture by GC.	159
FIGURE A.4.1	Saturation experiments for toluene (0.05 ml/min) in dense CO <sub>2</sub> at 40°C/10.0 MPa (replicate runs).	164
FIGURE A.4.2	Saturation runs for toluene (0.01 and 0.025 ml/min) in dense CO <sub>2</sub> at 40°C/10.0 MPa.	164
FIGURE A.4.3	Pressure-equilibrium phase composition diagram for the toluene/CO <sub>2</sub> binary system.	166
FIGURE A.4.4	The adsorption/desorption behavior of toluene/CO <sub>2</sub> mixture on $\alpha$ -cellulose at 40°C/10.0 MPa.	168
FIGURE A.4.5	The adsorption/desorption behavior of toluene/CO <sub>2</sub> mixture on activated carbon at 40°C/10.0 MPa.	169
FIGURE A.4.6	Effect of pressure on the desorption from carbon (at 40°C) previously loaded with toluene/CO <sub>2</sub> mixture.	169
FIGURE A.4.7	Moles toluene collected during blank run.	172

**LIST OF TABLES**

	<b>Page</b>	
TABLE 3.1.1	The key components of original origanum oil.	30
TABLE 4.4.1.	Experimental program for fractionating origanum oil.	63
TABLE 4.6.1.	Properties of activated carbon and silanized silica gel adsorbents.	67
TABLE 5.2.1.1	Normalized area percentages of original and residual origanum oil-components in 40°C/7.5 MPa extraction experiment.	76
TABLE 5.8.1.	Effect of pressure on activated carbon loadings from pure CO <sub>2</sub> .	147
TABLE A.2.1	Saturation experiments performed with the toluene/CO <sub>2</sub> binary system.	160
TABLE A.2.2	Adsorption/desorption experiments performed with toluene/CO <sub>2</sub> system.	161
TABLE A.4.1	Equilibrium phase composition of toluene/CO <sub>2</sub> system at 40°C.	167
TABLE B.1.	Temperature program of the analyses at GC/MS.	173
TABLE C.1.	Physical and chemical properties of origanum-oil components.	175
TABLE D.1.	Relative-distribution ratios of origanum-oil components in extraction experiment at 40°C/7.5 MPa.	179
TABLE D.2.	Relative-distribution ratios of origanum-oil components in extraction experiment at 40°C/10.0 MPa.	180

TABLE D.3.	Relative-distribution ratios of origanum-oil components in adsorption experiment at 40°C/7.5 MPa using two grams activated carbon.	181
TABLE D.4.	Relative-distribution ratios of origanum-oil components in adsorption experiment at 40°C/7.5 MPa using eight grams activated carbon.	182
TABLE D.5.	Relative-distribution ratios of origanum-oil components in adsorption experiment at 40°C/7.5 MPa using eight grams activated carbon (replicate exp.).	183
TABLE D.6.	Relative-distribution ratios of origanum-oil components in adsorption experiment at 40°C/7.5 MPa using eight grams activated carbon (replicate exp.).	184
TABLE D.7.	Normalized area counts (%) of origanum-oil components in desorption experiment at 40°C/14.5 MPa.	185
TABLE D.8.	Relative-distribution ratios of origanum-oil components in desorption experiment at 40°C/14.5 MPa.	186
TABLE D.9.	Relative-distribution ratios of origanum-oil components in desorption experiment at 40°C with step-wise pressure increase from 8.0 to 14.5 MPa.	187
TABLE D.10.	Relative-distribution ratios of origanum-oil components in desorption experiment at 40°C with step-wise pressure increase from 8.0 to 14.5 MPa (replicate exp.).	188
TABLE D.11.	Relative-distribution ratios of origanum-oil components in adsorption experiment at 40°C/7.5 MPa using eight grams silica gel.	189

TABLE D.12.	Relative-distribution ratios of organum-oil components in adsorption experiment at 40°C/7.5 MPa using 15 grams silica gel.	190
TABLE D.13.	Relative-distribution ratios of organum-oil components in desorption experiment at 40°C/14.5 MPa using eight grams silica gel.	191
TABLE D.14.	Relative-distribution ratios of organum-oil components in desorption experiment at 40°C/14.5 MPa using 15 grams silica gel.	192
TABLE D.15.	Relative-distribution ratios of organum-oil components in adsorption experiment at 40°C/10.0 MPa using eight grams activated carbon.	193
TABLE D.16.	Relative-distribution ratios of organum-oil components in desorption experiment at 40°C/14.5 MPa using eight grams activated carbon.	194

## LIST OF SYMBOLS

$A_{MT}$	Ratio of the area counts of the monoterpene component group in the sample to that in the original oil
$A_{NMT}$	Ratio of the area counts of the non-monoterpene component group in the sample to that in the original oil
$C_i$	Concentration of the $i$ 'th component in sample
$C_i^\circ$	Concentration of the $i$ 'th component in the original oil
$C_{i, MT}$	Concentration of the $i$ 'th monoterpene component in sample
$C_{i, MT}^\circ$	Concentration of the $i$ 'th monoterpene component in the original oil
$C_{i, NMT}$	Concentration of the $i$ 'th non-monoterpene component in sample
$C_{i, NMT}^\circ$	Concentration of the $i$ 'th non-monoterpene component in the original oil
$R_i$	Relative-distribution coefficient of the $i$ 'th component
$R_{MT}$	Relative-distribution coefficient of the monoterpene component group
$R_{NMT}$	Relative-distribution coefficient of the non-monoterpene component group
$R_{x, I}$	Liquid-phase relative-distribution coefficient of the $i$ 'th component
$x$	Liquid oil-phase composition
$y$	Dense gas-phase composition
$y^*$	Equilibrium composition of organum oil in the dense gas-phase
$z$	Overall composition of feed to the mixing cell
$\alpha$	Separation factor

## 1. INTRODUCTION

Natural materials are sources of lipophilic compounds and their extracts may contain up to hundreds of specific components. In general, these lipophilic natural extracts may be considered in two main classes, i.e., vegetable oils and essential oils. Essential oils are particularly relevant since they represent the vital basic materials for scented products in the perfume and cosmetic branches (Stahl et al., 1988). Further applications are in the pharmaceutical and prepared-food domains. Many essential oils such as origanum oil, possess pharmacological activity and thus find interesting application in therapy, in addition to their common uses in the food and human nutrition field.

Using fractionation methods, the composition of essential and vegetable oils may be changed and specialized products which are more useful than the naturally available oils as raw materials or as ingredients in a recipe may be obtained. Such purer materials usually command higher values in the pharmaceutical, food and cosmetics industries and have longer shelf-life. One of the most technologically advanced separation processes available to attain such separations of complex natural extracts is based on the use of supercritical fluids. Conventional methods like atmospheric, vacuum, hydro or steam distillation may cause product degradation to the large and heat-sensitive molecules of thermolabile materials because of the high temperatures they employ. Furthermore, solvent residue inherent in the solvent extraction process, even in the commonly used hexane, is also becoming increasingly unacceptable in products, especially if the product is going to be used for human consumption. Thus, supercritical fluid applications are considered to be a suitable alternative process to the conventional procedures for rectification and purification of higher-value oil fractions and can be used safely in industry due to their non-toxic and easily recoverable residues and their favorable operating conditions, which are usually below the thermal degradation limits of the essential-oil components.

Extraction of essential oils from plants and fractionation of these extracted oils into desired products is a promising field for the industrial application of supercritical processing. The knowledge of the phase behavior of the essential-oil/supercritical-solvent

system over a wide range of operating conditions is a prerequisite for the successful design, operation, and optimization of such supercritical-fluid-aided operations. It is known that solubilities of essential-oils components depend not only on the solute properties such as molecular weight, polarity and vapor pressure, but also on temperature and pressure of the solvent, which in turn directly affect the density and the solvating power of the solvent (Stahl et al., 1988). Furthermore, essential oils being complex multicomponent mixtures, these values are also affected by solute-solvent and solute-solute interactions.

Particularly, the supercritical-fluid-aided techniques developed to produce a high-quality essential-oil product almost free of its monoterpene (MT) hydrocarbons (deterpenation) exploits the solubility behavior of essential-oil components in supercritical-solvent CO<sub>2</sub>. The selective elimination of these unsaturated compounds is necessary since MT compounds can undergo structural rearrangements and are also rapidly oxidized by air. Furthermore, they do not contribute much to the flavor or fragrance of the oil. Thus, for the fractionation and successful deterpenation of essential oils, solubilities of essential-oil compounds in dense gas should vary as much as possible.

In recent years, supercritical fluid extraction (SFE) has gained popularity in producing essential oils with a low MT hydrocarbon content. In practice, an oil which has 50 per cent of its MTs removed is called a terpenless oil. However, drawbacks of the simple SFE process (high solubility and high selectivity are not compatible) has led to the development of different approaches in the supercritical fractionation of essential oils: supercritical desorption and countercurrent processing. The introduction of adsorbents into a SFE system is the other attractive method to increase the selectivity of the separation process.

As a consequence, the development of a new process arrangement for the fractionation and successful deterpenation of origanum oil (*Origanum Munituflorum*), or similar essential oils, is the objective of this thesis. For this purpose, an experimental set-up has designed, constructed and operated. The proposed operational scheme is constituted by a continuous adsorption/desorption process coupled with dense-CO<sub>2</sub> extraction. By taking the advantages of the solubility behavior of origanum-oil components in supercritical

solvent CO<sub>2</sub> and the different affinities of these essential-oil components for the adsorbent, improvement in product quality of origanum oil (or similar essential oils) is aimed through selectively removing its MT hydrocarbons.

Chapter two introduces the basic concepts about essential oils and supercritical fluids, and gives a detailed overview of the previous studies conducted for essential-oil applications using supercritical-solvent CO<sub>2</sub>. Chapter three, which is a “key” in understanding the following chapters of this dissertation, presents the different forms of operations and procedures implemented in order to achieve the purpose of this study, regarding the facts about the solubility behavior of origanum-oil components in supercritical CO<sub>2</sub>. The reasoning behind each process scheme, which is illustrated by simple diagrams, is explained considering various operational aspects. The detailed description of the experimental apparatus constructed (including materials and equipment used) and procedure applied is given in chapter four. The experimental results obtained in this work are discussed in chapter five. In detail, the effect of extraction pressure, of adsorbent quantity and type, of desorption pressure and of origanum-oil/CO<sub>2</sub> feed composition on the fractionation of origanum oil is analyzed in terms of the relative-distribution ratios (and normalized area percentages) of the twelve major components in origanum oil, of the MT and NMT fractions of oil collected during sampling and of the value of the separation factor, which is important in determining the degree of the fractionation. Finally, concluding remarks with possible research directions are provided in chapter six. The appendix part of this dissertation is divided into ten parts: In Appendix A, the approach followed and the experimental results obtained during the testing of the system with toluene/CO<sub>2</sub> binary mixture are presented. In Appendices B and C, information about sample analysis and properties of major origanum-oil components are provided. In Appendix D, experimental results (relative-distribution ratios) are tabulated and some examples of the chromatograms and “per cent area reports” obtained from GC/MS analyses are given in Appendices E to J.

## 2. BACKGROUND

In the first section of this chapter, properties of essential oils and of supercritical fluids are introduced, and in light of these fundamentals, the factors influencing the solubility behavior of essential-oil components in dense CO<sub>2</sub> are discussed. In the second section, an overview of the previous studies conducted for essential-oil extraction and fractionation/rectification applications using dense-CO<sub>2</sub> solvent is presented.

### 2.1. Basic Concepts

Essential oils are volatile materials derived from various parts of plants (leaf, fruit, seed, flower, etc.). The essence -odor and/or flavor- contained in these plants is usually the result of the complex interactions occurring among the hundreds of essential-oil components. Essential oils and its derivatives play an important role in food technology as flavoring agents and are basic constituents for the scented products in the perfume and cosmetics industries, in which they are processed directly in their pure state to yield high-grade natural perfumes. A further application is in the pharmaceutical domain; many essential oils possess pharmacological activity and antiseptic properties and thus find interesting application in therapy. However, essential-oil yield of plants is not high but, these oils are very concentrated in flavor; strength of flavor of a typical essential oil is about hundred times that of its parent plant (Memory, 1968).

Essential oils, which are mixtures of organic compounds, are insoluble in water and they are generally liquid at room temperature. These oils may be obtained in three product forms: concrete, absolute and isolate (Memory, 1968). "Concrete" is the product obtained after final concentration. It resembles a fatty wax that is quasi-solid at room temperature and is saturated with an aromatic substance. "Absolute" is the alcohol-soluble liquid or

semi-liquid oil saturated with an aromatic substance. "Isolate" is the pure substance separated from natural products.

Essential oils, though composed of chemically dissimilar compounds, mainly consist of mixtures of hydrocarbon terpene and sesquiterpene groups, which are the most characteristic component families present in many of these oils. The other major groups of essential-oil components are the oxygenated compounds (alcohols, aldehydes, ketones, acids, esters and ethers) and the benzene derivatives, which are the important flavor and perfume constituents of essential oils derived from benzene (more specially from n-propyl benzene).

Common characteristic of many of these oil constituents, mainly the monoterpene (MT) hydrocarbons of the terpene fraction, are their instability and the ease with which intramolecular rearrangements occur with heat and light effects. Such deformations and destructions usually run parallel with the loss of delicate nuances in smell, which is a certain indication that changes in the original composition of the oil have taken place (Guenther, 1952). For example, autoxidation of limonene to carvone and carveol has been suggested as one of the degradation paths responsible for terpene-like off-notes formation (Ziegler et al., 1991). Therefore, the selective elimination of these highly volatile terpene hydrocarbons (deterpenation) is required since in addition, these compounds do not contribute much to the flavor or fragrance of the oil. Essential oils free of MT components have longer shelf-life and higher market value. Thus, further processing of essential oils to reduce their terpene content to a minimum acceptable level, and to isolate and concentrate their valuable compounds/fractions, are of industrial importance because of the higher market values they exhibit due to improved qualities and longer shelf-life.

The most commonly used processes to concentrate the oxygenated fraction of essential oils are vacuum distillation, extraction with alcohol, partition between solvents of different polarity, and preparative adsorption chromatography. The drawbacks of all these processes are low yields, formation of thermal degradation products and contamination with organic solvents. These deficiencies of the conventional methods fostered research in

application of the supercritical fluid technology as an alternative means for the fractionation and purification to higher-value essential oil fractions.

The fundamentals of supercritical fluids (SCFs) have long been known, but their exploitation in laboratory and in commercial separation processes is of relatively recent origin. Figure 2.1.1 shows a generalized pressure-temperature phase diagram for a pure fluid, in which the solid, liquid and gas phases are indicated. Also shown on the diagram are the lines indicating the co-existence of two phases. The liquid-gas line extends from the triple point to the critical point where the properties of liquid and gas phases become identical. The critical temperature,  $T_c$ , of a gas is the temperature above which it cannot be

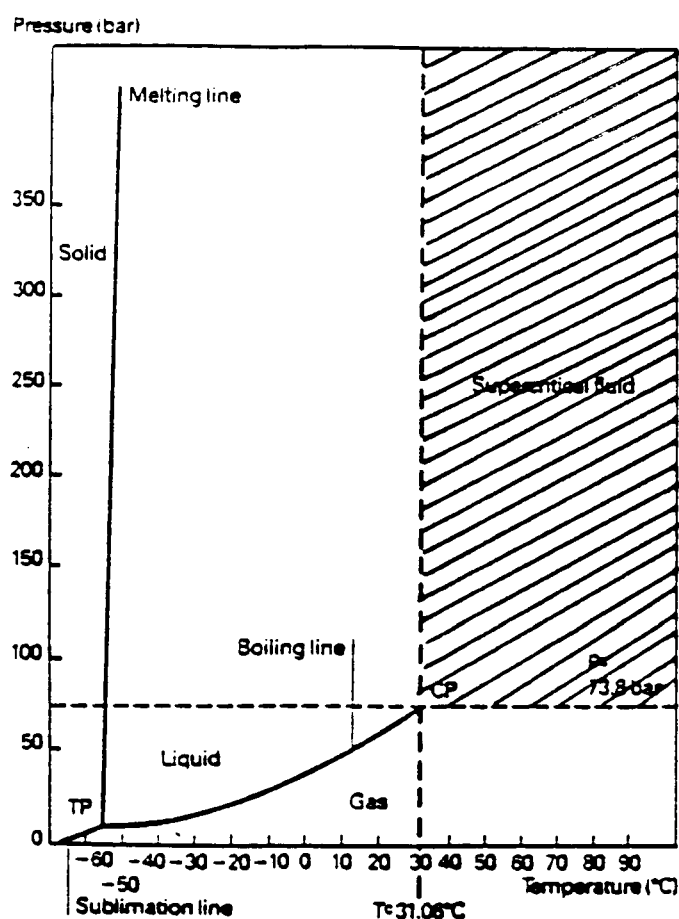


FIGURE 2.1.1. Typical pressure-temperature phase diagram for a pure material (McHugh and Krukoni, 1986).

liquefied, no matter how high the pressure. Similarly, the critical pressure,  $P_c$ , of a gas is the pressure below which it cannot be liquefied, no matter how low the temperature. Above the critical point, the substance is neither gas nor liquid and therefore, is named as the supercritical fluid. The region presented by the shaded area in Figure 2.1.1 is the supercritical-fluid region of  $\text{CO}_2$  ( $T_c$ :  $31.06^\circ\text{C}$ ,  $P_c$ : 73.8 bar). In this region or around the critical point, the supercritical fluid has the characteristics of both gases and liquids. It possesses gas-like viscosities and diffusion coefficients which are intermediate to those of liquids and gases. These properties provide SCFs the ability to penetrate into the solid material deeply and efficiently. Moreover, the liquid-like density of a SCF allows it to dissolve large amounts of organic compounds (even relatively non-volatile ones with high molecular weights) that usually have low solubility in ordinary liquid or gaseous states of the same fluid. However, the solubility of compounds in a SCF depends on solute and solvent properties. The dissolved compounds can be recovered from the fluid by decreasing the pressure or increasing the temperature, both of which reduce fluid density and allow the dissolved compounds to be separated from the fluid.

Supercritical  $\text{CO}_2$  is the most favorable solvent for essential-oil applications since it is nontoxic, does not leave any residue in the product and permits the extraction and fractionation operations on these vulnerable oils to be carried at mild conditions. The  $\text{CO}_2$  molecule is non-polar and hence it is classified as a non-polar solvent, although it has some affinity with polar solutes due to its large molecular quadrupole. Thus, pure  $\text{CO}_2$  can also be used as a solvent for many large organic solute molecules even if they have low polarity. However, for the extraction of more polar molecules, the solvating power of  $\text{CO}_2$  is not adequate. On other hand, other SCFs that appear to have good properties for supercritical-fluid extraction generally suffer from being too reactive (e.g. ammonia), too expensive (e.g. xenon) or flammable (e.g. ethane and propane form explosive mixtures with air). Therefore, the most practical approach is to increase the solvent power of  $\text{CO}_2$  by adding organic modifiers (co-solvent/entrainer), generally in the range of 1-10 per cent volume (Westwood, 1993). When co-solvents such as ethanol or methanol are used, the resulting solubility increase of the solute may be explained in terms of the hydrogen bonding between the solute and the entrainer (Schulz et al., 1991). When an apolar solvent (such as  $\text{CO}_2$ ) is

mixed with a polar co-solvent, apparent polarity of the modified solvent increases, thus more polar compounds of the solute matrix can be appreciably dissolved.

The effectiveness of the SCFs depends on the solubility behavior of the solute in the supercritical solvent. The solubility of a solute in a SCF is contributed to by the specific properties (volatility, molecular weight and polarity) of this compound and the solvating power of the solvent. The latter is primarily a function of the density of the fluid. Figure 2.1.2 shows the variation of the reduced density ( $\rho_R$ ) of a pure substance in the vicinity of its critical point. For a reduced temperature ( $T_R$ ) range of 0.9 to 1.2 and reduced pressure ( $P_R$ ) greater than 1.0, the reduced density of the solvent can change from a value of about 0.1, a gas-like density, to about 2.5, a liquid-like density. As the reduced densities become liquid-like, the SCF begins to act as a liquid solvent. However, as the reduced temperature is increased to a value 1.55, the SCF becomes more expanded. Hence, if liquid-like densities are to be reached, the reduced pressure must be increased to values as high as 10.0. When operating in the critical region both pressure and temperature can be used to regulate the density and therefore, the solvent power of a SCF (McHugh and Krukoni, 1986).

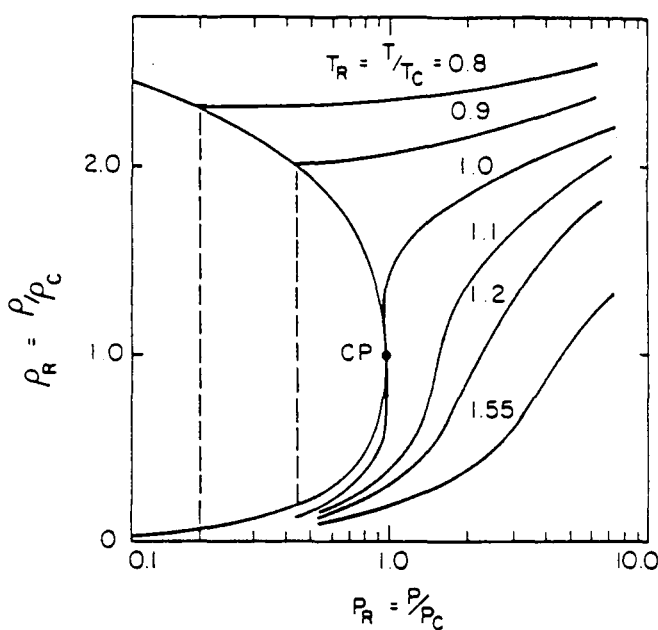


FIGURE 2.1.2. Variation of the reduced density of a pure component (McHugh and Krukoni, 1986).

The pressure/temperature effects on solubility behavior of a compound can be completely examined with the aid of Figure 2.1.3 and Figure 2.1.4. Figure 2.1.3 shows the solubility changes of the solute (benzoic acid) with pressure and temperature in CO<sub>2</sub> (McHugh and Krukoni, 1986). As can be seen from this diagram, at pressures lower than 100 atm, each solubility isotherm (65°C, 55°C and 45°C) passes through a minimum and then increases with pressure. At the beginning of the curves where pressure is lower than 35 atm, the effect of the solute's vapor pressure is more dominant on the solubility behavior than the solvent-power (solvent-density) effect. As pressure increases, the fractional contribution of vapor pressure to the total system pressure decreases and the solubility of benzoic acid is reduced to the minimum. After the minimum point up to 280 atm, solvent density becomes

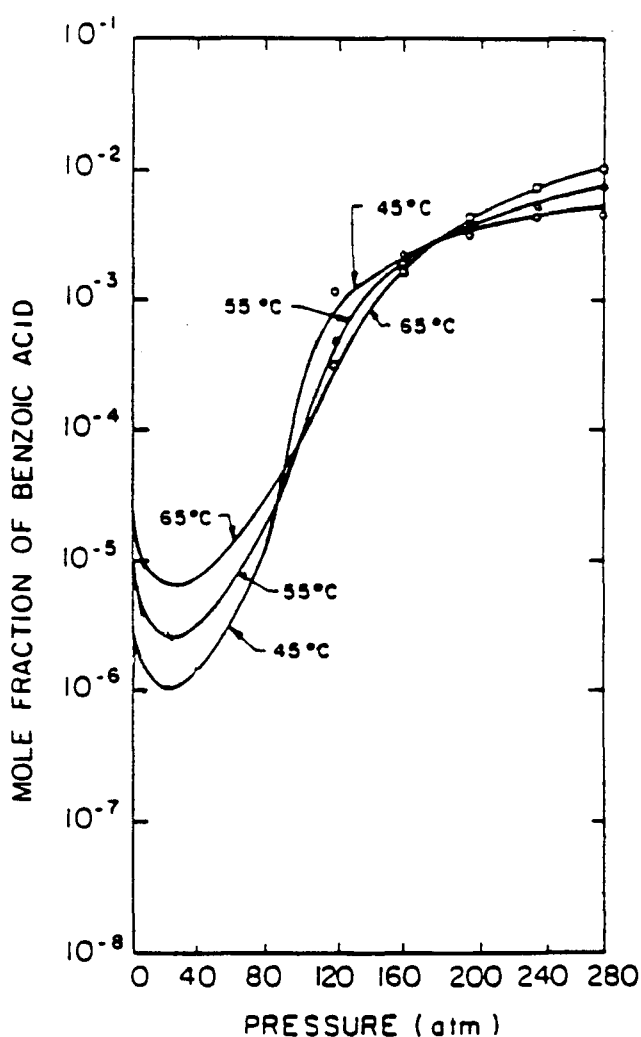


FIGURE 2.1.3. Solubility of benzoic acid in CO<sub>2</sub> (McHugh and Krukoni, 1986).

more effective on solubility, so the solubility increases with the increase of pressure at each temperature (pressure effect on solubility). In this region, solubility values at 65°C are higher than those at 45°C and 55°C, since when the temperature is increased, solvent density shows only minor reductions thus tending to decrease the solute solubility. At the same time, temperature increase causes a major vapor pressure increase, resulting in a large solubility increase (conventional temperature effect on solubility). Between 100 and 180 atm, solubility of benzoic acid at 45°C is higher than the value at 65°C. In this region, solvent power (solvent density) affects solubility behavior predominantly and solvent-power/solvent-density reduction with the increase of temperature is very large in comparison with the solute's vapor pressure increase. Hence, an increase in temperature brings about a decrease in solubility at the same pressure (retrograde temperature effect on solubility). Above 180 atm, conventional temperature effect is recovered and again the solubility value of benzoic acid at 65°C is more than the value at 45°C at the same pressure. In this region, solubility behavior is mostly determined by solute's vapor pressure.

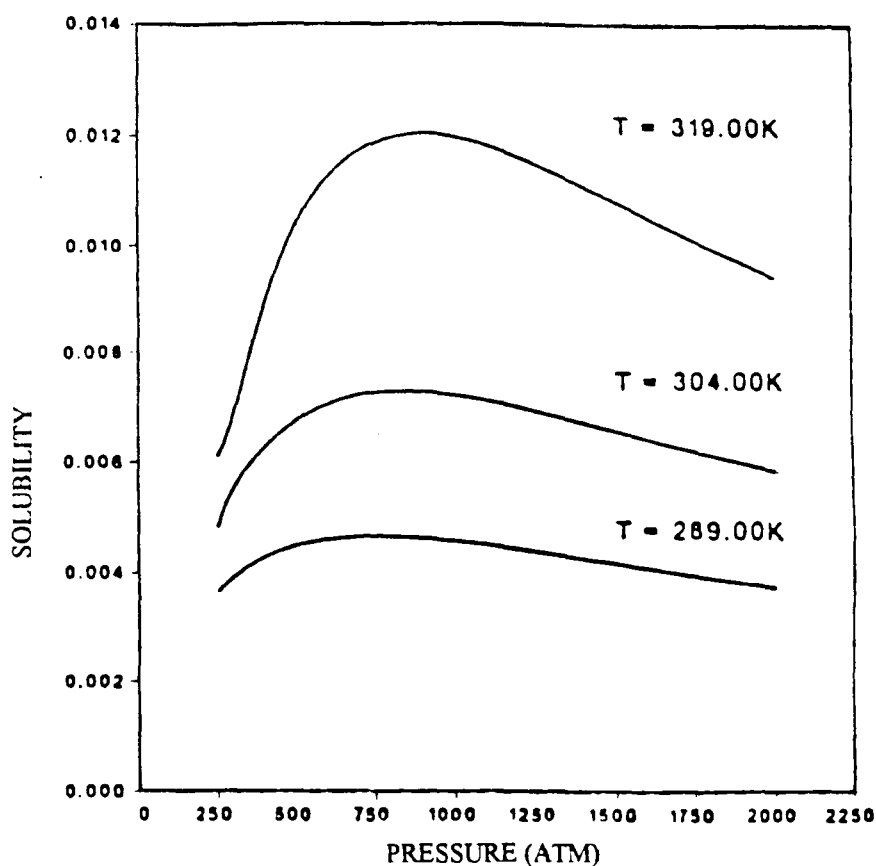


FIGURE 2.1.4. Solubility of 2,3-dimethylnaphthalene in CO<sub>2</sub> (Schulz et al., 1991).

The solubility of 2,3-dimethylnaphthalene in CO<sub>2</sub> as a function of pressure at three different temperatures (289K, 304K and 319K) is shown in Figure 2.1.4 (Schulz et al., 1991). At pressures above 250 atm, the solubility increases with the increase in temperature. It is a fact that at pressures higher than 250 atm, the CO<sub>2</sub> solvent is nearly incompressible. Hence, when temperature is increased, the solvent density shows only minor reductions (almost insensitive to temperature). On the other hand, the increase in temperature causes a significant increase in solute's vapor pressure. Therefore, the net result at higher pressures is a large solubility increase with temperature (the vapor-pressure effect dominates the density effects). At pressures below 400 atm, the density of CO<sub>2</sub> decreases appreciably as temperature rises. Hence, this effect combined with the increase in the vapor pressure of the solute results in lower temperature gradients below 400 atm as compared to those at higher pressures.

In addition to the solvent density, vapor pressure, molecular weight and polarity of the solute are properties which have a special influence on the solubility in dense gases. Dielectric constant (DC) of a compound is dependent upon the polarity of the molecule and affects the solubility behavior of the material. It is an accepted rule that polar compounds dissolve in solvents that are as polar as solute compounds. While a compound having no functional group has a low DC value (low polarity), increase in the number of functional groups in the molecular structure brings about compounds of higher DC value and of lower solubilities in a SCF with a relatively low DC value such as CO<sub>2</sub>. Likewise, it has been shown that compounds which have low molecular weight are completely soluble in the liquid state, for example in liquid CO<sub>2</sub> (Stahl et al., 1988). Vapor pressure is another factor contributing to the solubility of a solute in dense gases. Compounds having higher vapor pressures show higher solubilities in SCFs. Therefore, at prescribed temperature and pressure conditions, the lower the polarity, the smaller the molecular mass and the higher the vapor pressure is, the more soluble is the solute in the SCF.

Technical feasibility of essential-oil processing with SCF aided operations, thus require the solubility (or phase equilibrium) data of these essential-oil components in the supercritical solvent over a wide range of operating conditions. Comprehensive studies of the solubility behavior of volatile oils were carried out and so, the range of dense CO<sub>2</sub> in

which these substances could be obtained selectively was characterized. Figure 2.1.5 gives the solubility behavior (pressure and density dependence) of typical essential-oil components in dense CO<sub>2</sub> at 40°C. As can be seen from this figure, all essential-oil compounds are freely soluble in compressed CO<sub>2</sub>, even at relatively low gas densities. Their solubilities rise exponentially between 70 and 100 atm, as a result of the rapid rise in CO<sub>2</sub> density. If CO<sub>2</sub> is in more strongly compressed condition (high gas density), the miscibility may be total (Stahl et al., 1988).

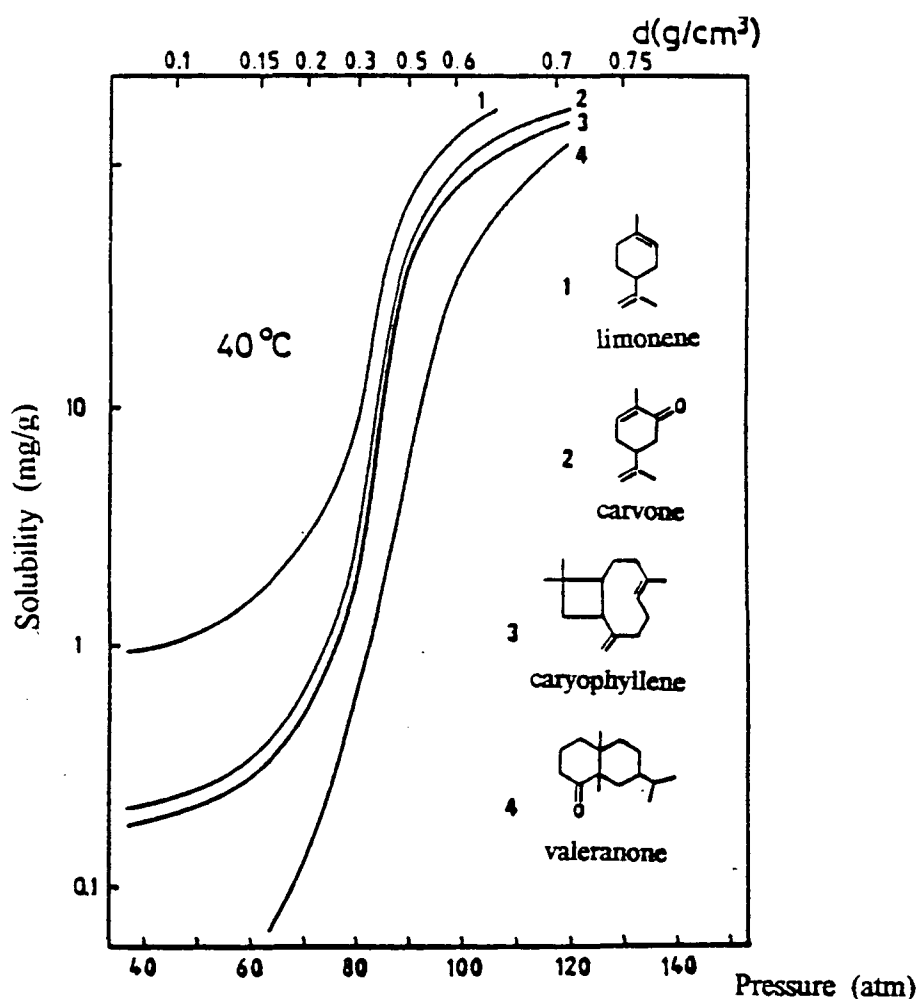


FIGURE 2.1.5. Solubility isotherms of typical essential-oil components in dense CO<sub>2</sub> at 40°C (Stahl et al., 1988).

As seen in Figure 2.1.5, the MT hydrocarbons (e.g. limonene) of essential oils exhibit higher solubilities in dense CO<sub>2</sub>, as compared to the other essential-oil constituents

due to their high vapor pressures, low polarities and small molecular masses (Stahl et al., 1988). Oxygen-containing MTs, e.g. carvone, and sesquiterpene hydrocarbons, e.g. caryophyllene, are equally soluble in dense CO<sub>2</sub>, therefore their solubility curves run very close together. Oxygen-containing sesquiterpene hydrocarbons, e.g. valeranone, with lower vapor pressures and higher molecular weights, are less soluble under the same conditions. As the gas density increases (pressure increases), however, the solubility of each component increases very markedly. At 40°C and above 90 atm, the solubility curves of all components approach to each other; a further increase in density (close to liquid CO<sub>2</sub> density) results in complete miscibility of all compounds.

Solubility behavior of a single essential-oil component in the SCF can also be used to determine the favorable conditions (temperature and pressure) of fractionating these highly volatile substances into component groups of differing volatilities and/or polarities. In such case, the solubilities of components in the supercritical solvent must show large differences so that selective extraction of a desired group can be achieved. As can be seen from Figure 2.1.6, it is evident from the solubility isobars of limonene and carvone that no fractionation is possible at CO<sub>2</sub> gas densities larger than 0.4 g/cm<sup>3</sup>, corresponding to temperatures below 35°C at 80 bar (Stahl and Gerard, 1985). Each solubility curve passes through a minimum when the temperature is raised isobarically. On the one hand, the dissolving capacity of the gas diminishes on account of the fall in its density, and on the other hand, the higher temperature leads to increase of vapor pressure of the substances. At higher temperatures, the differing volatilities together with the dissolving power of the supercritical CO<sub>2</sub> cause the oil components which are to be separated to have distinctly differing solubilities. The general statement can be made that the phase region of the dense CO<sub>2</sub> which permits fractionation of the essential-oil components into definite compound classes is characterized by density values between 0.2 to 0.4 g/cm<sup>3</sup>, and temperatures of 50 to 80°C bring additional advantages (Stahl et al., 1988). However, these temperature and pressure values do not represent optimum conditions for extraction and fractionation of all essential oils, therefore have to be adjusted for each case studied.

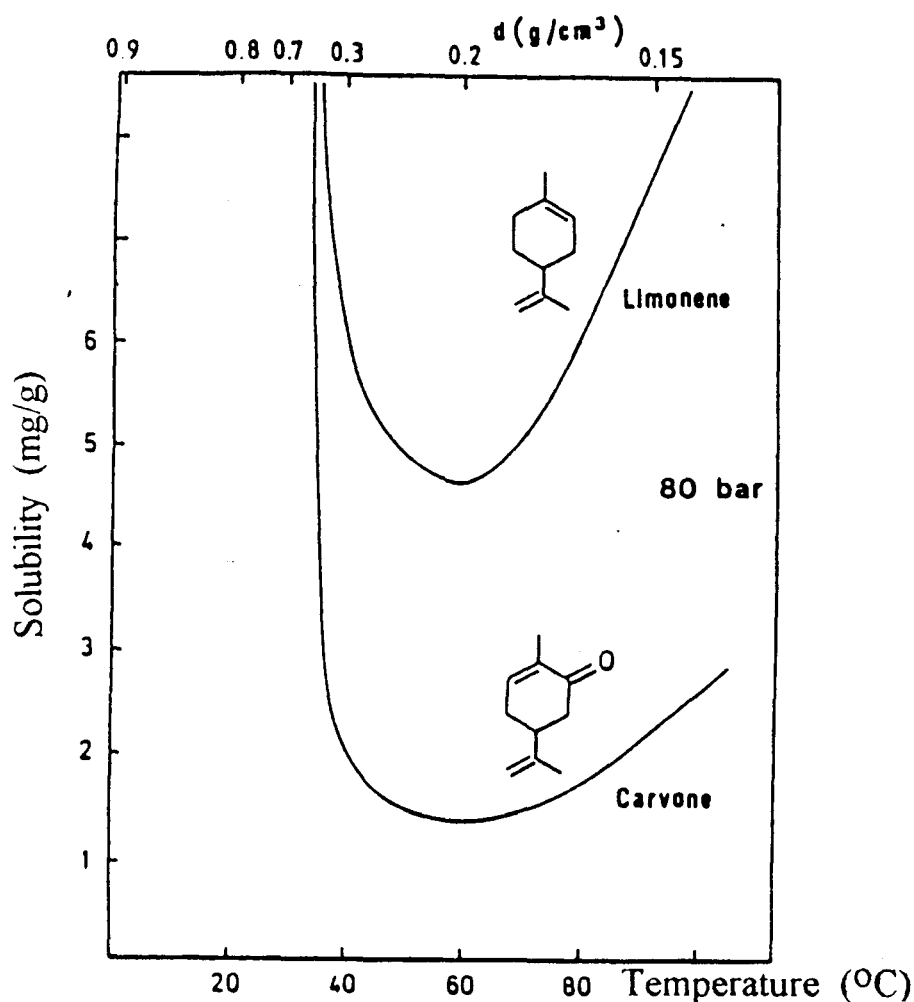


FIGURE 2.1.6. Solubility isobars of limonene and carvone, as functions of temperature and density of dense CO<sub>2</sub> at 80 bar (Stahl and Gerard, 1985).

However, solubility of a single essential-oil component in the SCF can only serve as guides for possible fractionation of essential oils, since typical essential-oil extracts obtained from plants contain over hundred components; ten to twenty of which constitute the bulk and thus characterize the essential oil. Undoubtedly, solubility of an isolated single essential-oil component in the SCF would be different than its solubility in the presence of other components of the essential oil. As a consequence, solubilities of these complex multicomponent mixtures will be affected by solute-solvent and solute-solute interactions. Di Giacomo et al. (1989) measured the solubility of the binary mixture of limonene and citral, which are the most characteristic components of citrus essential oils, in supercritical

CO<sub>2</sub> at 50°C and at pressures ranging from 9.49 to 10.0 MPa. In addition, the phase behavior of this ternary mixture was calculated and the results show that for the accurate prediction of this essential-oil/supercritical-solvent ternary system, binary interaction coefficients between the two solutes should be taken into account (Brandani et al., 1990).

Furthermore, Coppella and Barton (1987) measured the equilibrium solubility of lemon-oil/CO<sub>2</sub> system at 30°C, 35°C and 40°C and in the pressure range of 4.0 to 9.0 MPa. They observed that this system exhibited a single phase above 7.8 MPa at 35°C, however, a decrease in pressure of 0.15 MPa caused the single-phase system to revert to a two-phase system. In such case, a liquid-oil and a dense-gas phase in which CO<sub>2</sub> and the dissolved oil components appear were present, and the complete miscibility of the oil in CO<sub>2</sub> was rapidly lost. This observation further strengthens the complex behavior of an essential-oil/CO<sub>2</sub> system, since a small perturbation in pressure can cause a major change in the phase behavior of this binary system; verifying that solubility is also composition dependent.

Therefore, for the successful design, operation and optimization of SCF aided extraction of essential oils from plants and fractionation of essential-oil extracts into desired products, a detailed study on the solubility and separation (selectivity) behavior of at least the major components of essential oils, which may comprise as high as 200 species, would be highly beneficial.

## **2.2. Overview of the Previous Extraction and Fractionation Studies**

The advantageous properties of SCFs (particularly those of supercritical CO<sub>2</sub>) suggest that SCF applications are likely to become more important in chemical and food industries, since they can maximize product recovery and improve the product quality while minimizing energy requirements during production (Temelli et al., 1988). In this section the applications of SCFs to extraction and fractionation of essential oils are discussed.

### 2.2.1. Supercritical Fluid Extraction Applications

Figure 2.2.1.1 shows the different physical states of CO<sub>2</sub> at various temperatures and pressures, and identifies those regions where a supercritical process can perform functions applicable to essential-oil processing. The high pressure region is generally used for processes where total extraction of a target component (or group of related components) is desired, since most extractable compounds exhibit their maximum solubility in a SCF at higher pressures. The low pressure region can be suitable for crude separations or deodorization of a material containing components of diverse solubilities (Brogle, 1982).

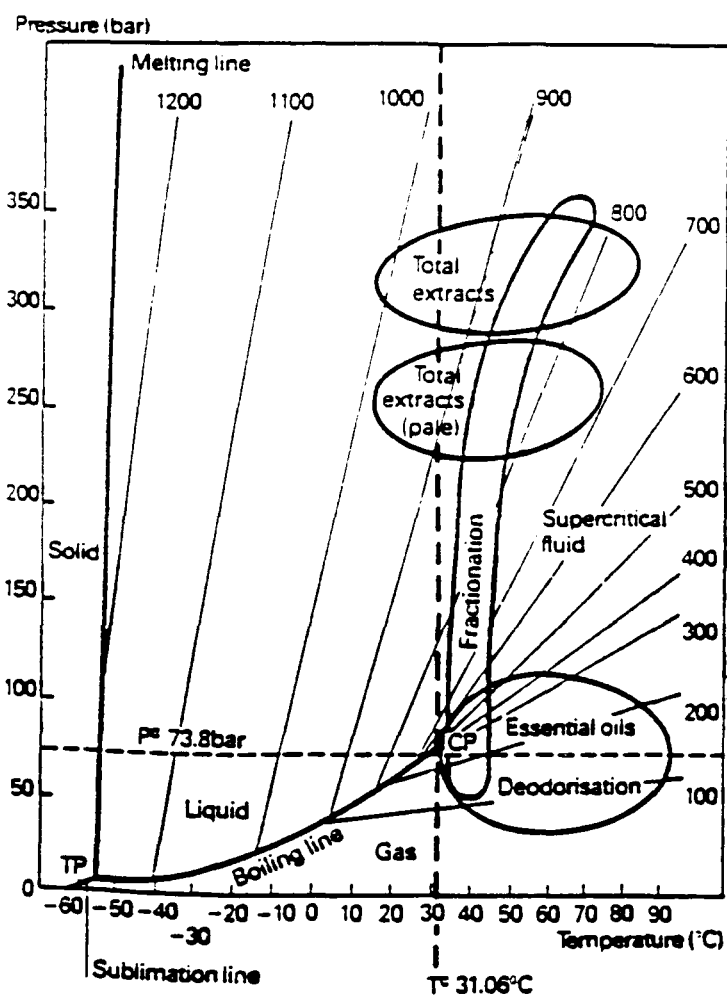


FIGURE 2.2.1.1. Physical states of CO<sub>2</sub> at various temperatures and pressures, illustrating regions useful for essential-oil applications (Brogle, 1982).

If a supercritical extraction of a multicomponent system is carried out over a range of conditions (temperature/pressure ranges), then some degree of selectivity, which is a measure of the ease of separation between two components (or two different groups of components, e.g. isolation of MTs from the oxygenated fraction of an essential oil) can be obtained as the solvent removes components according to their relative solubilities, starting with the most soluble and progressing through the components. Temelli et al. (1988) studied the removal of MT hydrocarbons from citrus essential oils in a single-stage pilot-scale supercritical fluid extraction (SFE) system (Figure 2.2.1.2) within the temperature and pressure ranges of 40-70°C and 8.3-12.4 MPa. It was found that highest selectivity of oxygenated compounds from MT constituents was achieved at 70°C/9.7 MPa but, the yield (amount of extract collected) was minimum under this condition. Likewise, the selectivity was the lowest at 40°C/12.4 MPa, where the largest amount of oxygenated compounds was extracted together with MTs, giving the highest yield among the conditions studied. Hence, based on these results, it was concluded that simple SFE process was successful in eliminating the MT constituents of citrus essential oils, but high solubility and high selectivity were not compatible. In this case, a lower pressure gave higher selectivity but lower extraction yield, whereas a higher pressure gave higher yield but poor selectivity.

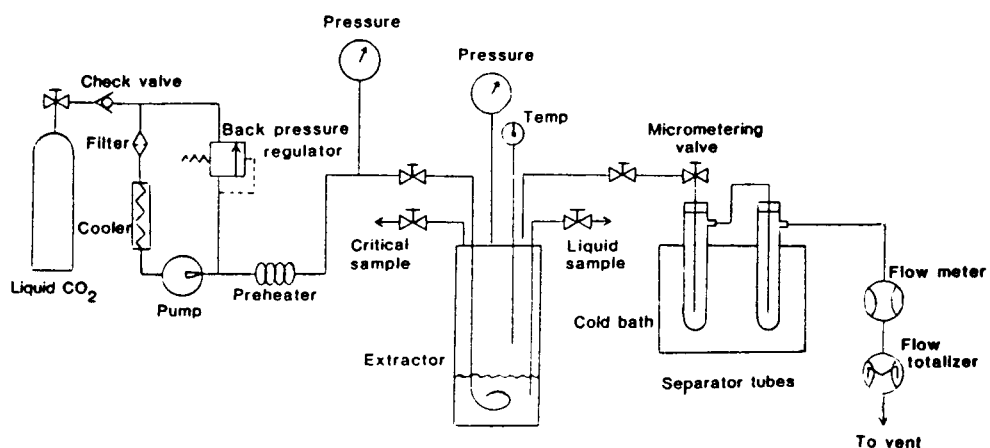
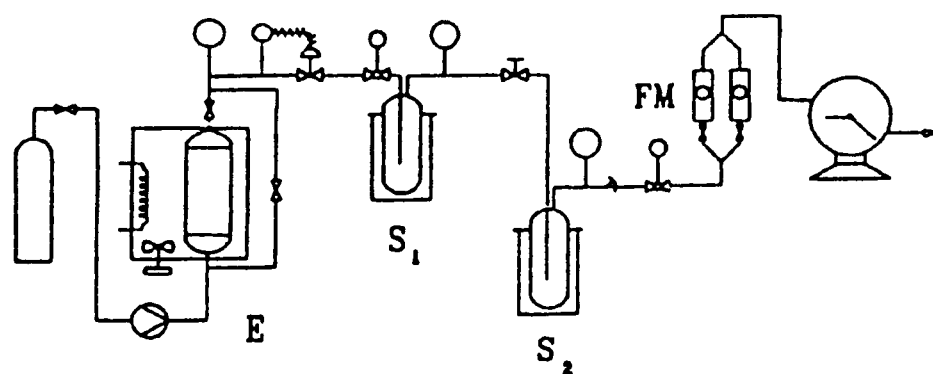


FIGURE 2.2.1.2. Flow diagram of pilot-scale supercritical fluid extraction system (Temelli et al., 1988).

However, the SFE performed by single-stage extraction and separation of essential oils from vegetable substrates (herb, leaf) produces the simultaneous extraction of several compound families that produce a quasi-solid extract. Indeed, hydrocarbon terpenes, oxygenated terpenes and other related products that constitute essential oils are extracted together with paraffins (cuticular waxes) and other undesired compounds (Reverchon, 1992). Therefore, the fractional separation of the extracts is required to isolate the essential oil in order to obtain high-quality products. Reverchon (1992) implemented a process arrangement (Figure 2.2.1.3) that allowed the production of extracts whose chemical, physical and organoleptic properties were similar to those of essential oils. This procedure was applied to the total extraction of marjoram-leaf essential oil followed by the fractional separation of the loaded  $\text{CO}_2$ -solvent through a series of separation vessels, where temperature and/or pressure perturbations were applied. This procedure allowed a nearly complete separation of cuticular waxes, which precipitated in the first separator operating at  $0^\circ\text{C}/80$  bar, and the essential-oil components were separated in the second separator operating at  $-25^\circ\text{C}/5$  bar.



E: extraction section

S1, S2: separators

FM: flow measurement section

FIGURE 2.2.1.3. Schematic representation of the experimental apparatus used in studying supercritical- $\text{CO}_2$  extraction of marjoram-leaf oil (Reverchon, 1992).

Likewise, the results of the single-cycle supercritical-CO<sub>2</sub> extraction of spearmint oil from mint leaves suggested that a two-cycle extraction may be more feasible to obtain a spearmint-oil extract free of MT hydrocarbons (Özer et al., 1996). Thus, if the volatilities of the components differ sufficiently and the conditions maintained in the separators mirror those differences, then a high degree of separation is theoretically possible via the SFE process using the fractional separation technique. On the other hand, if the mixture contains closely related components, it may only be possible to change the relative balance of the individual components in the extract, when compared to that of the original mixture. One disadvantage of this fractionation approach is that the system is capable of separating the original feed mixture into as many fractions as there are separating vessels (Rizvi et al., 1986). In addition, the engineering and operation of the system becomes more complicated and costly, especially if precise temperature and pressure differences must be maintained in the extraction vessels to achieve the desired products.

### **2.2.2. Supercritical Fluid Fractionation Applications**

The drawbacks of the above mentioned simple SFE processes have led to the development of a different approach (based on the use of supercritical CO<sub>2</sub>) to fractionation. This approach, which capitalizes on the temperature dependence of solubility, involves coupling an extraction system to columns designed to establish countercurrent rectification in a semibatch mode, as the separation is taking place. Several investigators (Nilsson et al., 1988, Suzuki et al., 1989) attempted the supercritical fluid fractionation (SFF) of fatty acid ethyl esters and urea-crystallized fish oil esters using rectification columns with axial temperature gradients, which was induced using an internal hot finger (Figure 2.2.2.1). In such cases, the mixture to be separated is placed into the supply vessel and the supercritical solvent is introduced into the vessel from below. The loaded solvent reaches the hot finger via the packed column (the temperature at the top of the column was kept higher than that at the bottom, i.e., the extractor). The dissolved solutes begin to separate out on the finger as a result of the increase in temperature, thus yielding an internal reflux, and flows back into the extraction vessel, setting up countercurrent flow against the

rising loaded solvent. The solutes still in solution in the supercritical solvent are separated by isothermally lowering the pressure. Hence, depending on the processing conditions in the column, an effective separation of the liquid feed material with relatively similar components could be achieved.

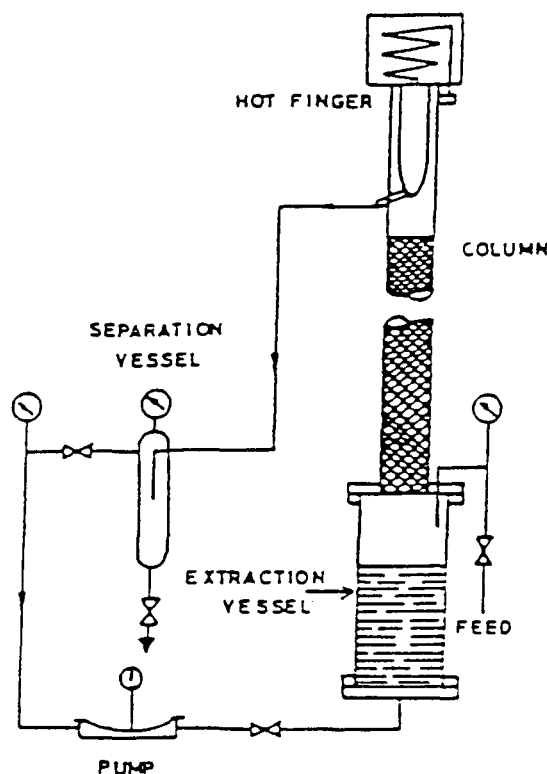


FIGURE 2.2.2.1. Supercritical fractionation apparatus (Rizvi et al., 1986).

SCF extraction with a rectification column (Figure 2.2.2.2) was applied to the separation of a model citrus oil mixture, which consists of limonene, linalool and citral, at various column temperature distributions of 313-333 K and pressures of 8.8-11.8 MPa (Sato et al., 1995). The selective separation was achieved due to the internal reflux in the column induced by an axial temperature gradient of 20 K (a linear temperature distribution from 313 K at the bottom to 333 K at the top). The extractor was operated in semibatch mode with continuous CO<sub>2</sub> flow, and the temperature of the column was controlled by five PID controllers. The effect of temperature distribution on the separation behavior was evaluated in comparison with the column controlled at a uniform temperature. In addition,

the effect of pressure and CO<sub>2</sub> flow rate on the separation of the model mixture was studied. It was concluded that the slight temperature gradient of 20 K improved fractional separation due to the considerable change of solubilities with temperature. A small increase in pressure accelerated the extraction rate; likewise the increase of CO<sub>2</sub> flow rate caused an increase in the extraction rate. Moreover, based on experimental results, it was proven that at pressures above 11.8 MPa, because of the formation of a homogeneous mixture of solutes and supercritical CO<sub>2</sub>, separation was not possible. Raw orange oil was also processed in the same apparatus (Figure 2.2.2.2) used for citrus oil model mixture. The semibatch extraction with internal reflux increased the separation selectivity between terpenes and oxygenated compounds as opposed to a column without a temperature gradient. However, the limitation of semibatch fractionation in a packed tower lies in the fact that a continuous procedure is not possible because all the components of the mixture are extracted in succession, for which pressure of the SCF may have to be increased stepwise.

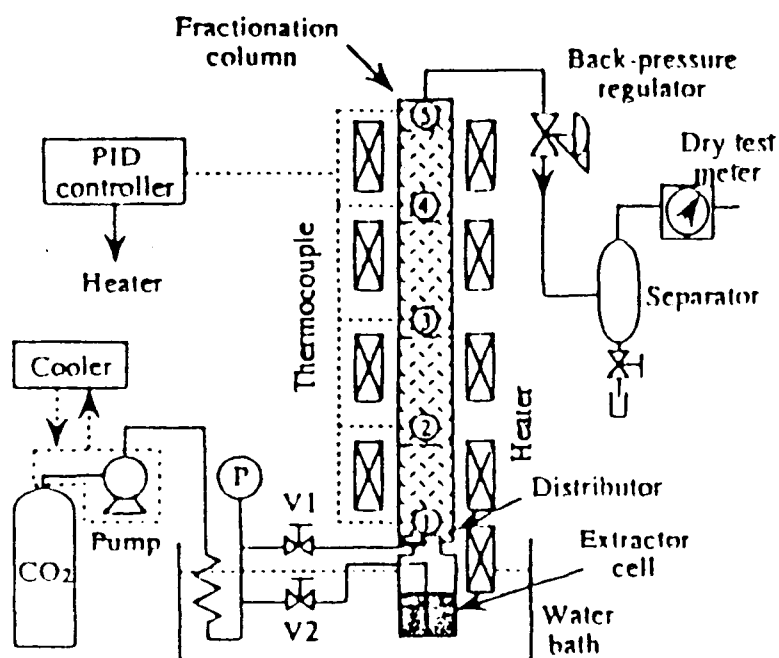


FIGURE 2.2.2.2. Semibatch fractionation apparatus (Sato et al., 1995).

On the other hand, Stahl and Gerard (1985) suggested the removal of terpenes from orange peel oils in a continuous countercurrent high-pressure extraction column (Figure 2.2.2.3). The fractionation column was operated in a continuous mode, and the terpene-containing oil was continuously fed into the middle of the column. Mass transfer takes place between dense gas and essential oil. In climbing through the column the gas becomes enriched preferentially with the more soluble and more volatile MTs which separate out as terpene fraction after leaving the column. The oil, of greatly reduced terpene concentration, is drawn off continuously at the bottom of the column. A definite internal reflux of head product is set via the difference in temperature between that of fractionation (in the middle of the column) and that at the head. Deterpenated orange peel oil (its MT content was reduced to 42 per cent compared to the composition of the starting oil, which was 90 per cent MTs) was obtained when operating in the pressure range between 70 and 90 bar and at temperatures below 80°C (Stahl and Gerard, 1985).

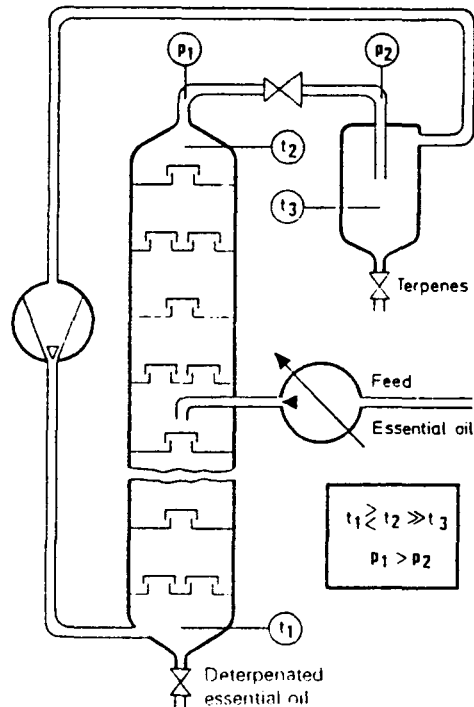


FIGURE 2.2.2.3. Continuous fractionation apparatus (Stahl and Gerard, 1985).

Recently, a more effective separation of essential-oil components was established by increasing the number of equilibrium stages in a continuous countercurrent extraction

column (Sato et al., 1996). In this process, oxygenated compounds were selectively fractionated and collected in the raffinate, and terpenes in the feed were removed in the extract. It was suggested that the extraction process operated at higher solvent-to-feed ratio, and with a longer stripping column will make more valuable products (Sato et al., 1996).

Semibatch or continuous deterpenation of essential oils in a packed tower is based on the difference solubilities of pure essential-oil components. However, some of the major compound families of essential oil exhibit similar solubility behavior in supercritical medium. In fact, oxygen-containing MTs and sesquiterpene hydrocarbons are equally soluble in supercritical CO<sub>2</sub> (Stahl et al., 1988). Therefore, the disadvantages of these processes are that they have low selectivities and a large number of equilibrium stages is required to obtain an effective separation. Moreover, small amounts of waxes contained in citrus peel oils cause problems during this type of fractionation. Not only they reduce the efficiency of the packing in the extraction column, but they concentrate in the raffinate with the oxygenated compounds of the product (Sato et al., 1998). Thus, these separation (continuous or semibatch extraction in a countercurrent packed tower) procedures cannot be used to eliminate the unwanted components of essential oils.

Introducing adsorbents into a SCF extraction system is an attractive method to improve the selectivity (separation between two components, or two groups of components) of the fractionation process. Several attempts and applications to utilize adsorption and desorption behavior in supercritical CO<sub>2</sub> for the deterpenation of essential oils and elimination of their allergenic compounds (like bergapten and oxypeucedanin, which can give a strong allergenic effect on human skin) have been published in literature (Barth et al., 1994). Cully et al. (1990) proposed the supercritical CO<sub>2</sub> desorption of citrus peel oils from several adsorbents, at a temperature range from 50 to 70°C and pressures from 70 to 90 bar. Silica gel proved to be the best adsorbent in fractionating peel oils, since it gives the maximum selectivity in the separation of MT hydrocarbons and oxygenated terpenes. More recently, other investigators suggested the deterpenation and elimination of the high molecular weight compounds (psoralens and coumarins) from lemon (Barth et al., 1994), bergamot (Chouchi et al., 1995), mandarin and lime peel oils (Della Porta et al.,

1997) by supercritical CO<sub>2</sub> from silica gel adsorbent. A high-quality essential oil (e.g. the content of oxygenated compounds in the dertepenated fraction was 20 times higher than in the crude lemon oil) and less nonvolatiles (these high molecular compounds were not detected in the desorbed fractions, but were concentrated in the residue, which was collected after washing the desorption column with ethanol) was obtained in experimental apparatus shown in Figure 2.2.2.4 (Barth et al., 1994). Fractionation of peel oils was started at 40°C/75 bar, and by stepwise increasing the desorption pressure to 85 and 100 bar, at 40°C. The desorbed fractions were precipitated in two cyclonic separators operated in series at 40°C/30 bar and 15°C/20 bar, respectively. However, a higher pressure environment or a co-solvent was required to regenerate the adsorbent and recover the nonvolatiles such as waxes and pigments, which were more strongly adsorbed on silica gel than oxygenated compounds during the dertepenation of these peel essential oils. Thus, an additional process for the removal waxes is required to maintain the activity of the adsorbent.

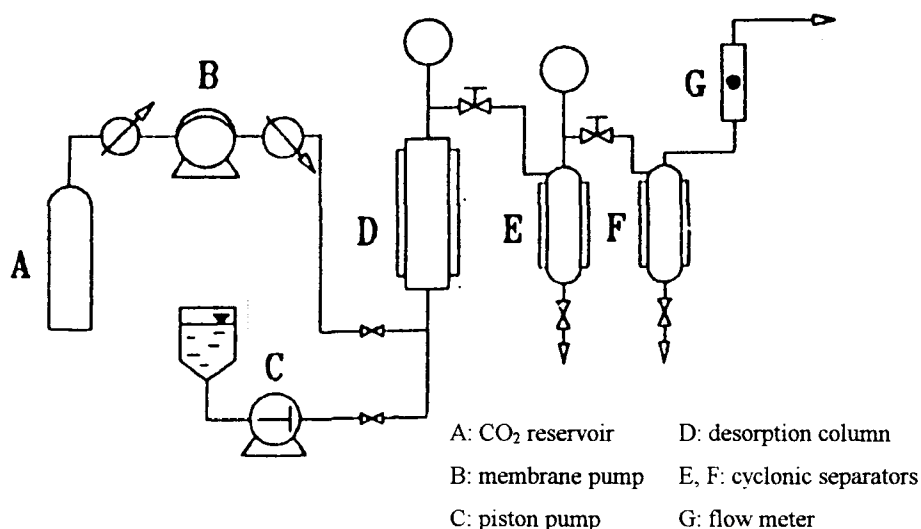


FIGURE 2.2.2.4. Schematic diagram of the desorption apparatus (Barth et al., 1994).

Sato et al. (1997) proposed a continuous cyclic operation (Figure 2.2.2.5) between the adsorption and desorption steps (performed at 40°C/8.8 MPa and 40°C/19.4 MPa, respectively) involving the rinse step (performed at 40°C/8.8 MPa) to remove solutes in the void region of the adsorber (pressure-swing adsorption, PSA, process) for citrus oil

processing with silica gel adsorbent in supercritical CO<sub>2</sub>. There were no terpenes or waxes in the bed at the end of the desorption step, hence derteneration and elimination of nonvolatiles of citrus oil was successfully obtained. However, large amounts of oxygenated compounds were still retained on the bed at the end of the desorption step, which indicated that only a small part of the bed was effectively used for the fractionation process.

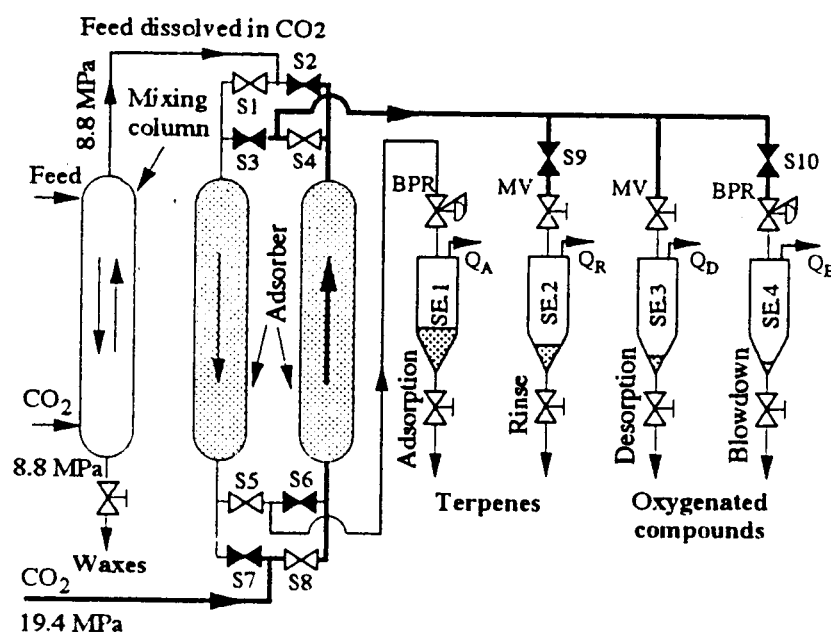


FIGURE 2.2.2.5. Schematic representation of the PSA apparatus (Sato et al., 1997).

Another limitation of the single-supercritical desorption processes stands in the fact that the desorption step is started after the equilibrium saturation between the essential oil and the adsorbent is maintained at ambient conditions; this was the procedure applied by Barth et al. (1994), Chouchi et al. (1995) and Della Porta et al. (1997) during the fractionation of citrus peel oils by supercritical-CO<sub>2</sub> desorption from silica gel adsorbent. In other words, citrus peel oil was charged to the desorption column already filled with the adsorbent, then a certain amount of period was allowed for the complete disappearance of the liquid phase. Therefore, these processes were semibatch since it was necessary to batchwise charge the oil to the desorption column. To overcome this limitation, and to develop a continuous process, the oil can be mixed with the supercritical fluid and fed

continuously to the column. Subra et al.(1998) studied supercritical adsorption on silica gel of a model mixture of terpenes that are among the characteristic components of citrus essential oils (Figure 2.2.2.6). The dynamic behavior of this system was analyzed via the breakthrough curves, and adsorption isotherms were obtained for each component of the mixture at 37°C and 47°C, at a fixed CO<sub>2</sub> density of 0.75 g/cm<sup>3</sup>. Their results suggested that the adsorption process should be performed at low CO<sub>2</sub> density (0.5 g/cm<sup>3</sup>) and low temperature (37°C) to get a higher loading of the sorbent and to maintain an enrichment in oxygenated compounds against the MT'hydrocarbons.

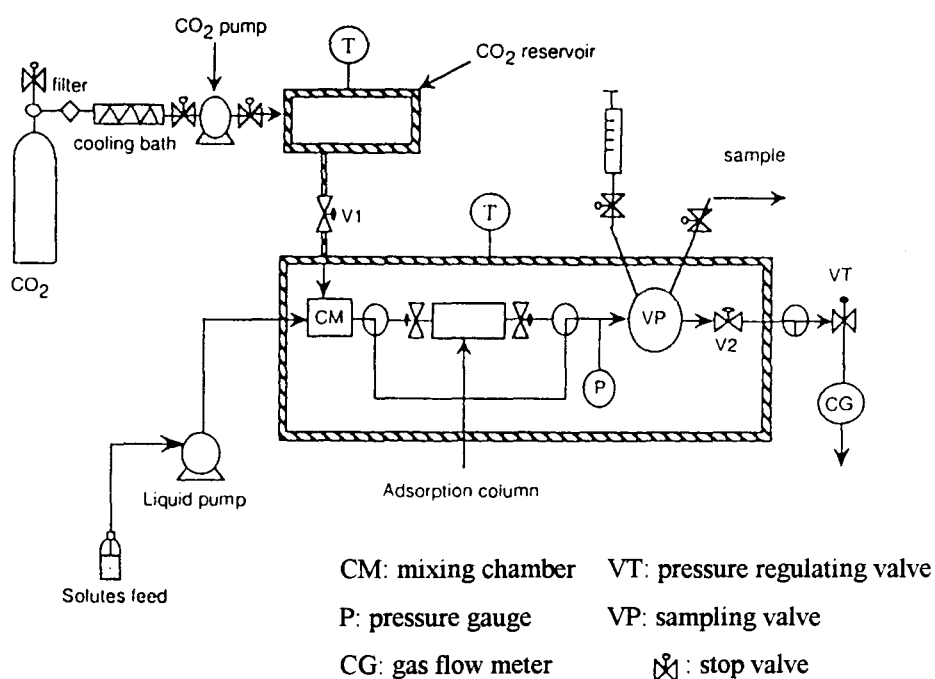


FIGURE 2.2.2.6. Experimental apparatus for the adsorption of supercritical mixtures (Subra et al., 1998).

Regarding the disadvantages of these studies conducted in the aim of extracting the essential oil as a whole or isolation and concentration of its valuable compounds/fractions imply that there still remains a lot of work to be done for the successful design, operation and optimization of SCF aided operations on essential-oil processing. In fact, for the success of future industrial applications of SCF technology to essential-oil extraction,

purification and/or rectification (such as deterpenation process), knowledge on the relative distribution of at least the major components of essential oils in supercritical solvents would be highly beneficial. Noting the above discussion, a new process arrangement which will capitalize on the solubility and selectivity information of the proposed procedures for essential oil processing would be highly valued. Since in such a case, the advantages of all the suggested operation schemes will be exploited. This approach has to be considered for the supercritical-based processing of essential oils, which are complex mixtures comprising of over 200 components, since an attempt might result in enhanced essential oil yields and improved essential oil qualities.

### 3. BASIC FACTS, INTENTIONS AND PROCEDURES

As a consequence of the previous work summarized in chapter two, the development of a new process arrangement based on supercritical fluid fundamentals, which will selectively remove the monoterpene (MT) hydrocarbons and thus, improve the product quality of a group of essential oils (in this case, origanum oil) was chosen as the aim of this study. In summary, the suggested process separated the MT constituents from the non-monoterpene (NMT) fraction of the oil (deterpenation) through a continuous phase separation (dense-CO<sub>2</sub> extraction) followed by an adsorption process coupled with a step-wise pressure increase desorption process. The simple supercritical-CO<sub>2</sub> extraction process can be used to separate origanum oil into groups of components of differing properties (volatility and/or polarity). Then, the adsorption process can be used to further increase the selectivity (separation between MT hydrocarbons and oxygenated fraction) of the fractionation process according to the different affinities of origanum-oil components for the sorbent. The adsorption process can be performed on a fixed bed filled with activated carbon (or silica gel) with a continuous feed of origanum-oil/CO<sub>2</sub> mixture. Last, desorption with pure supercritical CO<sub>2</sub> can be used to recover the adsorbed compounds (the oxygenated constituents of this origanum oil) using step-wise pressure increase method. The first step performed at a low pressure will produce the selective desorption of the MT hydrocarbons and the second performed at a high pressure will assure the fast desorption of the oxygenated compounds. A pilot-scale experimental apparatus has been designed and constructed in the laboratory in order to achieve the purpose of this study. In this chapter, the different forms of operations and procedures implemented in order to achieve the purpose of this study will be presented regarding the facts about origanum-oil components and supercritical CO<sub>2</sub>.

### 3.1. Key Components of Origanum Oil

Table 3.1.1 shows the twelve key components of this origanum oil (*Origanum Munituflorum*) identified by GC/MS, their classification (including their formulae and molecular weights), retention times (RT) and normalized concentrations (normalized area percentages). Information on boiling point, density and solubility of each key component in water and various solvents (ethanol and ether) is given in Table C.1, in Appendix C. In addition, the molecular structure of each key component is illustrated in Appendix C. The chromatogram (Figure E.1) and the area per cent report of the original oil is demonstrated in Appendix E. The major origanum-oil components that will be referred throughout this thesis are given in a different column in Table 3.1.1. This is because the peaks (generated by GC/MS chromatographic analysis) for pseudo-components *PC1* and *PC2* are not pure, but a mixture of two different classes of components. In fact, scanning through the peak of *PC1* suggested that the front of this peak was pure  *$\beta$ -phellandrene* (a monoterpene), whereas the end of the peak was pure *1,8 cineole* (an ether). Similarly, the front of the peak of *PC2* was pure *terpinen-4-ol* (an alcohol), whereas the end of the same peak was pure *caryophyllene* (a sesquiterpene). Consequently, it was not possible to obtain an area count result for each component forming *PC1* or *PC2*. Hence, the overall area count of the pseudo-component *PC1* and *PC2*, and the area counts of the other selected components of this origanum oil were used to calculate the normalized area percentages of the twelve key components of the original oil (refer to the area per cent report of the original oil given in Appendix E). As presented in Table 3.1.1, total monoterpene (MT) and non-monoterpene (NMT) hydrocarbon content in this origanum oil is 40.434 per cent and 59.566 per cent, respectively. The MT cut is comprised of six pure components and one pseudo-component, *PC1*, whereas the NMT cut (including alcohol, sesquiterpene and phenolic substances) is comprised of four pure components and one pseudo-component, *PC2*.

The distribution chart of origanum oil components in Figure 3.1.1 also shows that the oil mainly consists of the NMTs, and carvacrol, being the major component (48%) in the original oil. So, this oil can be called a “carvacrol-rich” origanum oil.

TABLE 3.1.1. The key components of original origanum oil.

Key components of original origanum oil identified by GC/MS	Formula and Molecular weight	Class	Component names referred in this thesis	RT (min)	Normalized area percentages
$\alpha$ -pinene	$C_{10}H_{16}$ 136.24	MT	$\alpha$ -pinene	7.10	3.109
camphene	$C_{10}H_{16}$ 136.24	MT	camphene	8.08	1.307
myrcene	$C_{10}H_{16}$ 136.24	MT	myrcene	10.64	1.620
$\alpha$ -terpinene	$C_{10}H_{16}$ 136.24	MT	$\alpha$ -terpinene	11.22	2.365
$\beta$ -phellandrene	$C_{10}H_{16}$ 136.24	MT	PC1	12.08	1.146
1,8 cineole	$C_{10}H_{18}O$ 154.26	Ether			
$\gamma$ -terpinene	$C_{10}H_{16}$ 136.24	MT	$\gamma$ -terpinene	13.09	12.547
p-cymene	$C_{10}H_{14}$ 134.22	HYD	p-cymene	13.80	18.340
<i><math>\Sigma</math> monoterpene hydrocarbons</i>					$\Sigma$ 40.434
linalool	$C_{10}H_{18}O$ 154.26	AL	linalool	20.45	1.769
terpinen-4-ol	$C_{10}H_{18}O$ 154.26	AL	PC2	22.24	5.848
caryophyllene	$C_{15}H_{24}$ 204.36	ST			
borneol	$C_{10}H_{18}O$ 154.26	AL	borneol	25.00	2.821
thymol	$C_{10}H_{14}O$ 150.22	PH	thymol	39.39	0.821
carvacrol	$C_{10}H_{14}O$ 150.22	PH	carvacrol	40.28	48.307
<i><math>\Sigma</math> non-monoterpene hydrocarbons</i>					$\Sigma$ 59.566
<i><math>\Sigma</math> total</i>					$\Sigma$ 100.000

Reference: Guenther, 1952 (MT: monoterpene, HYD: hydrocarbon, AL: alcohol, ST: sesquiterpene, PH: phenol).

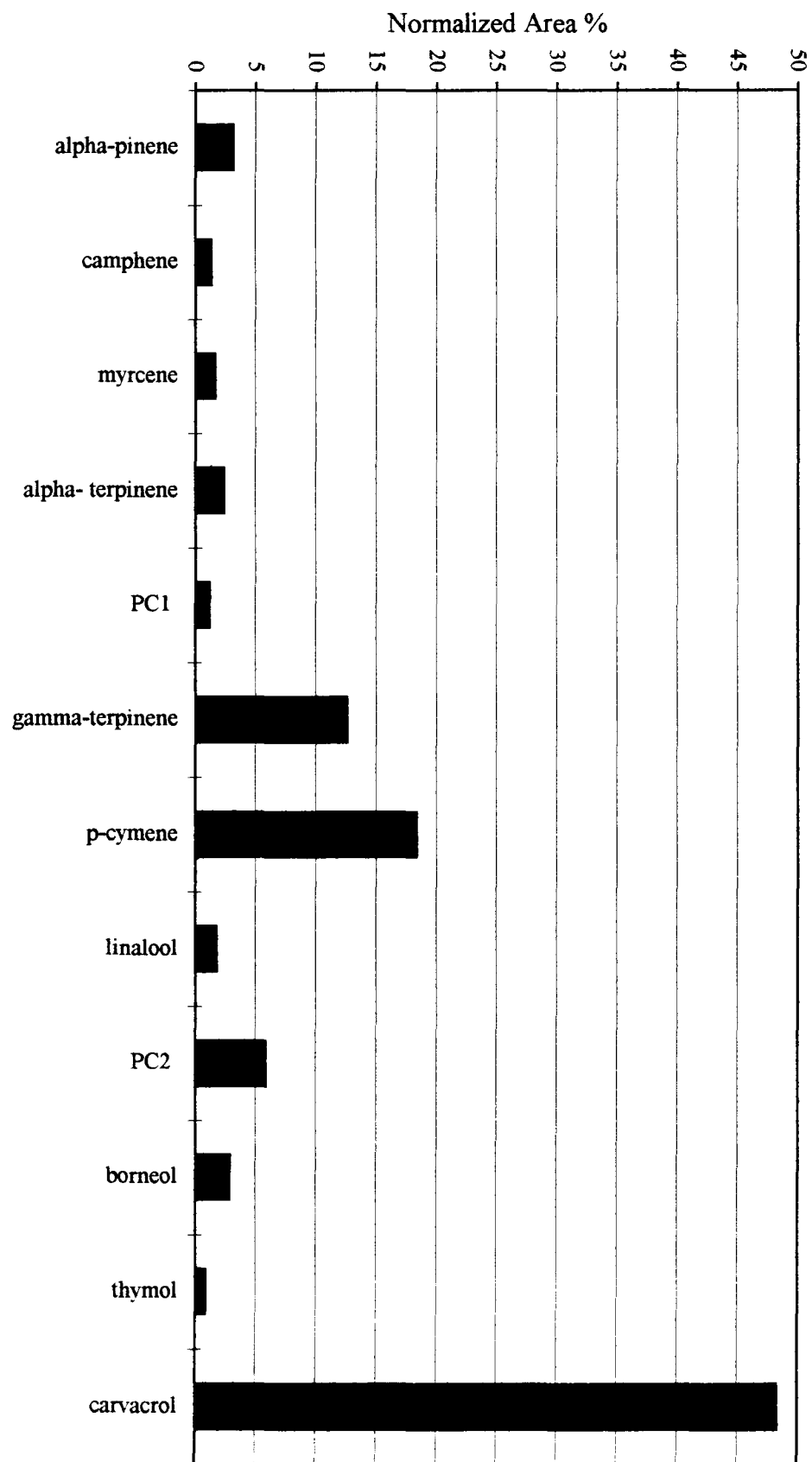


FIGURE 3.1.1. Distribution of *origanum* oil (*Origanum Muniflorum*) key components.

### 3.2. Intentions and Procedures

It is a fact that the quality of essential-oil products decreases with increasing fraction of the MT hydrocarbons. Decomposition of these unstable hydrocarbons generates compounds which impair the quality of the essential-oil product. On the other hand, oxygenated hydrocarbons are the real flavor and aroma donators of essential oils. Therefore, an experimental set-up has been constructed and operated in the aim of obtaining an origanum-oil product possibly free of MT hydrocarbons. In other words, the purpose of this experimental study is to remove the MT components (deterpenation) and leave the NMT hydrocarbons behind, thus a minimum amount of NMT components in the origanum-oil product is desired. This research is carried out with the understanding that the results of this work will be of importance in producing valuable products from origanum oil for the Turkish essential-oil industry.

It is known that, in a simple supercritical-fluid extraction process, it is often difficult to reconcile conditions that lead to high recovery (yield) with those that result in high selectivity. An alternative approach is the coupling of supercritical-fluid extraction to an adsorption process. Based on this idea and in lieu of the intentions of this study, supercritical-CO<sub>2</sub>-aided, a continuous adsorption/desorption process coupled with dense-gas extraction has been developed.

The plan of attack consisted of a number of experiments that have been conducted in order to achieve the purpose of this work. In each case, the evolution of the process performance was obtained by taking samples at fixed time intervals from the cold trap (sample collector). This sample was further diluted in ethanol, and the resulting mixture was analyzed by GC/MS. The detailed description of the experimental apparatus constructed and procedure applied will be given in chapter five. Here, the different forms of operations adopted are presented by simple diagrams, Figures 3.2.1 to 3.2.3. The reasoning behind each process scheme will also be explained considering various operational aspects.

First, simple supercritical-CO<sub>2</sub> extraction process was carried out in the aim of fractionating origanum oil and isolating its MT constituents. Two different forms of extraction experiments were performed, as schematically presented in Figures 3.2.1 and 3.2.2. As seen from these diagrams, the mixing cell (packed with glass beads) situated prior to the extractor, was used in preparing the feed solution through mixing the supercritical CO<sub>2</sub> and the origanum oil streams (tee preceding the mixing cell connects them); this feed was then allowed to enter the extractor. In reality, all the extraction process is taking place in the mixing cell thus, the second column denoted as extractor (packed with glass beads) can be named as “blank column” because there is nothing being extracted in this column; the feed mixture is simply traveling/diffusing through this packed vessel. Throughout this dissertation, in the experiments referred as extraction experiments performed in the mixing cell/extractor arrangement, comprised of two columns in series (shown within dashed lines in Figures 3.2.1 and 3.2.2), the extraction process is taking place in the first column (mixing cell, packed with glass beads) and the second column (extractor, packed with glass beads) is used to prevent the possible entrainment. This column (extractor) is then packed with adsorbent during the adsorption/desorption runs. In both figures, the overall composition of the feed stream entering the mixing cell is labeled as  $z$ .

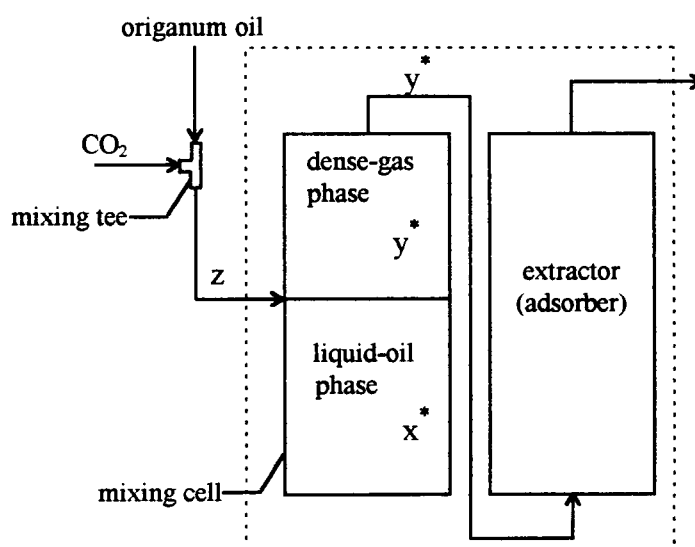


FIGURE 3.2.1. Supercritical-CO<sub>2</sub> extraction (or supercritical-CO<sub>2</sub> adsorption following dense-gas extraction) experiments at 40°C/7.5 MPa.

As can be seen in Figure 3.2.1, if at 40°C/7.5 MPa conditions, the origanum-oil/CO<sub>2</sub> system falls in the two-phase region, then a liquid-oil and a dense-gas phase in which CO<sub>2</sub> and the dissolved oil components appear are present. In this case, equilibrium conditions are attained, thus the feed mixture leaving the mixing cell has the composition of origanum oil in the dense-gas phase,  $y^*$ , and  $y^* \ll z$ . Hence, at this operating conditions, the mixing cell/extractor arrangement acts as a flash unit adding an extra degree of flexibility to the system. MT hydrocarbons definitely possess the highest vapor pressure among the key components of origanum oil. This property, coupled with their lower molecular mass and lower polarity (CO<sub>2</sub> is a nonpolar solvent) makes them easily soluble in CO<sub>2</sub> (Stahl et al., 1988). Therefore, the MT constituents of this origanum oil are expected to concentrate in the dense-gas phase (Figure 3.2.1), whereas NMT hydrocarbons are expected to show the opposite behavior, i.e., to remain in the liquid-oil phase (Figure 3.2.1). The validity of this argument was established experimentally, and the supercritical-CO<sub>2</sub> extraction experiment performed at 40°C/7.5 MPa conditions confirmed the presence of a liquid-oil phase accumulating in the bottom of the mixing cell (CO<sub>2</sub> continuously bubbled through it). During this experiment, 11.4 ml of origanum oil was charged to the mixing cell (by the HPLC pump) and at the end of the run, 3.7 ml residual oil was collected through the on-off valve placed in the bottom of the mixing cell (refer to Figure 4.2.3); this means that 7.7 ml of origanum oil was dissolved in dense-CO<sub>2</sub> phase. In other words, it was not possible to measure the volume of origanum oil collected in the sample collector at the end of this experiment (and all others) hence, the amount of oil solubilized in dense-CO<sub>2</sub> phase was calculated from the difference of the measured quantities. However, the composition of the original origanum oil and residual oil were characterized by GC/MS analysis. The distinct distribution of the origanum-oil components in the residual and original oil further strengthened the validity of the above hypothesis that indeed two-phases exist (the results of the GC/MS analysis will be demonstrated in Figure 5.2.1.4).

On the other hand, as can be seen in Figure 3.2.2, at 40°C/10.0 MPa conditions, the origanum-oil/CO<sub>2</sub> system is expected to be in the single-phase region. In this case, equilibrium conditions are not attained, thus the composition of the feed to the extractor is equal to the composition of the feed to the mixing cell, i.e.,  $z$  is equal to  $y$  and  $x$  is equal to zero (no liquid-oil phase). The validity of the single-phase occurrence was also established

experimentally, and the supercritical-CO<sub>2</sub> extraction experiment performed at 40°C/10.0 MPa conditions confirmed that all oil pumped was completely miscible in CO<sub>2</sub> (since no residual oil was collected through the on-off valve placed in the bottom of the mixing cell). In addition, at the end of the run, the glass beads within the mixing chamber were washed with ethanol to recover any oil that was not dissolved in dense CO<sub>2</sub>. The GC/MS analysis of this solution showed no peaks were detected, that further strengthened the presence of a single dense-gas phase at this operating conditions.

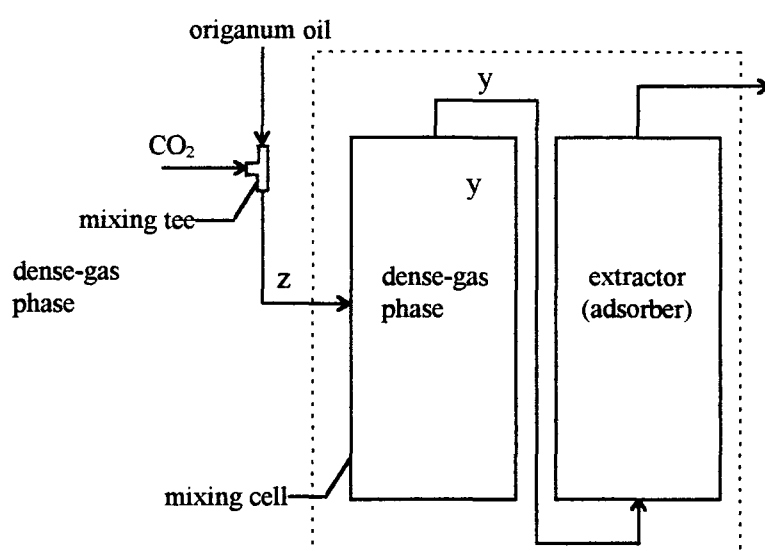


FIGURE 3.2.2. Supercritical-CO<sub>2</sub> extraction (or supercritical-CO<sub>2</sub> adsorption following dense-gas extraction) experiments at 40°C/10.0 MPa.

Next, supercritical-CO<sub>2</sub> adsorption following the dense-gas extraction was carried out in the aim of enhancing the separation between the MT and NMT components of organum oil. Two different forms of adsorption experiments were performed, as schematically presented in Figures 3.2.1 and 3.2.2. In the extraction runs, the extractor was packed with glass beads of 3 mm, whereas in the adsorption runs the same vessel was packed with the sorbent. The adsorption process was performed on a fixed bed filled with activated carbon (or silanized silica gel) with a continuous feed of organum-oil/CO<sub>2</sub> mixture. As seen from these diagrams, the mixing cell (packed with glass beads) situated prior to the adsorber, was used in preparing the feed solution through mixing the supercritical CO<sub>2</sub> and the organum oil streams (tee preceding the mixing cell connects

them); this feed was then allowed to enter the adsorber. It was proved through the simple supercritical extraction experiments that the mixing cell/extractor system acted as a flash unit at 40°C/7.5 MPa conditions. Therefore, as a first step prior adsorption, the mixing cell/extractor arrangement added an extra degree of flexibility to the system. This fact offers the advantage that the feed mixture entering the adsorber is already separated into groups of components of differing properties (volatility and/or polarity) in the mixing cell. In addition, the adsorption process was expected to enrich the column selectively according to the different affinities of origanum-oil components for the sorbent.

Last, supercritical-CO<sub>2</sub> desorption following the origanum-oil/CO<sub>2</sub> adsorption coupled with dense-gas extraction was executed in order to recover adsorbed compounds (Figure 3.2.3). Pure supercritical CO<sub>2</sub> (entering the desorber through a different connecting line) was used during the desorption process.

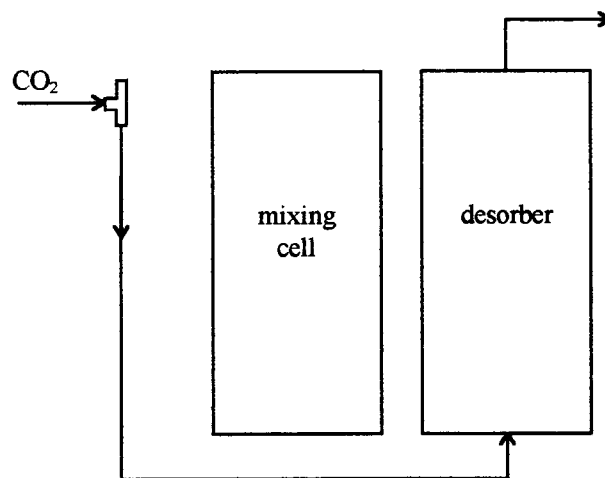


FIGURE 3.2.3. Desorption with pure supercritical CO<sub>2</sub>.

In constructing the pilot-scale deterpenation system, in which different types and forms of experiments could be conducted, several of the above stated facts were taken into account. These can be re-iterated as follows:

1. Samples collected in all the experiments i) supercritical-CO<sub>2</sub> extraction, ii) supercritical-CO<sub>2</sub> adsorption coupled with dense-gas extraction, and iii) pure supercritical-CO<sub>2</sub>

desorption following the origanum-oil/CO<sub>2</sub> adsorption coupled with dense-gas extraction) are not instantaneous but integral samples.

2. For each component, the area-count result obtained from the GC/MS analysis is directly related to the amount (mass) of this component in the mixture.
3. All essential-oil components and flavor substances are freely soluble in compressed CO<sub>2</sub>, even at relatively low gas density (Stahl et al., 1988).
4. At higher pressure, due to increased density of CO<sub>2</sub>, the effect of the solvating power of the solvent increases (Stahl et al., 1988).
5. MT hydrocarbons have higher vapor pressure, low polarity and smaller molecular weight compared to the other components of essential oils (Stahl et al., 1988).
6. NMT hydrocarbons possess lower vapor pressure, higher polarity and higher molecular weight among the essential-oil components (Stahl et al., 1988).
7. Oxygen-containing MTs and sesquiterpene hydrocarbons are equally soluble in supercritical CO<sub>2</sub> (Stahl et al., 1988).
8. *p-cymene* is the only aromatic hydrocarbon and possesses the lowest molecular weight among the twelve key components of origanum oil.
9. *myrcene* is the only acyclic hydrocarbon among the MT constituents of origanum oil (Guenther, 1952).
10. *PC1* is a pseudo-component since it is a mixture of *β-phellandrene* (a MT hydrocarbon) and *1,8 cineole* (an oxygenated compound, ether).
11. *PC2* is a pseudo-component since it is a mixture of *β-caryophyllene* (sesquiterpene hydrocarbon) and *terpinen-4-ol* (oxygenated terpene, alcohol).

12. *borneol* and *terpinen-4-ol* are both cyclic terpene alcohols, whereas *linalool* is the only aliphatic terpene alcohol among the NMT hydrocarbons of *origanum* oil (Guenther, 1952).
13. The phenolic constituents of the NMT group are *thymol* and *carvacrol*, which are isomers of each other (Guenther, 1952).
14.  $\alpha$ -*pinene* and *camphene* are the least polar components among the MT hydrocarbons of *origanum* oil (Adams, 1995).
15. The unique surface property of activated carbon is that its surface is nonpolar or slightly polar as a result of the surface oxide groups and inorganic impurities (Yang, 1987).
16. The stronger the components are adsorbed (favorable adsorption), the harder they will be desorbed (unfavorable desorption) (Ruthven, 1984).

## 4. EXPERIMENTAL WORK

The main purpose of this work was to develop a supercritical-CO<sub>2</sub>-based adsorption/desorption process (coupled with dense-gas extraction) to improve the quality of origanum oil (*Origanum Munituflorum*) through the removal of its monoterpene (MT) hydrocarbons, deterpenation. Before investigating the optimum conditions for the fractionation of origanum oil, the experimental set-up and procedure had to be tested. In Appendix A, the different types of experiments carried out with toluene/CO<sub>2</sub> binary mixture, the experimental procedure employed and the results obtained are demonstrated. Based on the information/experience gained with the toluene/CO<sub>2</sub> system, the experimental set-up (Figure A.1) constructed was modified (adjusted) prior to the fractionation of origanum oil via supercritical CO<sub>2</sub>. In this section, the materials used and a description of the equipment and the experimental procedure employed will be explained in detail.

### 4.1. Materials Used

As the feed material, origanum oil (*Origanum Munituflorum*) was used. The origanum oil, which was obtained from a processing plant in Antalya region, was supplied by Altes Ltd. Şirketi, İstanbul. Ethanol (Riedel de Haen, 99.9% pure) was used as the solvent of origanum oil during GC/MS analyses and hexane (commercial grade) was used as the cleaning solvent. Helium (99.9% pure), the carrier gas for the gas chromatograph, was obtained from BOS (Birleşik Oksijen Sanayii, İstanbul) and CO<sub>2</sub> (99.7% pure) in cylinders equipped with dip tubes was supplied from Hergaz A.Ş., İstanbul.

## 4.2. Experimental Set-up

The schematic diagram of the high-pressure continuous flow-type experimental apparatus used in performing the supercritical-CO<sub>2</sub> extraction and adsorption/desorption runs is depicted in Figure 4.2.1. Previously, in chapter three, the different forms of operations adopted were presented by simple diagrams (Figures 3.2.1 to 3.2.3) and the reasoning behind each process scheme was explained considering various operational aspects. In the experimental set-up designed for fractionation of origanum oil, all connecting lines used were made of stainless-steel tubing (Type 316, Alltech Co.) and all on-off, check and metering valves (Swagelok Co.) used were capable of withstanding high pressures up to 250 bar. Pressure measurements for the system were made using high-pressure gauges (Pakkens Instruments) having pressure ranges of 0-315 bar and sensitivity KL 1.0. Detailed information about the experimental apparatus constructed and operated in the aim of improving the quality of origanum oil through the removal of MT hydrocarbons (considering the facts listed in chapter three), is given below.

The solvent entry zone, where CO<sub>2</sub> is compressed to the operating pressure, of the experimental set-up is illustrated in Figure 4.2.2. CO<sub>2</sub> was supplied from a gas cylinder with dip tube attachment at a pressure of 60 bar at 15°C and the on-off valve SV1 enabled the flow of CO<sub>2</sub> to the system. The pressure in the gas cylinder was continuously monitored through the pressure gauge placed after the drier (silica gel bed, 6.15 cm inner diameter and 25 cm length), which was used to remove any water vapor that might be present in the commercial grade CO<sub>2</sub>. The drier was manufactured by Erikman Kardeşler Makine Sanayii, İstanbul. The solvent was then cooled to -6°C in the refrigerated bath (Heto CB7) containing water/monoethylene glycol mixture. In this way, the vapor pressure of CO<sub>2</sub> was kept below the atmospheric pressure and probable gasification was prevented. Inline filters, F1 and F2, were placed before the pump to trap any contamination which might be present in the solvent, hence allowing the cleaned fluid pass through the diaphragm pump. These filters (Nupro Co., TF Series) had a filtration rate of 40 µm at a 95-98 per cent efficiency.

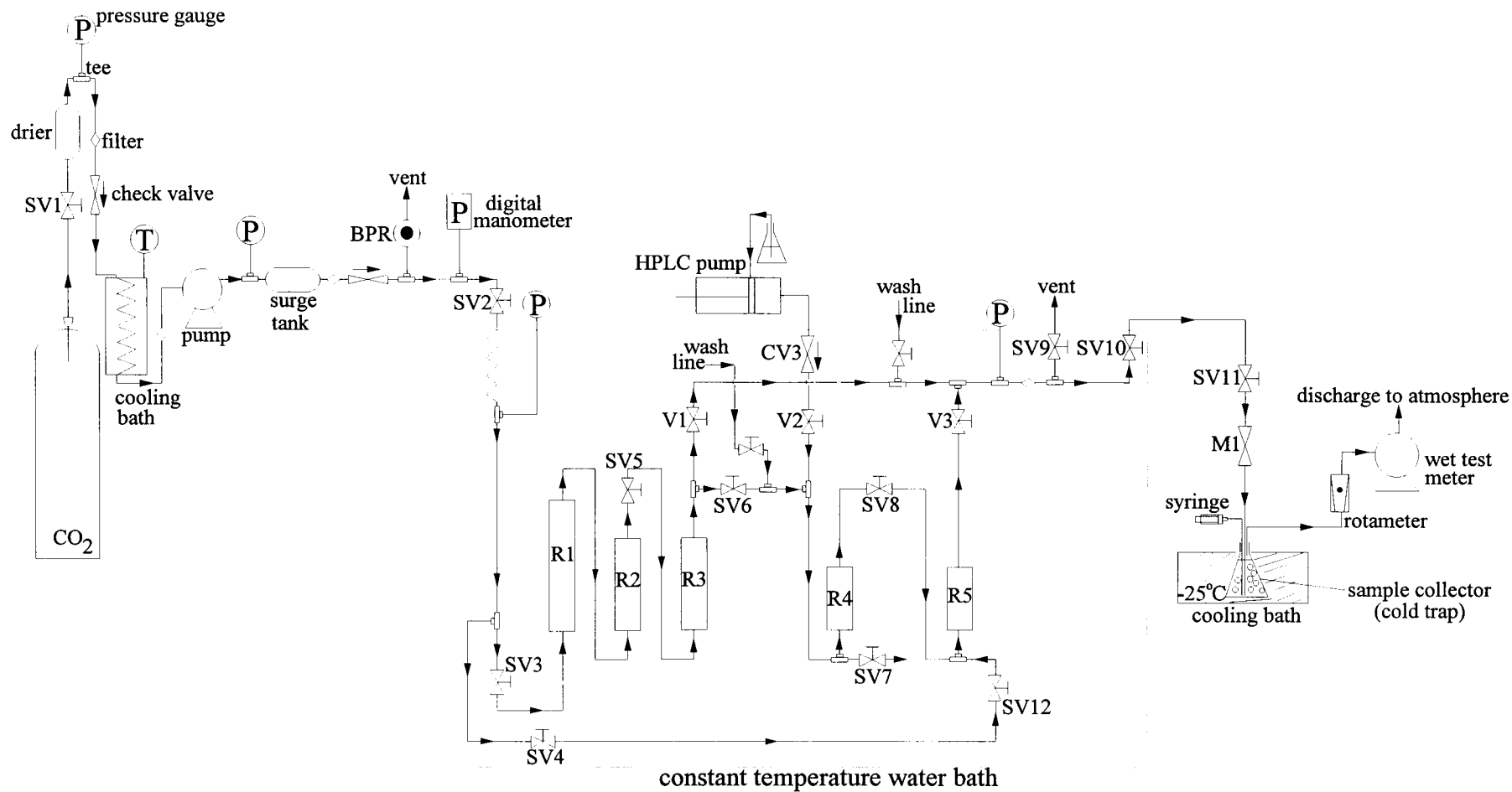


FIGURE 4.2.1. Experimental set-up for fractionating origanum oil (SV: 1/4" on-off valve, V: 1/8" on-off valve M: 1/4" metering valve, R: column).

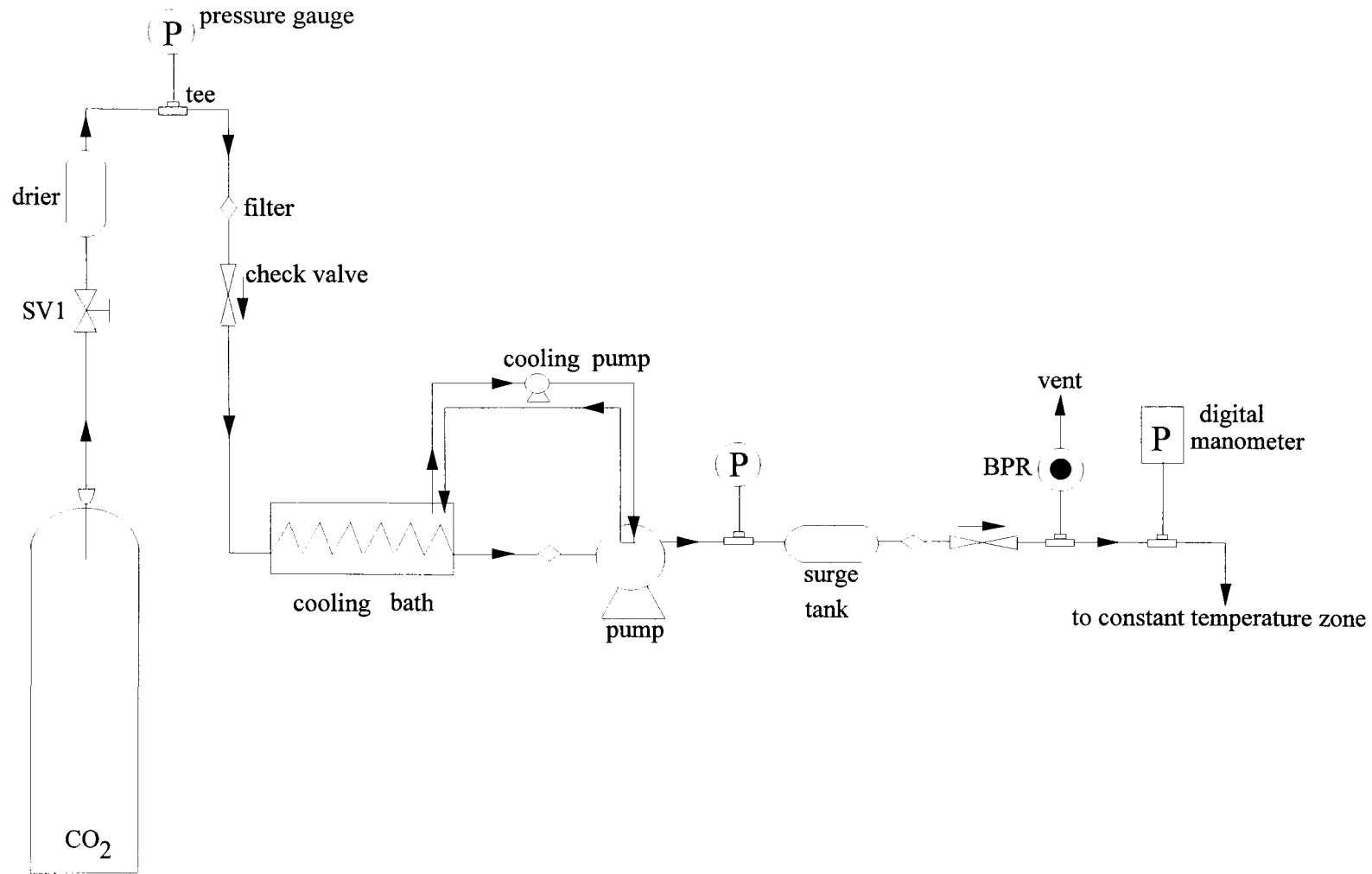


FIGURE 4.2.2. Solvent entry zone.

Liquid CO<sub>2</sub> was then compressed to the operating pressure by a diaphragm pump (Lewa, type EK), whose head was also cooled by the circulated refrigerant. Cooling was necessary because the compressibility of CO<sub>2</sub> increases dramatically at the critical point and therefore reducing the pump efficiency to a degree where no pumping occurs effectively. The diaphragm pump used was rated for a maximum operating pressure of 400 bar. The pressure gauge placed after the pump outlet enabled to monitor the pressure of the compressed CO<sub>2</sub>.

After compression, CO<sub>2</sub> was introduced into a surge tank (6.15 cm inner diameter and 25 cm length) to dampen the fluctuations generated by the operation of the pump. The surge tank was manufactured by Erikman Kardeşler Makine Sanayii, İstanbul. In order to maintain a constant pressure within the system, a hand adjustable back-pressure regulator with a stated accuracy of  $\pm 1$  per cent of the relief pressure range (Tescom Co. Series 26-1700, model 26-1724-24) was employed. During the operation of the system, it was found that best performance could be achieved by keeping this regulator always slightly open, after reaching the desired pressure. This approach permitted better pressure control of the system with fluctuations within  $\pm 1$  bar. The regulator was covered with an electrical heating mantle and heated constantly by a Powerstat (Fisher Scientific) to prevent clogging with solidified CO<sub>2</sub>. The controlled pressure range for this pressure regulator was 1-175 bar. The excess gas that discharged through the back-pressure regulator was relieved directly to the atmosphere. A digital pressure manometer (Delta OHM, HD 8804) was used for accurate pressure measurements of the CO<sub>2</sub> before it was allowed to enter the constant-temperature zone of the experimental set-up through the on-off valve SV2.

The structure holding the assembly of columns, R1 to R5, and the connecting lines (1/4"OD $\times$ 0.210"ID and 1/8"OD $\times$ 0.085"ID) and on-off valves were immersed in the constant temperature water bath, as shown in Figure 4.2.3. The rectangular structure (made up of aluminum) could be lifted up or brought down with a hand operated pulley mechanism which enabled the columns R4 and R5 to be charged with glass beads and adsorbent, respectively, before the experiment and to be cleaned easily after the experiment.

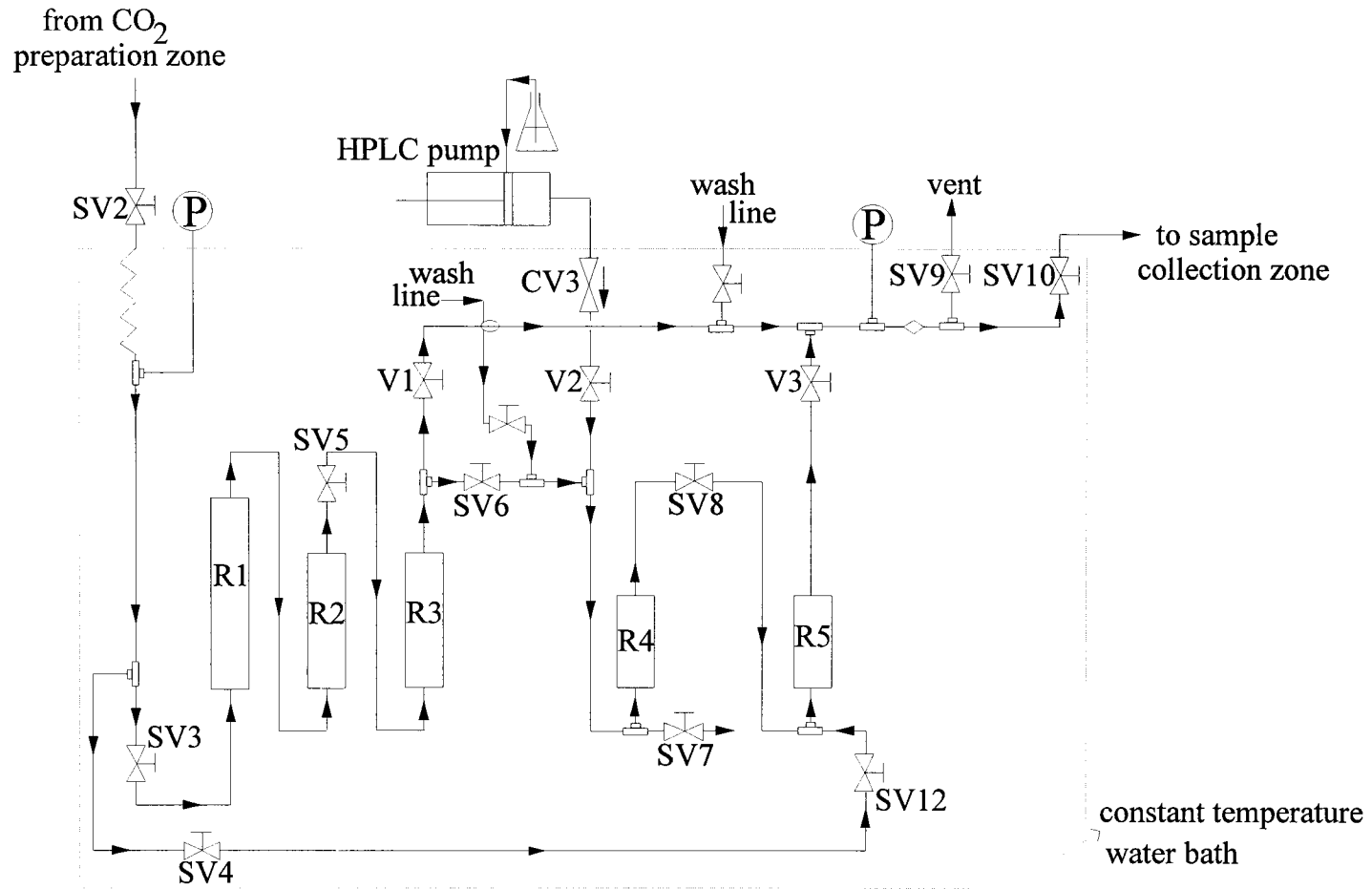


FIGURE 4.2.3. Constant temperature zone.

The assembly of columns immersed in the constant-temperature water bath were ideally appropriate for use at elevated pressures, i.e., they were capable of withstanding pressures up to 250 bar. Each stainless steel vessel (manufactured by Er Makine, İstanbul) consisted of three main parts: cap, cover and body. The cover was inserted in the body. A suitable teflon gasket was used to ensure proper seating of the cover on the body. The threaded cap was screwed onto this assembly first by hand then with the use a wrench, which tightly fit the hexagonal sides of the cap. The cover included one male connector which was used to link the column to the system via the connecting lines. The cap and cover arrangement was present at the two ends of the body.

After the operating pressure was adjusted to the desired value by the aid of the back-pressure regulator, the compressed CO<sub>2</sub> was preheated to the operating temperature by passing it through a 1/8" flattened stainless-steel coil (Alltech Co., free-flow pulse dampener). The temperature inside the water bath was maintained at constant pre-set values by means of a thermostat attached to the exterior of the bath and two heating resistances (2800 Watt) that were electronically connected to the thermostat were placed at the bottom of the water bath. The actual temperature of the bath was continuously measured by a K-type thermocouple (Keithley Ins., model 820) to  $\pm 0.1^{\circ}\text{C}$ .

The on-off valve SV3 directed the dense CO<sub>2</sub> to the assembly of columns and the on-off valve SV4 and SV12 enabled the same solvent to enter directly column R5. Columns R1, R2 and R3 were stainless-steel vessels of 2.7 cm in inner diameter, and 25, 20 and 20 cm in length, respectively, and each of them were packed with glass beads of 3 mm diameter. Cup-like wire netting was placed inside the bottom of each column to prevent the falling of the glass beads into the gas inlet line and also inside the top of each column to prevent the blocking of the connecting lines by the broken glass beads during the initial equilibration period of the experiments.

Columns R1 and R2 can be named as "blank columns" since the only reason they were included in the set-up was to assure that the compressed CO<sub>2</sub> was heated to the desired operating temperature. Column R3 (also named as "blank column") was used in maintaining the desired flow rate of the solvent before mixing the CO<sub>2</sub> and the origanum-oil

streams in the mixing chamber, column R4. After the temperature and pressure of the dense-gas solvent was attained at the desired values, the on-off valve V1 directed the CO<sub>2</sub> to the metering valve M1 via two other on-off valve SV10 and SV11. The pressure gauge before these on-off valves was used to monitor the constant the pressure in the system. The on-off valve SV9 was placed after the pressure gauge for safety reasons.

The liquid feed oil (origanum oil) to be fractionated by dense CO<sub>2</sub> was introduced to the system by an HPLC pump (HP 1050) through the connecting line (1/16"OD×0.010"ID) followed by an on-off valve, V2. The flow rate of the dense-CO<sub>2</sub> solvent was regulated at the diaphragm pump and the flow rate of the origanum oil was adjusted at the HPLC pump. The mixing tee, T8, connected the origanum oil stream (flowing through the on-off valve V2) and the CO<sub>2</sub> stream (flowing through the on-off valve SV6), then this feed mixture entered the mixing chamber column R4. This stainless-steel vessel (2.7 cm in inner diameter and 10 cm in length) was packed with glass beads of 3 mm diameter to eliminate the possibility of liquid-phase entrainment and channeling. Cup-like wire netting was placed inside the two ends of the column to prevent the falling of the glass beads into the gas inlet/outlet line. The on-off valve SV7 extending from the bottom of the mixing chamber was used to collect the residual oil, if any left, at the end of the experiments.

The on-off valve SV8 directed the flow of origanum-oil/CO<sub>2</sub> mixture to the column R5. This stainless-steel vessel of 2.7 cm in inner diameter and 10 cm in length acted as an extractor or adsorber/desorber according to the type of experiment performed (refer to chapter four). In the extraction step, the feed mixture was allowed to enter the extractor filled with glass beads of 3 mm diameter. Again cup-like wire netting was placed inside the two ends of the column to prevent the falling of the glass beads into the gas inlet line, but the cup-like wire netting used at the exit of the vessel was filled with inert  $\alpha$ -cellulose to prevent the contamination of the metering valve with origanum oil. In the adsorption step, the same feed mixture was allowed to enter the adsorber filled with adsorbent, activated carbon or silanized silica gel. Glass beads of 3 mm diameter were also packed above and below the adsorbent in order to achieve a uniform flow distribution in the column. Again cup-like wire netting was used at both ends of the column, but the netting at the exit of the vessel was filled with inert  $\alpha$ -cellulose to prevent the carry over of the activated carbon.

However, in the case of silica gel adsorbent, inert  $\alpha$ -cellulose was used at both ends of the adsorber due to the smaller size of adsorbent particles compared to activated carbon.

The product line from the top of the vessel R5 was connected to the on-off valve V3 which enabled the flow of the effluent from the extractor or adsorber/desorber to the sampling zone (Figure 4.2.4) via the heated on-off valve SV11 and the metering valve M1. M1 (1/4", Swagelok Co.) provided a fine adjustment of the output flow throughout the system. Through this valve, the high pressure in the system was reduced to atmospheric pressure where origanum oil started to separate from the dense-gas solvent. The basic features of M1 that allowed precise flow adjustments were a finely tapered stem, a fine operating thread and an orifice size of 0.79 mm. M1 was also wrapped with electrical heating mantle and heated constantly by a Powerstat (Fisher Scientific) to prevent clogging with the precipitated solute.

The origanum oil that precipitated during the pressure-reduction step was separated from the CO<sub>2</sub> gas in the sample collector containing 300 ml ethanol (Riedel de Haen, 99.9% pure) and immersed in a sub-zero water/monoethylene glycol bath (Heto CB60) at  $-25^{\circ}\text{C}$ . A plastic syringe was used in taking samples from the cold trap (sample collector) and a condenser (in which water/monoethylene glycol mixture was circulated at  $-25^{\circ}\text{C}$ ) was placed at the exit of the sample collector to further cool down the CO<sub>2</sub> gas before it was directed to the rotameter (Aalborg Instruments and Controls Inc., NY) in which the constant gas flow rate through the system was monitored. The volume of the expanded CO<sub>2</sub> during the process was measured by a wet-test meter (Precision Scientific Co.) to  $\pm 10\text{ cm}^3$ .

### **4.3. Experimental Procedure**

In chapter three, it was described and presented by simple diagrams (Figures 3.2.1 to 3.2.3) that in the experimental apparatus constructed, it was possible to perform different kinds of experiments. The details of the experimental procedure employed during the series

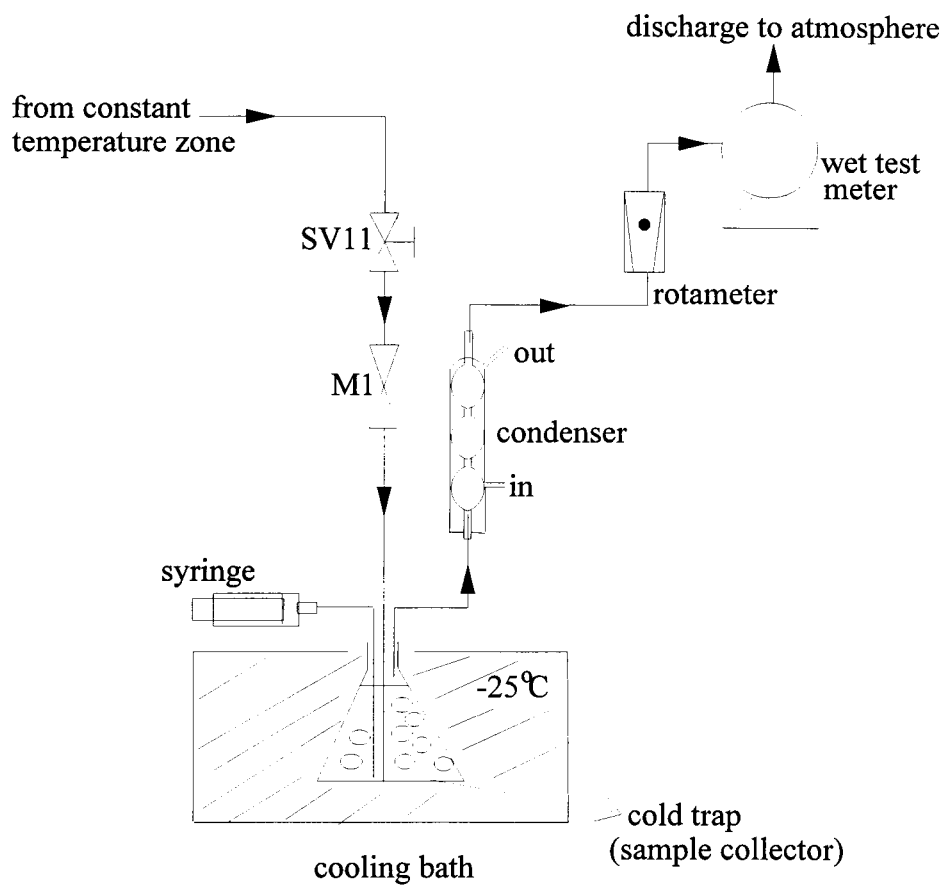


FIGURE 4.2.4. Sampling zone.

of experiments carried out in the aim of isolating the MT hydrocarbons of this origanum oil to obtain a high quality essential-oil product will be explained in this section.

#### **4.3.1. Preparing the System before Starting an Experiment**

Prior to beginning a run, the constant-temperature water bath, the refrigerated bath which is used to cool the CO<sub>2</sub> before entering the diaphragm pump, and the cooling bath that contained the sample collector were all brought to their respective run temperatures. The operating temperature of the refrigerated bath and of the cooling bath was held at  $-6^{\circ}\text{C}$  and  $-25^{\circ}\text{C}$ , respectively, for all runs. The electrical heating mantle covering the back-pressure regulator and that covering valves SV11 and M1 were activated to prevent them from freezing as a result of the Joule-Thompson effect, i.e., cooling upon sudden gas expansion. The pump head was cooled with water/monoethylene glycol mixture supplied from the cooling bath at  $-6^{\circ}\text{C}$ .

Initially, all on-off valves were kept closed. After obtaining the desired temperatures throughout the system, the valve of the CO<sub>2</sub> tube was opened and it was allowed to fill the drier and surge tank through the on-off valve SV1, provided the on-off valve SV2 was kept closed. The pressure of the CO<sub>2</sub> from the gas cylinder (equipped with a dip tube) was continuously monitored by the pressure gauge installed after the drier. It was necessary to observe the pressure in the tube since no pumping occurred at CO<sub>2</sub> pressures lower than 5 MPa, then the CO<sub>2</sub> tube was replaced with a new one before starting an experiment.

For the sake of simplicity, the experimental procedure will be described in the following sequential order:

1. Open the on-off valves SV2, SV3, SV5, V1, SV10 allowing CO<sub>2</sub> to flow through the heating coil and through vessels R1 to R3 to insure that it reached the desired operating temperature before contacting the oil.

2. Check that the metering valve M1 is almost closed, but not fully, since excessive closing force will damage the valve seat.
3. Open the on-off valve SV11, and very slowly open M1 (by turning its vernier knob counter-clockwise) until the flow of CO<sub>2</sub> is detected in the rotameter. Adjust the CO<sub>2</sub> flow rate to a low setting by regulating M1, provided the knob of the rotameter is in the fully open position.
4. Turn on the diaphragm pump. Initially operate it at maximum stroke, as the pressure of the CO<sub>2</sub> starts to increase (monitored by the pressure gauge after the pump), decrease the stroke by turning it clockwise.
5. The high-pressure pump delivered CO<sub>2</sub> continuously and the desired CO<sub>2</sub> flow rate was achieved by manipulating the flow rate adjuster of the pump and M1. The back-pressure regulator installed after the surge tank was manually set to control the system pressure, thus to maintain a constant pressure within the system.
6. Before starting an experiment, observe the CO<sub>2</sub> flow rate, pressure and temperature for some time (10 to 15 minutes) and make sure that a constant CO<sub>2</sub> flow rate is attained within the system (fluctuations in the CO<sub>2</sub> flow rate are easily detected at the rotameter).

#### **4.3.2. Experimental Procedure for Dense-CO<sub>2</sub> Extraction**

Once the operation variables i.e., CO<sub>2</sub> flow rate, pressure and temperature, were attained at their desired values, it was possible to perform any necessary type of experiment in order to accomplish the intentions summarized in chapter three. The dense-gas extraction of organum oil was conducted in two forms, as illustrated schematically in Figures 3.2.1 and 3.2.2. The only difference in these processes was the temperature and pressure, but the CO<sub>2</sub> flow rate was kept constant at about 1.5 g/min. Therefore, the experimental procedure

adopted was exactly the same in both cases. The steps followed during the dense-gas extraction of origanum oil are listed below:

1. Provided that the on-off valves V2, SV4, SV12, SV7, SV8, V3 are turned-off (as in the preparation procedure, close the on-off valve V1 and immediately open the on-off valve SV6 allowing CO<sub>2</sub> to fill the mixing chamber (R4).
2. Direct the CO<sub>2</sub> flow to the extractor (R5, which is packed with glass beads), through the on-off valve SV8. Once the operating pressure is achieved (continuously monitor the pressure within the system by the digital manometer), open the on-off valve V3.
3. Wait for some time until the system reaches equilibrium, in other words, desired pressure and CO<sub>2</sub> flow rate values are re-attained. If necessary, by manipulating M1 (preceding the sample collector) adjust the required CO<sub>2</sub> flow rate.
4. Adjust the flow rate of origanum oil at the HPLC pump, provided that the on-off valve V2 is closed. Start to pump the oil at 0.2 ml/min until the pressure at the HPLC pump displays a higher value than the operating pressure, then open the on-off valve V2. For example, if the operating pressure is 8.0 MPa, set the HPLC flow rate to 0.2 ml/min and let the pump supply origanum oil until the pressure in the connecting line before the on-off valve V2 is at least 9.0 MPa. Then, open the on-off valve V2 to start the continuous contact of CO<sub>2</sub> and origanum oil; thus this approach permits thorough mixing of the two streams. Furthermore, to avoid any entrainment of liquid droplets, the origanum-oil/CO<sub>2</sub> stream is delivered from the bottom of the mixing chamber (and extractor).
5. Let the HPLC pump continuously supply origanum oil to the system, specifically, at 0.2 ml/min for 15 minutes, then at 0.01 ml/min for the rest of the experimental period. This technique was applied in the experiments shown schematically in Figure 3.2.1. However, during the experiments shown schematically in Figure 3.2.2, origanum oil was pumped at a rate of 0.01 ml/min throughout the experimental period. Step four is similarly followed, but in this case, the oil is pumped at 0.01 ml/min until the pressure

at the HPLC pump displays a higher value than the operating pressure, then the on-off valve V2 is opened.

6. Enable the origanum oil/CO<sub>2</sub> mixture to enter the extractor, then permit the oil-laden gas from the extraction vessel to expand across the metering valve (the on-off valves SV8 and V3 were already opened in step two).
7. Trap the origanum oil components extracted by (solubilized in) dense-CO<sub>2</sub> in the sample collector and by a plastic syringe, take samples from the cold trap at 30 minute time intervals. Mix 10 drops of this product with 50µl ethanol (Riedel de Haen, 99.9% pure) in a separate bottle and inject the remaining sample in the syringe back into the cold trap in order to secure a constant volume within the sample collector. The small bottle holding the product sample is tightly closed and covered with a parafilm strip and stored in the refrigerator until required for chromatographic analyses. Remember to decrease the CO<sub>2</sub> flow rate to a lower value than the desired one by manipulating M1 in order to be able to take a sample, otherwise some amount of product bleeds off from the syringe-outlet connection of the sample collector. Once the sample taken, mixed with ethanol and the remaining part is injected back into the cold trap, then by re-manipulating M1, instantaneously adjust the CO<sub>2</sub> flow rate to its original value, which is continuously detected by the rotameter.
8. Analyze the composition of the fractions collected during the experiment by a gas chromatograph equipped with a mass selective detector (GC/MS, HP 5890/5971). Identify the 12 key components constituting bulk of the original oil (90.96 per cent of total GC area count) charged to the system via the HPLC pump and the oil extracts accumulated in the sample collector.
9. At the end of the run, determine the volume of the CO<sub>2</sub> leaving the system from the wet test meter reading.

The following shut-down procedure was next applied:

10. Close the on-off valves SV6, SV8 and V3 in order to isolate the mixing chamber (R4) and the extraction vessel (R5) from the system.
11. Close the on-off valve V2 and turn off the HPLC pump so that no more origanum oil is charged to the system.
12. Turn off the diaphragm pump and close the valve of the CO<sub>2</sub> tube.
13. Open the on-off valve V1 to depressurize the system. Then, slowly open the on-off valve V3 to empty R5, provided the on-off valve SV8 is closed. Lift up the rectangular structure immersed in the constant-temperature water bath after the pressure within the system shows zero, i.e., CO<sub>2</sub> is completely discharged from the system.
14. Provided the on-off valve SV6 (and SV8) is closed, open the on-off valve SV7 placed at the bottom of the mixing cell to recover the origanum-oil/CO<sub>2</sub> mixture remaining in the vessel R4. Store the fraction collected in the refrigerator until required for chromatographic analyses to determine its composition. This step was practiced in the extraction experiments shown schematically in Figures 3.2.1 and 3.2.2.
15. Bring the temperature of both of the cooling baths to 0°C and deactivate the heating mantles covering the back-pressure regulator and the metering valve.

#### **4.3.3. Experimental Procedure for Supercritical-CO<sub>2</sub> Adsorption Following Dense-Gas Extraction**

In the aim of enhancing the separation between the MT and non-monoterpene (NMT) hydrocarbons of origanum oil, a continuous adsorption process following dense-gas extraction was developed. This process was conducted in two forms, as illustrated schematically in Figures 3.2.1 and 3.2.2. Initially, the adsorption vessel R5, was packed with the required amount of activated carbon or silanized silica gel adsorbent. Before

starting an experiment, the preparation procedure explained in section 4.3.1 was exactly followed.

Once the operation variables i.e., CO<sub>2</sub> flow rate, pressure and temperature, were attained at their desired values, it was possible to perform either of the experiments referred above. The steps followed during the supercritical-CO<sub>2</sub> adsorption process following dense-gas extraction are listed below:

1. Provided that the on-off valves V2, SV4, SV12, SV7, SV8, V3 are turned-off (as in the preparation procedure), close the on-off valve V1 and immediately open the on-off valve SV6 allowing CO<sub>2</sub> to fill the mixing chamber.
2. Adjust the flow rate of organum oil at the HPLC pump, provided that the on-off valve V2 is closed. Start to pump the oil at 0.2 ml/min until the pressure at the HPLC pump displays a higher value than the operating pressure. For example, if the operating pressure is 10.0 MPa, set the HPLC flow rate to 0.2 ml/min and let the pump supply organum oil until the pressure in the connecting line before the on-off valve V2 is at least 11.0 MPa. Turn off the HPLC pump before an error is detected at the pump outlet due to the high-pressure load in the connecting line since the outlet of the pump (on-off valve V2) is closed.
3. Direct the CO<sub>2</sub> flow to the adsorption vessel, R5 (packed with activated carbon or silanized silica gel), through the on-off valve SV8. Once the operating pressure is achieved (continuously monitor the pressure within the system by the digital manometer), open the on-off valve V3.
4. Wait for some time until the system reaches equilibrium, i.e., when desired pressure and CO<sub>2</sub> flow rate are re-attained. If necessary, by manipulating M1 adjust the required CO<sub>2</sub> flow rate.
5. Turn on the HPLC pump and once the pressure in the connecting line before the on-off valve V2 reaches its original value (e.g. 11.0 MPa), open the on-off valve V2 to start

the continuous contact of CO<sub>2</sub> and origanum oil. This approach permits minimum adsorption of pure CO<sub>2</sub> onto the adsorbent because it takes a long time for the connecting line before the on-off valve V2 to be completely filled with origanum oil due to the low flow rate of the oil stream, 0.2 ml/min. In order to avoid any entrainment of liquid droplets, the origanum-oil/CO<sub>2</sub> stream is delivered from the bottom of the mixing cell (and adsorber).

6. Let the HPLC pump continuously supply origanum oil to the system, specifically, at 0.2 ml/min for 15 minutes, then at 0.01 ml/min for the rest of the experimental period. This technique was applied in the experiment shown schematically in Figure 3.2.1. However, during the experiment illustrated in Figure 3.2.2, origanum oil was pumped at a rate of 0.01 ml/min throughout the run. The operating principle in step two is similarly followed, but in this case, the oil is pumped at 0.01 ml/min until the pressure at the HPLC pump displays a higher value than the operating pressure.
7. Enable the origanum-oil/CO<sub>2</sub> mixture to enter the adsorption vessel, then permit the oil-laden gas from the adsorber to expand across the metering valve (the on-off valves SV8 and V3 were already opened in step three).
8. Trap the origanum oil components solubilized in dense-CO<sub>2</sub> in the sample collector and by a plastic syringe, take samples from the cold trap at 30 minute time intervals. Mix 10 drops of this product with 50µl ethanol (Riedel de Haen, 99.9% pure) in a separate bottle and inject the remaining sample in the syringe back into the cold trap in order to secure a constant volume within the sample collector. The small bottle holding the product sample is tightly closed and covered with a parafilm strip and stored in the refrigerator until required for chromatographic analyses. Remember to decrease the CO<sub>2</sub> flow rate to a lower value than the desired one by manipulating M1 in order to be able to take a sample, otherwise some amount of product bleeds off from the syringe outlet connection of the sample collector. Once the sample taken, mixed with ethanol and the remaining part is injected back into the cold trap, then by re-manipulating M1, instantaneously adjust the CO<sub>2</sub> flow rate to its original value, which is continuously detected by the rotameter.

9. Analyze the composition of the fractions collected during the experiment by a gas chromatograph equipped with a mass selective detector (GC/MS, HP 5890/5971). Identify the 12 key components constituting bulk of the original oil (90.96 per cent of total GC area count) charged to the system via the HPLC pump and the oil extracts accumulated in the sample collector.
10. At the end of the run, determine the volume of the CO<sub>2</sub> leaving the system from the wet test meter reading.

The following shut-down procedure was next applied:

11. Close the on-off valves SV6, SV8 and V3 in order to isolate the mixing chamber (R4) and the adsorption column (R5) from the system.
12. Close the on-off valve V2 and turn off the HPLC pump so that no more origanum oil is charged to the system.
13. Turn off the diaphragm pump and close the valve of the CO<sub>2</sub> tube.
14. Open the on-off valve V1 to depressurize the system through venting CO<sub>2</sub> to the atmosphere via M1, until the pressure within the system shows zero.
15. Let the rectangular structure holding the assembly of columns remain in the constant-temperature water bath. Maintain the temperature inside the water bath at constant desired value (at the operating temperature) by means of the thermostat.
16. Bring the temperature of both of the cooling baths to 0°C and deactivate the heating mantles covering the back-pressure regulator and the metering valve.

#### **4.3.4. Experimental Procedure for Supercritical-CO<sub>2</sub> Desorption Following the Origanum-oil/CO<sub>2</sub> Adsorption Coupled with Dense-Gas Extraction**

Pure supercritical CO<sub>2</sub> is utilized to desorb the origanum-oil components adsorbed on the sorbent (activated carbon or silanized silica gel) during the supercritical-CO<sub>2</sub> adsorption process following dense-gas extraction, as schematically shown in Figure 3.2.3. In the experimental set-up constructed, it was possible to perform the desorption operation in two ways: either at constant pressure or by step-wise increasing the pressure (first at a low-pressure then, at a high-pressure). The reasoning behind each of these methods will be explained in detail in chapter five. Before starting a desorption experiment, the preparation procedure explained in section 4.3.1 was exactly followed.

Once the operation variables i.e., CO<sub>2</sub> flow rate, pressure and temperature, were attained at their desired values, it was possible to perform either of the experiments referred above. Prior to starting the desorption process, the experimental set-up was freed from any oil components remaining on the inside walls of the tubing and valves, etc. The details of the cleaning procedure will be explained in section 4.3.5. It is important to mention that during the desorption experiment, origanum oil is not charged to the system, hence the HPLC pump is not operated and the on-off valve V2 is closed throughout the experiment. The steps followed during the desorption process (after the completion of the cleaning procedure) is given below:

1. Provided that the on-off valves SV6, SV7, SV8, V3 are closed, open the on-off valve SV4 allowing pure CO<sub>2</sub> to flow all the way up to the on-off valve SV12 placed just before the entrance of the desorption vessel.
2. Open the on-off valve SV12 and let the CO<sub>2</sub> fill the desorber, which was left at the operating pressure of the adsorption process (refer to step 11 in section 5.3.3). After desired pressure is reached in the desorber (continuously monitor the pressure within the system by the digital manometer), immediately open the on-off valve V3 and close the on-off valve V1. This approach permitted constant CO<sub>2</sub> flow rate within the system,

since until the pressure in the desorber attained its desired value, a continuous dense gas flow was maintained via the on-off valve V1, then the on-off valve V3 was opened and the on-off valve V1 was closed.

3. Enable the oil-laden gas from the desorption vessel to expand across the metering valve.
4. Trap the origanum oil components solubilized in dense-CO<sub>2</sub> in the sample collector and by a plastic syringe, take samples from the cold trap at 30 minute time intervals. Mix 10 drops of this product with 50µl ethanol (Riedel de Haen, 99.9% pure) in a separate bottle and inject the remaining sample in the syringe back into the cold trap in order to secure a constant volume within the sample collector. The small bottle holding the product sample is tightly closed and covered with a parafilm strip and stored in the refrigerator until required for chromatographic analyses. Remember to decrease the CO<sub>2</sub> flow rate to a lower value than the desired one by manipulating M1 in order to be able to take a sample, otherwise some amount of product bleeds off from the syringe outlet connection of the sample collector. Once the sample taken, mixed with ethanol and the remaining part is injected back into the cold trap, then by re-manipulating M1, instantaneously adjust the CO<sub>2</sub> flow rate to its original value, which is continuously detected by the rotameter.
5. Analyze the composition of the fractions collected during the experiment by a gas chromatograph equipped with a mass selective detector (GC/MS, HP 5890/5971). Identify the 12 key components in the oil extracts accumulated in the sample collector.
6. Continue with step 11 for the desorption process performed at constant pressure, otherwise continue with step seven.
7. If the desorption operation is the one with step-wise pressure increase method, after 240 minutes of supercritical-CO<sub>2</sub> desorption at constant pressure, increase the system pressure to the required value by manipulating the flow rate adjuster of the diaphragm pump (operate it a maximum stroke).

8. Manually set the back-pressure regulator to control the system pressure at its new value.
9. Maintain a constant pressure and flow rate within the system by manipulating M1. The series of arrangements should be done rapidly in order not to disturb the equilibrium in the desorption vessel. It is important to notice that the on-off valves SV4, SV12 and V3 are never closed during the pressure increase procedure.
10. Continue with steps three to five until the step-wise pressure increase desorption experiment is terminated.
11. At the end of the run, determine the volume of the CO<sub>2</sub> leaving the system from the wet test meter reading.

The following shut-down procedure was next applied:

12. Close the on-off valves SV12, V3 and SV4 in order to isolate the desorption vessel from the system.
13. Turn off the diaphragm pump and close the valve of the CO<sub>2</sub> tube.
14. Open the on-off valve V1 to depressurize the system through venting CO<sub>2</sub> to the atmosphere via M1, until the pressure within the system shows zero.
15. Slowly open the on-off valve V3 to discharge the CO<sub>2</sub> within the desorber.
16. Lift up the rectangular structure immersed in the constant-temperature water bath after the pressure within the system shows zero.
17. Provided the on-off valves SV6 and SV8 are closed, open the on-off valve SV7 to discharge the mixing chamber totally. The mixing cell could also been emptied through the desorber by opening the on-off valve SV8. This method is not appropriate because

the remaining origanum-oil/CO<sub>2</sub> mixture in the bottom of the mixing cell would instantaneously precipitate on the adsorbent, resulting in incorrect experimental data.

18. Disconnect the desorption vessel from the apparatus and pour its contents into a petri dish. Remove the glass beads from the activated carbon particles by the help of a tweezers and immediately weigh the adsorbent left on the container.
19. Add 30 ml of ethanol (Riedel de Haen, 99.9% pure) on the activated carbon sample and cover the petri-dish with folio-film. The volume of ethanol used is slightly larger than the amount required to wet the adsorbent surface fully. Store this sample in the refrigerator (for 24 hours) for GC/MS analysis to determine its composition.
20. Bring the temperature of both of the cooling baths to 0°C and deactivate the heating mantles covering the back-pressure regulator and the metering valve.

#### **4.3.5. Cleaning of the Equipment between Experiments**

It is a fact that some of the origanum oil components, most probable the heavier compounds, especially *carvacrol*, would inpart remain on the inside walls of the tubing and the valves, etc. of the experimental set-up. Thus, it is very important that preceding an experiment, the insides of the equipment is freed from these remnants in order to obtain precise and accurate experimental results. The experimental procedure employed during the cleaning process after the dense-gas extraction and after the supercritical-CO<sub>2</sub> desorption is exactly the same, whereas the one applied after the adsorption process following dense-gas extraction is slightly different.

Once the dense-gas extraction or the supercritical-CO<sub>2</sub> desorption experiment was ended, columns R4 and R5 were disconnected from the system and plastic tubing was attached in place of these vessels. Each stainless steel vessel was disassembled and each part (except the teflon gasket) of it was soaked in commercial grade hexane in order to remove

the remaining oil components on the inside walls of the columns. Then, all the connecting lines and valves (on-off and metering) were cleaned with hexane using a circulation pump (ProMinent Electronic). Hexane was collected in a container located at the exit of the metering valve, which was adjusted to its fully open position. Later, the plastic tubing was substituted with stainless steel tubing, and all the connecting lines and valves were cleaned with CO<sub>2</sub> at elevated pressures. Pure ethanol was charged to the sample collector and high-pressure CO<sub>2</sub> (at 14.5 MPa) was allowed to flow through the system. Extracts (though oil was not charged) accumulating in the sample collector were analyzed by GC/MS at different time cuts (in two hour time intervals). Once the analysis of the samples revealed that the extracts were free of oil constituents, the cleaning procedure was ceased. Unfortunately, about five days of cleaning period was needed to prepare the system prior to another experiment.

At the end of the adsorption process following dense-gas extraction, it was necessary to clean the connecting tubing extending from the on-off valve V1 to the sampling zone of the set-up. Initially, commercial grade hexane was circulated through the piping system and the metering valve. Then, pure ethanol was charged to the sample collector and high-pressure CO<sub>2</sub> (at 14.5 MPa) was allowed to flow through the system via the on-off valve V1, provided the on-off valves SV6, V2, SV7, SV8 and V3 were closed. Extracts (though oil was not charged) accumulating in the sample collector were analyzed by GC/MS at different time cuts (in two hour time intervals). Once the analysis of the sample revealed that the extracts were free of oil constituents, the cleaning procedure was ceased. This cleaning period took two days before the supercritical desorption experiment could be executed. Consequently, the experimental procedure described in section 4.3.4 was followed.

#### 4.4. Experimental Program for Fractionating Origanum Oil

The successful operation of the experimental apparatus designed and constructed in the aim of improving the quality of origanum oil (or similar essential oils) was initially tested by toluene/CO<sub>2</sub> binary mixture. The experimental program followed during these trials is given in Tables A.2.1 and A.2.2, in Appendix A. Based on the information/experience gained with the toluene/CO<sub>2</sub> system, the experimental set-up was accordingly modified, after which it was considered ready for the investigation of the optimum conditions for the fractionation of origanum oil via supercritical CO<sub>2</sub>. The experimental program implemented in order to achieve the purpose of this work is listed in chronological order in Table 4.4.1. The main variables at these different forms of operations (extraction, adsorption and desorption, which were explained in detail chapter three) are temperature, pressure, CO<sub>2</sub> flow rate, and adsorbent amount and kind. As can be seen from Table 4.4.1, the temperature was kept constant at 40°C, independent of operation type. This is because at temperatures around 40°C, even thermally unstable substances can be won undecomposed with dense CO<sub>2</sub> (Stahl et al., 1988). However, at temperatures less than 40°C, in other words, closer to the critical temperature of CO<sub>2</sub> (31°C), the gas-phase density approaches the density of liquid CO<sub>2</sub>, and it is known that all essential oil components and flavor substances are freely soluble in liquid CO<sub>2</sub> (Stahl et al., 1988). Therefore, a temperature of 40°C was assumed as the optimum value for the experiments to be conducted. In addition, independent of operation type, the CO<sub>2</sub> flow rate was kept at about 1.5 g/min, since this was the highest observable flow at the rotameter, in which constant gas flow rate through the system was monitored.

It is important to notice in Table 4.4.1 that the amount of origanum oil fed to the system varied between runs, this is because of the experimental time. In other words, although the flow rate of origanum oil, which was adjusted at the HPLC pump, was kept constant (ml/min), the experimental duration affected the amount (ml) of oil introduced to the system.

TABLE 4.4.1. Experimental program for fractionating origanum oil.

Run no.	Oil Used (ml)	Extraction T, P and Time (°C, MPa, min)	Adsorption T, P and Time (°C, MPa, min)	Desorption T, P and Time (°C, MPa, min)	CO <sub>2</sub> Flow-rate (g/min)	Adsorbent (type, g)
1	11.4	40, 7.5, 840	–	–	1.54	–
2	8.4	–	40, 7.5, 540	–	1.53	non-dried carbon, 2
3	11.4	–	40, 7.5, 840	–	1.52	non-dried carbon, 8
4	–	–	–	40, 14.5, 690	1.54	–
5	9.3	–	40, 7.5, 630	–	1.52	dried silica, 8
6	–	–	–	40, 14.5, 570	1.53	–
7	11.4	–	40, 7.5, 840	–	1.52	non-dried carbon, 8
8	–	–	–	40, 8.0/14.5, 690	1.54	–
9	9.3	–	40, 7.5, 630	–	1.53	dried silica, 15
10	–	–	–	40, 14.5, 630	1.52	–
11	11.4	–	40, 7.5, 840	–	1.53	non-dried carbon, 8
12	–	–	–	40, 8.0/14.5, 690	1.54	–
13	–	–	–	40, 7.5, 840	1.53	non-dried carbon, 8
14	–	–	–	40, 7.5, 840	1.53	non-dried carbon, 8
15	–	–	–	40, 14.5, 840	1.52	non-dried carbon, 8
16	–	–	–	40, 7.5, 840	1.53	dried carbon, 8
17	–	–	–	40, 7.5, 840	1.52	dried carbon, 8
18	–	–	–	40, 14.5, 840	1.52	dried carbon, 8
19	5.4	40, 10.0, 540	–	–	1.53	–
20	8.4	–	40, 10.0, 840	–	1.54	non-dried carbon, 8
21	–	–	–	40, 14.5, 540	1.54	non-dried carbon, 8

The influence of adsorbent quantity (g) and type on the separation between the monoterpene (MT) and non-monoterpene (NMT) hydrocarbons was also examined, as seen in Table 4.4.1. Experiments were performed at the same operating conditions (T, P and CO<sub>2</sub> flow rate) using activated carbon and silanized silica gel adsorbents. Moreover, the effect of activated carbon treatment (prior to an adsorption run) i.e., dried or non-dried form, was studied.

The effect of pressure on the fractionation of origanum oil was investigated. Simple supercritical-CO<sub>2</sub> extraction runs were carried out at 7.5 and 10.0 MPa (the reason behind this selection of pressure was explained in chapter three). At these operating conditions, supercritical-CO<sub>2</sub> adsorption following dense-gas extraction runs were performed to determine the effect of an adsorbent on the selectivity of the process. Likewise, during the desorption process performed with pure CO<sub>2</sub>, the influence of pressure on the origanum oil quality was studied.

#### 4.5. Analysis of Origanum Oil Fractions by Gas Chromatography

In this work, the origanum oil charged to the continuous flow system and the fractions accumulated in the sample collector were characterized by gas chromatography/mass spectrometry technique (GC/MS). The identification of the origanum-plant essential-oil major components (called “key components”) was obtained on a quadrupole mass spectrometer (HP 5971) directly coupled to a gas chromatograph (HP 5890), using an Innowax Column: 0.25-mm i.d.×60m×0.25 $\mu$ m film thickness, crosslinked polyethylene glycol capillary column.

Origanum oil fractions were dissolved in pure ethanol (Riedel de Haen, 99.9%) prior to injection to the gas chromatograph. The mixture was immediately vaporized at the injection port at 250°C. The essential-oil components moved in the column (together with the carrier gas, He) with different velocities due to different adsorption/desorption affinities for the coating material in the column. Electronic pressure controller (EPC) was equipped with the gas chromatograph to maintain a constant flow of the carrier gas at 1 ml/min. It is known that as the column temperature increases, the flow rate of the carrier gas will decrease; thus by the aid of the EPC, the inlet pressure rises automatically to keep the flow rate within the column constant. An oven temperature programming, given in Appendix B, was used to separate the numerous complex origanum-oil components. A temperature program (step-wise increase with time), which benefited on the temperature dependence of competitive adsorption/desorption equilibria, allowed a good resolution, i.e., maximum difference between the retention times of the individual component peaks. Hence, the chromatographic part prepared pure components for the mass selective detector (MSD), which then identified them. The MSD placed at the end of a capillary column identified the components using a reference library data (Wiley) by matching the mass spectrum (mass-to-charge pattern) for each particular component of the mixture.

After all experimental samples (and original origanum oil) were analyzed, the area counts obtained were normalized to 100 per cent and used for the calculation of the relative-distribution coefficients (see section 5.1). The direct application of the GC/MS

results without a calibration (injection of a mixture of known concentration) may not be very convincing for a quantitative analysis, however, this problem becomes insignificant when the results are discussed in terms of ratios. R values are ratios of concentrations, and even if the area per cents are corrected to concentrations (normalized area counts), the correction factors will be canceled in the ratio. Therefore, for all calculations, the area count results were used after normalization to 100 per cent. The results of GC/MS analyses of the original origanum oil and of the fractions collected at different time intervals (during the different operations performed) are given in Appendices E, F, G, H, I, and J.

#### **4.6. Characterization of Activated Carbon and Silica Gel Adsorbents**

The adsorbents used in this work were activated carbon (commercial grade) and silanized silica gel 60 (Merck 7719). Fresh samples were used for each adsorption experiment. Silica gel was dried prior to use for 12 hours in a vacuum oven at 100°C. Similarly, in a few experiments conducted with activated carbon (Table 4.4.1), this sorbent (after being screened) was washed in deionized water to remove fines and then was dried under vacuum at 100°C for 24 hours. However, in the rest of experiments performed to investigate the optimum conditions for fractionating origanum oil, the activated carbon sorbent was only screened to 18-20 mesh-fraction prior to use. The justification for this may be as follows: The main objective of this work was to establish a supercritical-fluid-aided process in order to enhance the product quality of origanum oil (or similar essential oils). Therefore, in large scale plants, the quantity of activated carbon utilized will accordingly be very high (compared to laboratory scale operations), thus it will not be possible to wash and dry the sorbent, but instead it will be used directly (without any treatment) as supplied by the manufacturer.

Some characteristics of the sorbents are listed in Table 4.6.1. Activated carbon adsorbent was characterized by measuring its total surface area and total pore volume. The properties of silica gel were obtained from the manufacturer (Merck).

TABLE 4.6.1. Properties of activated carbon and silanized silica gel adsorbents.

Silanized silica gel		Activated carbon	
Property	Value	Property	Value
surface area <sup>a</sup> (N <sub>2</sub> BET) (m <sup>2</sup> /g)	480-540	total surface area (N <sub>2</sub> BET) (m <sup>2</sup> /g)	773 ± 20
particle size <sup>a</sup> (μm)	63-200	particle size (mesh size)	18-20
mean particle diameter <sup>a</sup> (μm)	105-130	total pore volume (m <sup>3</sup> /g)	0.50
porous volume <sup>a</sup> (ml/g)	0.74-0.84		
mean pore diameter <sup>a</sup> (nm)	6		

<sup>a</sup> Data from manufacturer.

#### 4.6.1. Total Surface Area Measurement

Primarily, total surface area measurement of an activated carbon with specified properties (Merck 9631) was done. Once the experimental findings were in good agreement with data from manufacturer, the characterization of the employed activated carbon was studied using the multi-point BET method. The sample is first dried and degassed under helium flow for two and a half hours at 250°C and then cooled to room temperature. The Flowsorb 2300 unit is calibrated by injecting one milliliter of nitrogen at ambient conditions, calculating the corresponding volume of gas at standard conditions and setting the instrument to indicate thereafter adsorbed and desorbed gas volumes at standard conditions. Then, a flow of the measuring gas (five per cent to 25 per cent nitrogen/helium mixture) was allowed to pass over the sample at liquid nitrogen temperature of (77.4 K) and equilibrate. After the adsorption equilibrium was established, as indicated by the threshold lamp, the temperature of the sample was raised to ambient temperature and the amount of nitrogen desorbed was measured by the thermal conductivity detector. This nitrogen adsorption/desorption procedure was repeated four times with different composition of nitrogen-helium gas mixtures. The total surface area was calculated by using software supplied by Micromeritics Inc. along with the Flowsorb 2300 unit.

#### **4.6.2. Total Pore Volume Measurement**

The total pore volume measurement with the Flowsorb 2300 unit requires the determination of the volume of gas which, when condensed as a liquid, is taken up by the sample from the 95 per cent nitrogen/five per cent helium gas mixture at liquid nitrogen temperature. The sample is first dried and degassed at 250°C for two and a half hours and then cooled to room temperature. The Flowsorb 2300 unit is calibrated by injecting ten milliliters of nitrogen at ambient conditions, calculating the corresponding volume of gas at standard conditions and setting the instrument to indicate thereafter adsorbed and desorbed gas volumes at standard conditions. The sample is first saturated using 100 per cent nitrogen and then equilibrated with a 95 per cent nitrogen/five per cent helium gas mixture at liquid nitrogen temperature. The quantity of gas desorbed from this latter equilibration establishes the total pore volume.

## 5. RESULTS AND DISCUSSION

The research here aimed the design, construction and successful operation of a supercritical-CO<sub>2</sub>-aided process in order to improve the product quality of essential oils through selectively removing the monoterpene (MT) hydrocarbons. The suggested process arrangement constituted by a continuous adsorption/desorption process coupled with dense-CO<sub>2</sub> extraction was utilized for the fractionation and deterpenation of origanum oil (*Origanum Munituflorum*). Experiments were conducted to investigate the influence of extraction pressure, of adsorbent quantity and type, of desorption pressure and of origanum-oil/CO<sub>2</sub> feed composition on the selectivity of the fractionation process. In this chapter, these factors affecting the product quality are discussed and the process performance is analyzed in terms of the relative-distribution ratios of the twelve major components in origanum oil, of the MT and NMT fractions of oil collected during sampling, and of the separation factor, the value of which indicates the degree of fractionation.

### 5.1. Relative-Distribution Coefficients and Separation Factor

To analyze the experimental results quantitatively, the relative-distribution coefficients (ratios) were defined. The normalized area per cents for each key component (identified by GC/MS analysis) or monoterpene (MT) / non-monoterpene (NMT) groups in the original feed,  $C_i^o$  (Table 3.1.1), and in samples,  $C_i$ , were used to calculate the dense-gas phase CO<sub>2</sub>-free relative-distribution ratios  $R_i$ ,

$$R_i = C_i / C_i^o \quad i = 1, \dots, n \quad (i \neq \text{CO}_2) \quad (5.1)$$

The  $C_i$  values were found by analyzing the liquid samples accumulated in the sub-cooled sample collector. These samples were obtained from the condensation of the dense-gas phase in which the origanum oil was dissolved.

Based on the normalized area per cents for MT and NMT groups in the original feed and in samples, the relative-distribution ratios for MT and NMT groups were defined as:

$$R_{MT} = \sum C_{i, MT} / \sum C_{i, MT}^o \quad (5.2)$$

and similarly,

$$R_{NMT} = \sum C_{i, NMT} / \sum C_{i, NMT}^o \quad (5.3)$$

The value of  $R_i$  is important in determining whether the amount of component is increased or decreased in the sample with respect to the feed oil. This may be summarized as follows:

- $R_i > 1$ : The R value greater than one means that the component (or, MT / NMT group) concentration is higher in the recovered oil than in the original essential oil.
- $R_i = 1$ : The R value equal to one means that the component (or, MT / NMT group) concentration is the same in the recovered oil and in the original essential oil.
- $R_i < 1$ : The R value less than one means that the component (or, MT / NMT group) concentration is lower in the recovered oil than in the original essential oil.

Separation factor,  $\alpha$ , was defined as:

$$\alpha = \frac{\sum C_{i, MT} / \sum C_{i, NMT}}{\sum C_{i, MT}^o / \sum C_{i, NMT}^o} = R_{MT} / R_{NMT} \quad (5.4)$$

The value of the separation factor  $\alpha$  is important in determining the degree of the fractionation. It is impossible to separate MT hydrocarbons in origanum oil from the oxygenated flavor compounds (NMTs) when  $\alpha$  becomes equal to unity because in that case, both MT and NMT hydrocarbons will be equally soluble in dense CO<sub>2</sub>. The condition for desirable deterpenation is at  $\alpha$  values greater than unity, where the MT constituents of the origanum oil are preferentially removed by CO<sub>2</sub>.

## **5.2. Fractionation of Origanum Oil by Supercritical-CO<sub>2</sub> Extraction**

The aim of performing a supercritical-CO<sub>2</sub> extraction run was to improve the quality of origanum oil through the removal of its monoterpene (MT) constituents. In chapter three, the different types of extraction experiments carried out were shown schematically (Figures 3.2.1 and 3.2.2), and the facts considered in performing these distinct operations were explained in detail. In this section, the experimental results obtained during the supercritical-CO<sub>2</sub> extraction runs at 40°C/7.5 MPa and 40°C/10.0 MPa conditions will be discussed in terms of the twelve major components of origanum oil, and the MT and non-monoterpene (NMT) fractions of oil collected during sampling.

### **5.2.1. Supercritical-CO<sub>2</sub> Extraction at 40°C/7.5 MPa**

The relative-distribution ratios of the key components in origanum oil obtained via supercritical-CO<sub>2</sub> extraction at 40°C/7.5 MPa are given in Table D.1, in Appendix D, and illustrated in Figure 5.2.1.1. It should be understood that the samples collected in all the extraction experiments (Figures 3.2.1 and 3.2.2), are not instantaneous but integral samples. Therefore, and since the MT components are extracted preferentially (early) than the NMT constituents of the oil, the fraction of the MTs in the samples collected decreases as their amount in the original origanum oil (in the stream going to the collector) decreases with

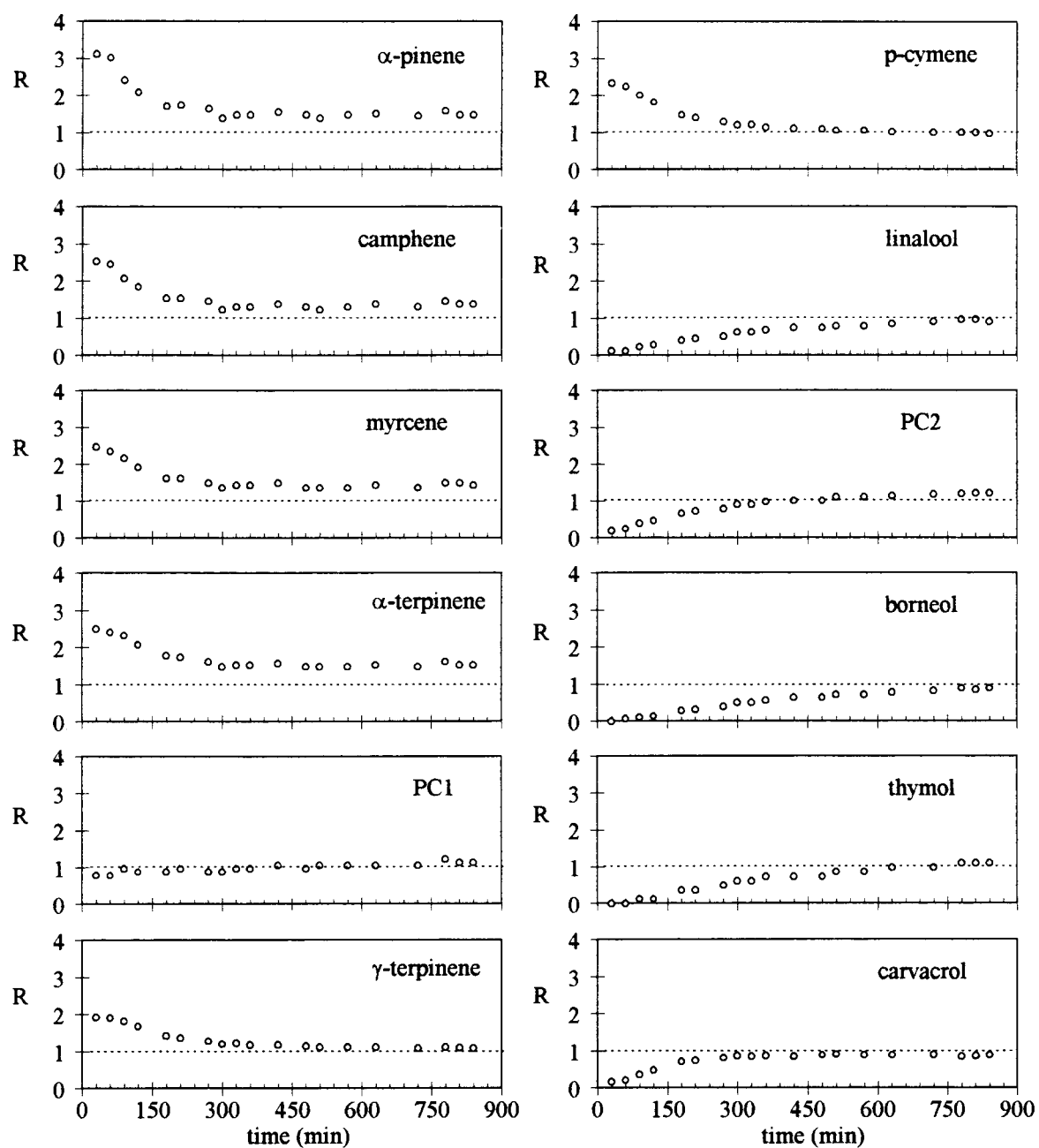


FIGURE 5.2.1.1. Relative-distribution ratios of origanum-oil components in extraction experiment at 40°C/7.5 MPa.

time. Consequently, the concentration of the NMT hydrocarbons in the integral samples increases with time.

As seen in Figure 5.2.1.1, all MT hydrocarbons demonstrate similar extraction behavior in dense CO<sub>2</sub>. As extraction time proceeds, the relative-distribution ratios of the MTs have a tendency to decrease asymptotically as the NMT components start to appear in the samples collected. CO<sub>2</sub> preferentially dissolves the MTs and the NMTs with  $R_i < 1$  tend to concentrate in the liquid-oil phase remaining in the bottom of the extraction vessel (see Figure 3.2.1). This is because MT hydrocarbons can be extracted earlier with ease by supercritical CO<sub>2</sub> due to fact five, as stated in chapter three, keeping in mind that CO<sub>2</sub> is a non-polar solvent. This reasoning also explains the relative-distribution behavior of *p-cymene*. Although *p-cymene* is not a MT hydrocarbon, it behaves like a MT hydrocarbon, because of possessing the lowest molecular weight among the twelve key components of origanum oil. Compared to the other MT hydrocarbons, the relative-distribution ratio of *PCI* does not change significantly as the extraction time proceeds (Figure 5.2.1.1). This can be explained by considering fact ten, as stated in chapter three. The oxygenated part of *PCI* (*1,8 cineole*) is expected to show a behavior similar to MTs, but with lower R-values since it has a vapor pressure close to those of the MT hydrocarbons (its boiling point is lower than that of the *γ-terpinene*, as can be seen in Table C.1, in Appendix C).

All NMT components exhibit comparable extraction behavior in supercritical CO<sub>2</sub> at 40°C/7.5 MPa extraction, as seen in Figure 5.2.1.1. Fact seven, as stated in chapter three, explains the relative-distribution behavior of the alcohols (*linalool*, *terpinen-4-ol*, *borneol*) and phenolics (*thymol*, *carvacrol*) because of their relatively high polarities and low vapor pressures, and the sesquiterpene (*β-caryophyllene*) because of its high molecular weight are not preferentially extracted.

Figure 5.2.1.2 shows the relative-distribution ratios of the MT and NMT groups of the extracts obtained via supercritical-CO<sub>2</sub> extraction at 40°C/7.5 MPa. Since the purpose of extraction is to remove the MT hydrocarbons and leave the NMT compounds behind, a minimum amount of NMT in the extracts is desired. Figure 5.2.1.2 indicates that, the MT

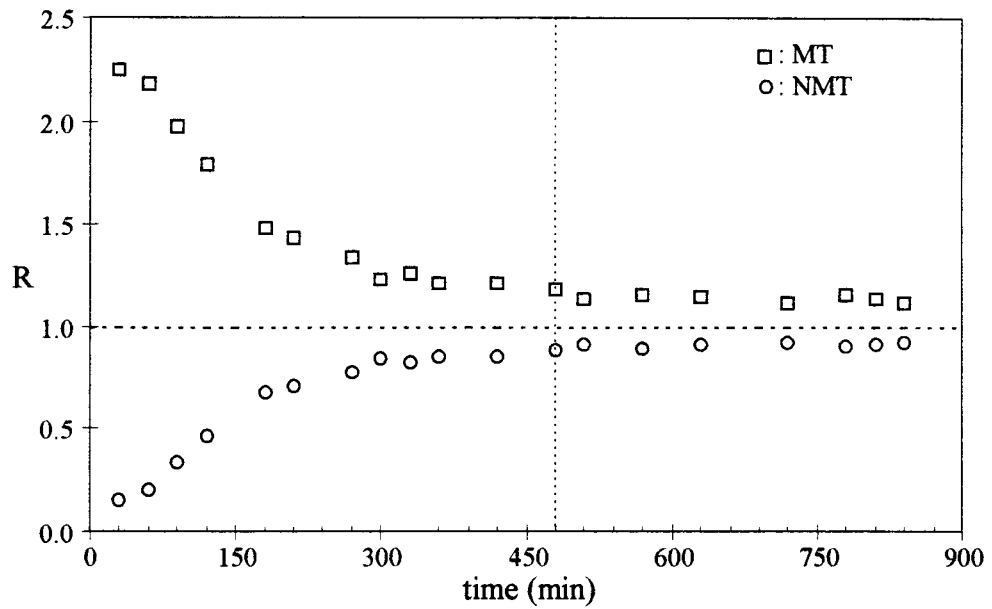


FIGURE 5.2.1.2. Relative-distribution ratios of MT and NMT cuts in extraction experiment at 40°C/7.5 MPa.

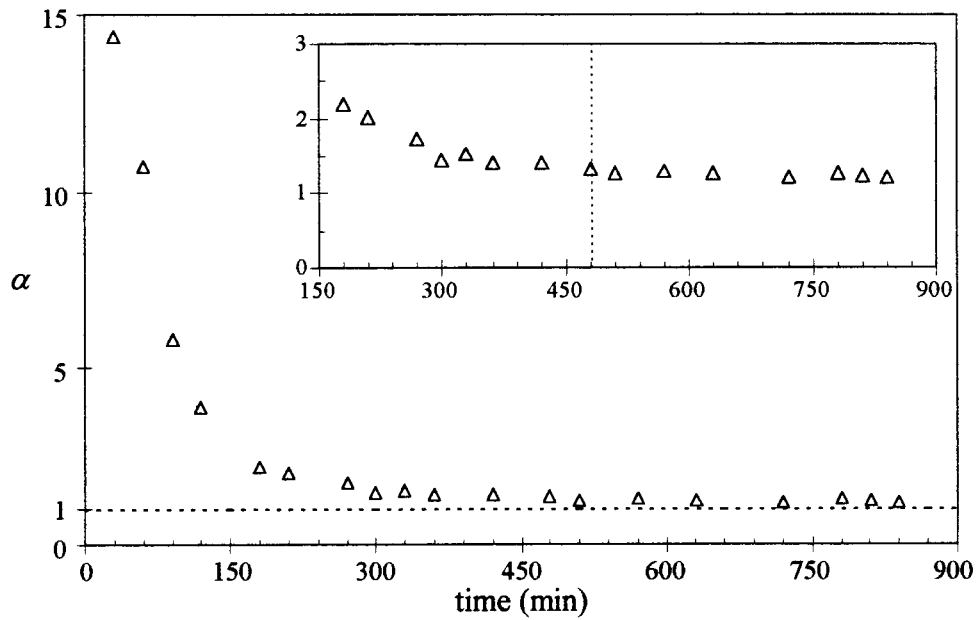


FIGURE 5.2.1.3. Separation factor in extraction experiment at 40°C/7.5 MPa.

components were extracted ( $R > 1$ ) by dense  $\text{CO}_2$  to a greater extent and the NMT components ( $R < 1$ ) were left in the liquid-oil phase remaining in the bottom of the extraction vessel (Figure 3.2.1), almost independent of the extraction time. It is important to note that the extraction experiment was carried out for an extended period of time, 840 minutes. The optimum extraction time for the fractionation of origanum-oil components can be estimated as 480 minutes since after that period, the  $R$ -values of the MT and NMT groups do not change significantly. Figure 5.2.1.2 also gives the evidence that the relative-distribution ratios of both MT and NMT groups approach to unity, as time proceeds.

Figure 5.2.1.3 is a plot of the selectivity, or separation factor,  $\alpha$ , as a function of the extraction time. The analysis of the extracts showed that under  $40^\circ\text{C}/7.5$  MPa extraction conditions,  $\text{CO}_2$  had some selectivity for the MT hydrocarbons since  $\alpha$ -values are greater than unity during the entire extraction run. There was a decrease in selectivity as extraction proceeded, but above 480 minutes of extraction period the composition of the origanum oil in dense- $\text{CO}_2$  phase did not change significantly ( $\alpha$  remained nearly constant at 1.25). Hence, approximately 480 minutes of extraction time was sufficient to reach some degree of selectivity of MTs over the NMT hydrocarbons.

It was assumed that at  $40^\circ\text{C}/7.5$  MPa conditions, the origanum-oil/ $\text{CO}_2$  system falls in the two-phase region, i.e., a liquid-oil and a dense-gas phase in which  $\text{CO}_2$  and the dissolved oil components appear are present. The validity of this argument was established experimentally and in chapter three, the operational arrangement used (Figure 3.2.1) was described in detail. Table 5.2.1.1 shows the composition of the original oil and residual oil (liquid-oil phase accumulating in the bottom of the mixing cell) in terms of normalized area per cent (obtained by GC/MS analysis) of the twelve major components of this origanum oil. Figure 5.2.1.4 demonstrates the distribution of the residual-oil components relative to the original-oil components,  $R_x$ . As can be seen from this figure, the liquid-oil phase is mainly composed of the NMT hydrocarbons and *PCI* ( $R_x > 1$ ); the MT components tend to concentrate in the dense-gas phase ( $R_x \ll 1$ ) due to fact five, as stated in chapter three; and the NMT fraction accumulates in the liquid-oil phase (Figure 3.2.1). Among the NMT group, the relative-distribution ratio of *carvacrol*, which constitutes bulk of the original origanum oil, is the lowest and closest to unity, but still higher than unity, showing that

*carvacrol* preferentially remains in the liquid-oil phase. It is also seen from Figure 5.2.1.2 that the dense-gas relative-distribution ratios,  $R_y$ , (simply named  $R$ ), of the NMT cut is less than unity, which is in good agreement with the above discussion. On the other hand, the liquid phase relative-distribution ratio,  $R_x$ , of *PCI* is greater than unity (Figure 5.2.1.4); this may be explained regarding fact ten, as stated in chapter three. It is also evident from Figure 5.2.1.1 that the oxygenated part of *PCI* (*1,8 cineole*) has a pronounced effect on the behavior of this component since, as compared to the observed behavior of the MT group, the dense-gas relative-distribution ratios of *PCI* do not change significantly and remain around unity throughout the duration of the extraction at 40°C/7.5 MPa. Based on the results of this discussion, it is obvious that the mixing cell, which acts as a flash cell prior to extraction of origanum oil by supercritical CO<sub>2</sub>, provides additional separation between the more soluble components in CO<sub>2</sub> and the hard-to-extract substances by CO<sub>2</sub> of this oil, i.e., between the MT and NMT hydrocarbons.

TABLE 5.2.1.1. Normalized area percentages of original and residual origanum oil-components in 40°C/7.5 MPa extraction experiment.

Components	A	B	$R_x = B/A$
	Normalized area % original origanum oil	Normalized area % residual oil	
$\alpha$ -pinene	3.109	0.600	0.193
camphene	1.307	0.200	0.153
myrcene	1.620	0.501	0.309
$\alpha$ -terpinene	2.365	0.901	0.381
PC1	1.146	1.475	1.287
$\gamma$ -terpinene	12.547	5.395	0.430
p-cymene	18.340	6.602	0.360
linalool	1.769	4.700	2.657
PC2	5.848	14.702	2.514
borneol	2.821	8.899	3.155
thymol	0.821	2.211	2.693
carvacrol	48.307	53.814	1.114

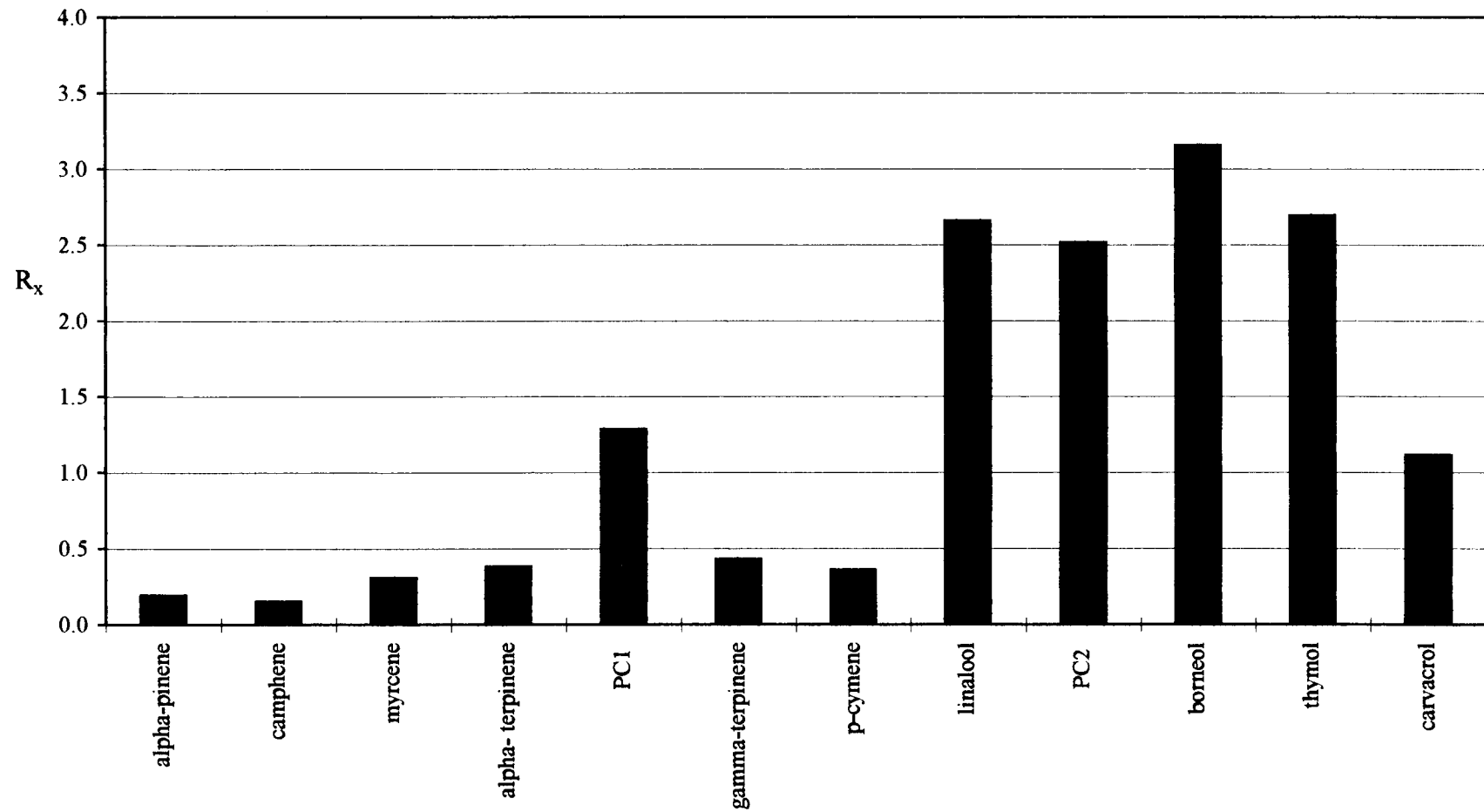


FIGURE 5.2.1.4. Liquid phase relative-distribution ratios of residual-oil components in 40°C/7.5 MPa extraction experiment.

One would expect a better quality product with a higher proportion of oxygenated compounds since these hydrocarbons are the real aroma donators of the essential oils. On the other hand, the MT hydrocarbons contribute little to the flavor, and their decomposition products impair the quality of the oil. The results of this work show that deterpenation of origanum oil with dense CO<sub>2</sub> is thus possible at 40°C/7.5 MPa conditions (corresponding to a pure CO<sub>2</sub> density of about 0.25 g/cm<sup>3</sup>) through selective extraction of the MTs from the oxygenated compounds. It is known that the optimum pressure for extracting MT hydrocarbons is 7.0-9.0 MPa and CO<sub>2</sub> densities between 0.2-0.4 g/cm<sup>3</sup> are suitable for fractionation of essential oils (Stahl et al., 1988).

### 5.2.2. Supercritical-CO<sub>2</sub> Extraction at 40°C/10.0 MPa

The relative-distribution ratios of the key components in origanum oil obtained via supercritical-CO<sub>2</sub> extraction at 40°C/10.0 MPa are given in Table D.2, in Appendix D, and illustrated in Figure 5.2.2.1. At this operating conditions, all MT hydrocarbons, with the exception of *γ-terpinene* and *p-cymene*, exhibit similar extraction behavior in supercritical CO<sub>2</sub>. Compared to the behavior observed in Figure 5.2.1.1 (extraction at 40°C/7.5 MPa), the peaks of the relative-distribution ratios of the MT components, with the exception of *γ-terpinene* and *p-cymene*, are more dilated and shifted toward longer breakthrough times (to about 120 minutes). These changes, which occurred with increase in pressure, may be explained as follows: Both of these runs were performed at comparable CO<sub>2</sub> flow rates; 1.54 g/min and 1.53 g/min in 40°C/7.5 MPa and 40°C/10.0 MPa extractions, respectively. However, the volumetric flow rate of the supercritical solvent within the extractor (cm<sup>3</sup>/min at operating conditions) is reduced by a factor of about three at elevated-pressure extraction as a result of increasing gas density (0.64 g/cm<sup>3</sup> pure CO<sub>2</sub> density at 40°C/10.0 MPa versus 0.25 g/cm<sup>3</sup> pure CO<sub>2</sub> density at 40°C/7.5 MPa). This argument explains the delayed elution times of all of the key components, with the exception of *γ-terpinene*, *p-cymene* and *carvacrol*. These components, which constitute bulk of this origanum oil, rapidly elute from the extractor and appear in the samples collected after 60 minutes of the extraction period.

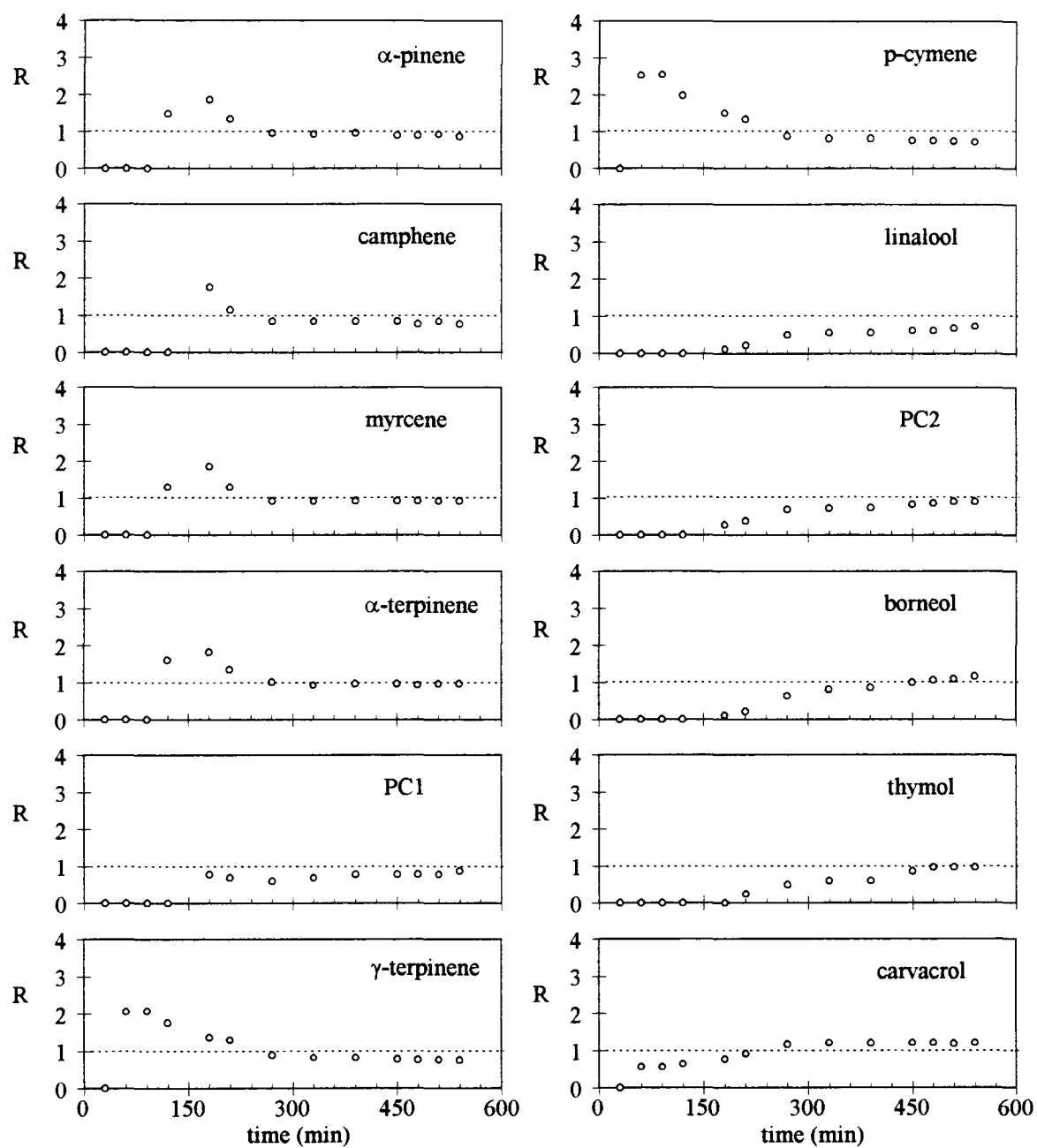


FIGURE 5.2.2.1. Relative-distribution ratios of organum-oil components in extraction experiment at 40°C/10.0 MPa.

At this operating conditions, the origanum-oil/CO<sub>2</sub> system is believed to be in the single-phase region meaning that all the oil pumped is completely miscible in the supercritical CO<sub>2</sub>. The validity of this argument was established experimentally and in chapter three, the operational arrangement used (Figure 3.2.2) was described in detail. It is also known that at pressures above 9.0 MPa at 40°C (corresponding to CO<sub>2</sub> densities above 0.5 g/cm<sup>3</sup>), the solubilities of the typical essential-oil components increase so rapidly that no fractionation of the oil is possible (Stahl et al., 1988). In that case, the concentration of each component in dense CO<sub>2</sub> is close to that in the original origanum oil fed to the extractor ( $R_i$  values close to unity). Consequently, all the components, being equally soluble, are extracted together (without selectivity) and appear at the same instant in the sample collector once the extraction process is started. On the contrary, as can be seen in Figure 5.2.2.1, all of the key components of origanum oil move along very slowly (very long tails are observed in the extraction profiles) as if they are faced with some kind of resistance on their way to the sample collector. This behavior can be related to the dynamics in the connecting lines and that the solubility of these compounds in supercritical CO<sub>2</sub> is not the only limiting step of the extraction process.

Examination of Figure 5.2.2.1 shows that with increasing pressure, the effect of the solvating power of the solvent increases, and the relative-distribution ratios of most of the key components show an asymptotic approach to unity, which reveals that these MT and NMT components of the origanum oil are equally soluble in CO<sub>2</sub>. However, the relative-distribution ratios of *γ-terpinene* and *p-cymene* are less than unity indicating that part of MT hydrocarbons might have not been recovered in the sample collector but have been lost in the CO<sub>2</sub> flow at the exit of the set-up. In that case, the relative-distribution curves of the MT hydrocarbons at 40°C/7.5 MPa extraction conditions would have shifted upwards. Even in this situation, the preferential loading of MT constituents into supercritical phase would have not been altered because the relative-distribution ratios of these components would still have R values greater than unity. As can be seen in Figure 5.2.1.1, this reasoning is consistent with the already observed behavior of the MT hydrocarbons with  $R > 1$  (due to fact five, as stated in chapter three). It is also seen from Figure 5.2.2.1 that all NMT hydrocarbons, with the exception of *borneol* and *carvacrol* with  $R > 1$ , show analogous extraction behavior in supercritical CO<sub>2</sub> at 40°C/10.0 MPa.

Figures 5.2.2.2 and 5.2.2.3 show the pressure and extraction-time dependence of the relative-distribution ratios of the MT and NMT cuts and of the separation factor in the extracts obtained via supercritical-CO<sub>2</sub> extraction at 40°C. The behaviors observed in these figures contradict the validity of the single-phase argument since at 10.0 MPa, the relative-distribution ratios of the MT cut is less than unity, and that of the NMT cut is greater than unity. Moreover, it takes a long time for the key components of origanum oil to appear in the sample collector once extraction is started. In that case, the fact that no residual oil was collected in the bottom of the mixing cell at the end of the extraction is the only indication to verify that the origanum-oil/CO<sub>2</sub> system is in the single-phase region (Figure 3.2.2).

The results of these experiments show that deterpenation of origanum oil with supercritical-CO<sub>2</sub> extraction at 40°C/7.5 MPa conditions is more successful than that at 40°C/10.0 MPa conditions since in the former case,  $\alpha$ -values are higher (Figure 5.2.2.3) as a result of the preferential recovery of MT hydrocarbons in the dense-CO<sub>2</sub> phase. Therefore, in light of these experimental results, it can be concluded that the supercritical-CO<sub>2</sub> extraction process utilizing the mixing cell as a flash chamber is better in obtaining an origanum-oil product having its MT hydrocarbon content reduced to some extent compared to its initial MT hydrocarbon content. Fractionation of the oil, can be enhanced by introducing adsorption and desorption steps to the supercritical extraction system, as represented schematically in Figures 3.2.1 to 3.2.3, in chapter three. The experimental results will be demonstrated and discussed in detail in the next section.

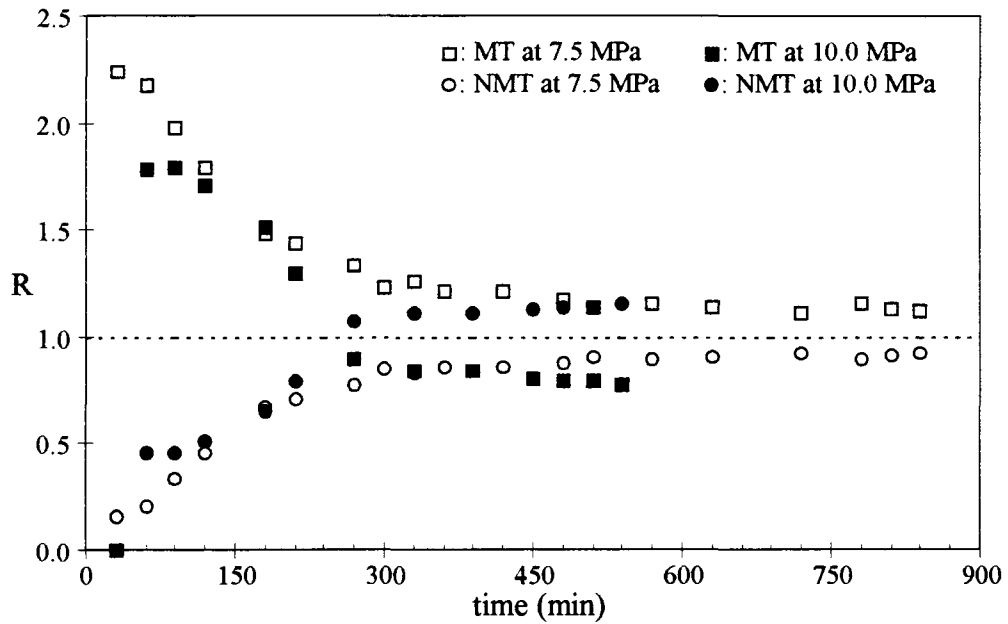


FIGURE 5.2.2.2. Pressure-dependence of the relative-distribution ratios of MT and NMT cuts in extraction experiments at 40°C/7.5 MPa and 40°C/10.0 MPa.

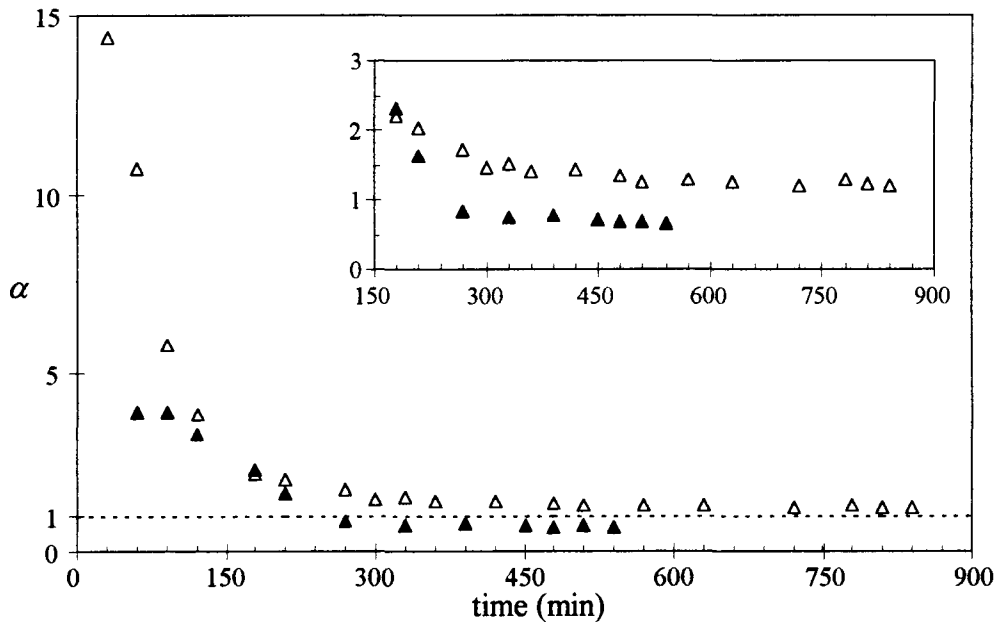


FIGURE 5.2.2.3. Pressure-dependence of the separation factor in extraction experiments at 40°C ( $\Delta$ : 7.5 MPa,  $\blacktriangle$ : 10.0 MPa).

### **5.3. Fractionation of Origanum Oil by Supercritical-CO<sub>2</sub> Adsorption Following Dense-Gas Extraction at 40°C/7.5 MPa Using Activated Carbon Adsorbent**

It is known that in a simple supercritical-fluid extraction process, it is often difficult to reconcile conditions that lead to high recovery yield with those that result in high selectivity. An alternative approach is the coupling of supercritical-fluid extraction to an adsorption process. Based on this idea, in this work, supercritical-CO<sub>2</sub>-aided, a continuous adsorption/desorption process coupled with dense-gas extraction has been developed. The introduction of the adsorption column to the system was expected to enhance the selectivity of the process according to the different affinities of the origanum-oil components for the adsorbent. Last, desorption with pure supercritical CO<sub>2</sub> was executed in order to recover adsorbed compounds.

In chapter three, the different types of supercritical-CO<sub>2</sub> adsorption (following the dense-gas extraction) experiments carried out were shown schematically (Figures 3.2.1 and 3.2.2), and the facts considered in performing these distinct operations were explained in detail. The adsorption from a supercritical feed (origanum oil solubilized in dense-CO<sub>2</sub> phase) was studied on a bed of activated carbon, first at 40°C/7.5 MPa conditions (Figure 3.2.1). In this section, the experimental results obtained, in which the influence of the quantity of adsorbent (activated carbon) charged into the adsorption column was investigated, will be discussed in terms of the twelve major components of origanum oil, and the monoterpene (MT) and non-monoterpene (NMT) fractions of oil collected during sampling. From now on, for the sake of simplicity, the process “supercritical-CO<sub>2</sub> adsorption following the dense-gas extraction” will be named as “supercritical-CO<sub>2</sub> adsorption”.

### 5.3.1. Supercritical-CO<sub>2</sub> Adsorption Following Dense-Gas Extraction on Two Grams Activated Carbon

The relative-distribution ratios of the key components in origanum oil obtained via supercritical-CO<sub>2</sub> adsorption at 40°C/7.5 MPa using two grams of activated carbon are given in Table D.3, in Appendix D, and illustrated in Figure 5.3.1.1. All MT hydrocarbons, with the exception of *PCI*, emerged in the effluent earlier than the NMT components indicating a weaker affinity towards the activated carbon sorbent. *PCI* was retained more than the other MT hydrocarbons; this can be explained by considering fact ten, as stated in chapter three. The oxygenated part of *PCI* (*1,8 cineole*), which is characterized by high polarity, has a pronounced effect on the behavior of this component.

The relative-distribution ratios of the MT and NMT groups of the extracts obtained at 40°C/7.5 MPa via supercritical-CO<sub>2</sub> extraction and supercritical-CO<sub>2</sub> adsorption (following the dense-gas extraction) using two grams of activated carbon are shown in Figure 5.3.1.2. As can be seen from this figure, the relative-distribution ratios of the MT cut obtained during adsorption are higher than those obtained during extraction, independent of extent of the experiments. Similarly, the relative-distribution ratios of the NMT cut obtained during adsorption are lower than those obtained during extraction. These results point to the fact that MTs show a low affinity for the sorbent in conjunction with a high affinity for CO<sub>2</sub>, whereas NMTs exhibit an opposite behavior. As seen in Figure 5.3.1.3, considering the sample collected after 360 minutes in both extraction and adsorption experiments, the separation,  $\alpha$ , achieved between the MT and NMT groups is 1.41 and 2.98, respectively. These results show that the NMT components were more selectively adsorbed on the activated carbon than the MT constituents, and that the separation factor had doubled in the presence of an adsorbent. This conclusion also supports the argument that the more soluble the components are in supercritical CO<sub>2</sub> (fact five, as stated in chapter three) the less strongly they will be adsorbed on the activated carbon. Hence, even two grams of adsorbent (activated carbon) was powerful in further fractionating (compared to simple supercritical-CO<sub>2</sub> extraction) origanum oil into its fractions, namely MT and NMT groups.

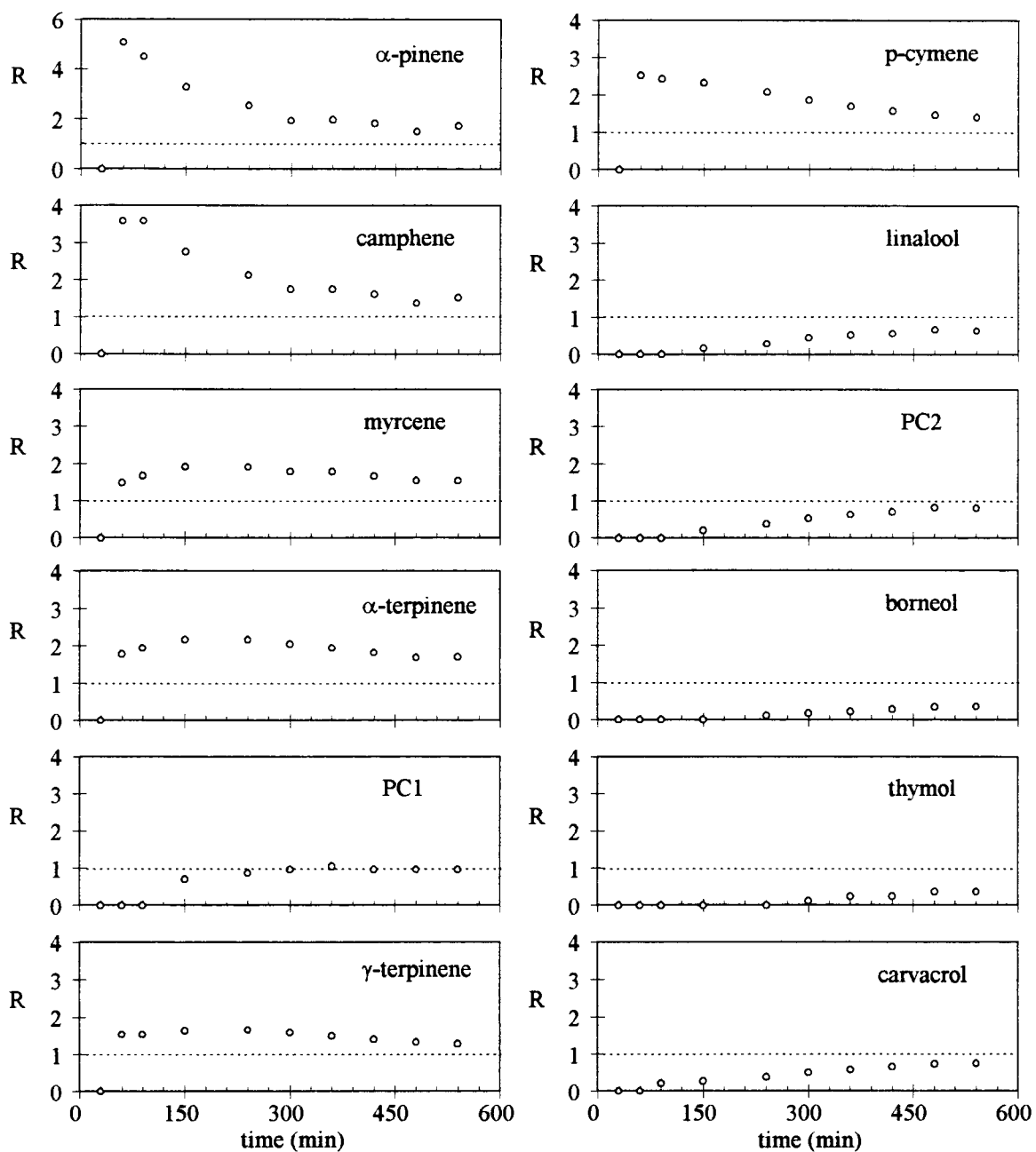


FIGURE 5.3.1.1. Relative-distribution ratios of origanum-oil components in adsorption experiment at 40°C/7.5 MPa using two grams activated carbon.

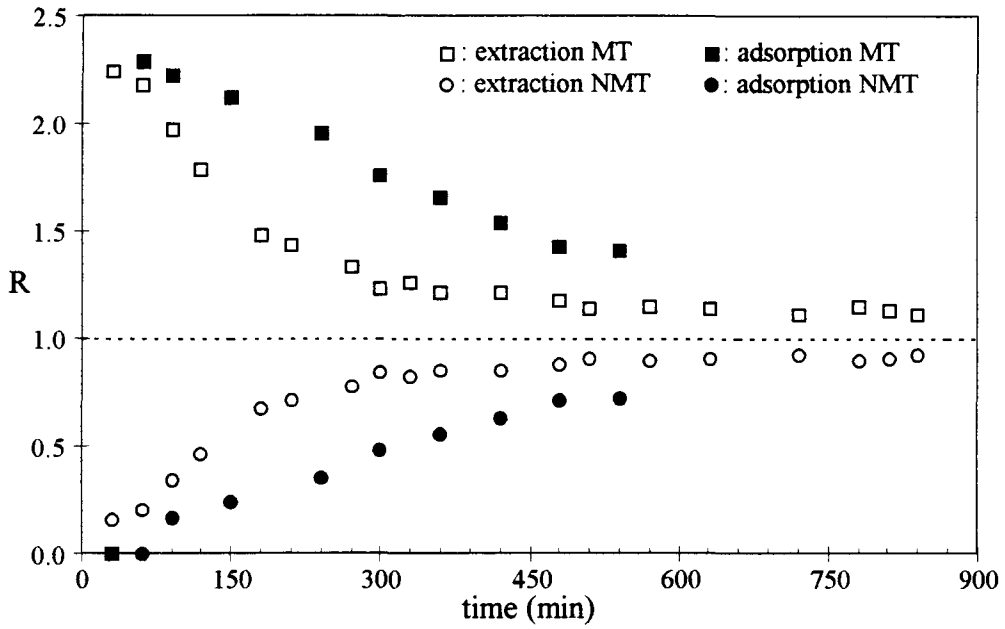


FIGURE 5.3.1.2. Relative-distribution ratios of MT and NMT cuts at 40°C/7.5 MPa in extraction run, and adsorption on two grams activated carbon run.

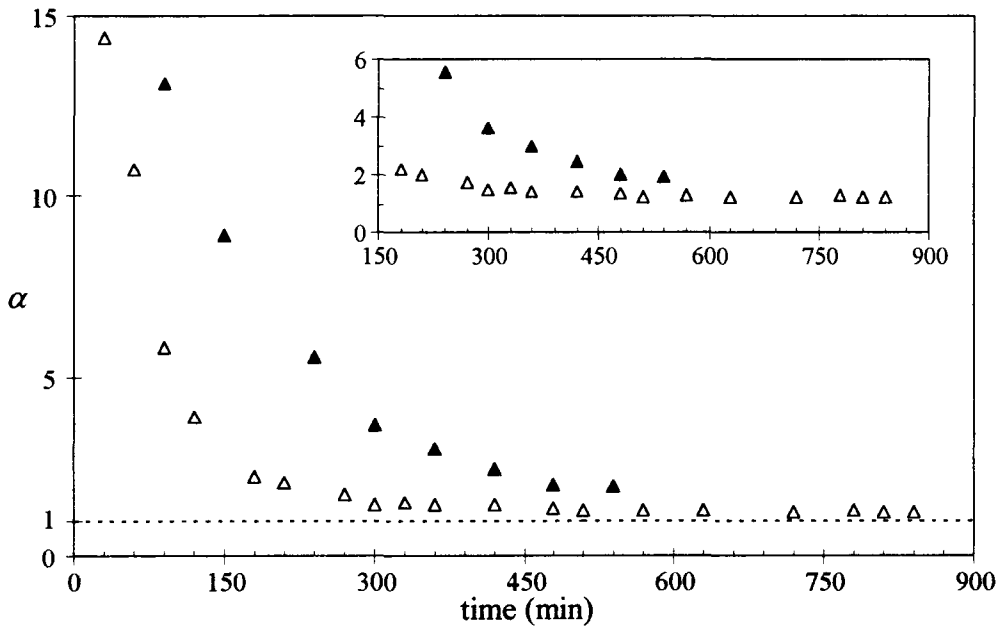


FIGURE 5.3.1.3. Separation factor at 40°C/7.5 MPa conditions ( $\Delta$ : extraction,  $\blacktriangle$ : adsorption on two grams activated carbon).

The supercritical-CO<sub>2</sub> adsorption of origanum oil on activated carbon was terminated after 540 minutes, then the carbon sample was removed and weighed prior to washing it with ethanol to recover the adsorbed fraction of the oil. 21.5 per cent increase was found in the weight of the activated carbon indicating a significant amount of origanum oil was adsorbed on the carbon. Figure 5.3.1.4 shows the composition (relative-distribution coefficient for each key component) of the ethanol-extracted activated-carbon residue and of the last sample taken (from the sample collector) during the adsorption run at 40°C/7.5 MPa. The most important characteristic of the activated-carbon residue were the high NMT content and the appearance of additional components belonging to the MT group. On the other hand, at the end of the adsorption, MT components with  $R > 1$ , with the exception of *PCI*, were found to be concentrated in the dense-gas phase, whereas the NMT hydrocarbons were preferentially adsorbed on the carbon. These results, coupled with the above observations, suggest that the fractionation of the origanum oil can be rationalized on the basis of the degree of adsorption on activated carbon and the different solubilities these components exhibit in supercritical CO<sub>2</sub>.

Desorption with pure supercritical CO<sub>2</sub> was not executed at the end of this adsorption run (performed using two grams of activated carbon) because it was only a preliminary experiment in determining the optimum amount of activated carbon to be used in the next runs.

It is also important to notice in Figure 5.3.1.1 that the relative-distribution ratios of the MT components decreased with time as that of the NMT hydrocarbons increased as adsorption proceeded. This behavior can be explained regarding fact one, as stated in chapter three. In other words, as the MTs were eluted earlier (due to low affinity for the sorbent and high to CO<sub>2</sub>) than the NMTs, they were already present in the effluent as the NMT hydrocarbons started to emerge in the effluent. Figure 5.3.1.5 shows the ratio of the area counts (obtained from the GC/MS analysis) of the MT and NMT cuts in the samples collected to that in the original origanum oil in the adsorption run at 40°C/7.5 MPa using two grams activated carbon. As clearly seen, the area counts (see fact two, as stated in chapter three) of both groups increase with time because the amount of origanum-oil components solubilized in supercritical CO<sub>2</sub> continuously aggregate in the sample collector.

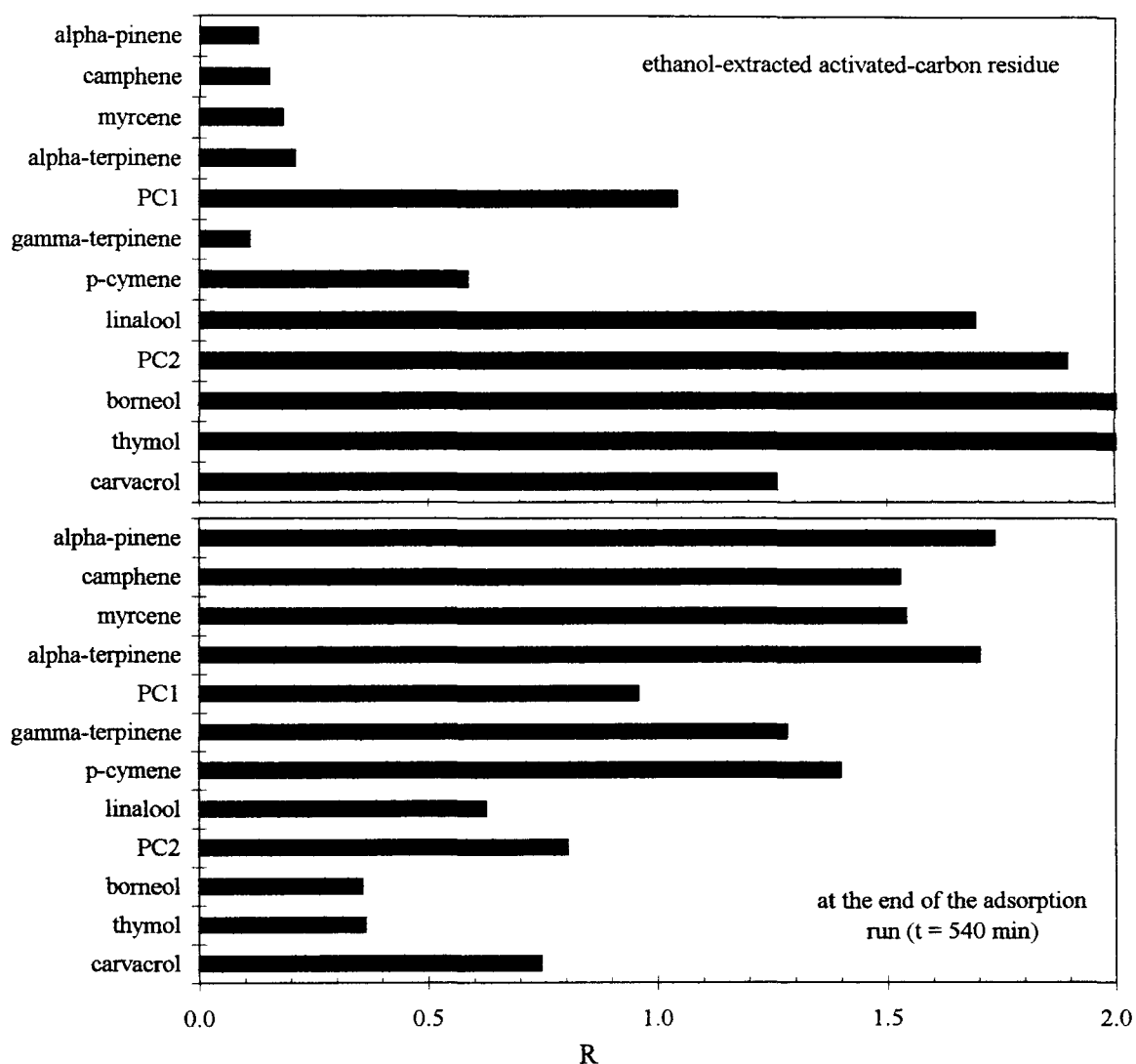


FIGURE 5.3.1.4. Composition of the ethanol-extracted activated-carbon residue and of the last sample taken during the adsorption run at 40°C/7.5 MPa using two grams activated carbon.

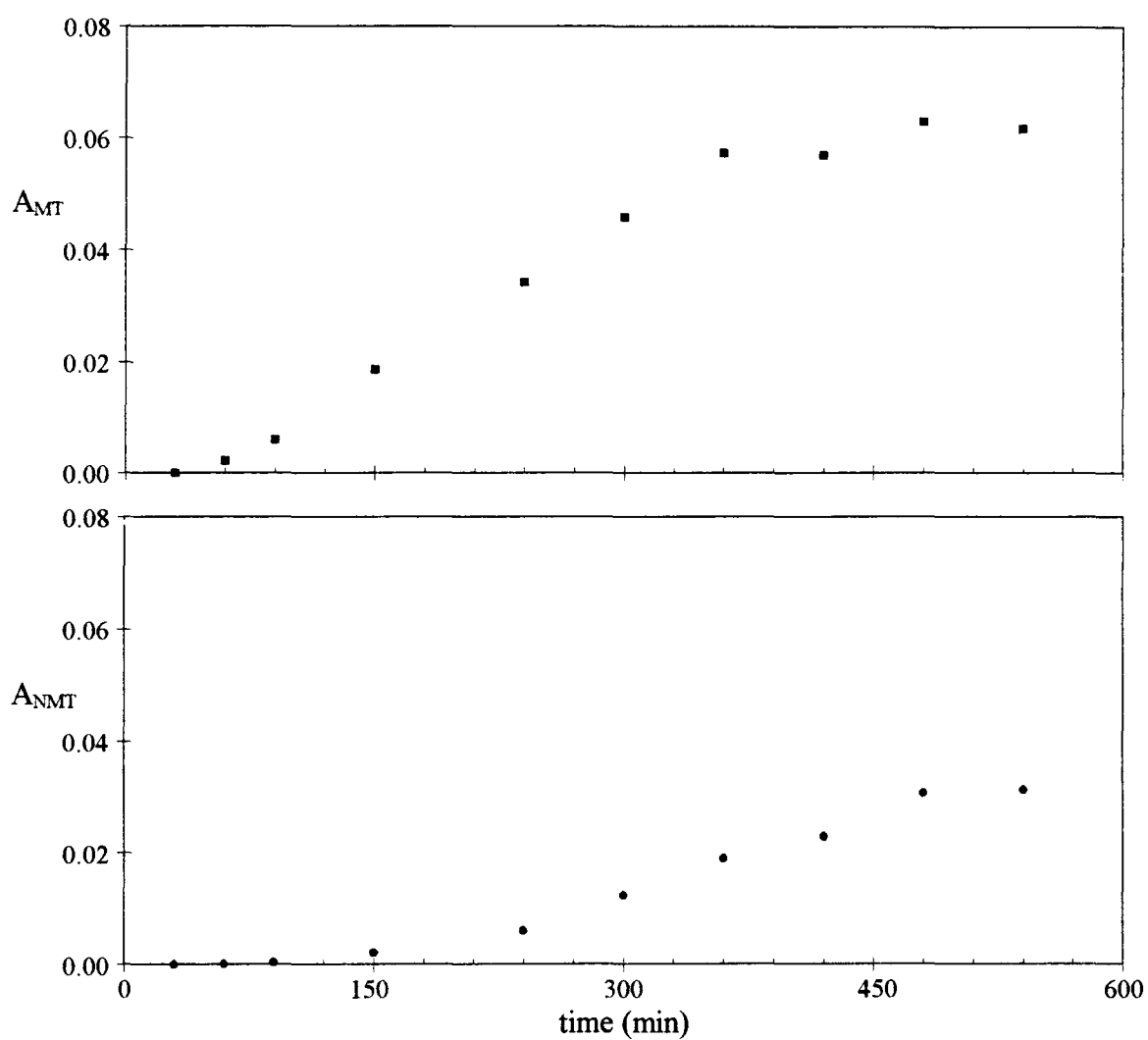


FIGURE 5.3.1.5. Ratio of the area counts of the MT and NMT cuts in the sample to that in the original origanum oil in adsorption run at 40°C/7.5 MPa using two grams activated carbon.

Therefore, the decrease in the relative-distribution ratios of the MTs does not imply that these hydrocarbons did not emerge and accumulate in the samples collected during the adsorption run. If the area count ratios of the MT or NMT components with respect to original organum oil were to remain constant, then that revealed the appearance of only pure CO<sub>2</sub> in the effluent.

### **5.3.2. Supercritical-CO<sub>2</sub> Adsorption Following Dense-Gas Extraction on Eight Grams Activated Carbon**

It had been found that at 40°C/7.5 MPa conditions even two grams of activated carbon adsorbent enhanced fractionation of organum-oil components, thus improving the quality of the oil through selectively retaining the NMT hydrocarbons. A series of adsorption runs using eight grams of activated carbon were also executed in order to identify the operating conditions that produce the maximum process selectivity, i.e., the best fractionation of the organum oil. In this section, the experimental results obtained in these runs will be discussed in terms of the twelve major components of organum oil, and the monoterpene (MT) and non-monoterpene (NMT) fractions of oil collected during sampling.

The relative-distribution ratios of the key components in organum oil obtained via supercritical-CO<sub>2</sub> adsorption at 40°C/7.5 MPa using eight grams of activated carbon are given in Table D.4, in Appendix D. Replicate runs at these operating conditions were performed to obtain accuracy and precision in the adsorption experiments. The relative-distribution ratios of the individual components obtained in these replicate experiments are given in Tables D.5 and D.6, in Appendix D. Yet, for comparison purposes, all of these results are illustrated in Figure 5.3.2.1.

The general pattern of the breakthrough curves reveals that the MT and NMT components of the organum oil showed different behavior as adsorption proceeded. The breakthrough order can be explained regarding the relative strength of interactions occurring during adsorption between the solute, the sorbent and the fluid phases.

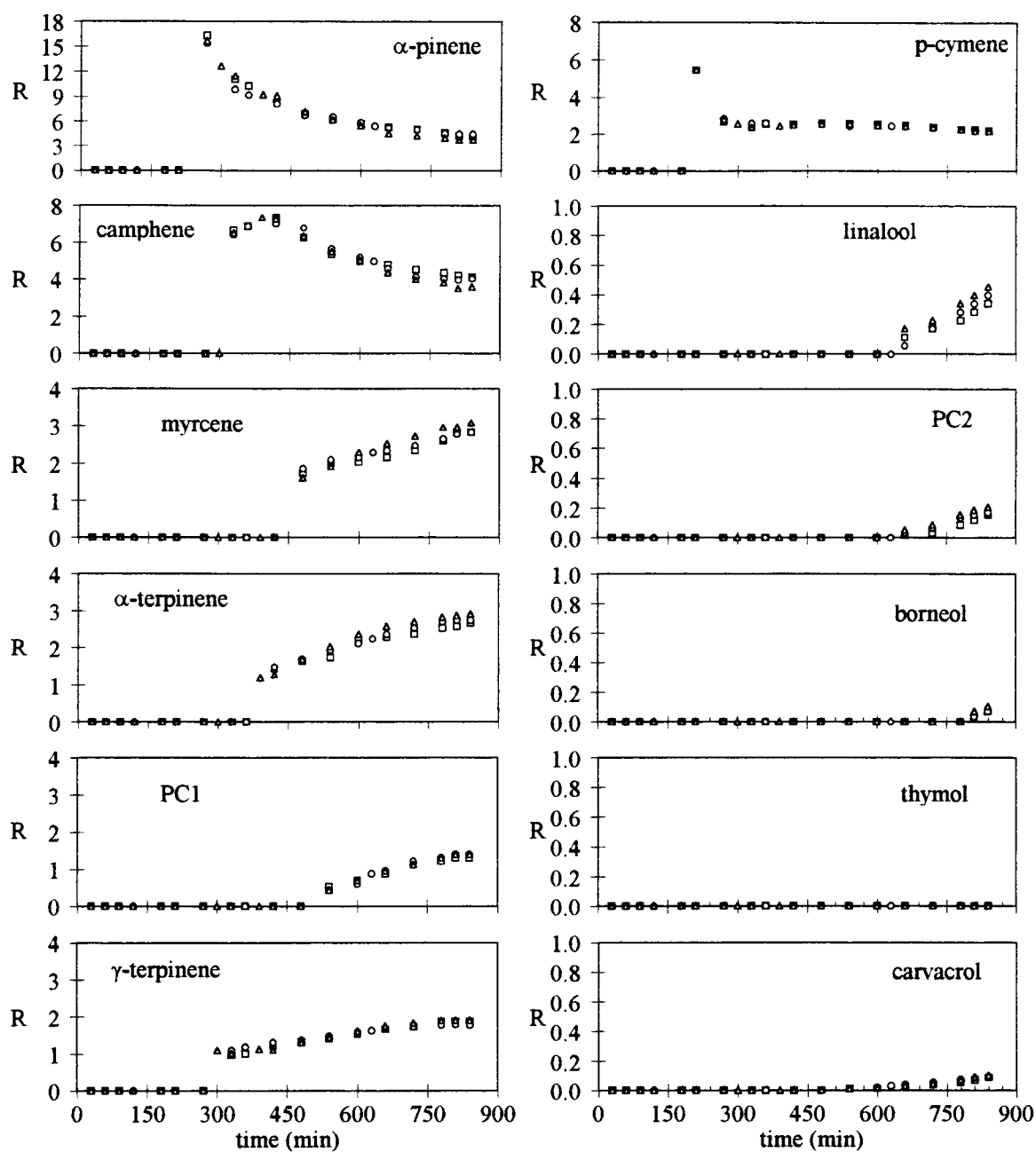


FIGURE 5.3.2.1. Relative-distribution ratios of origanum-oil components in adsorption experiment at 40°C/7.5 MPa using eight grams activated carbon (○, □, Δ: replicate runs).

Dealing with a supercritical medium, vapor pressure, polarity and molecular mass are properties which have a special influence on solubility. MT hydrocarbons possess the highest vapor pressures among the key components of the origanum oil and it is known that they have vapor pressures of a few millibar even at room temperature masses (Stahl et al., 1988). Hence, due to fact five, as stated in chapter three, MT hydrocarbons are more soluble in dense CO<sub>2</sub> than other essential-oil components. On the other hand, due to fact 15, as stated in chapter three, the MT hydrocarbons would have an affinity for the nonpolar surface, but the oxygenated compounds could also compete with the MTs for the same apolar sites due to the nonpolar part of their molecule (Reverchon and Iacuzio, 1997). As can be seen in Figure 5.3.2.1, in the earlier stages of adsorption, all the key components of origanum oil were adsorbed on the activated carbon. Later, compounds which had a stronger affinity with the adsorbent replaced the ones with a weaker affinity. In other words, NMT compounds (oxygenated, sesquiterpene and phenolic) emerged in the effluent after the MT hydrocarbons indicating a stronger affinity towards the carbon sorbent. As a result, the MT constituents of the origanum oil exhibited a low affinity for activated carbon in conjunction with a high affinity for the fluid phase, whereas the NMTs showed an opposite behavior. This conclusion also supports the argument that the more soluble the components are in supercritical CO<sub>2</sub> the less strongly they will be adsorbed on activated carbon.

It is important to notice in Figure 5.3.2.1 that the relative-distribution ratios of the MT hydrocarbons are higher than that of the NMT components. Furthermore, the relative-distribution ratios of *α-pinene*, *camphene* and *p-cymene* are even higher than that of the other MT constituents of this origanum oil. This behavior can be explained by considering the possible interactions of these components with the active sites of the adsorbent. In the earlier stages of the adsorption, all of the MT components were adsorbed on the activated carbon. Later, compounds *α-pinene*, *camphene* and *p-cymene* were rapidly replaced by the more polar MTs; in other words MT components with a higher polarity and stronger affinity with the adsorbent displaced the weakly adsorbed MTs from the adsorption site in which they were located. The presence of displacement resulted in a peak in the breakthrough curves of these components (*α-pinene*, *camphene* and *p-cymene*), i.e., their relative-distribution ratios sharply increased attaining very high values and then slowly

decreased as the other MT components emerged in the effluent. The argument based on the competitive adsorption or displacement effect (Ruthven, 1984) among the MT hydrocarbons explains their different adsorption behavior. It is important to remark in Figure 5.3.2.1 that even though the relative-distribution ratios of components *α-pinene*, *camphene* and *p-cymene* decreased with time, their amount increased in the samples collected (refer to fact two, as stated in chapter three).

As seen in Figure 5.3.2.1, MT components *myrcene*, *α-terpinene*, *PC1* and *γ-terpinene* exhibited comparable breakthrough behavior as adsorption proceeded. These components emerged later (in the sample collector) than the MT components *α-pinene*, *camphene* and *p-cymene*, with the exception of *γ-terpinene* which appeared in the effluent at the same time with *camphene*. The delayed behavior of these components may be explained as follows: *Myrcene* is the only acyclic hydrocarbon in these MT hydrocarbons. *PC1* (refer to fact ten, as stated in chapter three) is included into the MT group since it exhibited adsorption behavior approximately similar to MT components, and *PC1* with  $R > 1$  tended to concentrate in the dense-CO<sub>2</sub> phase. Furthermore, *α-pinene* and *camphene* are the least polar components among the MT hydrocarbons. Although *p-cymene* is not a MT hydrocarbon, it behaves like a MT hydrocarbon, because of possessing the lowest molecular weight among the twelve key components of origanum oil. These arguments confirms the validity that essential-oil components with lower molecular mass, lower polarity and higher vapor pressures are more soluble in dense CO<sub>2</sub> (Stahl et al., 1988).

At 40°C/7.5 MPa (Figure 5.3.2.1), compared to the MT behavior, the breakthrough curves of NMT hydrocarbons are more distinct and spread out. However, the breakthrough curves for *linalool* and *PC2* show similar behavior, but the relative-distribution ratios of *linalool* are higher than that of *PC2*. This behavior may be explained as follows: *linalool* is the only aliphatic terpene alcohol among the NMT hydrocarbons, whereas *terpinen-4-ol* is a cyclic terpene alcohol, which is characterized by higher polarity compared to *linalool*. Moreover, *β-caryophyllene*, the only sesquiterpene hydrocarbon in the mixture, possesses the highest molecular weight among the origanum-oil components. This argument, coupled with fact 11, as stated in chapter three, revealed that *PC2* exhibited higher affinity towards activated carbon compared to *linalool*. Likewise, *thymol* was very strongly retained by

carbon since it did not appear in the effluent even after 840 minutes of adsorption time, whereas *carvacrol* emerged in the effluent after 540 minutes. As a result, MT hydrocarbons (due to weak affinity towards the carbon) were eluted earlier than the NMT compounds. Since MT were eluted first, they were always present in the effluent as adsorption proceeded. The breakthrough order is thus understandable regarding the strength of the interactions with both the fluid and the sorbent.

The evolution of the relative-distribution ratios of the individual components is represented in Figure 5.3.2.2. As can be seen in this figure, the fraction accumulated in the sample collector from zero to 480 minutes was formed by only MT hydrocarbons, but *PCI* did not appear in the effluent yet. The fraction between zero to 600 minutes contained all the MT hydrocarbons and the phenolic compound, *carvacrol*. All the NMT compounds except *thymol* were collected in the subsequent fraction between zero to 840 minutes together with the other origanum-oil constituents (MTs). Longer adsorption times were required for *thymol* to elute from adsorber. The breakthrough order, coupled with the breakthrough location of the twelve key components of origanum oil, suggests the possibility of improving the quality of the oil through the removal of MT hydrocarbons by supercritical-CO<sub>2</sub> adsorption followed by dense-gas extraction at 40°C/7.5 MPa conditions using eight grams of activated carbon.

Furthermore, since the purpose of this work was to remove the MT hydrocarbons and leave the NMT compounds behind, a minimum fraction of MTs is desired in the adsorption column. As can be seen in Figure 5.3.2.3, the analysis of the samples collected during supercritical-CO<sub>2</sub> adsorption at 40°C/7.5 MPa conditions using eight grams of activated carbon produced an origanum oil with the highest MT hydrocarbons composition (lowest NMT fraction) indicating that MTs were preferentially extracted ( $R > 1$ ) by dense-CO<sub>2</sub> and the NMT components ( $R \ll 1$ ) were strongly retained on the sorbent. The selectivity (separation factor) corresponding to these operating conditions is the highest when compared to supercritical-CO<sub>2</sub> adsorption on two grams of activated carbon or simple supercritical-CO<sub>2</sub> extraction (Figure 5.3.2.4). As adsorption proceeded, the separation factor indicating the degree of fractionation decreased sharply due to the appearance of the NMTs in the effluent. Sample collected after 540 minutes of supercritical-CO<sub>2</sub> treatment of

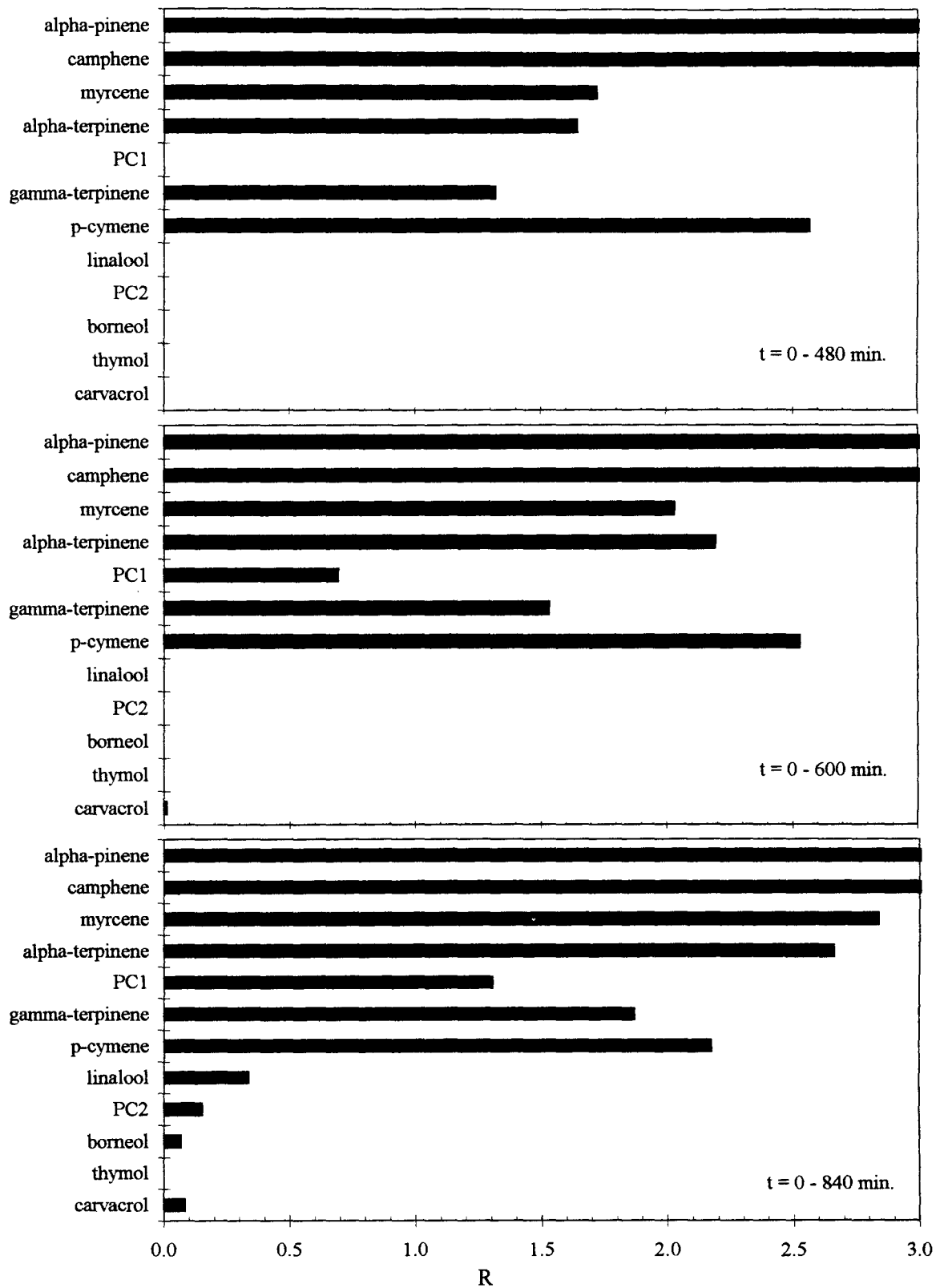


FIGURE 5.3.2.2. Evolution of the relative-distribution ratios of individual components in adsorption run at 40°C/7.5 MPa using eight grams activated carbon.

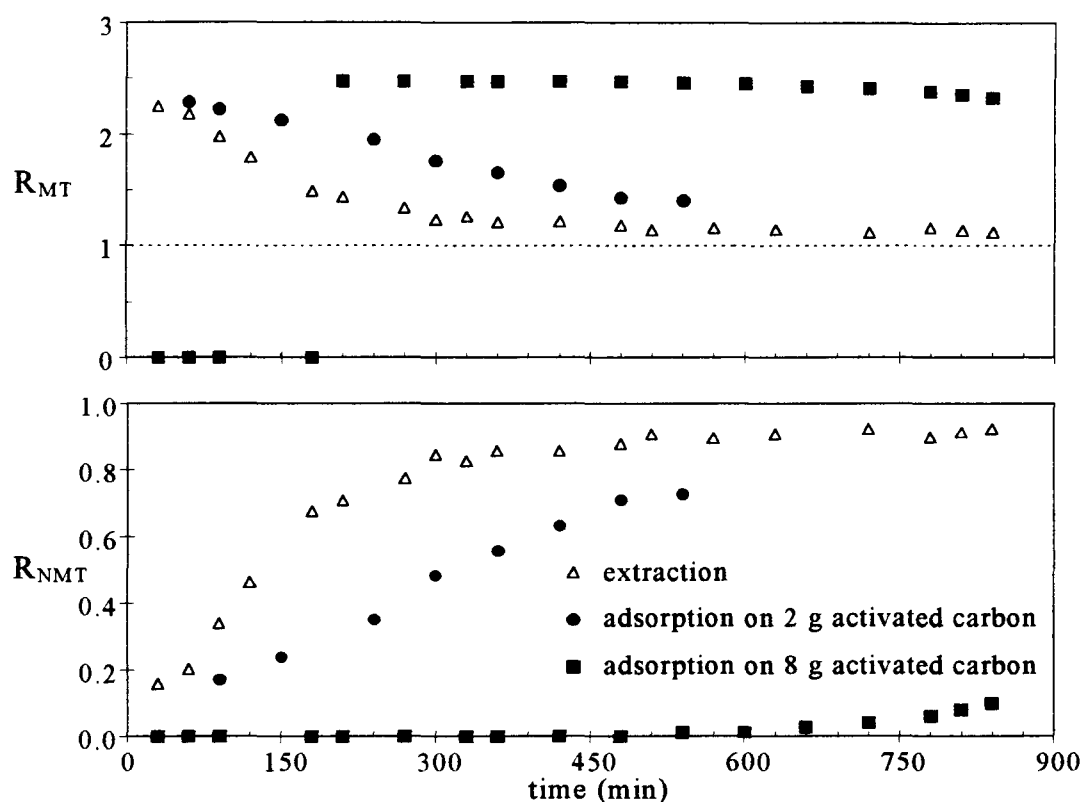


FIGURE 5.3.2.3. Relative-distribution ratios of MT and NMT cuts at 40°C/7.5 MPa in extraction and adsorption runs.

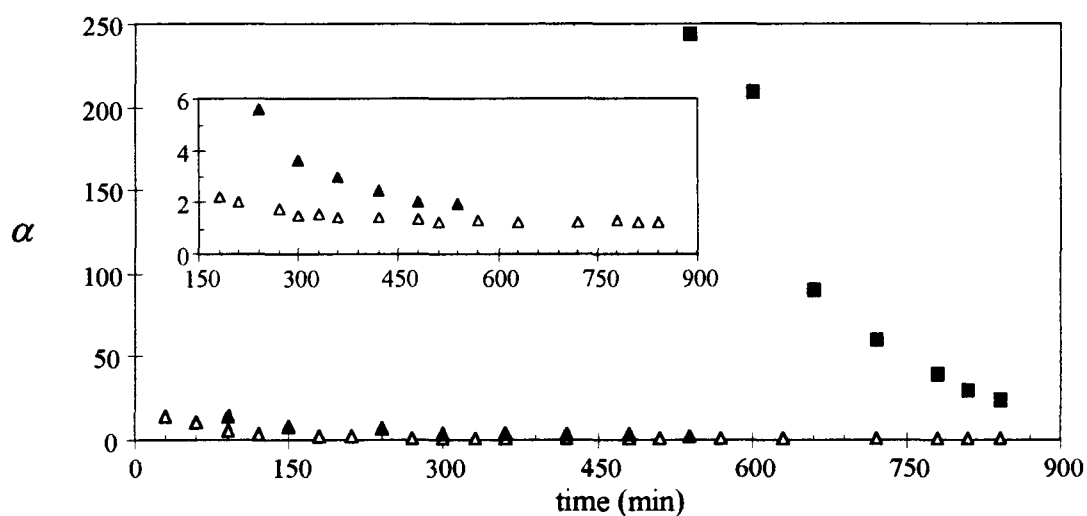


FIGURE 5.3.2.4. Separation factor at 40°C/7.5 MPa in extraction and adsorption runs ( $\Delta$ : extraction, adsorption on activated carbon:  $\blacktriangle$ : 2 g,  $\blacksquare$ : 8 g).

origanum oil at 40°C/7.5 MPa conditions showed that the separation between MT and NMT groups was around 1.26, 1.97, and 244.34 in the case of extraction; adsorption on two grams of carbon; and adsorption on eight grams of carbon, respectively. Based on these results, it can be concluded that activated carbon adsorbent enhanced dewatering of origanum oil, higher carbon loadings were obtained as the quantity of the sorbent increased. However, breakthrough-times of NMT components increase as the amount of carbon introduced into the column increases due to their strong affinity towards the sorbent. Therefore, in the aim of improving origanum oil quality, the trade-off between adsorption duration and elimination of MT hydrocarbons should be prudently taken into consideration in optimizing the operating conditions. As can be seen from Figure 5.3.2.4, until 540 minutes of adsorption period, there is no breakthrough of any component indicating that the activated carbon bed is not fully utilized. However, if an adsorbent bed is to be introduced into the simple extraction system, then at least it is required to wait until the bed is fully saturated. Hence, this argument implies that the optimum adsorption duration would be between 540 to 630 minutes, where at the same time the selectivity of the process is highest (Figure 5.3.2.4).

#### **5.4. Supercritical-CO<sub>2</sub> Desorption Following Origanum-oil/CO<sub>2</sub> Adsorption on Activated Carbon Coupled with Dense-Gas Extraction at 40°C**

In this section, for the sake of simplicity, the process “supercritical-CO<sub>2</sub> desorption following the origanum-oil/CO<sub>2</sub> adsorption coupled with dense-gas extraction” will be named as “supercritical-CO<sub>2</sub> desorption”. The supercritical-CO<sub>2</sub> adsorption (following the dense-gas extraction) experiments performed at 40°C/7.5 MPa conditions revealed that using eight grams of activated carbon as sorbent maintained an enrichment in the non-monoterpene (NMT) compounds (oxygenated, sesquiterpene and phenolic) against the monoterpene (MT) hydrocarbons. In the aim of improving the quality of origanum oil, desorption with pure supercritical CO<sub>2</sub> at 40°C/14.5 MPa conditions was carried out to desorb MT hydrocarbons and selectively recover the valuable essential-oil constituents. It is

important to notice that both adsorption and desorption experiments were performed at the same temperature. This is because at temperatures around 40°C, even thermally unstable substances can be won undecomposed with dense CO<sub>2</sub> (Stahl et al., 1988). However, at temperatures less than 40°C, in other words, closer to the critical temperature of CO<sub>2</sub> (31°C), the gas-phase density approaches the density of liquid CO<sub>2</sub>, and it is known that all essential oil components and flavor substances are freely soluble in liquid CO<sub>2</sub> (Stahl et al., 1988). Therefore, a temperature of 40°C was assumed as the optimum value for the supercritical-CO<sub>2</sub> desorption runs.

#### 5.4.1. Supercritical-CO<sub>2</sub> Desorption at 14.5 MPa

The normalized area counts (per cent) of the origanum-oil components obtained via supercritical-CO<sub>2</sub> desorption at 40°C/14.5 MPa (following the adsorption run at 40°C/7.5 MPa using eight grams of activated carbon) are given in Table D.7, in Appendix D. It was observed that MT hydrocarbons were rapidly desorbed at the beginning of the desorption process and were collected in the sample collector in high percentages (90-95%). All samples collected at desorption times higher than 60 minutes demonstrated a progressive increase in NMT compounds. For example, the desorbed fraction analyzed after 90 minutes comprised mainly of MT hydrocarbons (85.2%), with *p-cymene* (67.5%) being the major component. NMT compounds (14.8%) were also detected in this fraction. At the end of the process, the NMT hydrocarbons (70.5%) were substantially increased over the MT group (29.5%), with increased quantities of *carvacrol* (62.1%) and *thymol* (0.4%), which appeared in the effluent after 210 minutes of desorption time.

The relative-distribution ratios of the key components in origanum oil obtained via supercritical-CO<sub>2</sub> desorption at 40°C/14.5 MPa are reported in Table D.8, in Appendix D, and illustrated in Figure 5.4.1.1. In this figure, the relative-distribution ratios that had been obtained during the adsorption process are also included. The desorption behavior observed for each component is in good agreement with its adsorption behavior, i.e., components which were weakly adsorbed on the carbon (such as *α-pinene*, *camphene*) were easily and

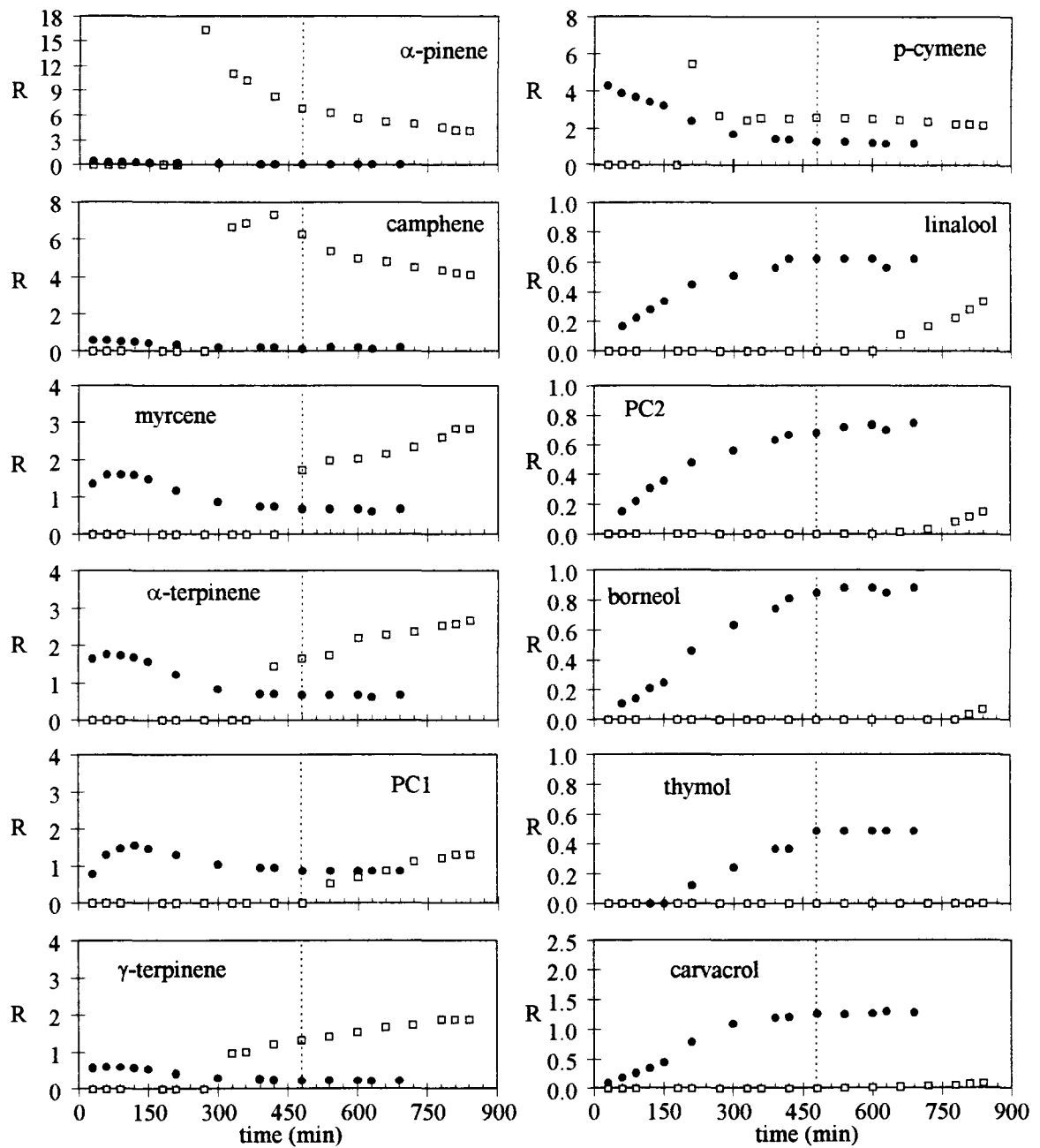


FIGURE 5.4.1.1. Relative-distribution ratios of origanum-oil components at 40°C using eight grams activated carbon (□: adsorption at 7.5 MPa, ●: desorption at 14.5 MPa).

completely desorbed, hence very low R values (close to zero) were obtained for these components. Likewise, in the early stages of the desorption process, MT hydrocarbons which were strongly retained by the sorbent, namely *myrcene*,  *$\alpha$ -terpinene* and *PCI*, were preferentially desorbed by supercritical CO<sub>2</sub> ( $R > 1$ ). Even though *p-cymene* was first to breakthrough during the adsorption process, this component tended to concentrate in the supercritical-CO<sub>2</sub> phase with  $R > 1$ . Similar behavior was observed for *carvacrol*; it was rapidly desorbed by supercritical CO<sub>2</sub> attaining R values greater than unity. Furthermore, NMT hydrocarbons appeared in the desorbed fractions later than the MT components due to their strong affinity for the carbon and lower solubility in CO<sub>2</sub>. At these operating conditions, the major families of compounds, i.e., MT and NMT hydrocarbons, exhibited fast desorption rates, but after 480 minutes the relative-distribution-ratio curves flattened indicating that the desorption was no more effective. On the other hand, due to the increased CO<sub>2</sub> density at 14.5 MPa (compared to CO<sub>2</sub> density at 7.5 MPa), it should have been possible to desorb all the key components of origanum oil since the solubility of all essential-oil components increases due to fact four, as stated in chapter three. This fact, coupled with the above observation, suggests that the complete recovery of the origanum-oil constituents at 40°C/14.5 MPa could be related to adsorption-equilibrium limitations and that the solubility of these compounds in supercritical-CO<sub>2</sub> does not represent the limiting factor of the desorption process.

It is important to notice in Figure 5.4.1.1 that samples collected in this desorption experiment were not instantaneous but integral samples. Hence, even though the relative-distribution ratios of MT constituents decreased with time, their amount (mass) increased in the samples collected (refer to fact two, as stated in chapter three).

The supercritical-CO<sub>2</sub> desorption of origanum oil from activated carbon was terminated after 690 minutes, then the carbon sample was removed and weighed prior to washing it with ethanol to remove the strongly adsorbed fraction of the oil. As opposed to the expected behavior, there was a decrease (4.63%) in the weight of the activated carbon. Figure 5.4.1.2 shows the composition (relative-distribution ratio for each key component) of the fraction collected at the end of the supercritical-CO<sub>2</sub> adsorption run, at the end of the supercritical-CO<sub>2</sub> desorption run and of the ethanol-extracted activated-carbon residue. The

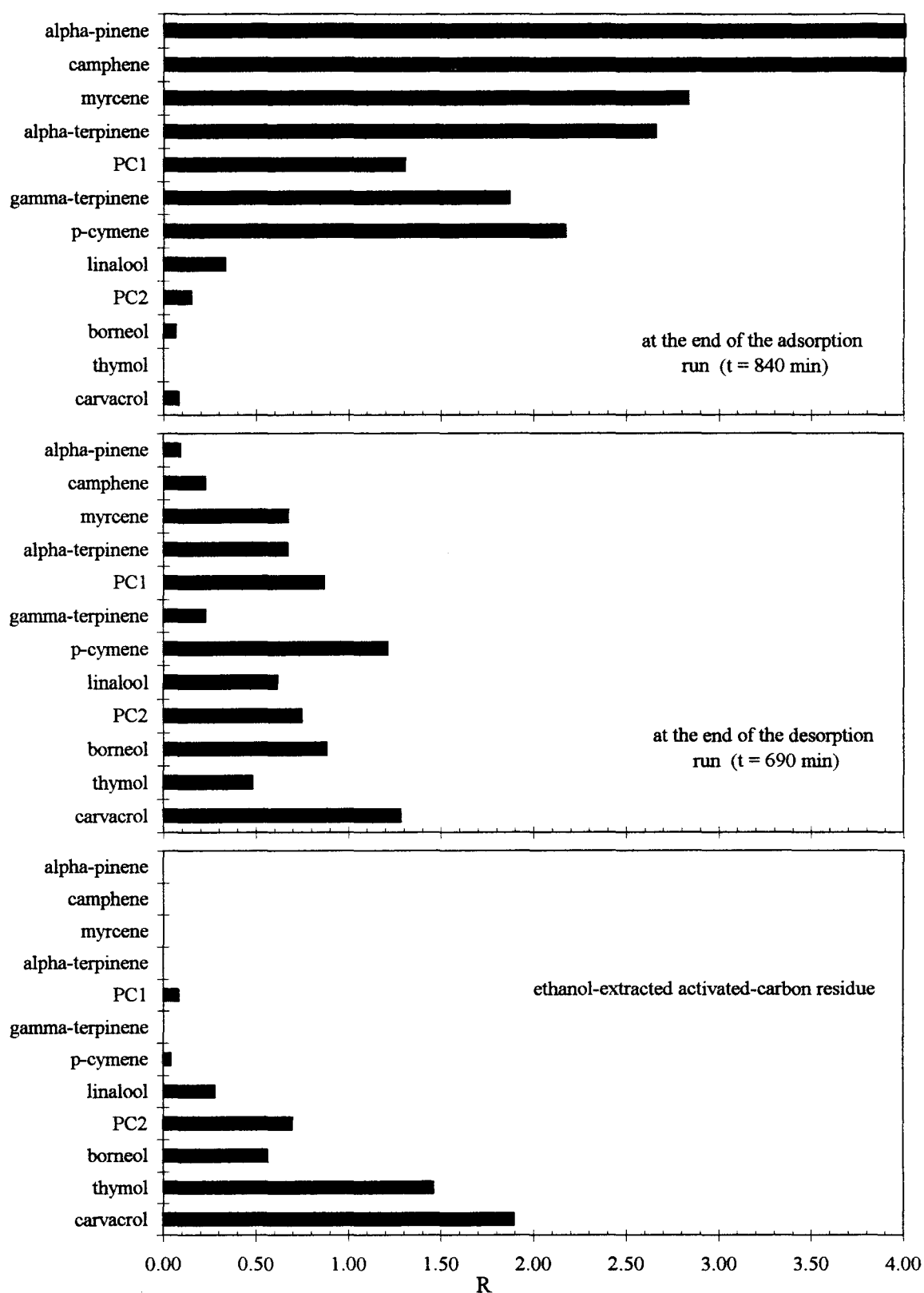


FIGURE 5.4.1.2. Relative-distribution ratios of individual components in the adsorbed (7.5 MPa) and desorbed (14.5 MPa) fractions and of the ethanol-extracted activated-carbon residue, using eight grams activated carbon.

most important characteristic of the activated-carbon residue was its low MT hydrocarbon content (0.9%), as reported in Table D.7, in Appendix D. Hence, MT components were successfully eliminated from the carbon, but a small quantity of *PCI* and *p-cymene* was still present on the sorbent. The minor content of MT constituents in the residue indicates that perhaps longer processing times were necessary to obtain a thorough desorption of these highly volatile compounds. However, an optimum should exist between the recovered quantities and the processing time. On the contrary, this residue contained a high percentage of NMT compounds (99.1%), the major component being *carvacrol* (91.7%). Therefore, the desorption of origanum oil from activated carbon at this temperature and pressure provided effective deterpenation of the oil. The remaining part (residue) which was rich in oxygenated components like alcohols and phenolics (*carvacrol* and *thymol*) will have the essential odor and properties of the origanum oil. The low performance of the desorption process towards the recovery of these compounds may be due to the fact that the bonding forces between the NMT hydrocarbons and the activated carbon were stronger than those between the MTs and the sorbent. For complete desorption of these valuable compounds which contribute to the flavor and aroma of origanum oil, a higher pressure or a higher temperature (since increase in temperature lowers the adsorptive capacity) would be needed. Based on the results of this experiment, a two-step pressure desorption process was implemented: first step at low pressure, 8.0 MPa, to remove the weakly adsorbed MT hydrocarbons followed by desorption at a moderately higher pressure, 14.5 MPa, for the complete recovery of the strongly adsorbed NMT compounds.

#### **5.4.2. Supercritical-CO<sub>2</sub> Desorption with Step-wise Pressure Increase**

Desorption of origanum oil from activated carbon via supercritical CO<sub>2</sub> (desorption following the origanum-oil/CO<sub>2</sub> adsorption coupled with dense-gas extraction) at 40°C /14.5 MPa was proved to be a selective process in removing the unstable MT hydrocarbons of the oil. However, the use of supercritical-CO<sub>2</sub> desorption with a gradual increase of pressure had been demonstrated by several authors (Chouchi et al., 1995, Della Porta et al., 1997) in the aim of fractionating citrus oils using silica gel as adsorbent. They proposed that

the optimum fractionation conditions for these peel oils were 40°C and pressure increasing from 7.5 to 10.0 MPa. Thus, comparable operating conditions were applied to origanum oil desorption since similar compound families were present in both cases. In detail, desorption was started at 40°C and 8.0 MPa for 240 minutes, after which the pressure was increased to 14.5 MPa for the subsequent 450 minutes of desorption.

The relative-distribution ratios of the key components in origanum oil obtained via supercritical-CO<sub>2</sub> desorption from eight grams of activated carbon at 40°C during the two successive pressure steps of 8.0 and 14.5 MPa are reported in Table D.9, in Appendix D. A replicate run at this operating conditions was performed to assess the reproducibility in the desorption experiments. The relative-distribution ratios of the individual components obtained in the replicate run are given in Tables D.10, in Appendix D. All the results are illustrated in Figure 5.4.2.1. The dashed line indicates the instant after which the pressure was increased from 8.0 to 14.5 MPa.

At 40°C, the influence of the desorption pressure on the fractionation of origanum-oil components can be best viewed by comparing the amount (area count) of each component desorbed against the desorption time, in the constant-pressure method at 14.5 MPa, and step-wise pressure increase method (from 8.0 to 14.5 MPa), in Figure 5.4.2.2. (It is important to mention that in this figure, for the sake of simplicity, all area count values obtained from GC/MS analysis were divided by a factor of 10000000). The end of the first step performed at a low pressure was decided by monitoring the GC/MS area counts of the MT compounds, i.e., the desorption pressure was increased when their area counts at 8.0 MPa almost remained constant. As can be seen in Figure 5.4.2.3, the transition between the two desorption steps is clearly marked by the sudden change of curvature in the relative-distribution ratios for all components. But, the effect of pressure increasing from 8.0 to 14.5 MPa was reflected in the desorbed fractions after 60 minutes. This delayed effect may be explained as follows: Both of the desorption steps (8.0 and 14.5 MPa) were carried out at similar CO<sub>2</sub> flow rates; 1.53 g/min and 1.54 g/min at 40°C/8.0 MPa and 40°C/14.5 MPa, respectively. However, the volumetric flow rate of the supercritical solvent within the system (cm<sup>3</sup>/min at operating conditions) is reduced by a factor of about three during the high pressure desorption step as a result of increasing gas density (0.78 g/cm<sup>3</sup> pure CO<sub>2</sub>

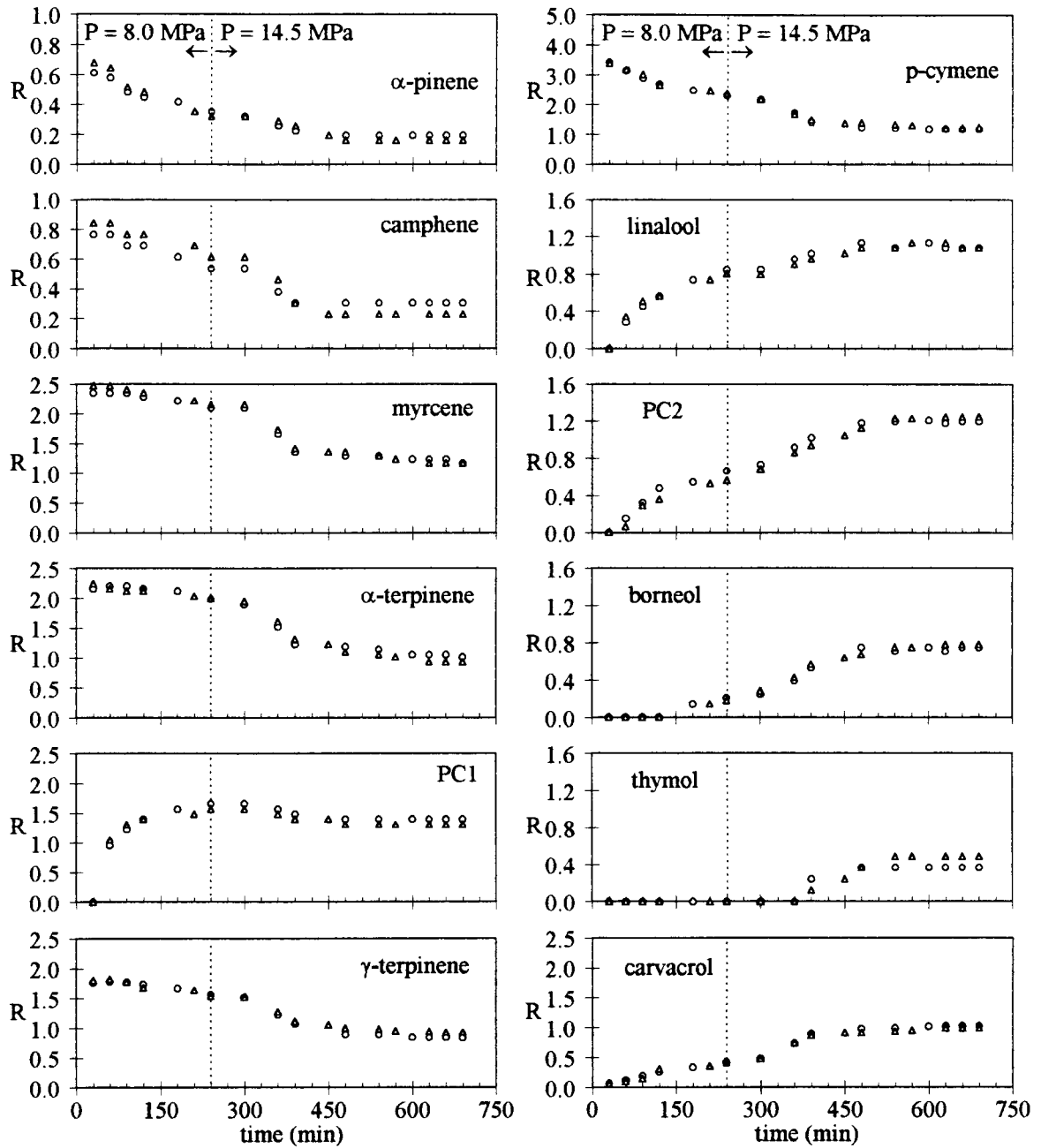


FIGURE 5.4.2.1. Relative-distribution ratios of origanum-oil components in desorption experiment at 40°C with step-wise pressure increase from 8.0 to 14.5 MPa (o, Δ: replicate runs).

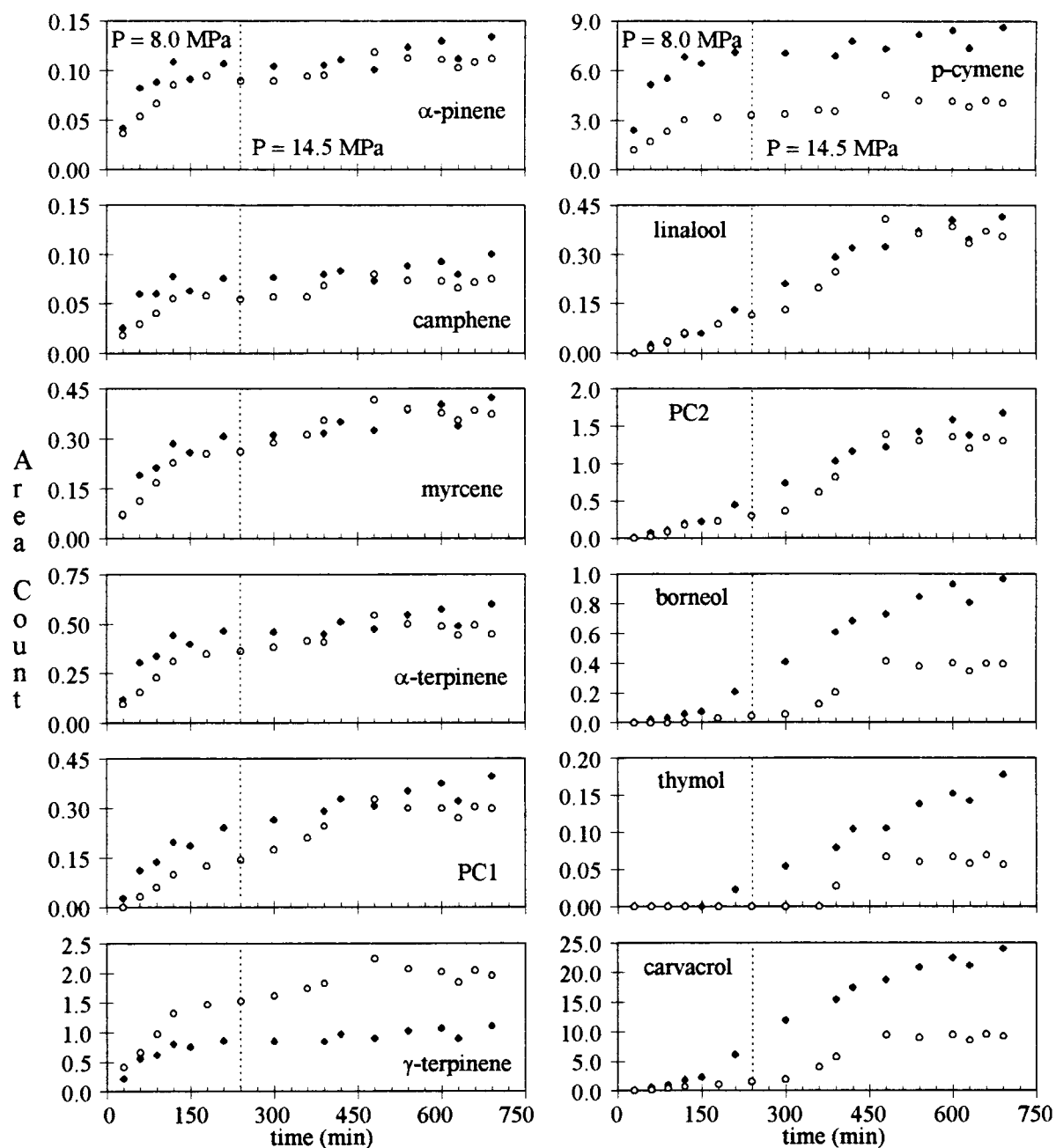


FIGURE 5.4.2.2. Area count results of origanum-oil components in desorption experiment at 40°C (o: with step-wise pressure increase from 8.0 to 14.5 MPa, ◆: with constant-pressure at 14.5 MPa).

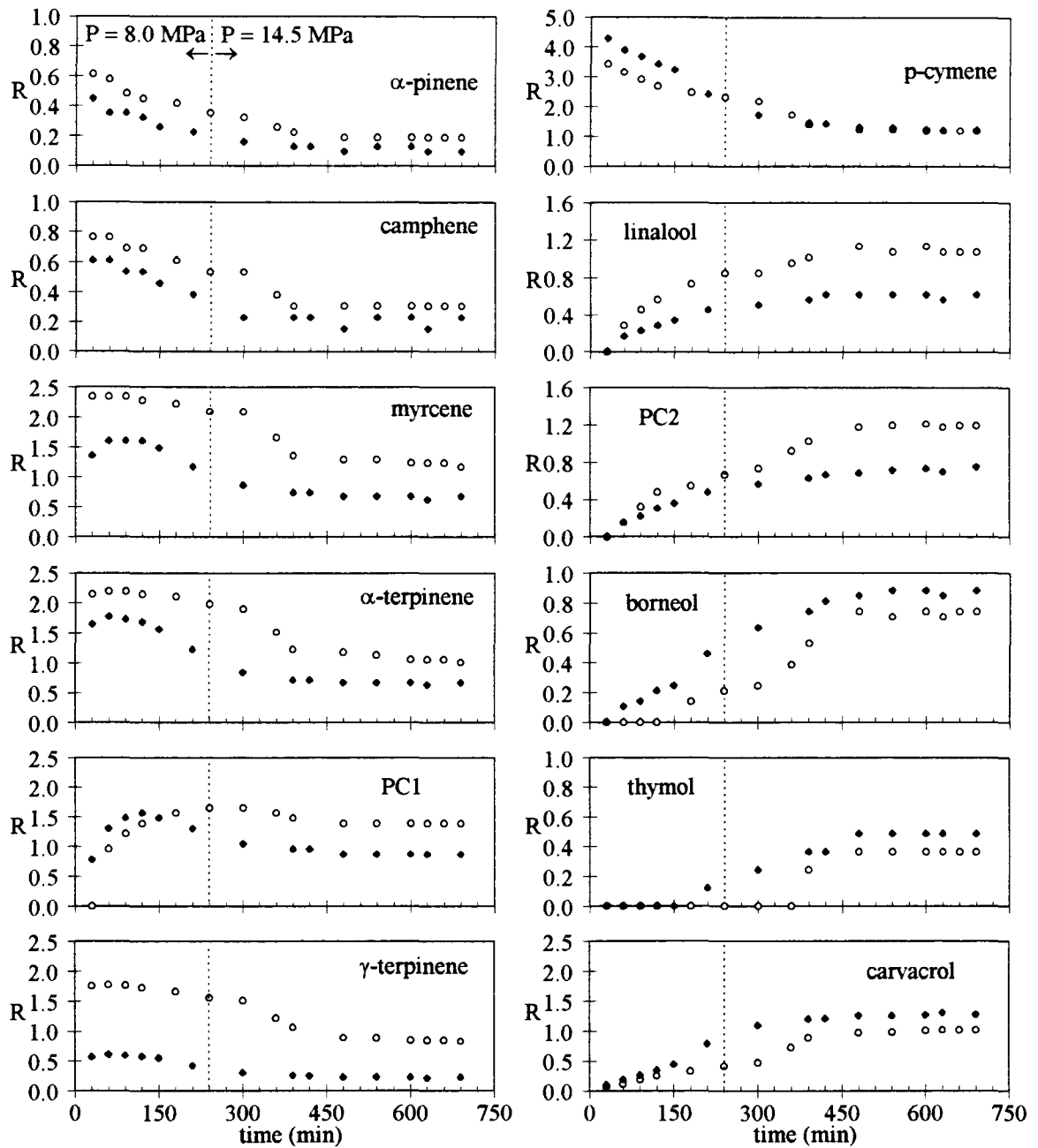


FIGURE 5.4.2.3. Relative-distribution ratios of origanum-oil components in desorption experiment at 40°C (○: with step-wise pressure increase from 8.0 to 14.5 MPa, ◆: with constant-pressure at 14.5 MPa).

density at 40°C/14.5 MPa versus 0.30 g/cm<sup>3</sup> pure CO<sub>2</sub> density at 40°C/8.0 MPa). This argument explains the dead time encountered as the desorption pressure was increased from 8.0 to 14.5 MPa.

As seen in Figure 5.4.2.2, in the first step of the desorption process at 8.0 MPa, the composition of NMT components in the desorbed fractions, with the exception of *linalool*, did not change much with desorption time. Moreover, in the earlier stages of the desorption, the area counts of the NMT components obtained during the constant-pressure process at 14.5 MPa were very close to those obtained at 8.0 MPa conditions. This observation reveals that for the NMT constituents of origanum oil, the transport mechanism of desorption is diffusion limited. In other words, the controlling step in the desorption was the rate of diffusion inside the pores of the activated carbon, and thus interparticle resistances were important. However, as the pressure was increased from 8.0 to 14.5 MPa in the second step of the desorption process, the NMT components were rapidly desorbed. The transition between the two steps is characterized by a sharp increase in the desorption rate of these compounds (slope of the area-count curves changed). This behavior can be explained through fact four, as stated in chapter three. Hence, solubility of oxygenated hydrocarbons in supercritical CO<sub>2</sub> increased and these hard-to-desorb substances (due to higher mass and/or polarity) were desorbed with ease. This pressure effect, coupled with the prompt availability of the NMT components on the porous carbon surface as a consequence of the desorption step at 8.0 MPa (diffusion limited), eventuated increased desorption rates (high mass-transfer coefficients). This conclusion is further strengthened by the significant difference between the area-count curves obtained during the constant-pressure and two-step pressure desorption processes (in the time interval between 240 to 690 minutes).

On the contrary, the desorption of MT components at 8.0 MPa compared to the constant-pressure desorption at 14.5 MPa revealed that the solvating power of the solvent was the controlling step of the desorption process. In other words, as seen in Figure 5.4.2.2, MT hydrocarbons were preferentially desorbed by supercritical CO<sub>2</sub> at higher pressure, with the exception of *γ-terpinene*. This argument explains the significant difference between the area-count curves obtained during the constant-pressure and two-

step pressure desorption processes (in the time interval between 0 to 240 minutes). Once the pressure was increased to 14.5 MPa in the second step, this difference developed to be almost negligible, with the exception of *p-cymene*, and in some parts the curves even overlapped. This experimental evidence also justified the fact that at constant temperature, both fluid-side and particle-side solid-gas mass-transfer coefficients decrease with increasing pressure (Akman, 1991).

It is important to notice in Figure 5.4.2.2 that the area counts of the twelve key components of the origanum oil, with the exception of *γ-terpinene*, during the constant-pressure desorption process at 14.5 MPa were higher than those obtained throughout the step-wise pressure increase procedure. In other words, the preferential loading of both MT and NMT hydrocarbons, with the exception of *γ-terpinene*, into the supercritical phase throughout the desorption process at 14.5 MPa (constant-pressure desorption) compared to the two-step pressure procedure corroborates the fact that increased solvating-power effects on solubility of these essential-oil components in dense-gas solvents are revealed distinctly at pressures higher than the critical pressure of the solvent (critical pressure of CO<sub>2</sub> is 7.3 MPa).

It is also seen from Figure 5.4.2.3 that at the beginning of the two-step desorption process, there existed a jump in the relative-distribution ratios of the MT hydrocarbons, with the exception of *PCI*. This is because MT compounds were desorbed earlier with ease by supercritical CO<sub>2</sub> at 40°C/8.0 MPa conditions. As desorption proceeded, the relative-distribution ratios of these components gradually decreased, and flattened as the pressure was increased to 14.5 MPa (data points at 240 and 300 minutes desorption time), then sharply decreased for a limited time and leveled-off (constant R values after 600 minutes). On the other hand, at 40°C/8.0 MPa conditions, the NMT constituent *borneol* appeared in the effluent after 180 minutes, and *thymol* were not desorbed at all. The increase in pressure from 8.0 to 14.5 MPa resulted in a sharp increase in the relative-distribution ratios of all the NMT hydrocarbons (300-390 minutes), but the curves flattened quickly.

The influence of desorption pressure on the relative-distribution ratios of the MT and NMT cuts of origanum oil is shown in Figure 5.4.2.4. In the earlier stages of

desorption, both component families of the essential oil exhibited comparable behavior, i.e., similar relative-distribution ratios were obtained, independent of desorption pressure (Figure 5.4.2.4). Yet, after 120 minutes of treatment time, the effect of desorption pressure becomes important; most pronounced during the time interval of 180 to 390 minutes (where the difference between the curves is largest). At 8.0 MPa, fast desorption of MT hydrocarbons was observed, whereas NMT hydrocarbons were desorbed slowly. However, as the pressure was increased after 240 minutes of desorption, since the solvating power of the solvent is higher at elevated pressures, fast desorption of both MT and NMT components was obtained. In other words, significant change in the relative-distribution ratios of these compound families is achieved by increasing the desorption pressure. The increase in pressure was encountered by the change in the slope of the relative-distribution curves, but after a limited time (after 480 minutes of desorption), the curves flattened indicating that no further appreciable gain was accomplished by increasing the pressure. Similar behavior was detected towards the end of the constant-pressure desorption process performed at 40°C/14.5 MPa conditions. This observation suggests that adsorption-equilibrium limitations were dominating the supercritical desorptions and that the solubilities of these compounds in supercritical CO<sub>2</sub> were not controlling the transport mechanism.

Figure 5.4.2.5 shows the pressure dependence of the selectivity (separation factor) against the desorption time. For example, the separation between the MT and NMT cuts obtained after 300 minutes of desorption was 1.01 and 3.50 for the constant-pressure and two-step pressure processes, respectively. In other words, at higher pressures, relative-distribution ratio of the MT cut was equal to that of the NMT cut, indicating no selectivity of supercritical CO<sub>2</sub> for either of the groups. On the other hand, at low pressures (8.0 MPa), MT components tended to concentrate in the dense-gas phase ( $R_{MT}=1.74$ ), as opposed to the NMT compounds which were strongly retained on the sorbent ( $R_{NMT}=0.50$ ). This behavior can be explained by the fact that the MT hydrocarbons, being the most volatile substances of the origanum oil, were selectively desorbed by supercritical CO<sub>2</sub>. Hence, desorption at 40°C/8.0 MPa conditions via supercritical CO<sub>2</sub> proved to be effective in fractionating origanum oil since the separation between MT and NMT cuts in the desorbed fraction were about four times higher than the one obtained at 40°C/14.5 MPa desorption. However, once the pressure was increased to 14.5 MPa in the second step of

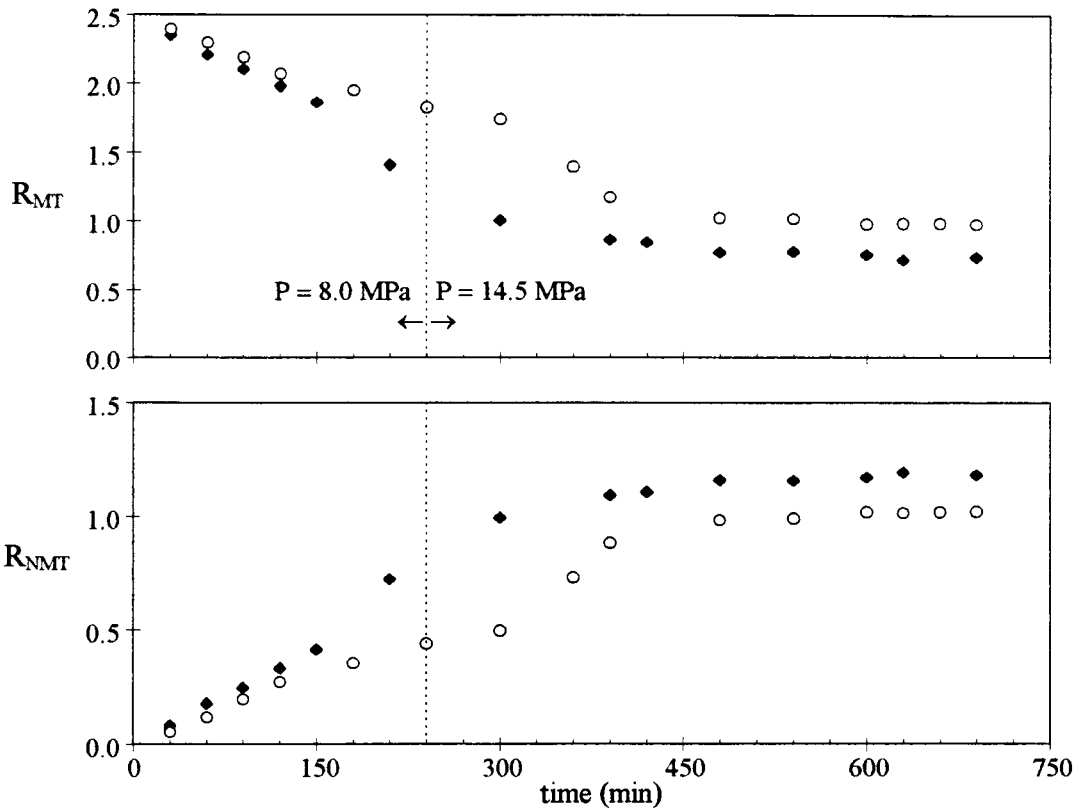


FIGURE 5.4.2.4. Pressure dependence of the relative-distribution ratios of MT and NMT cuts in desorption run at 40°C (○: with step-wise pressure increase from 8.0 to 14.5 MPa, ◆: with constant-pressure at 14.5 MPa).

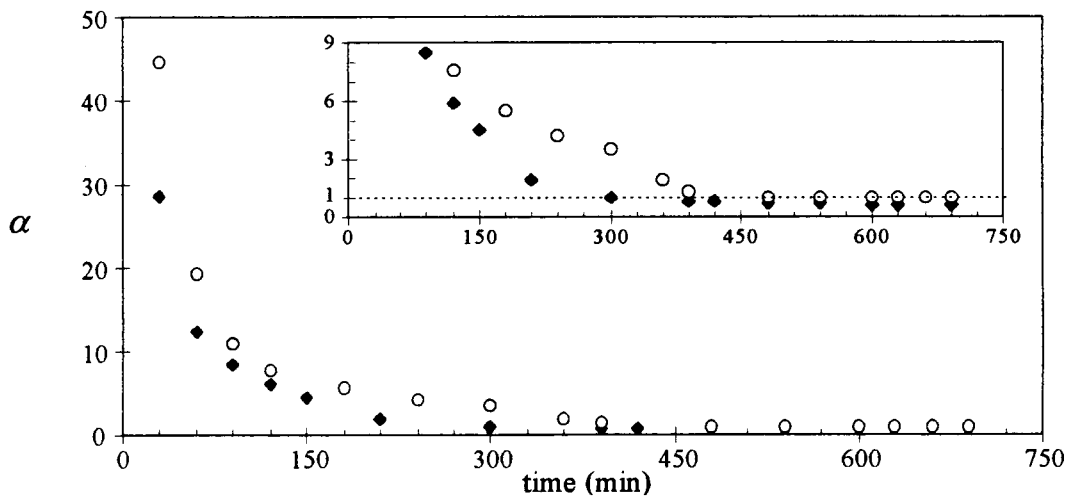


FIGURE 5.4.2.5. Pressure dependence of the separation factor in desorption run at 40°C (○: with step-wise pressure increase from 8.0 to 14.5 MPa, ◆: with constant-pressure at 14.5 MPa).

the desorption process, a faster desorption of both compound families was obtained, but after 690 minutes of desorption, a large decrease in the desorption selectivity was observed ( $\alpha=0.95$ ). The decrease in selectivity is because with increasing pressure, the solubilities of these essential-oil components grow dramatically due to strong increase of solvent density. Hence, a greater quantity of NMT hydrocarbons is co-desorbed. A similar result was also observed during the desorption of *mandarin peel oil* by supercritical CO<sub>2</sub> (Della Porta et al., 1997). A decrease in desorption selectivity,  $\alpha$ , was also detected at the end of the constant-pressure desorption process, i.e., the separation between the MT and NMT cuts obtained after 690 minutes of desorption was 0.62. The decrease in desorption selectivity was expected since the amount of MT hydrocarbons in the activated carbon decreased with time. Consequently, the concentration of the harder-to-desorb substances (NMT constituents; due to high molecular mass coupled with their strong affinity with the sorbent) increased with time. Therefore, in fractionating origanum oil via supercritical-CO<sub>2</sub> desorption and in optimizing the operating policies, the trade-off between complete recovery of NMT hydrocarbons and selectivity of the process should be prudently taken into consideration.

The supercritical-CO<sub>2</sub> desorption of origanum oil performed by the step-wise pressure increase procedure was terminated after 690 minutes, then the carbon sample was removed and weighed prior to treatment with ethanol to remove the strongly-adsorbed fraction of the oil. As opposed to the expected behavior, there was a decrease (3.13%) in the weight of the activated carbon; similar behavior was observed after the constant-pressure desorption performed at 40°C/14.5 MPa conditions. Figure 5.4.2.6 shows the composition (normalized area percentages for each key component) in the fraction collected at the end of the low-pressure desorption step, at the end of the high-pressure desorption step and in the ethanol-extracted activated-carbon residue. At the end of the low-pressure desorption step, after 240 minutes of desorption at 40°C/8.0 MPa conditions, the ratio between the MT and NMT hydrocarbons (0.74:0.26) was different from the one in the original oil (0.40:0.60) due to the fact that MT components were desorbed faster than NMTs as a consequence of fact five, as stated in chapter three. These properties, coupled with the weak bonding forces between the sorbent and MT compounds (recall fact 15, as stated in chapter three), makes them easily desorbable by supercritical CO<sub>2</sub>. After 690

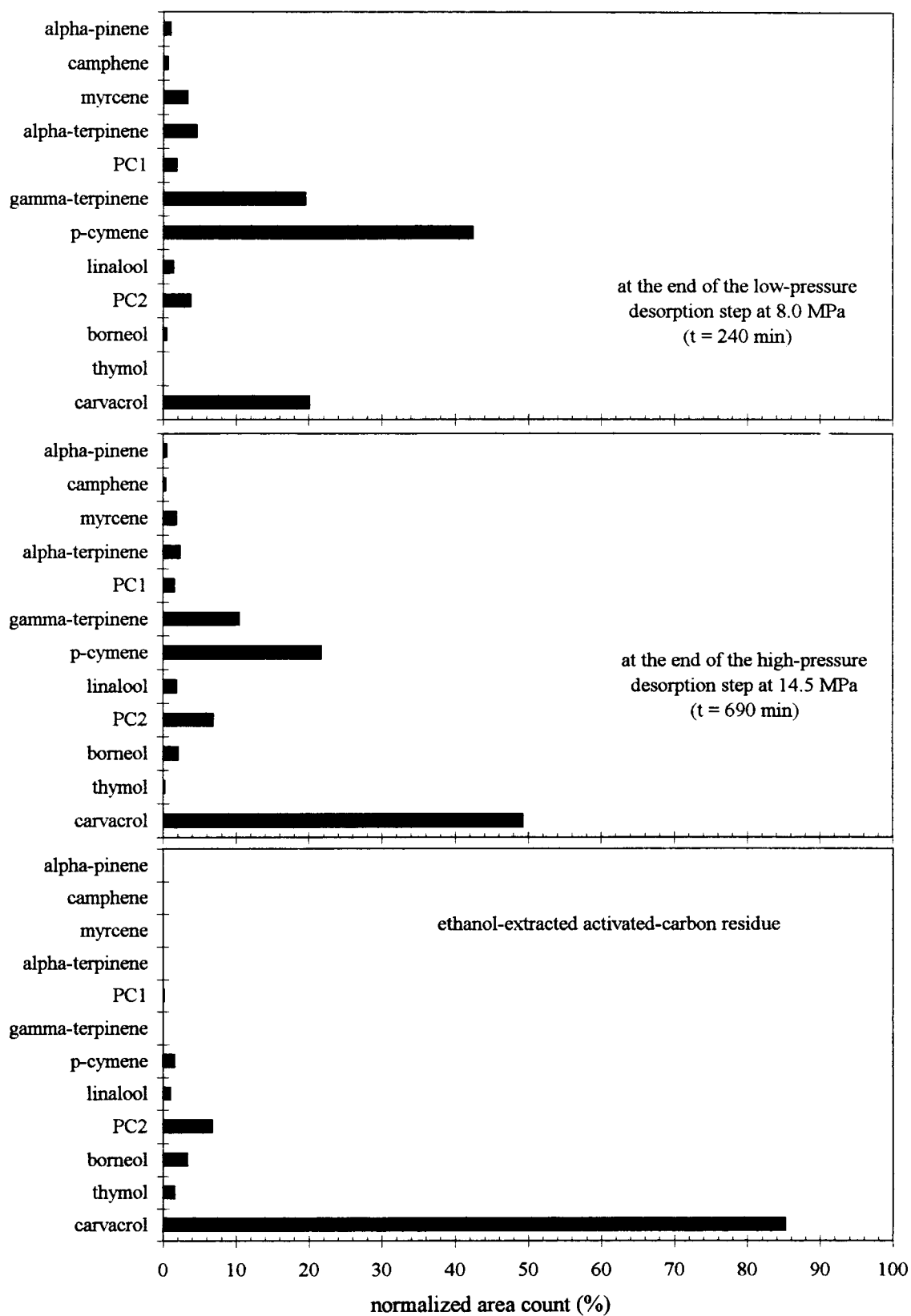


FIGURE 5.4.2.6. Normalized area counts of individual components in the desorption run at the end of 40°C/8.0 MPa step, 40°C/14.5 MPa step and in the ethanol-extracted activated-carbon residue.

minutes of desorption, the solubility of NMT hydrocarbons increased due to fact four, as stated in chapter three; hence large quantities of NMT constituents (60.7%) were co-desorbed with small quantities of MT components (39.3%). This evidence could demonstrate that the first step performed at 8.0 MPa produced the selective desorption of the MT hydrocarbons and the second one performed at 14.5 MPa assured the fast desorption of the NMT components.

Furthermore, the low MT hydrocarbon content in the ethanol-extracted activated-carbon residue (1.8%), as seen in Figure 5.4.2.6, indicates that MT components were successfully eliminated from the carbon, but a small quantity of *PCI* and *p-cymene* still remained on the sorbent. Hence, the minor content of MT constituents in the residue indicates that perhaps longer processing times were necessary to obtain a thorough desorption of these highly volatile compounds. However, an optimum should exist between the recovered quantities and the processing time. On the contrary, the residue contained a high-percentage of NMT compounds (98.2%), the major component being *carvacrol* (85.3%). The remaining part (residue) which was rich in oxygenated components like alcohols and phenolics (*carvacrol* and *thymol*) will have the essential odor and properties of the origanum oil. Therefore, these two steps allowed a fast and quasi-complete recovery of all NMT constituents contained in this origanum oil. The proposed fractionation scheme (by supercritical-CO<sub>2</sub> desorption) is not the only procedure that it is possible to apply. For example, a larger pressure increase after 240 minutes of desorption could produce faster processing.

### 5.5. Fractionation of Origanum Oil by Supercritical-CO<sub>2</sub> Adsorption Following Dense-Gas Extraction at 40°C/7.5 MPa Using Silica Gel Adsorbent

Selective elimination of the unstable monoterpene (MT) hydrocarbons, which impair the essential-oil quality, were obtained by starting the adsorption (following the dense-gas extraction) process on a bed of activated carbon with a continuous feed of origanum-oil/CO<sub>2</sub> mixture at 40°C/7.5 MPa conditions. Then, desorption with pure supercritical CO<sub>2</sub> was executed in order to recover the valuable essential-oil constituents of this origanum oil, namely non-monoterpene (NMT) hydrocarbons. It could be concluded that activated carbon is a promising adsorbent in deterring origanum oil by supercritical CO<sub>2</sub>. However, several authors (Cully et al., 1990, Dugo et al., 1995) proposed silica gel as the best adsorbent in fractionating citrus oils by supercritical CO<sub>2</sub>. Therefore, a number of adsorption/desorption experiments coupled with dense-gas extraction using silanized silica gel as the adsorbent were performed by supercritical CO<sub>2</sub> at the same process conditions (temperature, pressure, CO<sub>2</sub> flow rate and amount of oil pumped) applied in the case of activated carbon.

In chapter three, the different types of supercritical-CO<sub>2</sub> adsorption (following the dense-gas extraction) experiments carried out were shown schematically (Figures 3.2.1 and 3.2.2), and the facts considered in performing these distinct operations were explained in detail. In this section, the supercritical-CO<sub>2</sub> adsorption of origanum-oil/CO<sub>2</sub> mixture onto silanized silica gel at 40°C/7.5 MPa conditions (Figure 3.2.1) will be discussed. Two sets of runs were performed: first using eight grams of silica gel, second using 15 grams of silica gel. The experimental results will be discussed in terms of relative-distribution ratios (and normalized area counts) of the twelve major components and of the MT and NMT cuts of origanum oil. Comparison with simple supercritical-CO<sub>2</sub> extraction and supercritical-CO<sub>2</sub> adsorption (following the dense-gas extraction) using activated carbon will also be presented in this section. From now on, for the sake of simplicity, the process “supercritical-CO<sub>2</sub> adsorption following the dense-gas extraction” will be named as “supercritical-CO<sub>2</sub> adsorption”.

### 5.5.1. Supercritical-CO<sub>2</sub> Adsorption Following Dense-Gas Extraction on Eight Grams Silica Gel

The relative-distribution ratios of the key components in organum oil obtained via supercritical-CO<sub>2</sub> adsorption at 40°C/7.5 MPa using eight grams of silanized silica gel are given in Table D.11, in Appendix D, and illustrated in Figure 5.5.1.1. All MT hydrocarbons, with the exception of *PCI*, emerged in the effluent earlier than the NMT components indicating a weaker affinity towards the silica gel sorbent. Since MTs were eluted first, they were always present in the effluent as adsorption proceeded. *PCI* was retained more than the other MT hydrocarbons; this can be explained by considering fact ten, as stated in chapter three. The oxygenated part of *PCI* (*1,8 cineole*) characterized by high polarity (due to the presence of -OH group) has a pronounced effect on the behavior of this component.

At 40°C/7.5 MPa, compared to the MT behavior, the breakthrough curves of NMT hydrocarbons are more distinct and spread out. It is important to notice in Figure 5.5.1.1 that *PC2* was retained slightly more than the MTs, but appeared in the effluent earlier than the other NMT hydrocarbons. This is because *β-caryophyllene* (the sesquiterpene fraction of *PC2*) has a high molecular mass, but vapor pressure of this substance is close to that of limonene, a MT component (Platin et al., 1994). Similar breakthrough behavior of pure *β-caryophyllene* is also found in literature (Subra et al., 1998). Hence, the experimental results obtained using silica gel adsorbent were almost similar with those of activated carbon. In other words, NMT hydrocarbons were preferentially adsorbed on silanized silica gel ( $R < 1$ ), whereas MTs showed an opposite behavior; they tended to concentrate in the dense-gas phase with  $R$  values greater than unity.

The general pattern of the breakthrough curves reveals that the MT and NMT components showed different behavior as adsorption proceeded. The breakthrough order can be explained regarding the relative strength of interactions occurring during adsorption between the solute, the sorbent and the fluid phases. Dealing with a supercritical medium, vapor pressure, polarity and molecular mass are properties which have a special influence on solubility. MT hydrocarbons possess the highest vapor pressures among the key

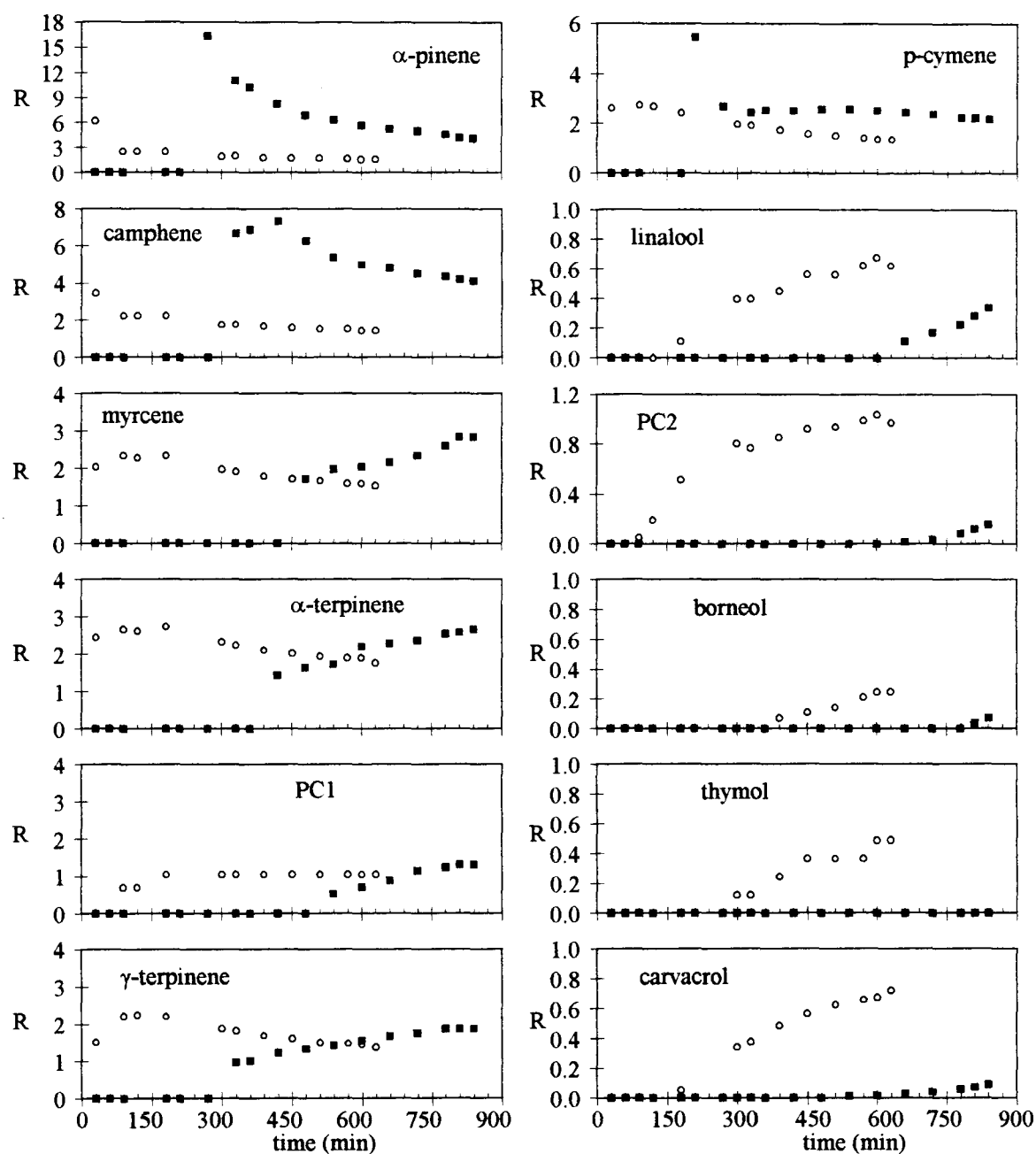


FIGURE 5.5.1.1. Relative-distribution ratios of origanum-oil components in adsorption experiment at 40°C/7.5 MPa using eight grams adsorbent (■: activated carbon, ○: silica gel).

components of this origanum oil (Stahl et al., 1988). Hence, due to fact five, as stated in chapter three, MT hydrocarbons are more soluble in dense CO<sub>2</sub> than other essential-oil components. On the other hand, the surface of silanized silica gel offers two sites of interaction: apolar SiCH<sub>3</sub> sites and polar SiOH sites. The presence of OH-groups imparts a degree of polarity to the surface of silica gel, in this case, the alcohols (*linalool*, *terpinen-4-ol*, *borneol*) and the phenols (*thymol* and *carvacrol*) would have an affinity for the polar sites of the surface, but also for the apolar ones due to the non-polar part of their molecule (Reverchon and Iacuzio, 1997). MT hydrocarbons (*α-pinene*, *camphene*, *myrcene*, *α-terpinene*, *γ-terpinene* and *p-cymene*) and sesquiterpenes (*β-caryophyllene*) can be adsorbed on CH<sub>3</sub>-groups of silica gel, so they would have a greater affinity for the apolar sites only. The breakthrough order is thus understandable regarding the strength of the interactions with both the fluid and the sorbent.

Supercritical-CO<sub>2</sub> adsorption on activated carbon and silanized silica gel can be compared regarding the evolution in the normalized area count (per cent) of the individual components (Figure 5.5.1.2) and of the MT and NMT cuts (Figure 5.5.1.3). As can be seen in Figure 5.5.1.2, after 330 minutes of adsorption on carbon, the fraction accumulated in the sample collector was formed by solely MT hydrocarbons, with *p-cymene* (44.8%) and *α-pinene* (34.3%) being major, but not all the key compounds of this family were eluted. Hence, the MT content of the effluent was 100% (Figure 5.5.1.3). However, in the case of adsorption on silica gel, NMT hydrocarbons (23.4%), with the exception of *borneol*, were also detected in this fraction, but together with MT components (76.6%). In both cases, all samples collected at higher adsorption times demonstrated a progressive decrease in MT compounds, consequently an increase in NMT hydrocarbons. For example, the sample analyzed after 600 minutes of adsorption on carbon, comprised mainly of MT hydrocarbons (99.3%) and the phenolic compound *carvacrol*, whereas all NMT components (41%) together with MT hydrocarbons (59%) were present in the case of adsorption on silica. This observation can be explained by the fact that the bonding forces between MT hydrocarbons and activated carbon are stronger compared to that between MT hydrocarbons and silanized silica gel. Moreover, NMT hydrocarbons also have a stronger affinity towards the activated carbon compared to silanized silica gel.

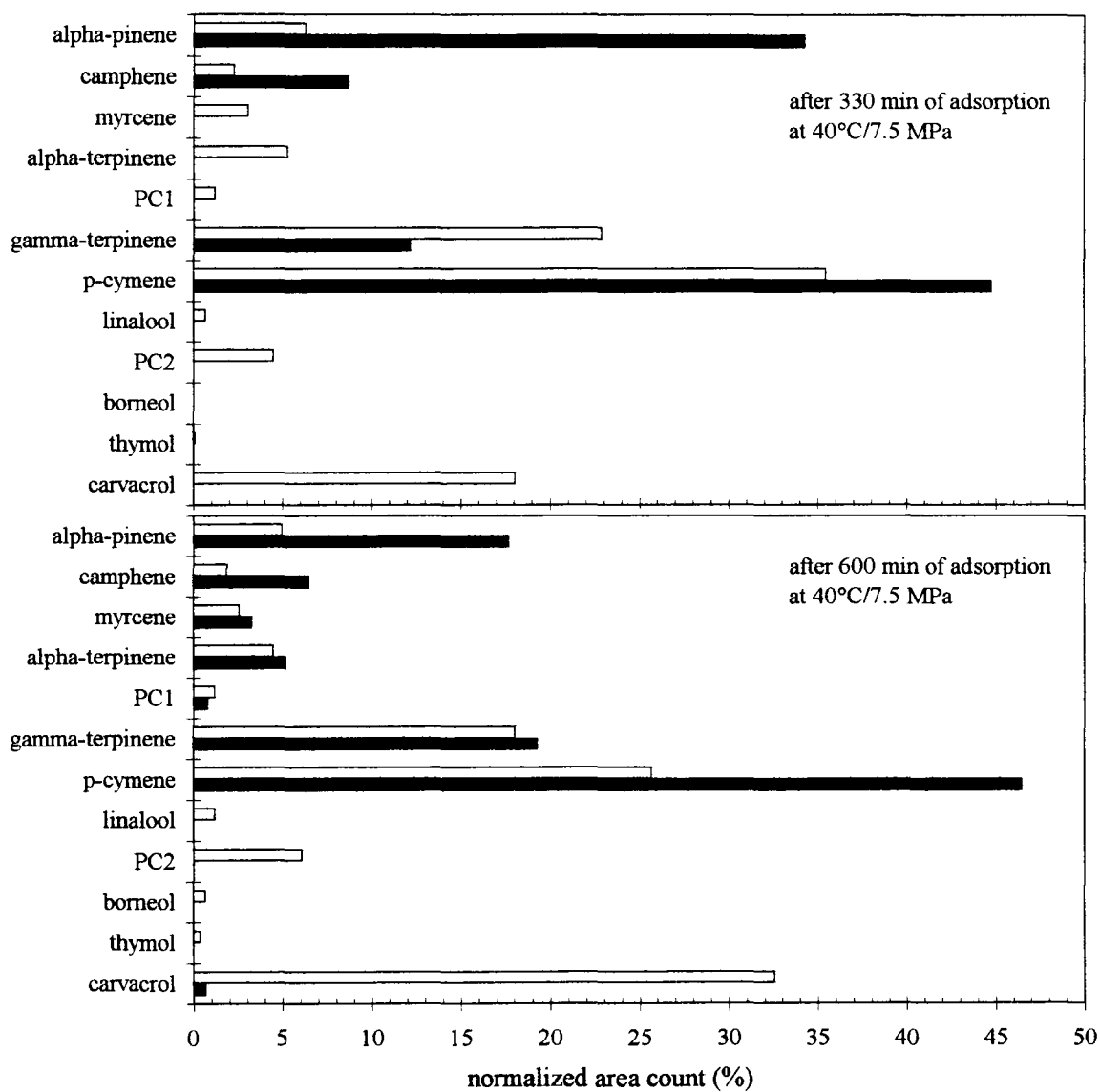


FIGURE 5.5.1.2. Time dependence of the normalized area count of individual components in adsorption runs at 40°C/7.5 MPa (□: silica gel, ■: activated carbon).

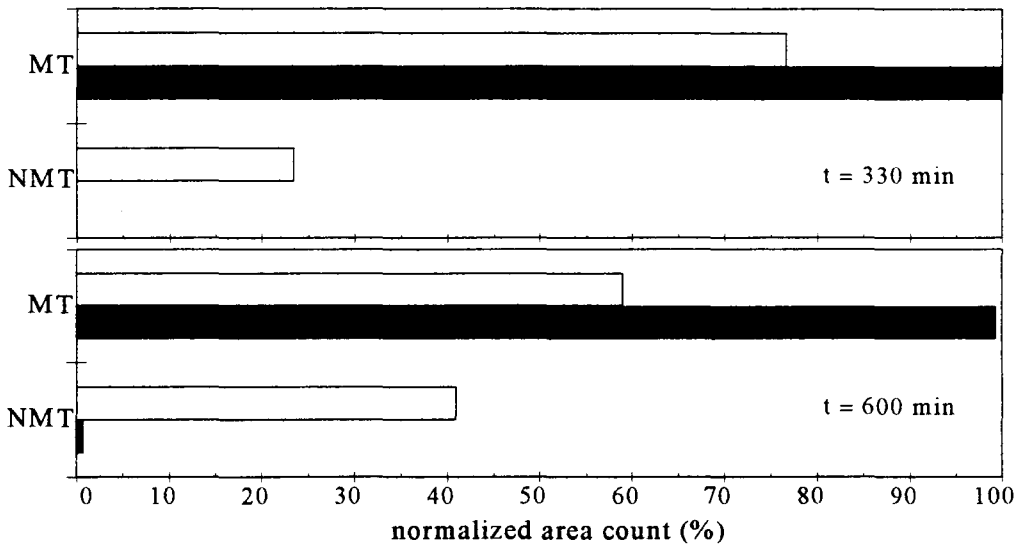


FIGURE 5.5.1.3. Time dependence of the normalized area count of MT and NMT cuts in adsorption runs at 40°C/7.5 MPa (□: silica gel, ■: activated carbon).

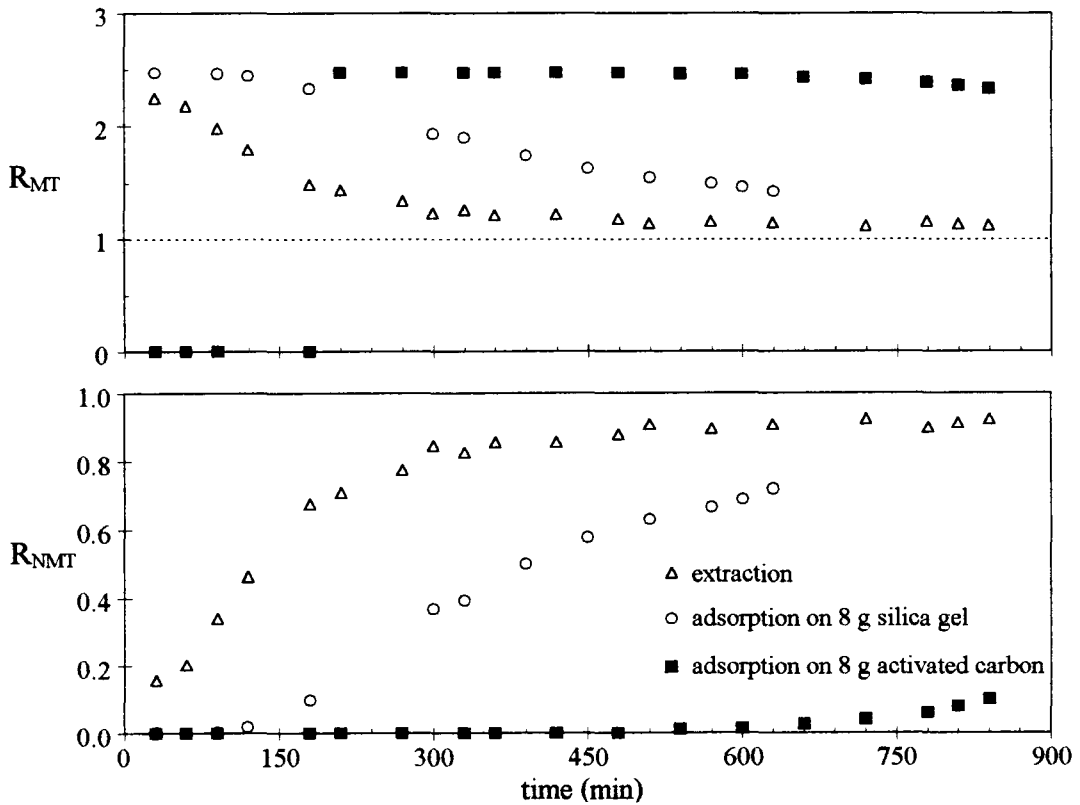


FIGURE 5.5.1.4. Relative-distribution ratios of MT and NMT cuts during extraction and adsorption experiments at 40°C/7.5 MPa.

The purpose of the supercritical-CO<sub>2</sub> adsorption experiments was to remove the MT hydrocarbons and leave the NMT compounds behind, hence a minimum amount of NMT components in the fractions collected is desired. This criteria was successfully achieved during the adsorption process on activated carbon since NMT key compounds of this organum oil were selectively retained by the sorbent and MT constituents were preferentially concentrated in the dense-gas phase. Thus, a deterpenated fraction of this essential oil was obtained on the adsorbent. Next, desorption with pure supercritical CO<sub>2</sub> was carried out to collect the valuable NMT hydrocarbons in a separate collector. Based on the experimental evidence, it can be concluded that activated carbon is a superior adsorbent compared to silanized silica gel in fractionating and eliminating the unstable hydrocarbons of organum oil.

Relative-distribution ratios of the MT and NMT cuts of the extracts obtained via supercritical-CO<sub>2</sub> extraction, adsorption on eight grams silica gel and adsorption on eight grams activated carbon at 40°C/7.5 MPa conditions are represented in Figure 5.5.1.4. As can be seen from this figure, the relative-distribution ratios of the MT cut obtained during adsorption on carbon were much higher than those obtained during extraction or adsorption on silica, but, in all these experiments, with R values greater than unity, MT hydrocarbons tended to concentrate in the dense-gas phase. The relative-distribution ratios of the NMT cut obtained during adsorption with carbon were much lower than those obtained in the other runs. It is important to notice in this figure that during the adsorption process on silanized silica gel, MT components emerged in the effluent at the same instant (after 30 minutes) as in the extraction run, however their appearance was delayed for 210 minutes during the adsorption process on carbon. However, the breakthrough time of the NMT components in the extraction and adsorption with silica gel runs was different (30 and 90 minutes, respectively), but these components were collected in the effluent after 540 minutes of adsorption on carbon. These results point to the fact that MT hydrocarbons show a low affinity for the carbon sorbent, yet lower affinity for the silica gel sorbent, in conjunction with a high affinity for CO<sub>2</sub>. On the contrary, the NMTs show a high affinity for the silica gel sorbent, even higher affinity for the carbon sorbent, in conjunction with a low affinity for CO<sub>2</sub> since R values of this cut is less than unity. Moreover, from the point of view of organum oil fractionation, the closer the breakthrough curves of the MT and NMT

hydrocarbons are, the less the composition of the effluent would vary, hence it would be very hard to obtain a deterpenated essential-oil product. The validity of this argument was ascertained in Figure 5.5.1.1, activated carbon is better in fractionating origanum oil into its major components.

It is also important to notice in Figure 5.5.1.4 that the relative-distribution ratios of the MT cut decreased with time as that of the NMT cut increased, independent of process type. This behavior can be explained regarding fact one, as stated in chapter three. In other words, as the MT hydrocarbons were eluted earlier (due to high solubility in supercritical fluid and/or low affinity towards the sorbent) than the NMT components, they were already present in the effluent as the NMT hydrocarbons started to emerge in the effluent. Figure 5.5.1.5 shows the ratio of the area counts (obtained from the GC/MS analysis) of the MT and NMT cuts in the samples collected to that in the original origanum oil. As clearly seen, the area counts (recall fact two, as stated in chapter three) of both groups increase with time because the amount of origanum-oil components continuously aggregate in the sample collector. Therefore, the decrease in the relative-distribution ratios of the MTs does not imply that MT hydrocarbons did not accumulate in the samples collected. It is also important to notice in Figure 5.5.1.5 that the area count ratios of the MT cut obtained during the extraction run were the highest followed by those obtained during adsorption on silica and those obtained during adsorption on carbon. This is because during the extraction experiment, since the column following the mixing cell was filled with glass beads (Figure 3.2.1), only the solubility of origanum-oil components in supercritical CO<sub>2</sub> was controlling the process, whereas by the introduction of activated carbon or silica gel, the affinity of the origanum-oil components for the sorbent also becomes important. In that case, both MT (to some degree) and NMT (preferentially) hydrocarbons tend to accumulate on the sorbent, hence the amount of origanum-oil components solubilized in the supercritical CO<sub>2</sub> phase decreases, and consequently, their amount in the sample collector diminishes. This argument also confirms the validity of the fact that the higher the area counts are the more the essential-oil components will be accumulated in the sample collector.

As seen in Figure 5.5.1.6, considering the sample collected after 330 minutes of extraction, adsorption on eight grams of silica gel, and adsorption on eight grams of

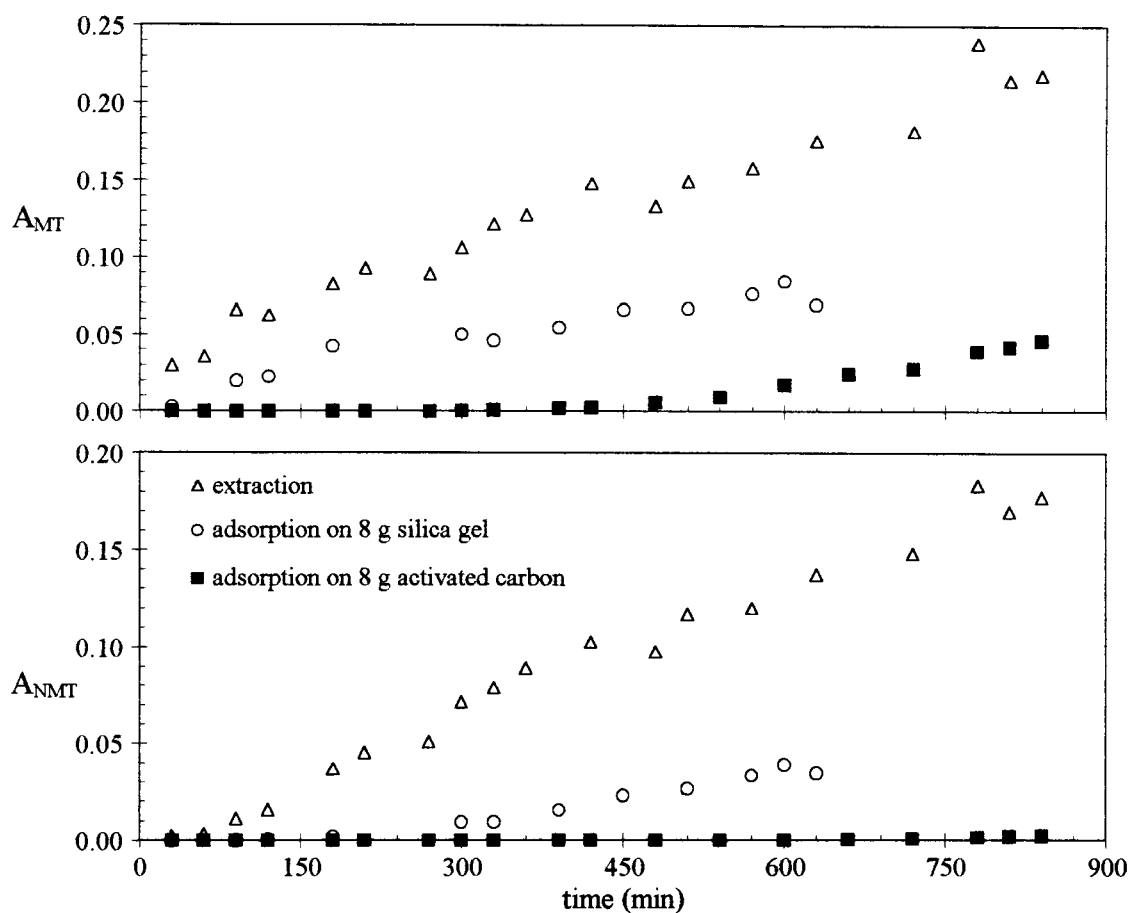


FIGURE 5.5.1.5. Ratio of the area counts of the MT and NMT cuts in the sample to that in the original oil at 40°C/7.5 MPa during extraction and adsorption runs.

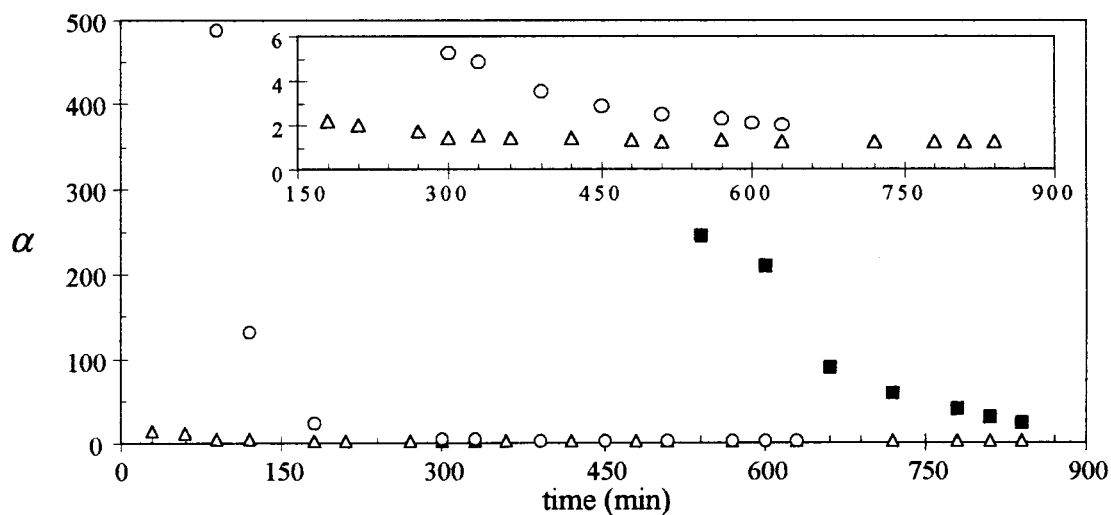


FIGURE 5.5.1.6. Separation factor at 40°C/7.5 MPa during extraction and adsorption runs ( $\Delta$ : extraction, adsorption:  $\circ$ : 8 g silica gel,  $\blacksquare$ : 8 g activated carbon).

activated carbon experiments, the separation,  $\alpha$ , achieved between MT and NMT hydrocarbons is 1.52, 4.82 and infinity (since  $R_{\text{NMT}}$  is equal to zero), respectively. These results show that the NMT components were more selectively adsorbed on either sorbent than the MT constituents, and the separation factor has tripled in the presence of silica gel compared to extraction. Considering the sample collected after 600 minutes in extraction, adsorption on eight grams of silica gel, and adsorption on eight grams of activated carbon experiments, the separation,  $\alpha$ , achieved between these two groups is 1.27, 2.12 and 209.01, respectively. The decrease in selectivity with time is expected as the amount of NMT components in the sample collector increases with time. Based on the results of this experiment, it can be concluded that, compared to silanized silica gel, activated carbon is a more promising adsorbent in fractionating origanum oil (or similar oils), thus improving the quality of this oil through the removal of the MT hydrocarbons (deterpenation). On the other hand, compared to silanized silica gel, longer adsorption times were required for saturating the activated carbon adsorbent. Therefore, in the aim of improving origanum oil quality, the trade-off between adsorption duration and elimination of MT hydrocarbons should be prudently taken into consideration in optimizing the operating conditions.

### **5.5.2. Supercritical-CO<sub>2</sub> Adsorption Following Dense-Gas Extraction on 15 Grams Silica Gel**

The supercritical-CO<sub>2</sub> adsorption on silanized silica gel was studied, with the aim of comparing the effectiveness of the adsorbent to activated carbon. It was concluded that silica gel improved the selectivity of the simple supercritical-CO<sub>2</sub> extraction process through the different affinities of the MT and NMT hydrocarbons for the sorbent. However, supercritical-CO<sub>2</sub> adsorption on activated carbon was more promising since compared to silica gel, enhanced fractionation of origanum-oil components was obtained. On the other hand, it was noticed that the experimental studies in the literature performed via supercritical CO<sub>2</sub> used higher amounts of silica gel in the aim of fractionating citrus peel oils. Therefore, adsorption run was conducted using 15 grams of silanized silica gel at

40°C/7.5 MPa conditions and at the same operating conditions (CO<sub>2</sub> flow rate and amount of oil pumped) as used in the adsorption on eight grams of silanized silica gel.

The relative-distribution ratios of the key components in origanum oil obtained via supercritical-CO<sub>2</sub> adsorption at 40°C/7.5 MPa using 15 grams of silanized silica gel are given in Table D.12, in Appendix D, and illustrated in Figure 5.5.2.1. As can be seen from this figure, the breakthrough behavior obtained is similar to that during the adsorption process performed at 40°C/7.5 MPa using eight grams of silanized silica gel (Figure 5.5.1.1). It is important to point out that increasing the amount of silica gel adsorbent does not affect the breakthrough behavior of the MT hydrocarbons. This experimental observation strengthens the validity of the argument that MT compounds are weakly adsorbed on silanized silica gel. However, the appearance of the NMT constituents in the effluent, with the exception of *carvacrol*, was delayed as the amount of silica gel was increased. Since NMT hydrocarbons exhibit higher affinity towards the silica gel, extended breakthrough times of these components was expected because the number of active sites available for adsorption was increased. The breakthrough location of *carvacrol* did not change with the sorbent amount, but the relative-distribution ratios obtained during adsorption on 15 grams silica gel were lower indicating that this phenolic constituent of origanum oil was strongly retained by silanized silica gel.

Relative-distribution ratios of the MT and NMT groups in the samples collected during the supercritical-CO<sub>2</sub> adsorption experiments on eight and 15 grams silica gel at 40°C/7.5 MPa conditions are represented in Figure 5.5.2.2. For the MT cut, relative-distribution ratios did not vary significantly as the amount of silica gel adsorbent was increased, moreover, in the early stages of adsorption their R values overlapped. It is important to notice in this figure that MT hydrocarbons with R values greater than unity, tended to concentrate in the dense-gas phase, independent of adsorbent amount, whereas NMT hydrocarbons, with R values less than unity, were strongly adsorbed. The effect of silica gel amount was more important for substances exhibiting a higher affinity for the sorbent. Indeed, the increase of silica gel quantity lead to lower relative-distribution ratios and longer breakthrough time of the NMT cut. From the point of view of origanum oil fractionation, the modification of the breakthrough location of the NMT hydrocarbons is

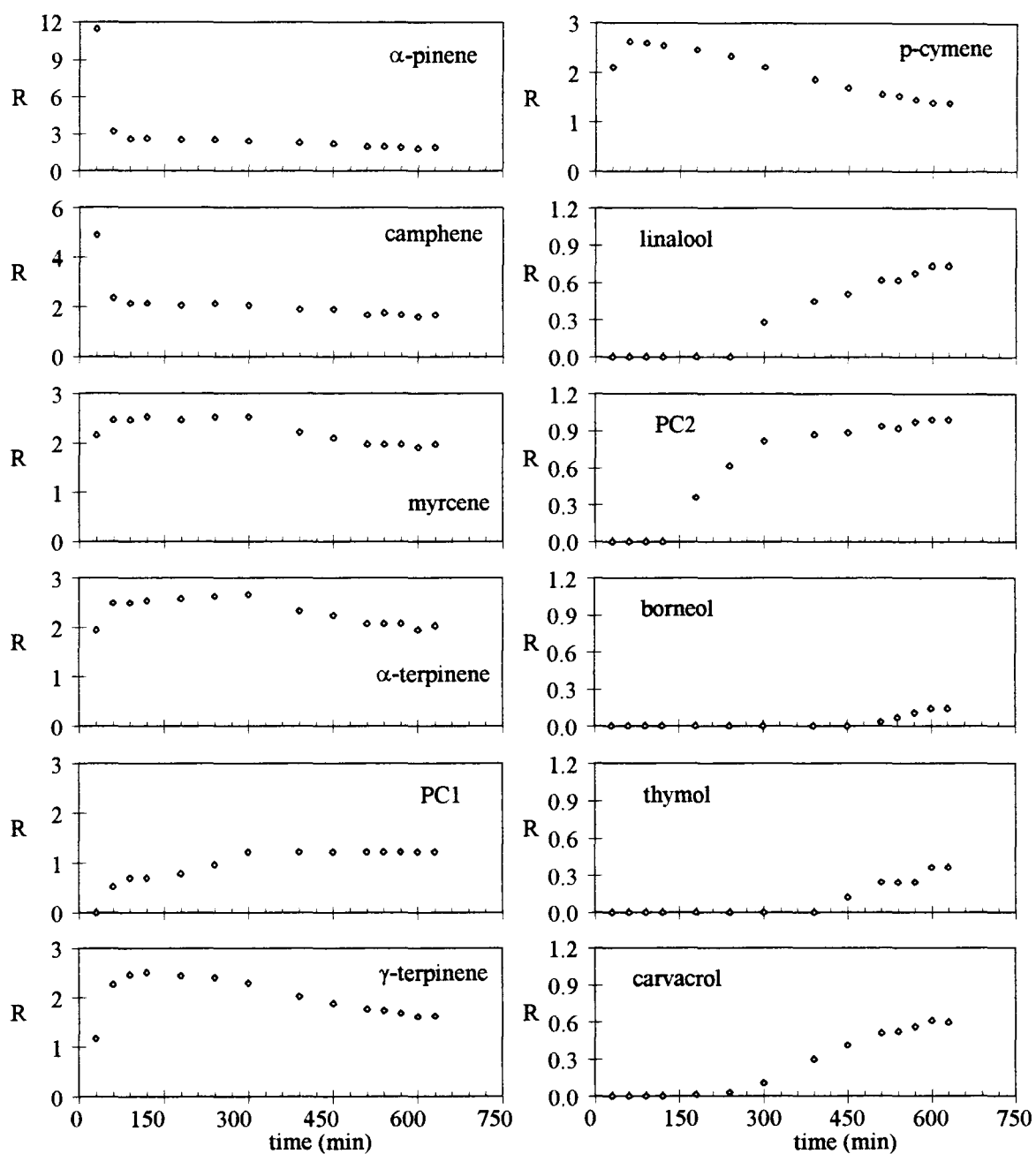


FIGURE 5.5.2.1. Relative-distribution ratios of organum-oil components in adsorption experiment at 40°C/7.5 MPa using 15 grams silica gel adsorbent.

significant, since the composition of the effluent would be more diversified. Hence, it will be easier to obtain a deterpenated fraction of origanum oil via supercritical-CO<sub>2</sub> adsorption at 40°C/7.5 MPa conditions using 15 grams of silanized silica gel.

For comparison purposes, Figure 5.5.2.2 also shows the relative-distribution ratios of the MT and NMT groups in the samples collected during the supercritical-CO<sub>2</sub> adsorption experiment with eight grams of activated carbon at 40°C/7.5 MPa conditions. As can be seen from this figure, relative-distribution ratios of the MT cut were higher, consequently, those of the NMT cut were lower compared to the ones obtained during the adsorption experiments on silica gel. In other words, MT hydrocarbons showed a low affinity for the carbon sorbent, yet lower affinity for the silica gel sorbent, in conjunction with a high affinity for CO<sub>2</sub>. On the contrary, the NMTs demonstrated a high affinity for the silica gel sorbent, even higher affinity for the carbon sorbent, in conjunction with a low affinity for CO<sub>2</sub>.

Figure 5.5.2.3 shows the evolution of the separation factor with respect to adsorption time. It is important to notice in this figure that during 540 minutes of adsorption (on activated carbon), the separation between the MT and NMT groups was infinity, since R values of the NMT cut was zero. As adsorption proceeded, the separation factor decreased sharply due to the appearance of the NMTs in the effluent. Samples collected after 600 minutes of supercritical-CO<sub>2</sub> treatment of origanum oil at 40°C/7.5 MPa conditions showed that the separation between major families of origanum oil was 209.01, 2.12, and 2.48 in the case of adsorption using eight grams of carbon, eight grams of silica gel and 15 grams of silica gel, respectively. Based on these results, increased quantities of silica gel adsorbent does not maintain a significant enrichment of the NMT components over the MT hydrocarbons, since  $\alpha$  values does not change much with time and amount of silica gel (enlarged portion of Figure 5.5.2.3). Furthermore, since the purpose of this work was to remove the MT hydrocarbons and leave the NMT compounds behind, a minimum fraction of MTs was desired in the adsorber. This argument suggests that improved fractionation of origanum-oil components can be achieved by using activated carbon as the adsorbent since the adsorption capacity of silanized silica gel is much weaker than activated carbon. However, in the aim of improving origanum oil quality, the trade-off between

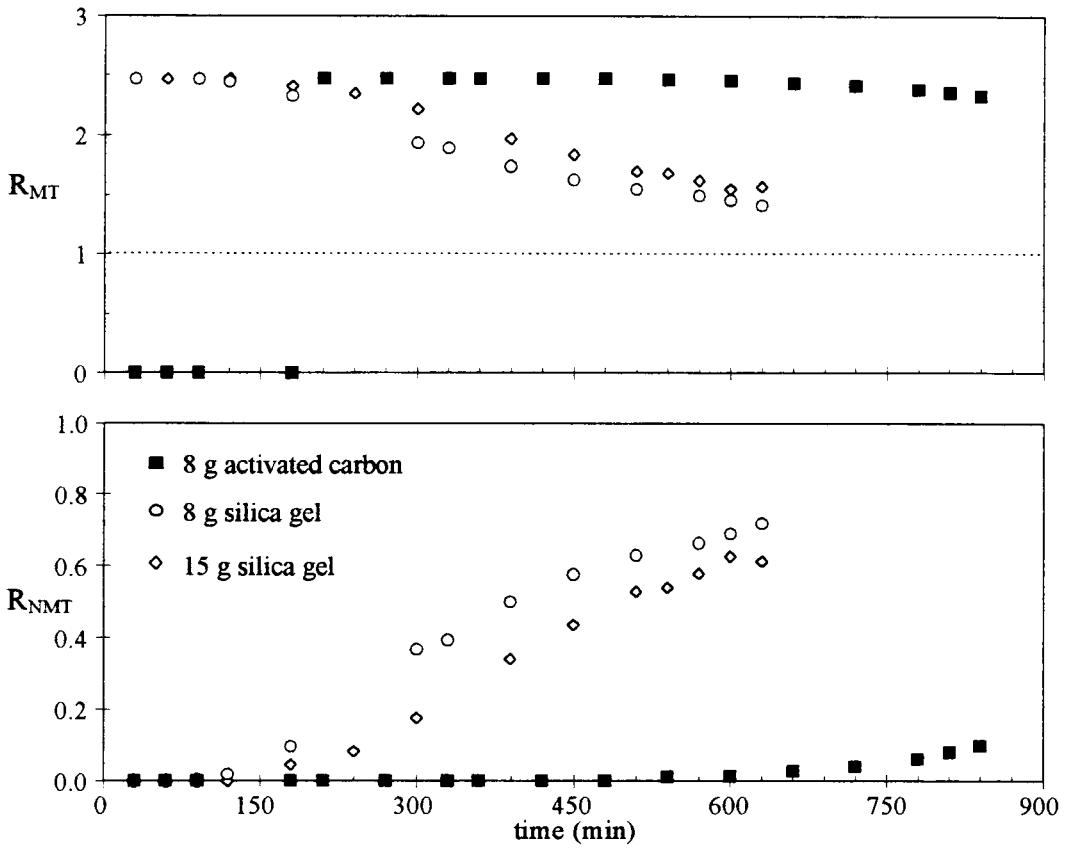


FIGURE 5.5.2.2. Relative-distribution ratios of MT and NMT cuts in adsorption experiments at 40°C/7.5 MPa.

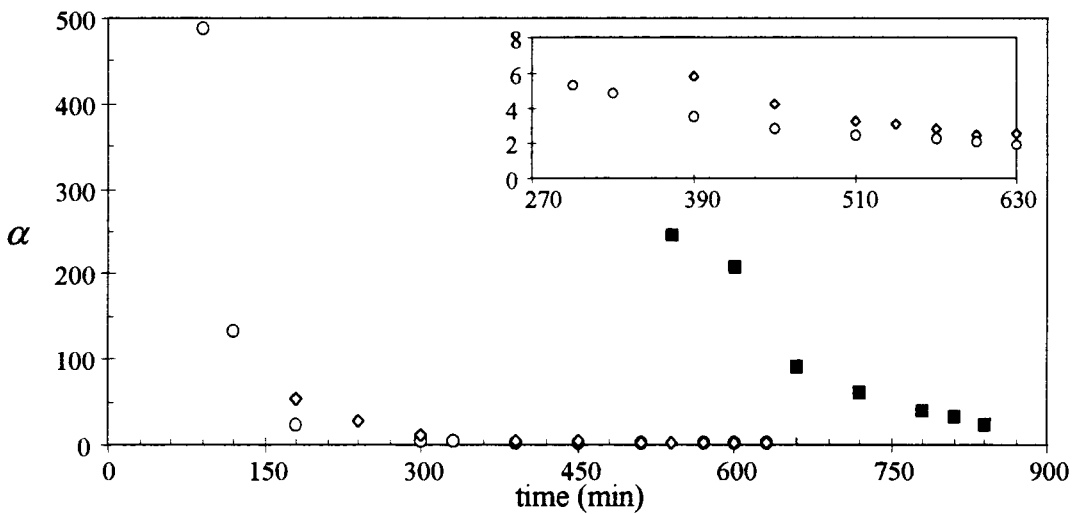


FIGURE 5.5.2.3. Separation factor in adsorption runs at 40°C/7.5 MPa (■: 8 g activated carbon, ○: 8 g silica gel, ◇: 15 g silica gel).

adsorption duration and elimination of MT hydrocarbons should be prudently taken into consideration in optimizing the operating conditions.

### **5.6. Supercritical-CO<sub>2</sub> Desorption Following the Origanum-oil/CO<sub>2</sub> Adsorption on Silica Gel Coupled with Dense-Gas Extraction at 40°C/14.5 MPa**

In this section, for the sake of simplicity, the process “supercritical-CO<sub>2</sub> desorption following origanum-oil/CO<sub>2</sub> adsorption coupled with dense-gas extraction” will be named as “supercritical-CO<sub>2</sub> desorption”. The supercritical-CO<sub>2</sub> adsorption (following the dense-gas extraction) experiments performed at 40°C/7.5 MPa conditions using silanized silica gel adsorbent revealed that it was possible to obtain a deterpenated fraction of origanum oil capitalizing on different affinities of the essential-oil components for the sorbent. In the aim of improving origanum oil quality, desorption with pure supercritical CO<sub>2</sub> (refer to Figure 3.2.3) at 40°C/14.5 MPa conditions (the step-wise pressure increase procedure was not employed in this case) was carried out to desorb MT hydrocarbons and selectively recover the valuable essential-oil constituents. It is important to notice that both adsorption and desorption experiments were performed at the same temperature of 40°C.

#### **5.6.1 Supercritical-CO<sub>2</sub> Desorption from Eight Grams Silica Gel**

The relative-distribution ratios of the twelve key components in origanum oil obtained via supercritical-CO<sub>2</sub> desorption at 40°C/14.5 MPa from eight grams of silanized silica gel are given Table D.13, in Appendix D, and illustrated in Figure 5.6.1.1. In this figure, the relative-distribution ratios that had been obtained during the adsorption process at 40°C/7.5 MPa are also included. As can be seen, the desorption behavior observed for each component is in good agreement with its adsorption behavior, i.e., components which were weakly retained by the sorbent were weakly retained by the sorbent (such as *α-pinene*,

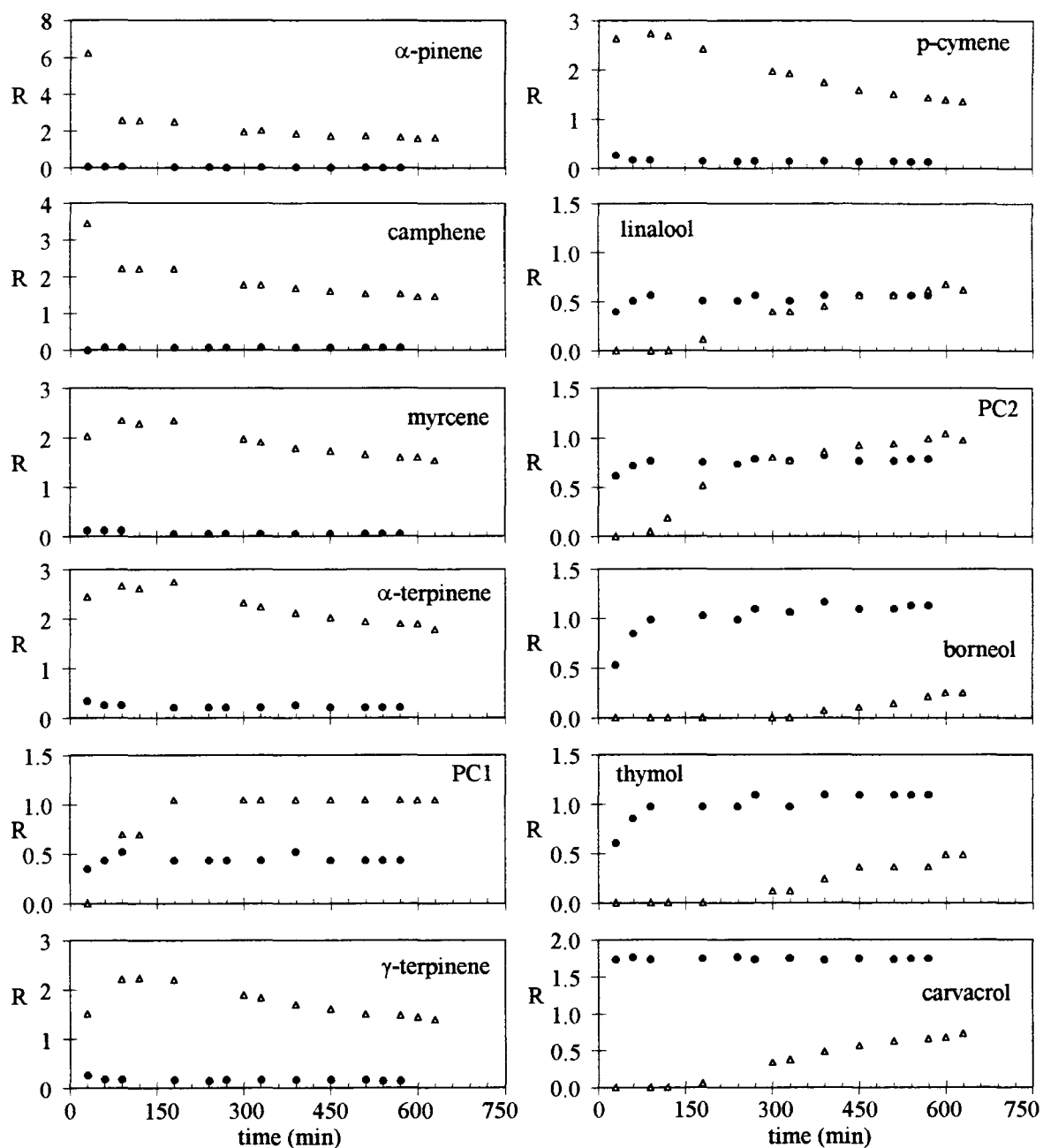


FIGURE 5.6.1.1. Relative-distribution ratios of origanum-oil components at 40°C using eight grams silica gel adsorbent ( $\triangle$ : adsorption at 7.5 MPa,  $\bullet$ : desorption at 14.5 MPa).

*camphene*) were easily and completely desorbed, hence very low R values (close to zero) were obtained for these components. Both MT and NMT compounds emerged in the effluent after 30 minutes of desorption time indicating that all component exhibited fast desorption. This can be explained by considering fact four, as stated in chapter three, which results in an increase in the solubility of all essential-oil components; therefore, at 14.5 MPa, it was possible to desorb from silica gel adsorbent all the key components of origanum oil. Moreover, MT hydrocarbons showed a low affinity for silica gel, whereas NMT hydrocarbons were strongly retained on the sorbent. This argument, coupled with the increased solvating power of the supercritical fluid, explains the desorption behavior of the origanum-oil components.

The supercritical-CO<sub>2</sub> desorption of origanum oil from silanized silica gel was terminated after 570 minutes, then the sorbent was removed and washed with ethanol to recover the adsorbed fraction of the oil. Figures 5.6.1.2 and 5.6.1.3 show the evolution in the normalized area counts (%) of each key component of origanum oil and of the MT and NMT cuts in the fractions collected at the end of the supercritical-CO<sub>2</sub> adsorption and desorption runs, respectively. At the end of the adsorption process, appreciable quantities of MT constituents (57.2%) were co-desorbed with significant quantities of NMT components (42.8%). On the other hand, MT hydrocarbons with R values greater than unity tended to concentrate in the dense-gas phase, whereas as NMT components remained on the sorbent (Figure 5.6.1.1). Desorption of origanum oil from silica gel provided effective fractionation of the oil, since the desorbed fraction at the end of the process contained a high percentage of NMT compounds (94.0%), the major component being *carvacrol* (84.3%). Thus, a deterpenated, *carvacrol-rich* fraction may be obtained from the origanum oil. Moreover, in practice an oil which has 50 per cent of its terpenes removed is called terpenless oil, consequently the results mentioned here are completely acceptable.

After the desorption experiment, as usual, the sorbent was removed and weighed to determine the loading of origanum oil at the experimental conditions. However, it was not possible to exactly determine the weight of silica gel sorbent due to its powder-like form (some part of it remained on the walls of the column) and moreover, after washing with ethanol no significant amount of origanum oil was detected on the silanized silica gel

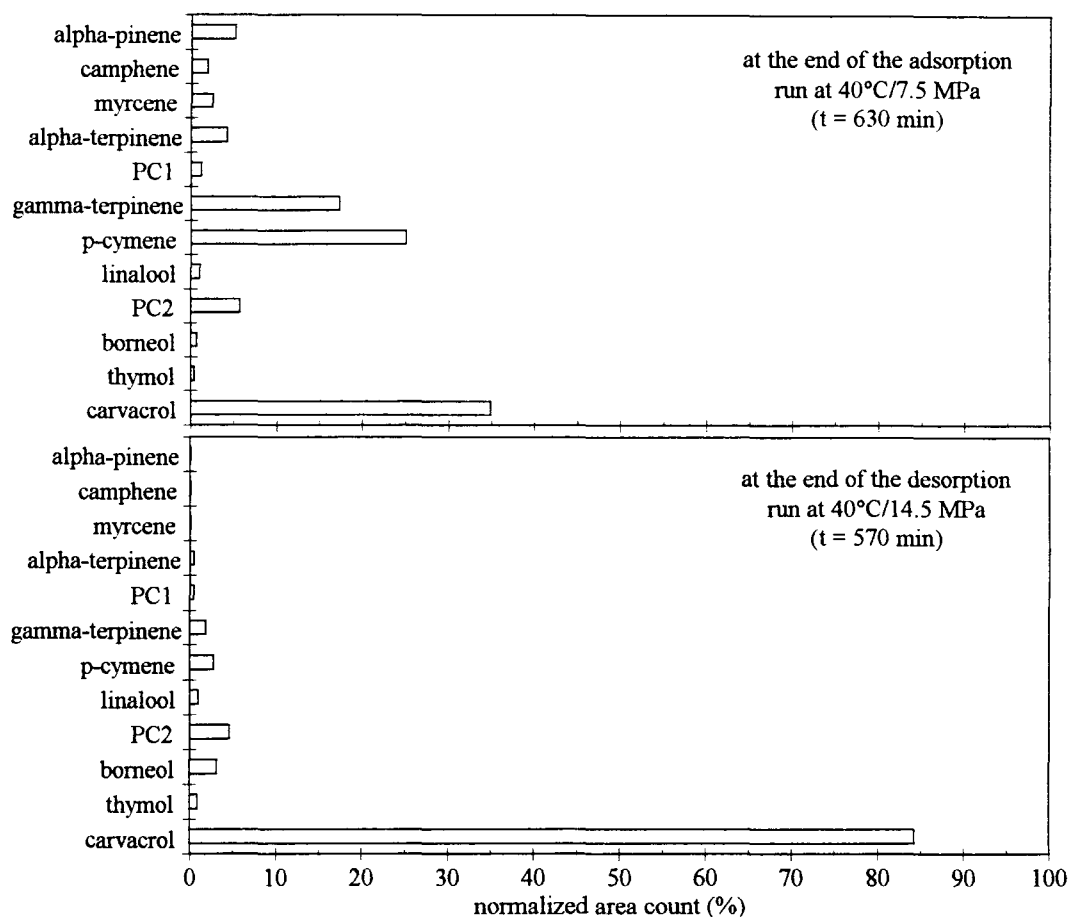


FIGURE 5.6.1.2. Normalized area counts of individual components at the end of the adsorption and desorption runs using eight grams silica gel adsorbent.

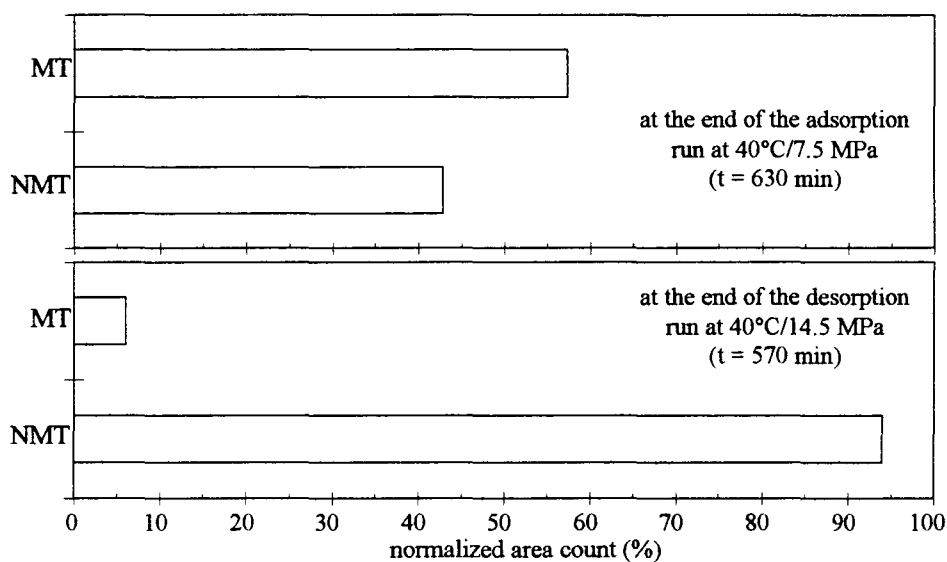


FIGURE 5.6.1.3. Normalized area counts of the MT and NMT cuts at the end of the adsorption and desorption runs using eight grams silica gel adsorbent.

(GC/MS analysis). This could be explained by the fact that ethanol-insoluble components were probably not desorbed from the silica gel adsorbent. But if that were the case, then it should have not been possible to obtain a residue after washing the activated carbon sorbent with ethanol at the end of the desorption runs. For complete satisfaction, silica gel was also washed with hexane, but again no significant amount of oil was detected on the sorbent. Therefore, the only rationalization is that complete removal of the essential-oil components was achieved at the operating conditions of 40°C/14.5 MPa via supercritical CO<sub>2</sub>. The argument based on the bonding forces between the key components of origanum oil and silanized silica gel strengthens the validity of the above discussion. It is important to recall that it was not possible to achieve a complete recovery of NMT compounds during supercritical-CO<sub>2</sub> desorption from activated carbon; even in the step-wise pressure increase procedure a significant amount of NMTs along with a small amount of MTs remained on the carbon.

#### **5.6.2. Supercritical-CO<sub>2</sub> Desorption from 15 Grams Silica Gel**

The relative-distribution ratios of the twelve key components in origanum oil obtained via supercritical-CO<sub>2</sub> desorption at 40°C/14.5 MPa from 15 grams of silanized silica gel are given Table D.14, in Appendix D, and illustrated in Figure 5.6.2.1. In this figure, the relative-distribution ratios that had been obtained during the adsorption process at 40°C/7.5 MPa are also included. As can be seen from this figure, the general shape of the desorption curves observed for each component is in good agreement with the breakthrough behavior obtained during the adsorption process. In other words, components which showed low affinity for the sorbent produced relative-distribution ratios very close to zero during desorption. It is important to notice in this figure that in the beginning of the desorption process, relative-distribution ratios for NMT hydrocarbons sharply increased, but remained almost constant throughout the duration of the experiment. Hence, these components exhibited fast desorption. This can be explained by considering fact four, as stated in chapter three, which results in an increase in the solubility of all essential-oil components; therefore, it was possible to desorb all the key components of origanum oil.

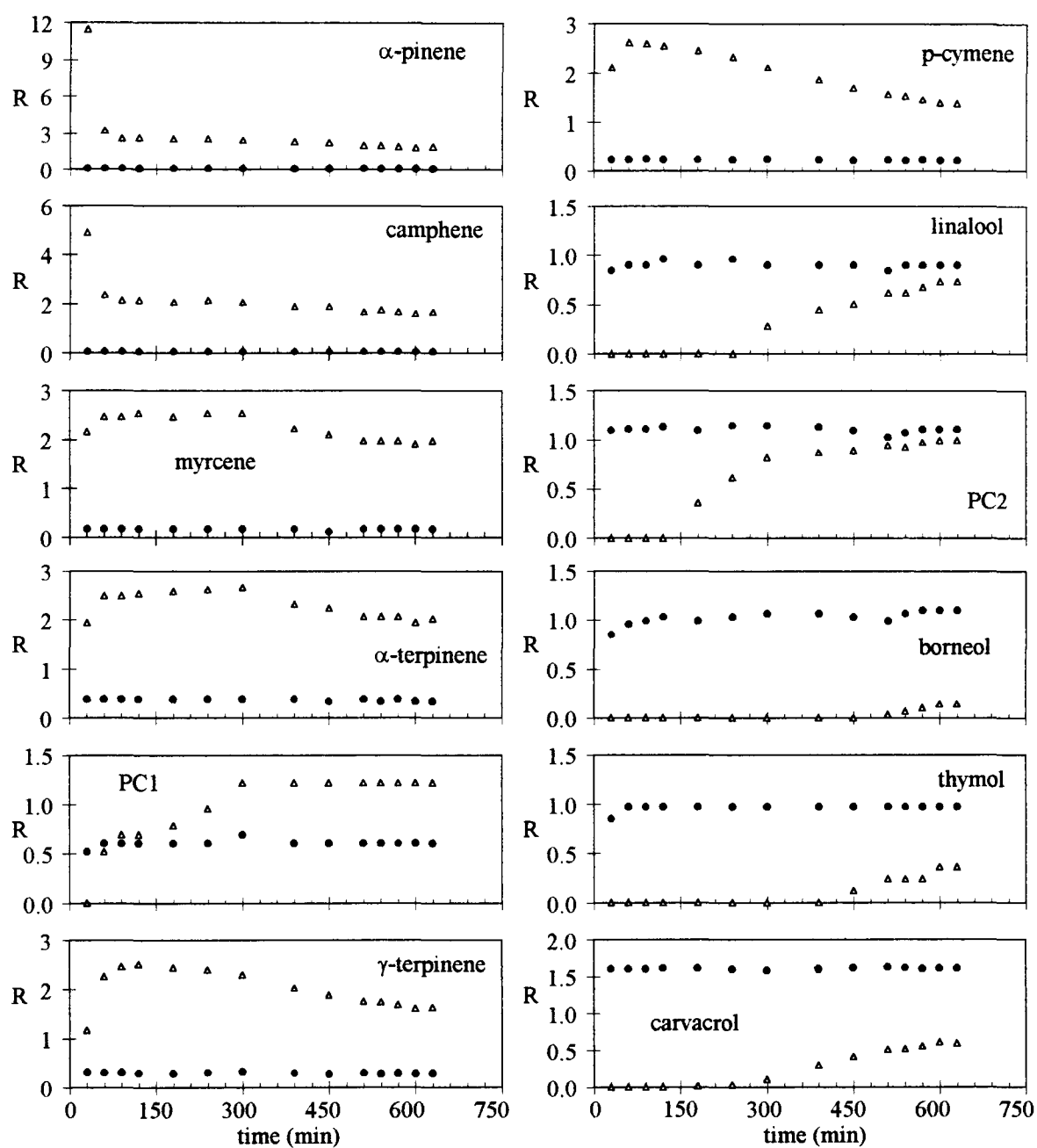


FIGURE 5.6.2.1. Relative-distribution ratios of origanum-oil components at 40°C using 15 grams silica gel adsorbent( $\Delta$ : adsorption at 7.5 MPa,  $\bullet$ : desorption at 14.5 MPa).

Moreover, MT hydrocarbons showed a low affinity for silica gel, whereas NMT hydrocarbons were strongly retained on the sorbent. This argument, coupled with the increased solvating power of the supercritical fluid, explains the desorption behavior of the origanum-oil components.

The supercritical-CO<sub>2</sub> desorption of origanum oil from silanized silica gel was terminated after 630 minutes, then the sorbent was removed and washed with ethanol to recover the adsorbed fraction of the oil. Figure 5.6.2.2 shows the evolution in the normalized area count of each key component of origanum oil and Figure 5.6.2.3 shows the evolution of the MT and NMT cuts in the fraction collected at the end of the supercritical-CO<sub>2</sub> adsorption and desorption runs. At the end of the adsorption process, appreciable quantities of MT constituents (63.5%) were co-desorbed with significant quantities of NMT components (36.5%). This fraction comprised of a higher MT content and, consequently, of a lower NMT content compared to adsorption on eight grams of silica gel. Hence, the increase in adsorbent quantity enhanced the selectivity of the adsorption process. Desorption of origanum oil from silica gel provided effective fractionation of the oil, since the desorbed fraction at the end of the process contained a high percentage of NMT compounds (90.0%), the major component being *carvacrol* (78.0%). Thus, a diterpenated, *carvacrol-rich* fraction may be obtained from the origanum oil.

After the desorption experiment, the sorbent was removed and weighed to determine the loading of origanum oil at the experimental conditions. However, it was not possible to exactly determine the weight of silica gel sorbent due to its powder-like form (some part of it remained on the walls of the column). After washing with ethanol, the only component detected in the residue was *carvacrol*. Hence, the increase in the adsorbent amount lead to incomplete recovery of this phenolic compound of origanum oil indicating that perhaps longer processing times were necessary.

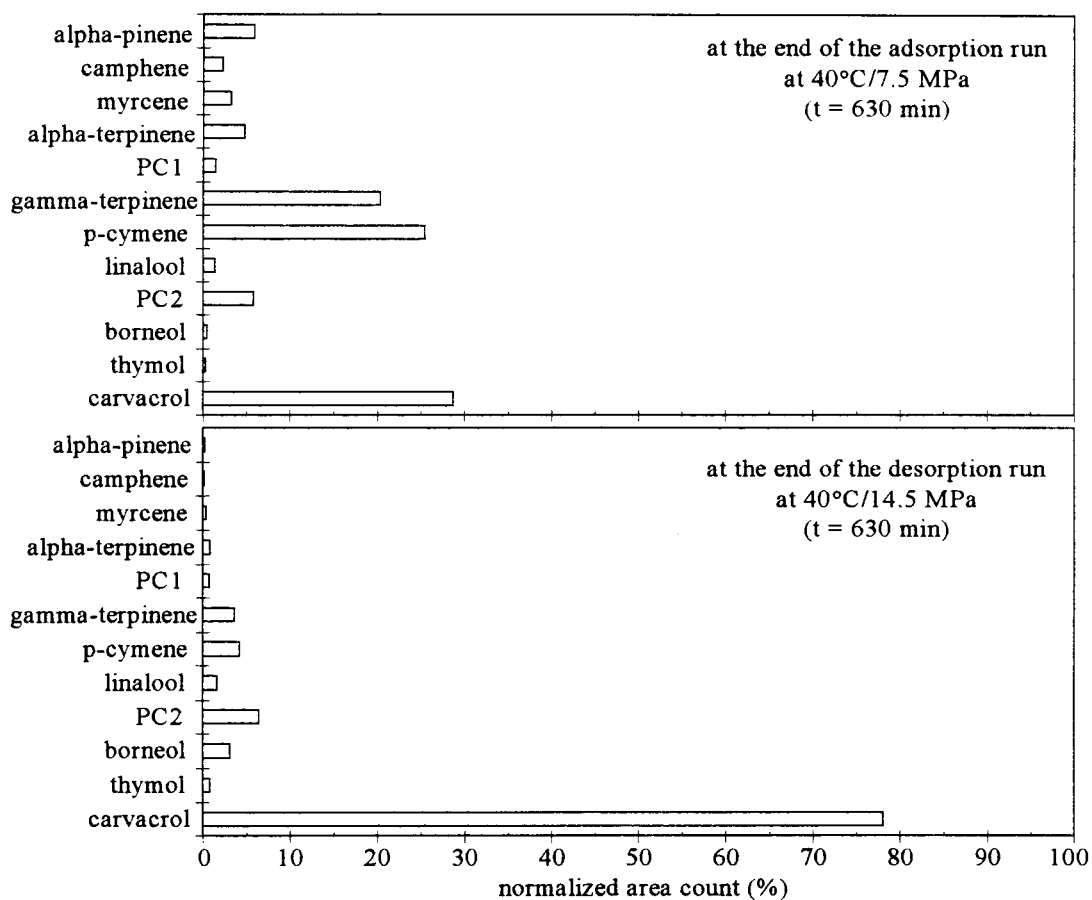


FIGURE 5.6.2.2. Normalized area counts of individual components at the end of the adsorption and desorption runs using 15 grams silica gel adsorbent.

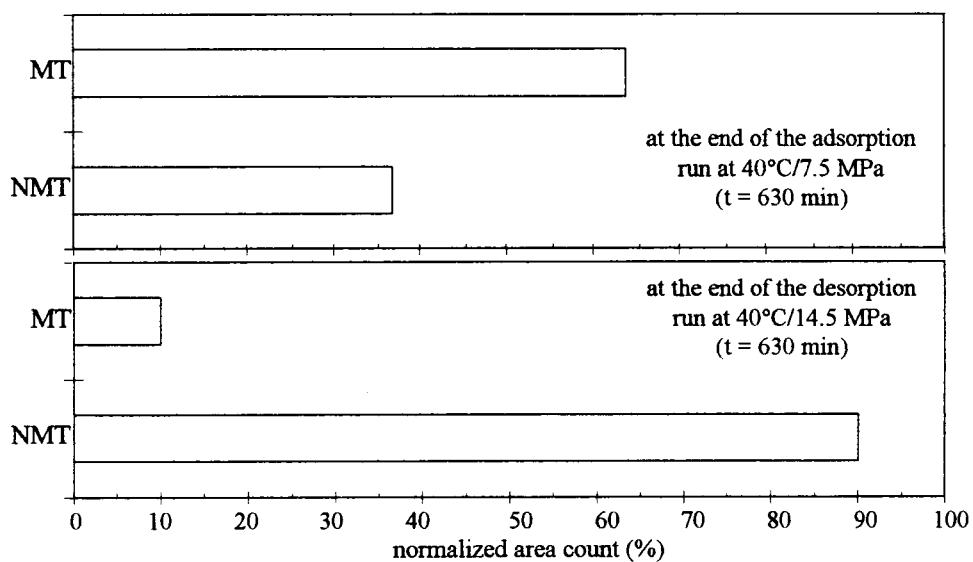


FIGURE 5.6.2.3. Normalized area counts of the MT and NMT cuts at the end of the adsorption and desorption runs using 15 grams silica gel adsorbent.

### 5.7. Effect of Origanum-oil/CO<sub>2</sub> Mixture Composition on the Fractionation of Origanum Oil at 40°C Using Activated Carbon

In this work, the feed solution was prepared through the continuous contact of the supercritical CO<sub>2</sub> and origanum oil streams in the mixing chamber. Then, the origanum-oil/CO<sub>2</sub> mixture was allowed to enter the extraction vessel. In chapter three, the different types of extraction experiments performed were shown schematically (Figures 3.2.1 and 3.2.2), and the facts considered in performing these distinct operations were explained in detail. Based on the results of these experiments, in which the influence pressure on the process selectivity was studied, it was concluded that at 40°C/7.5 MPa conditions, the feed mixture entering the extractor (leaving the mixing cell) had the equilibrium composition of origanum oil in the dense-gas phase. In the aim of enhancing the separation between the monoterpene (MT) and non-monoterpene (NMT) hydrocarbons of the oil, an adsorption column was introduced into the system (Figures 3.2.1 and 3.2.2). The adsorption from a supercritical feed (origanum oil solubilized in dense-CO<sub>2</sub> phase) was studied on a bed of activated carbon (and silanized silica gel). It was found that at 40°C/7.5 MPa conditions, the supercritical-CO<sub>2</sub> adsorption following the dense-gas extraction maintained an enrichment in the process selectivity according to the different affinities of the origanum-oil components for the sorbent. Last, desorption with pure supercritical CO<sub>2</sub> was carried out to desorb MT hydrocarbons and recover the valuable essential-oil constituents (Figure 3.2.3).

Feed concentration is one of the most important parameters affecting the design of continuous adsorption columns since the process is supposed to deal with feeds ranging from dilute to highly concentrated mixtures. Based on the results of the simple supercritical-fluid experiment at 40°C/7.5 MPa (Table 5.2.1.1), it was confirmed that the mixing cell situated prior to the adsorption column acted as a flash chamber, hence improving the fractionation of origanum oil. However, to further support the validity of this conviction a supercritical-CO<sub>2</sub> adsorption (following the dense-gas extraction) run was performed with a continuous feed of origanum-oil/CO<sub>2</sub> mixture in the single-phase region. It was already ascertained that at 40°C/10.0 MPa conditions, origanum-oil components exhibited complete

miscibility in CO<sub>2</sub> (section 5.2.2). Therefore, the supercritical-CO<sub>2</sub> adsorption (following the dense-gas extraction) of the origanum-oil/CO<sub>2</sub> feed mixture on eight grams of activated carbon was studied at 40°C/10.0 MPa conditions. In this section, the experimental results obtained will be discussed in terms of relative-distribution ratios of the twelve key components and of the MT and NMT cuts of origanum oil. Comparison with adsorption process performed with the origanum-oil/CO<sub>2</sub> feed mixture in the two-phase region, i.e., at 40°C/7.5 MPa conditions, will also be presented. From now on, for the sake of simplicity, the process “supercritical-CO<sub>2</sub> adsorption following the dense-gas extraction” will be named as “supercritical-CO<sub>2</sub> adsorption”.

### 5.7.1. Supercritical-CO<sub>2</sub> Adsorption Following Dense-Gas Extraction at 10.0 MPa

The relative-distribution ratios of the key components in origanum oil obtained via supercritical-CO<sub>2</sub> adsorption at 40°C/10.0 MPa using eight grams of activated carbon are given in Table D.15, in Appendix D, and illustrated in Figure 5.7.1.1. For comparison purposes, the relative-distribution ratios that had been obtained during the supercritical-CO<sub>2</sub> adsorption at 40°C/7.5 MPa are also included. It is important to notice in this figure that in the earlier stages of adsorption, all the key components of origanum oil were adsorbed on the activated carbon, independent of the adsorption pressure. Later, compounds (NMTs) which had a stronger affinity for the adsorbent replaced the ones (MTs) with a weaker affinity.

As can be seen in Figure 5.7.1.1, compared to the behavior observed at 40°C/7.5 MPa, both MT and NMT hydrocarbons breakthroughed earlier. Moreover, the pressure increase effect was more significant for components exhibiting higher affinity towards the activated carbon sorbent. Indeed, the breakthrough time for the NMT components was shortened to a great extent, even *thymol* appeared in the effluent. This behavior may be explained by considering the influence of feed concentration (g oil/g CO<sub>2</sub>) in both runs. At 7.5 MPa, the feed to the adsorber has the equilibrium composition of origanum oil in the dense-gas phase,  $y^*$  (Figure 3.2.1), which is not known. But an approximate value for the

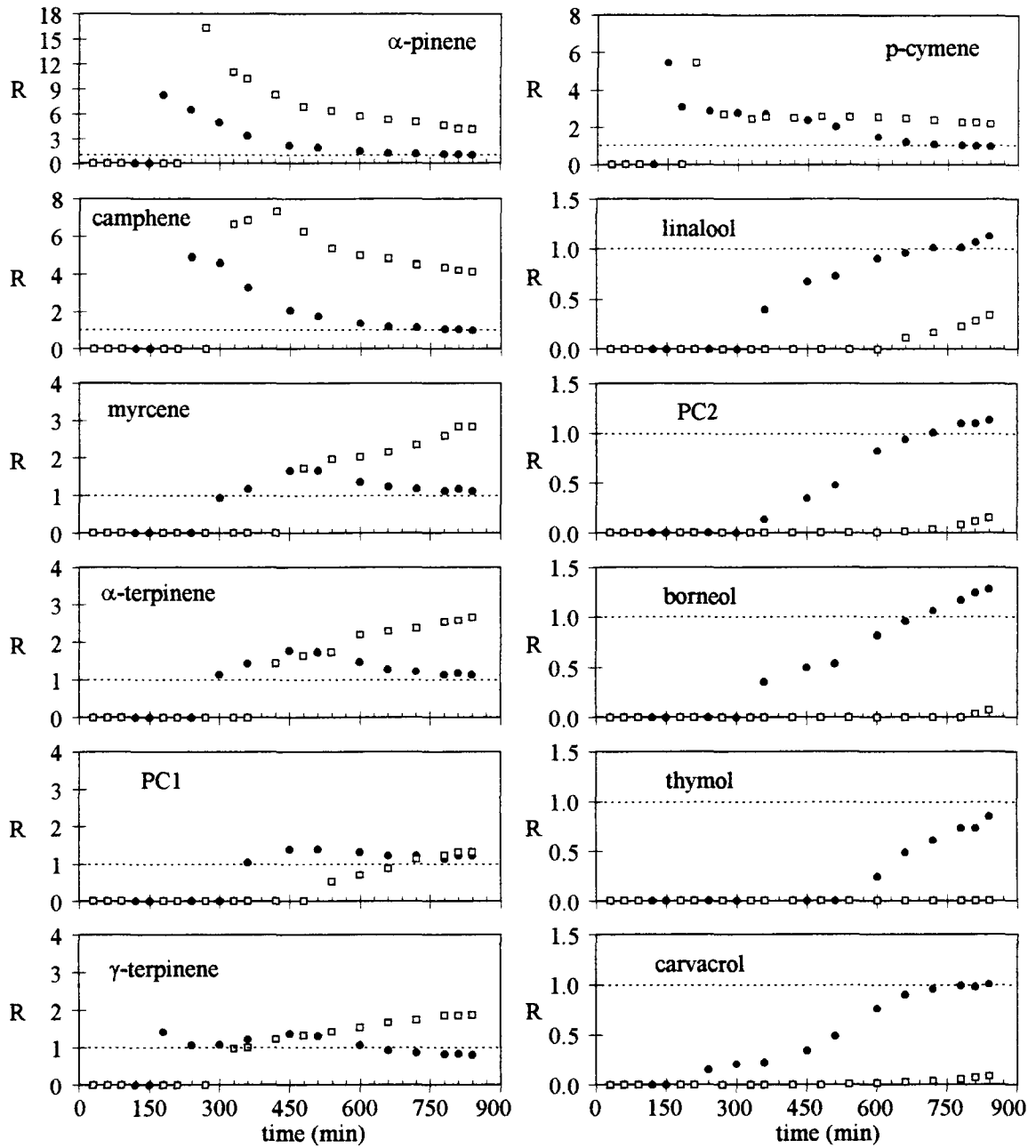


FIGURE 5.7.1.1. Relative-distribution ratios of origanum-oil components in adsorption experiments at 40°C using eight grams activated carbon (□: 7.5 MPa, ●: 10.0 MPa).

amount of oil entering the adsorber could be calculated through measuring the amount of liquid-phase accumulating in the bottom of the mixing cell during the experiment with a feed in the two-phase region. It was found that 11.4 ml of origanum oil was pumped and 3.7 ml of it remained in the mixing chamber, hence about 67.5% of the total amount was carried to the adsorber with the CO<sub>2</sub> flow rate. On the other hand, during the adsorption experiment with a feed in the single-phase region, all the oil pumped (8.4 ml) was assumed to enter the adsorber due to complete miscibility of origanum-oil components in CO<sub>2</sub>. However, both of these runs were performed at comparable CO<sub>2</sub> flow rates, 1.52 g/min and 1.54 g/min at 7.5 MPa and 10.0 MPa conditions, respectively. As a result of increased gas density (pure CO<sub>2</sub> density at 7.5 MPa and 10.0 MPa is 0.25 and 0.64 g/cm<sup>3</sup>, respectively), the volumetric flow rate of the supercritical solvent within the adsorber (cm<sup>3</sup>/min at operating conditions) was reduced (by a factor of two and a half) at higher pressure adsorption. Based on these arguments, the feed concentrations calculated for both runs turned out to be very similar. It is important to mention that this calculation is just an approximation, therefore the experimental evidence is the only verification that the feed concentration at 7.5 MPa must be lower than that at 10.0 MPa. The fact that an increase in the feed concentration leads to shorter breakthrough times, and that this effect is more remarkable for solutes showing a higher affinity towards the sorbent especially supports the data obtained in these runs. Similar behavior was also found in literature (Subra et al., 1998).

Figure 5.7.1.2 shows the pressure dependence of the relative-distribution ratios of the MT and NMT cuts during supercritical-CO<sub>2</sub> adsorption at 40°C. The most striking characteristic in this figure is that, at 10.0 MPa, the relative-distribution ratios of the both major compound families of origanum oil asymptotically approach to unity. In fact, towards the end of this adsorption process, the R values of both groups were very close to unity. However, at the beginning of adsorption at 10.0 MPa, both MT and NMT hydrocarbons were strongly adsorbed on the carbon. Then, compounds with a weak affinity towards the sorbent (and high to CO<sub>2</sub>) emerged in the effluent. In other words, MTs exhibited a low affinity for the sorbent in conjunction with a high affinity for the fluid phase. As compounds with a stronger affinity towards activated carbon (and lower to CO<sub>2</sub>) appeared in the effluent, the R values of the MT cut sharply decreased, consequently, that of the NMT cut

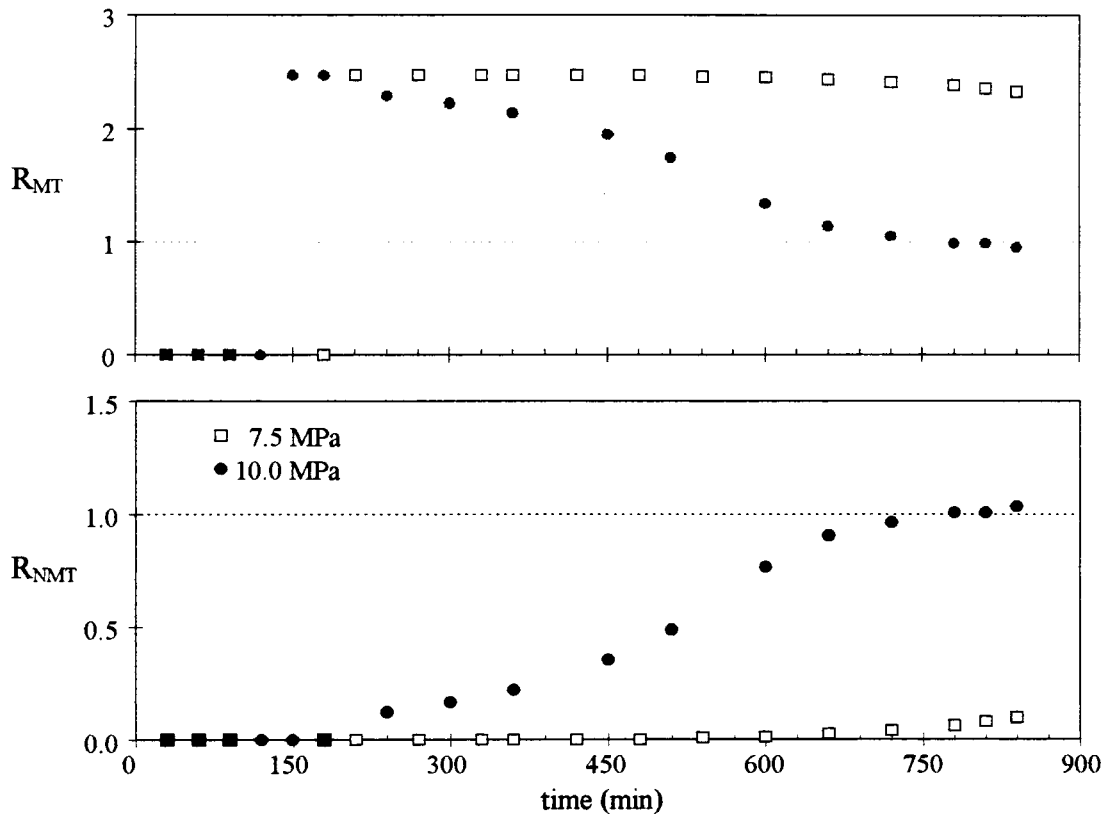


FIGURE 5.7.1.2. Pressure dependence of the relative-distribution ratios of MT and NMT cuts in adsorption runs at 40°C using eight grams activated carbon.

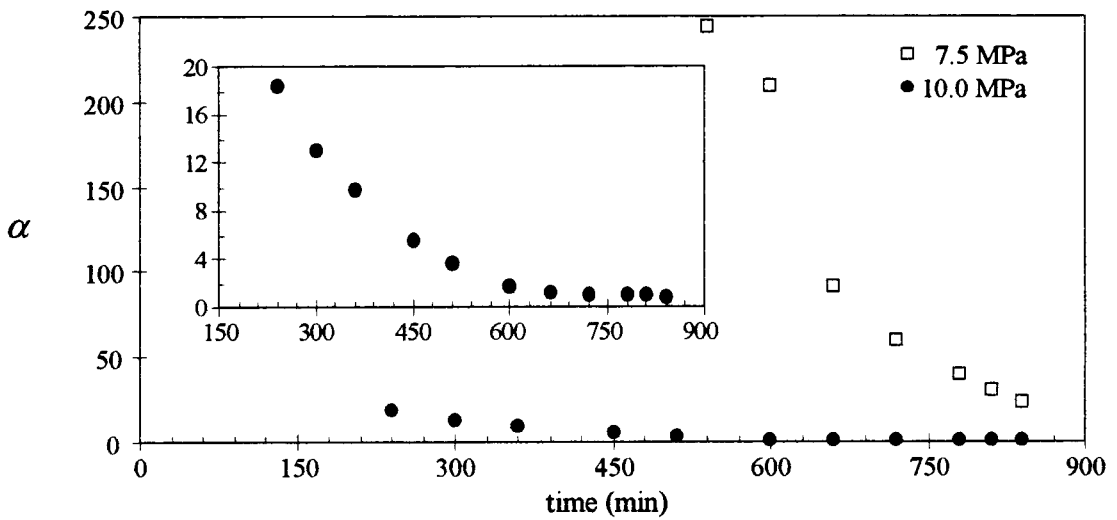


FIGURE 5.7.1.3. Pressure dependence of the separation factor in adsorption runs at 40°C using eight grams activated carbon.

sharply increased. Similar breakthrough behavior was also observed during supercritical- $\text{CO}_2$  adsorption at 7.5 MPa. In this case, the relative-distribution ratios of the MT cut were greater than unity indicating that these components tended to concentrate in the dense-gas-phase, whereas NMT compounds were preferentially adsorbed on the sorbent with  $R \ll 1$ . This is because with increasing pressure (from 7.5 to 10.0 MPa), the effect of solvating power of the solvent increases, and the R values of most of the key components show an asymptotic approach to unity (Figure 5.7.1.1), which reveals that MT and NMT constituents of origanum oil become equally soluble in  $\text{CO}_2$ . The above changes, which occurred with the increase in pressure, corroborate the validity of the single-phase argument.

As seen in Figure 5.7.1.2, adsorption with origanum-oil/ $\text{CO}_2$  feed mixture of composition  $y^*$  (Figure 3.2.1) gave more diversified fractions, whereas during adsorption with the same feed mixture in the single phase region, the selectivity of the process with respect to the effluent composition was rapidly lost. Figure 5.7.1.3 shows the pressure dependence of the separation factor against the adsorption time. As clearly seen, compared to adsorption at 10.0 MPa, deterpenation of origanum via supercritical adsorption at 7.5 MPa is more favorable since enhanced separation between MT and NMT components is obtained. Therefore, the presence of the flash chamber before the adsorber maintains an enrichment in MTs over the NMT hydrocarbons. Then, the origanum-oil/ $\text{CO}_2$  feed mixture comprised of a high content of MT components can be further fractionated according to the different affinity of origanum-oil components with activated carbon. Last, desorption with pure supercritical- $\text{CO}_2$  can be performed in order to recover the valuable constituents (NMTs) of origanum oil. For example, one possible way to deterpenate origanum oil may be as follows: At  $40^\circ\text{C}/7.5$  MPa operating conditions, the fraction accumulated in the sample collector during 480 minutes, is formed by only MT hydrocarbons, but *PCI* does not appear in the effluent yet. The carbon, containing both MT and NMTs hydrocarbons, can be desorbed by implementing the step-wise pressure increase method. First, desorption at 8.0 MPa will result in the selective elimination of most of the MT components. Then, by increasing the pressure to 14.5 MPa, NMT hydrocarbons will be desorbed together with the remaining MT compounds. If necessary, the desorption pressure can be further increased for complete recovery of the NMT hydrocarbons. This procedure suggests the possibility of

improving the quality of the oil through the removal of MT hydrocarbons by supercritical-CO<sub>2</sub> adsorption at 40°C/7.5 MPa conditions activated carbon adsorbent.

### **5.7.2. Supercritical-CO<sub>2</sub> Desorption at 40°C/14.5 MPa Following the Origanum-oil/CO<sub>2</sub> Adsorption on Activated Carbon at 40°C/10.0 MPa**

In the aim of improving origanum oil quality, desorption with pure supercritical CO<sub>2</sub> at 40°C/14.5 MPa conditions was carried out to desorb MT hydrocarbons and to recover the valuable essential-oil constituents. It is important to notice that both adsorption and desorption experiments were performed at the same temperature of 40°C. The relative-distribution ratios of the key components in origanum oil obtained via supercritical-CO<sub>2</sub> desorption at 40°C/14.5 MPa are reported in Table D.16, in Appendix D, and illustrated in Figure 5.7.2.1. In this figure, the relative-distribution ratios that had been obtained during the adsorption process (with eight grams of activated carbon at 40°C/10.0 MPa) are also included. The desorption behavior observed for each component is in good agreement with its adsorption behavior, i.e., components which were weakly retained by the sorbent (such as *α-pinene*, *camphene*) were easily and completely desorbed, hence very low R values (close to zero) were obtained for these components. As can be seen, both MT and NMT compounds exhibited fast desorption. This is because of the increased CO<sub>2</sub> density at 14.5 MPa compared to CO<sub>2</sub> density at 10.0 MPa, (pure CO<sub>2</sub> density at 14.5 MPa and 10.0 MPa is 0.78 and 0.64 g/cm<sup>3</sup>, respectively), since increased solvating power of the solvent results in an increase in the solubility of all essential-oil components; therefore, it was possible to desorb all the key components of origanum oil. Moreover, MT hydrocarbons showed a low affinity for carbon, whereas NMT hydrocarbons were strongly retained on the sorbent. This argument, coupled with the increased solvating power of the supercritical fluid, explains the desorption behavior of the origanum-oil components.

The effect of feed mixture composition on normalized area counts of the individual components in the adsorbed and desorbed fractions and in the ethanol-extracted activated-carbon residue can be seen in Figure 5.7.2.2. As mentioned before, at 40°C/7.5 MPa

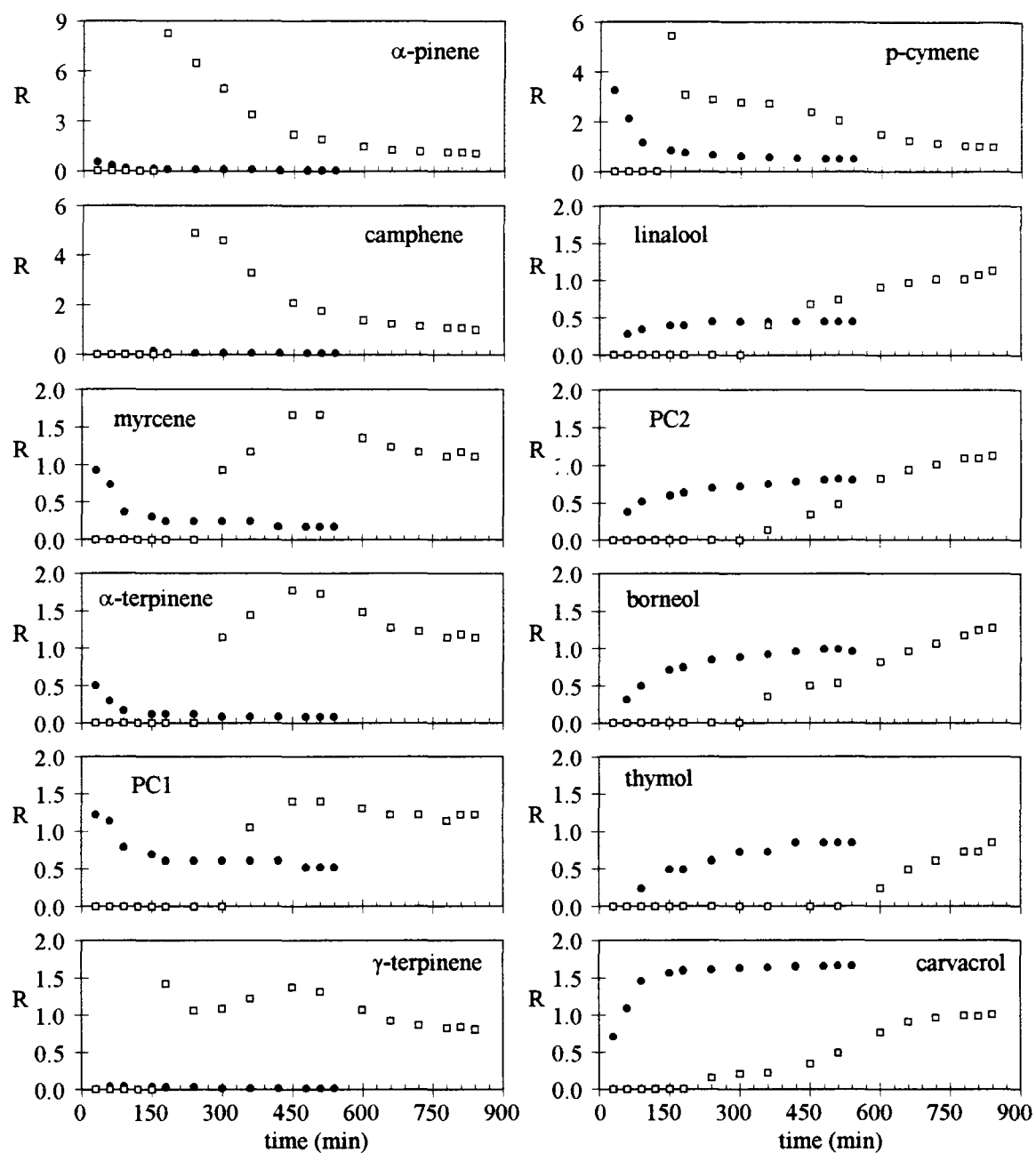


FIGURE 5.7.2.1. Relative-distribution ratios of organum-oil components at 40°C using eight grams activated carbon ( $\square$ : adsorption at 10.0 MPa,  $\bullet$ : desorption at 14.5 MPa).

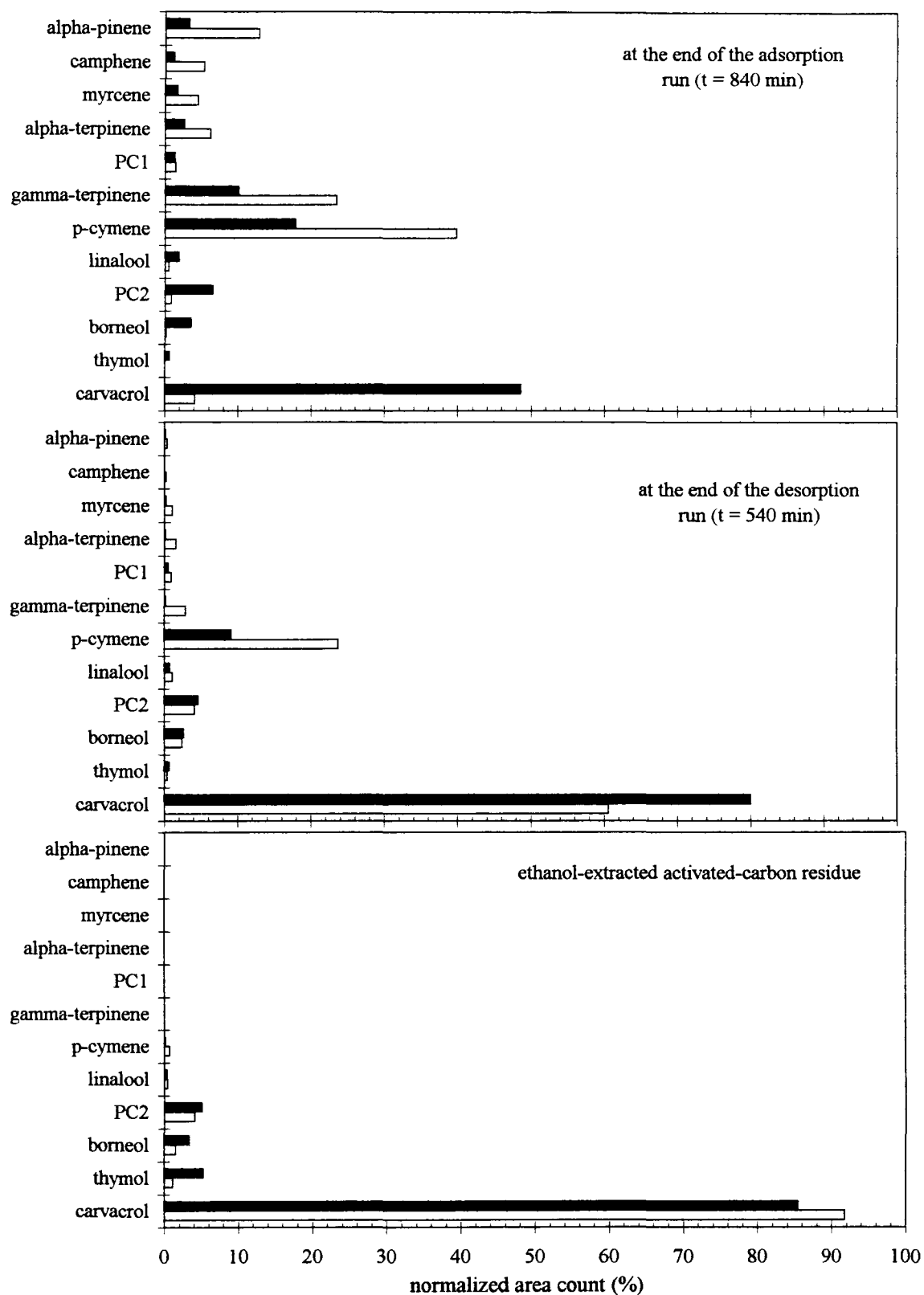


FIGURE 5.7.2.2. Effect of feed composition on normalized area counts of key components in the adsorbed and desorbed fractions and in the ethanol-extracted activated-carbon residue (■: single-phase feed, □: two-phase feed).

conditions, the origanum-oil/CO<sub>2</sub> feed mixture was proved to be in the two-phase region (Figure 3.2.1), whereas the same feed mixture at 40°C/10.0 MPa conditions was in the single-phase region (Figure 3.2.2). For the two-phase feed, the fraction collected at the end of the adsorption run comprised mainly of MT hydrocarbons (94.1%), whereas all NMT components (61.6%) together with MT hydrocarbons (38.4%) were present at the end of the adsorption process executed with a single-phase feed. This observation indicates that when a single-phase feed is introduced to the adsorber, the selectivity of the process with respect to the effluent composition is lost, since at this operating conditions, all components are equally soluble in CO<sub>2</sub>.

Ensuing the adsorption runs, desorption with pure supercritical-CO<sub>2</sub> was performed at 40°C/14.5 MPa conditions. As seen in Figure 5.7.2.2, after 540 minutes of desorption following the adsorption with a single-phase feed, the fraction accumulated in the sample collector was formed mainly by NMT hydrocarbons, with carvacrol (80.1%) being major. However, in the case of desorption following the adsorption with a two-phase feed, NMT hydrocarbons (68.9%) together with a significant MT content (31.1%) were detected. This observation can be explained by the fact that due to complete miscibility of origanum-oil components during adsorption with a single-phase feed at 40°C/10.0 MPa, most of the NMT content of the origanum oil was already recovered during adsorption. The remaining NMT fraction was easily collected during desorption since at increased CO<sub>2</sub> densities, these components show high solubility in CO<sub>2</sub>. This argument, coupled with the fact that at higher density, the interaction forces between the solute and the CO<sub>2</sub> molecules increase compared to the bonding forces between the solute and the carbon surface, justifies the high content of NMT hydrocarbons in the desorbed fraction (following the adsorption with a single-phase feed) after 540 minutes of treatment with pure supercritical CO<sub>2</sub>.

The supercritical-CO<sub>2</sub> desorption of origanum oil from activated carbon was terminated after 540 minutes, then the carbon sample was removed and weighed prior to treatment with ethanol to remove the strongly adsorbed fraction of the oil. As opposed to the expected behavior, there was a decrease in the weight of the activated carbon. The most important characteristic of the activated carbon residue was its low MT hydrocarbon content (0.3%). Hence, MT components were successfully eliminated from the carbon, but

a small quantity of *PCI* and *p-cymene* was still present on the sorbent. The minor percentage content of MT constituents in the residue indicates that perhaps longer processing times were necessary to obtain a thorough desorption of these highly volatile compounds. However, an optimum should exist between the recovered quantities and the processing time. On the contrary, this residue contained a high percentage of NMT compounds (99.7%). However, as seen in Figure 5.7.2.2, the composition of this residue was very similar to that obtained by introducing a feed to the adsorber with a composition of  $y^*$  (Figure 3.2.1). For complete desorption of these valuable compounds which contribute to the flavor and aroma of origanum oil, a higher pressure or a higher temperature (since increase in temperature lowers the adsorptive capacity) would be needed.

### 5.8. Pure Supercritical-CO<sub>2</sub> Adsorption on Activated Carbon at 40°C

After each supercritical-CO<sub>2</sub> adsorption/desorption experiment, the activated carbon sorbent was removed and weighed to determine the loading of origanum oil at the experimental conditions. It was observed that after the adsorption run performed at 40°C/7.5 MPa using two grams activated carbon, as expected there was a significant increase (21.5 per cent) in the weight of the sorbent. However, a decrease in the weight of the sorbent was detected when similar measurements were taken (exactly in the same manner) after the desorption experiments performed at constant-pressure or by step-wise pressure increase method. These results were controversial, therefore in an attempt of explaining the above behavior preliminary tests using pure supercritical CO<sub>2</sub> were conducted 40°C and 8.0 and 14.5 MPa conditions. It is important to note that these runs were carried out for an extended period of time, 840 minutes.

Adsorption from a supercritical feed has to be regarded as a competitive phenomenon between the solvent and the solute molecules towards the active sites of the sorbent surface. This argument points to the fact that the solvent could also been adsorbed

on the activated carbon, hence experiments were executed, without any solute (origanum oil), to determine the amount of adsorbed CO<sub>2</sub> present on the activated carbon. Two sets of experiments were carried out: first set without drying the carbon; second set after drying the carbon to constant weight under vacuum at 100°C for 24 hours. The results are given in Table 5.8.1.

TABLE 5.8.1. Effect of pressure on activated carbon loadings from pure CO<sub>2</sub>.

<i>Activated carbon, as is</i>				
T (°C)	P (MPa)	initial charge (g)	carbon loading after run (g)	change in weight (%)
40	7.5	8.00	7.47	-6.63
40	7.5	8.00	7.52	-6.00
40	14.5	8.00	7.50	-6.25
<i>Activated carbon, dried</i>				
T (°C)	P (MPa)	initial charge (g)	carbon loading after run (g)	change in weight (%)
40	7.5	8.00	7.49	-6.38
40	7.5	8.00	7.48	-6.50
40	14.5	8.00	7.52	-6.00

It was found that definite decrease in the weight of the carbon could be measured after depressurizing the system at the end of each experiment. Repeated weighings at different pressures (low or high) or distinct handling of the carbon showed the same behavior. This evidence points to the fact that supercritical CO<sub>2</sub> might be extracting some things from the activated carbon. However, if that were the case then, component peak(s) should have been identified by the GC/MS analysis of the sorbent after being washed in ethanol (residue), as was done in the desorption experiments with origanum oil. Therefore, the only explanation may be that the granular activated carbon when exposed to high pressures (8.0 or 14.5 MPa), breaks into smaller particles during depressurizing and some fraction of it becomes

dust-like. Hence, a fraction of the activated carbon introduced into the adsorber is lost by the continuous flow of the solvent, while another fraction of it sticks to the walls of the adsorption column. This argument also explains the measured weight loss of the carbon samples observed after supercritical-CO<sub>2</sub> desorption of origanum oil. However, adsorption of pure CO<sub>2</sub> onto activated carbon has already been investigated (Kander and Paulaitis, 1983) and it was found that no significant change in the weight of the carbon bed could be measured, thus CO<sub>2</sub> adsorption onto activated carbon could be neglected.

## 6. CONCLUSIONS AND RECOMMENDATIONS

The conclusions which can be drawn from the experimental findings of this study will be given in the first section, and possible research directions along with some recommendations will be provided in the second section of this chapter.

### 6.1. Conclusions

Fractionation and successful deterpenation of an essential oil, in this case, organum oil (*Origanum Munituflorum*), was accomplished through a dense-CO<sub>2</sub> extraction coupled with continuous adsorption/desorption process. This new process arrangement was developed by taking the advantages of the solubility behavior of organum-oil components in supercritical-solvent CO<sub>2</sub>. In addition, the introduction of an adsorption column to the simple extraction system proved to be very effective in enhancing the selectivity of the process according to the different affinities these essential-oil components for the adsorbent. Supercritical-CO<sub>2</sub> desorption with step-wise pressure increase produced a high-value product having the essential odor and properties of the organum oil; thus an organum-oil product almost free of its monoterpene (MT) hydrocarbons was obtained.

The experimental results obtained during the simple supercritical-CO<sub>2</sub> extraction runs performed at 40°C, in which the influence of pressure was studied, showed that better deterpenation of organum oil was achieved at 7.5 MPa compared to that at 10.0 MPa since in the former case, the separation factor,  $\alpha$ , between the MT and NMT hydrocarbons was higher as a result of the preferential recovery of MT hydrocarbons in the dense-CO<sub>2</sub> phase. The selectivity of the process decreased as extraction proceeded, but 480 minutes of extraction time was sufficient to reach some degree of selectivity of MTs over the NMTs.

It was also demonstrated that at 40°C/7.5 MPa, the origanum-oil/CO<sub>2</sub> system fell in the two-phase region, whereas at 40°C/10.0 MPa, this binary mixture was in the single-phase region. This evidence offered the advantage that the feed mixture entering the extractor at 40°C/7.5 MPa conditions was already separated into groups of components of differing properties (volatility and/or polarity) since a liquid-oil and a dense-gas phase in which CO<sub>2</sub> and the dissolved oil components appeared were present in the mixing cell. On the other hand, at 40°C/10.0 MPa conditions, origanum oil was completely miscible in supercritical CO<sub>2</sub> and the relative-distribution ratios of the key components showed an asymptotic approach to unity; hence the separation between MT and NMT groups deteriorated. In light of these results, it can be concluded that simple supercritical-CO<sub>2</sub> extraction process at 40°C/7.5 MPa conditions was more successful than that at 40°C/10.0 MPa, since in the former case, the mixing cell acted as a flash chamber providing additional separation between the more soluble components in CO<sub>2</sub> and the hard-to-extract substances by CO<sub>2</sub> of this oil, i.e., between the MT and NMT hydrocarbons.

The supercritical-CO<sub>2</sub> adsorption following the dense-gas extraction runs performed at 40°C/7.5 MPa conditions showed that activated carbon sorbent was powerful in further fractionating (compared to simple supercritical-CO<sub>2</sub> extraction) origanum oil into its fractions, MT and NMT cuts, since the activated carbon column maintained an enrichment in MTs over the NMT hydrocarbons. This is because the MT constituents (nonpolar) of the origanum oil exhibited a low affinity for activated carbon surface (apolar) in conjunction with a high affinity for the fluid phase (due to high vapor pressure, low polarity and small molecular weight), whereas the NMTs (polar) showed an opposite behavior.

Furthermore, it was observed that enhanced deterpenation of origanum oil, i.e., higher carbon loadings, was obtained as the quantity of the activated carbon charged into the adsorption column increased. However, breakthrough-times of NMT components increased as the amount of carbon introduced into the column increased due to their strong affinity towards the sorbent. Based on the experimental results obtained at 40°C/7.5 MPa, it can be concluded that with eight grams of activated carbon sorbent, optimum adsorption duration would be between 540 to 630 minutes (required time for full saturation of bed), where at the same time the selectivity of the process is highest.

Based on the experimental results obtained during the supercritical-CO<sub>2</sub> adsorption (following the dense-gas extraction) runs using silanized silica gel at the same process conditions applied in the case of activated carbon (temperature, pressure, CO<sub>2</sub> flow rate, amount of oil pumped and amount of adsorbent), it can be concluded that compared to silanized silica gel, activated carbon is a more promising adsorbent in fractionating and eliminating the unstable MT hydrocarbons of origanum oil. This is because MT hydrocarbons show a low affinity for the carbon sorbent, yet lower affinity for the silica gel sorbent, in conjunction with a high affinity for CO<sub>2</sub>. On the contrary, the NMT hydrocarbons show a high affinity for the silica gel sorbent, even higher affinity for the carbon sorbent, in conjunction with a low affinity for CO<sub>2</sub>.

In addition, the effect of silica gel adsorbent quantity was studied. Although this effect was more important for substances exhibiting higher affinity for the sorbent, namely NMTs, it was demonstrated that increased quantities of silica gel did not provide a significant enrichment of the NMT components over the MT hydrocarbons, since  $\alpha$  values did not change much with time and amount of silica gel, as compared to the effect of activated carbon quantity. Therefore, it can be concluded that improved fractionation of origanum-oil components can be achieved by using activated carbon as the adsorbent since the adsorption capacity of silanized silica gel is much weaker than activated carbon.

At 40°C, the influence of desorption pressure on the selectivity of the process was investigated. Based on the experimental results, it can be concluded that the step-wise pressure increase method provided enhanced fractionation of origanum oil compared to the constant-pressure method; the low pressure step at 8.0 MPa produced the selective desorption of the weakly adsorbed MT hydrocarbons and the high pressure step at 14.5 MPa assured the fast desorption of the strongly adsorbed NMT components. Therefore, by this method, larger separation between MT and NMT cuts could be obtained as compared to the constant-pressure desorption process at 14.5 MPa, since in the latter case, due the preferential loading of both MT and NMT components into the supercritical phase, the relative-distribution ratio of the MT cut was equal to that of the NMT cut, hence  $\alpha$ -value was equal to one.

Furthermore, it was proved that the complete recovery of the origanum-oil constituents was related to adsorption-equilibrium limitations and that the solubility of these compounds in CO<sub>2</sub> did not represent the limiting factor of the desorption process. This is because, although the solubilities of essential-oil components grow dramatically as the effect of solvating power of the solvent increases due to the increase in CO<sub>2</sub> density, the desorption process was not effective after 480 minutes of CO<sub>2</sub> treatment, thus it was not possible to desorb all the key components of origanum oil from activated carbon.

On the other hand, the high-percentage of NMT compounds in the ethanol-extracted activated-carbon residue indicated that supercritical-CO<sub>2</sub> desorption of origanum oil from activated carbon at 40°C with step-wise pressure increase method, provided effective dewatering of the oil. The remaining part (residue) which was rich in oxygenated components like alcohols and phenolics (*carvacrol* and *thymol*) will have the essential odor and properties of the origanum oil. Therefore, these two steps allowed a fast and quasi-complete recovery of all NMT constituents contained in this origanum oil.

To determine the effect of the origanum-oil/CO<sub>2</sub> mixture composition on the fractionation of origanum oil and to further support the validity of the conclusion that the mixing cell situated prior to the adsorption column acted as a flash chamber, a supercritical-CO<sub>2</sub> adsorption (following the dense-gas extraction) run was performed with a continuous feed of origanum-oil/CO<sub>2</sub> mixture in the single-phase region, i.e., at 40°C/10.0 MPa using activated carbon sorbent. The experimental results gave the evidence that at this operating conditions, the separation between MT and NMT groups deteriorated, since the relative-distribution ratios of both MT and NMT cuts were very close to unity indicating that all components were equally soluble in CO<sub>2</sub>. Hence, compared to adsorption at 10.0 MPa, (adsorption with a single-phase feed) dewatering of origanum via supercritical adsorption at 7.5 MPa (adsorption with a two-phase feed) is more favorable since enhanced separation between MT and NMT components is obtained.

In light of all the experimental results, it can be concluded that the process utilizing the mixing cell as a flash chamber was better in obtaining an origanum-oil product possibly free of its MT hydrocarbons. In addition, the activated carbon column proved to be very

effective in enhancing the selectivity of the process. Last, desorption with pure supercritical- $\text{CO}_2$  enabled the elimination of the undesirable MT components, thus improving the oil quality.

## 6.2. Recommendations for Further Work

For possible research alternatives, several modifications are necessary in the experimental set-up constructed: First of all the biggest limitation of the apparatus is that  $\text{CO}_2$  flow rates beyond 1.5 g/min value cannot be monitored at the rotameter. By manipulating the metering valve, higher  $\text{CO}_2$  flow rates could be adjusted, but it was not possible to claim the uniformity of these increased flow rates throughout the experimental period. A larger scale rotameter would be more feasible, since at increased solvent flow rate the residence time of the system will be reduced, thus the breakthrough time of the origanum-oil components in the effluent will be shortened. However, it is important to mention that high solvent flow rates may disturb the equilibrium between the liquid-oil and dense-gas phases present in the mixing cell, consequently, the separation between the MT and NMT cuts might deteriorate. Therefore, the optimum  $\text{CO}_2$  flow rate can be determined by conducting preliminary experiments at different solvent flow rates at the suggested temperature and pressure, at which best fractionation of this origanum oil was obtained.

It was observed that the ethanol-extracted activated-carbon residue contained a high-percentage of NMT compounds. For complete desorption of these valuable compounds which contribute to the flavor and aroma of origanum oil, a higher pressure or a higher temperature (since increase in temperature lowers the adsorptive capacity). Another possible method that can be implemented to increase the low performance of the desorption process might be the continuous mixing of various polar entrainers (co-solvents such as ethanol) with the pure  $\text{CO}_2$  flow entering the desorber.

Some additions may be made to the sampling zone of the experimental set-up, which will make the sampling procedure easier and at the same time, applicable to essential oils containing high molecular weight compounds. Precisely, two separators operating in series at different temperatures and pressures may be used instead of a single sample collector operating at  $-25^{\circ}\text{C}$ /atmospheric pressure. In this study, the evolution of the process performance was obtained by taking samples at fixed time intervals from the sample collector; thus, the samples collected were not instantaneous but integral samples. Through this recommended arrangement, periodical discharge of the product from the bottom of each separator would be possible, i.e., a different product cut could be allowed to accumulate into a different collector. In such case, the task of securing a constant volume within the sample collector is not required, although the applied method in this study was successful in obtaining precise and accurate data. Furthermore, the distinct operation temperature and pressure in the separators may also be used to produce supersaturation and precipitation of selected compounds, such as waxes that usually are present in most essential oils produced by cold pressing. It is important to note that origanum oil does not contain any high molecular weight compounds because it is produced by hydrodistillation (Guenther, 1952).

Finally, this study might be extended by investigating the effect of using oregano leaves (instead of origanum oil) on the selectivity of the suggested process. In that case, the mixing cell will be packed with oregano leaves, and the origanum oil extracted (from the leaves) by dense  $\text{CO}_2$  will be allowed to enter the adsorber packed with activated carbon. Pure supercritical- $\text{CO}_2$  desorption with step-wise pressure increase method will be used in recovering the adsorbent compounds.

## APPENDIX A: TESTING THE SYSTEM WITH TOLUENE/CO<sub>2</sub> BINARY MIXTURE

The main purpose of this work was to develop a supercritical-CO<sub>2</sub>-based adsorption/desorption process (coupled with dense-gas extraction) to improve the quality of origanum oil (*Origanum Munituflorum*) through the removal of its monoterpene (MT) hydrocarbons, deterpenation. Before investigating the optimum conditions for the fractionation of origanum oil, the experimental set-up and procedure had to be tested. In this section, the different types of experiments carried out with toluene/CO<sub>2</sub> binary mixture, the experimental procedure employed and the results obtained will be demonstrated. The main aim in working with toluene was that vapor and liquid equilibrium-phase composition data for the toluene/CO<sub>2</sub> system were available (Ng and Robinson, 1978) and therefore, experimental data obtained could be easily compared with literature data.

### A.1. Experimental Procedure

Primarily the solubility behavior of toluene in CO<sub>2</sub> was studied, then the adsorption behavior of this binary mixture onto  $\alpha$ -cellulose and activated carbon was examined. Last, pure supercritical CO<sub>2</sub> was used to desorb the adsorbed toluene from the sorbent. Depending on the set of experiments, all measurements during both extraction and adsorption/desorption experiments were carried out in the high-pressure continuous flow-type apparatus, as shown in Figure A.1.1. As stated before, this set-up was modified prior to fractionation of origanum oil, but the equipment used was exactly the same in both cases, however the experimental procedure employed for the fractionation of origanum oil (for details refer to chapter five) was slightly different than the one applied for the toluene/CO<sub>2</sub> mixture. Briefly it can be summarized as follows:

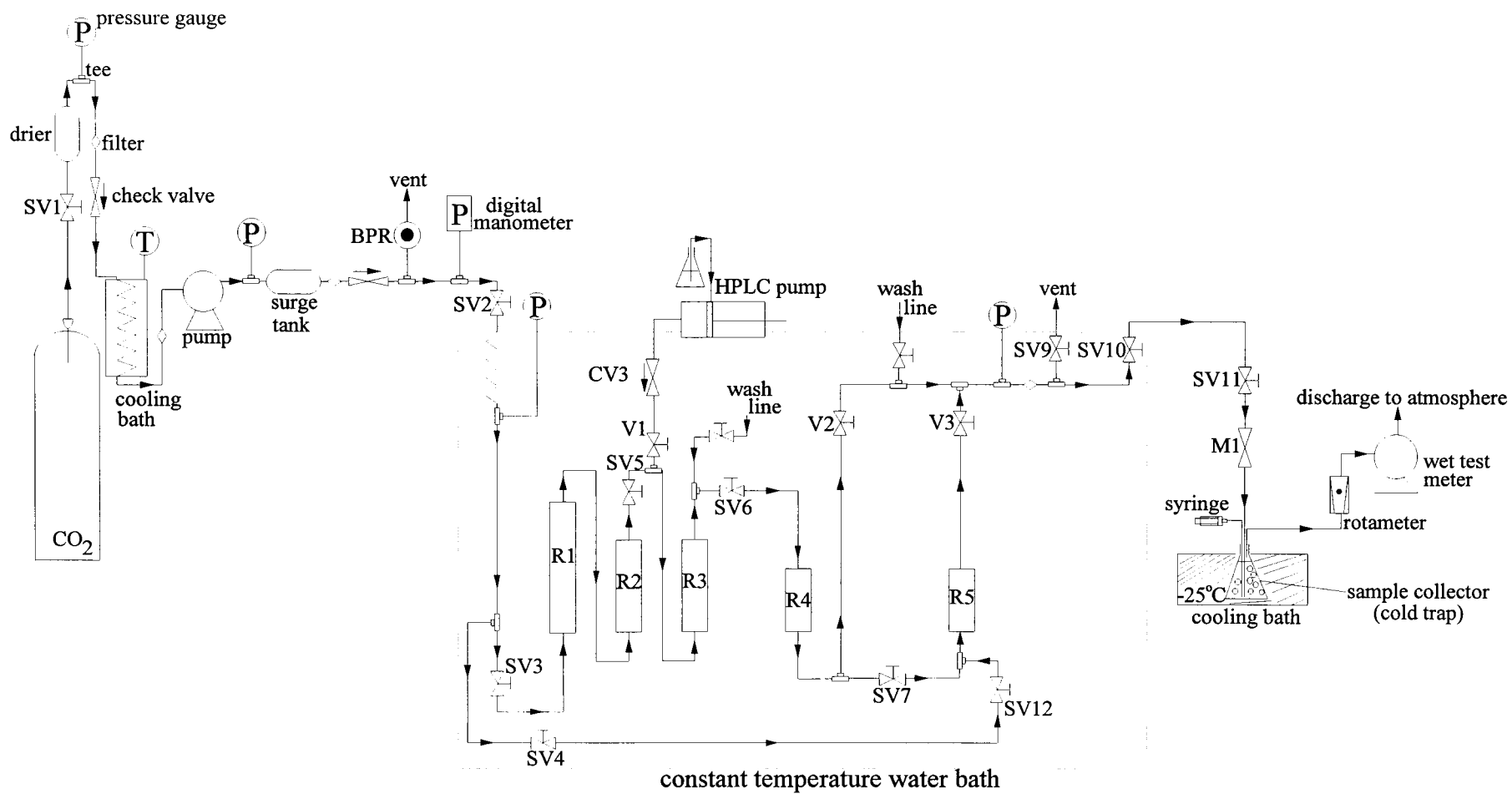


FIGURE A.1.1. Experimental set-up used in studying toluene/CO<sub>2</sub> binary mixture.

Prior to beginning a run, the constant-temperature water bath, the refrigerated bath which is used to cool the CO<sub>2</sub> before entering the diaphragm pump, and the cooling bath that contained the sample collector were all brought to their respective run temperatures. The electrical heating mantle covering the back-pressure regulator and that covering valves SV11 and M1 were activated to prevent them from freezing. The pump head was also cooled with water/monoethylene glycol mixture supplied from the cooling bath.

Initially, all on-off valves were kept closed. After obtaining the desired temperatures throughout the system, the valve of the CO<sub>2</sub> tube was opened and it was passed through the drier and surge tank via the on-off valve SV1. Then, the on-off valves SV2, SV3, SV5, SV6, V2 and SV10 were opened allowing CO<sub>2</sub> to flow through the system. Prior to turning on the diaphragm pump, the on-off valve SV11 and the metering valve M1 were opened. The high-pressure pump delivered CO<sub>2</sub> continuously at a desired flow rate and pressure was adjusted to the predetermined value by a back pressure regulator. The compressed CO<sub>2</sub> flowed through a heating coil and through columns R1-R4 (packed with glass beads) to insure that it reached the desired temperature before contacting toluene. Once the operation variables, i.e., temperature, pressure and CO<sub>2</sub> flow rate, were adjusted at their desired values, toluene (HPLC grade) was charged into the mixing chamber R3 (via on-off valve V1) using an HPLC pump. Throughout the extraction and adsorption experiments toluene was continuously pumped to the system at a constant flow rate. To assure a thorough mixing of these two streams and to avoid any entrainment of liquid droplets, the toluene/CO<sub>2</sub> stream was delivered from the bottom of the mixing cell. The feed mixture was then allowed to enter the extractor (saturator) R4. As CO<sub>2</sub> continuously flowed through column R4, it distributed through toluene. Solubilized material was carried out of the extractor and was expanded across the metering valve. The volume of the CO<sub>2</sub> leaving the system was determined by a wet test meter. The condensed toluene was collected in a cold trap immersed in a water/monoethylene glycol bath at -25°C. All collected solute was recovered in the cold trap containing 300 ml ethanol (Riedel de Haen, 99.9%). Samples from the cold trap were taken every 15 minutes by a syringe and 10 drops of this sample was mixed with 50 µl ethanol (Riedel de Haen, 99.9%). The remaining sample in the syringe was immediately injected back into the sample collector to provide constant volume within the cold trap. The composition of the fractions collected during the experiment was

analyzed by gas chromatograph (HP 5890 Series II) equipped with a flame ionization detector (FID) at every 15 minute time intervals.

The adsorption experiment was started when a constant composition of the toluene/CO<sub>2</sub> mixture, determined by regular sampling as explained above, was obtained. In that case, the adsorption experiment was initiated by closing the on-off valve V2, and switching the toluene/CO<sub>2</sub> mixture flow to enter the adsorber (R5) through the on-off valve SV7. Once the pressure in the adsorber reached the operating pressure (continuously the pressure within the system was monitored by the digital manometer), the on-off valve V3 was opened. Regular sampling, as described above, allowed to trace the breakthrough behavior of the toluene. When the exit concentration reached the inlet concentration, the adsorption experiment was terminated. Then, pure supercritical CO<sub>2</sub> flow was allowed to enter the desorber via the on-off valves SV4 and SV12, provided the on-off valves SV7, V3, SV5 and SV6 were instantaneously closed, and the on-off valve V3 was opened. During the desorption step, toluene was not charged to the system, hence the HPLC pump was not operated and the on-off valve V1 was kept closed throughout the experiment. The composition of the fractions collected during the desorption experiment was monitored in a similar way as described above.

A calibration curve was prepared in order to determine the change in moles of toluene with respect to time in the sample collector. Since gas chromatography analysis gives area per cent results, which are directly proportional to the mass of a component in a solution, samples of different weight fractions of toluene in ethanol were prepared and analyzed by gas chromatography (GC) method. Each prepared sample was injected three times to account for the replicability of the GC analysis. Figure A.1.2 shows the calibration curve, i.e., mass fraction of toluene in ethanol versus per cent area graph, which was used to calculate moles of toluene dissolved in supercritical CO<sub>2</sub>, assuming ethanol volume in the sample collector remained constant at all times during the experiment. Specifications of the column and temperature program of the chromatograph are given in section A.3.

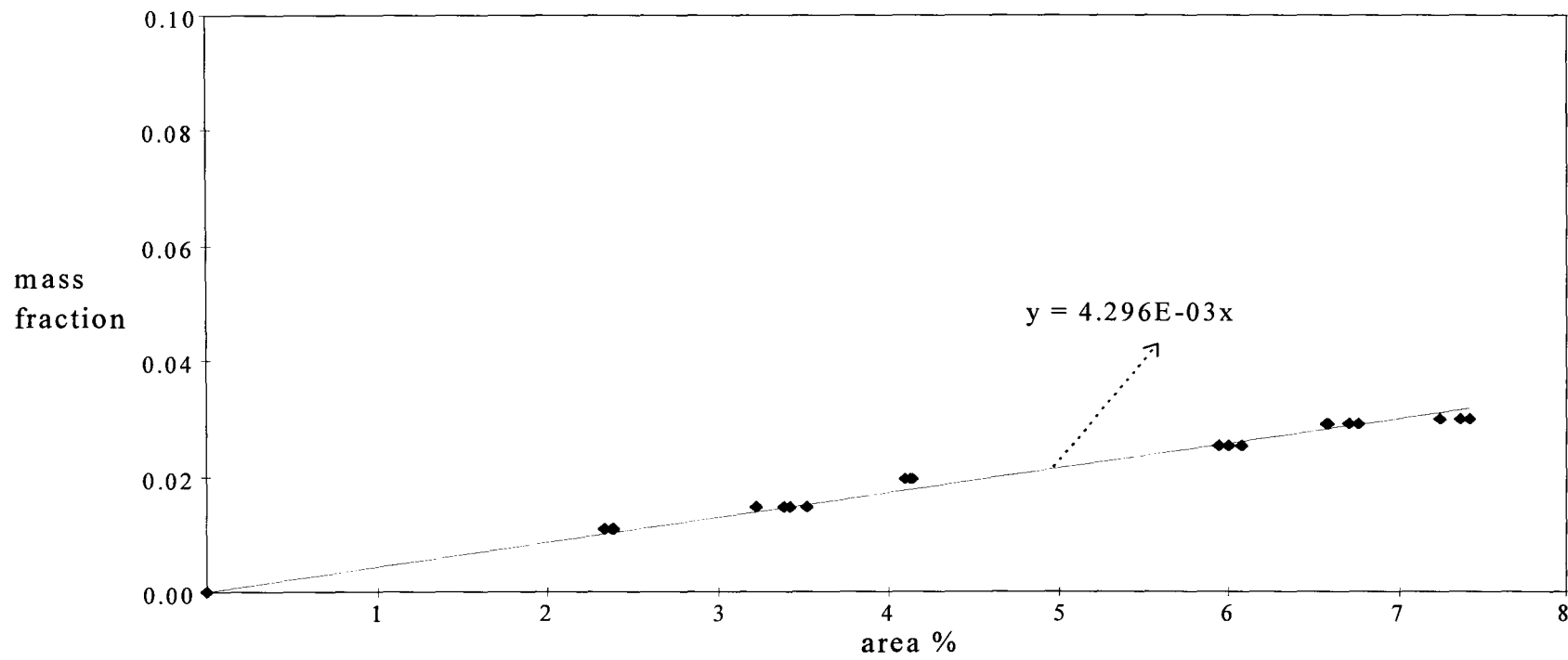


FIGURE A.1.2. Calibration curve of toluene/ethanol mixture by GC.

## A.2. Experimental Program

First, solubility behavior of the binary mixture of toluene and CO<sub>2</sub> was investigated at 40°C/10.0 MPa over a range of toluene flow rates from 0.025 to 0.1 ml/min. Toluene was first mixed with CO<sub>2</sub> to obtain a saturated mixture of toluene in supercritical CO<sub>2</sub>. Table A.2.1 shows the set of saturation experiments performed with different toluene concentrations in the feed mixture. Replicate runs were done to obtain accuracy and precision in the experiments. Between successive trials the whole set-up was cleaned (the same cleaning procedure was used as explained in section 5.3.5) until toluene was not detected in the sample collector.

TABLE A.2.1. Saturation experiments performed with the toluene/CO<sub>2</sub> binary system.

Run no.	Pressure (MPa)	Temperature (°C)	Toluene flow rate (ml/min)	CO <sub>2</sub> flow rate (cm <sup>3</sup> /min)	Run time (min)
1	10.0	40	0.05	1.26	255
2	10.0	40	0.05	1.29	255
3	10.0	40	0.10	1.31	255
4	10.0	40	0.10	1.31	255
5	10.0	40	0.05	1.30	255
6	10.0	40	0.025	1.30	255

After saturation experiments were completed, then the adsorption behavior of this binary mixture on  $\alpha$ -cellulose and activated carbon was examined at 40° C /10.0 MPa and at 0.05 ml/min toluene flow rate. Once the adsorption process was completed, pure supercritical CO<sub>2</sub> was used to desorb the adsorbed toluene from the sorbent. Sets of runs, listed in Table A.2.2 were performed to study the effect of an adsorbent,  $\alpha$ -cellulose, in the extraction of toluene from toluene/CO<sub>2</sub> binary system.

TABLE A.2.2. Adsorption/desorption experiments performed with toluene/CO<sub>2</sub> system.

Run no.	CO <sub>2</sub> flow rate (cm <sup>3</sup> /min) during extraction	CO <sub>2</sub> flow rate (cm <sup>3</sup> /min) during adsorption	CO <sub>2</sub> flow rate (cm <sup>3</sup> /min) during desorption	adsorbent (g, kind)
1	1.28	1.27	1.26	2, α-cellulose
2	1.28	1.27	1.26	5, α-cellulose
3	1.29	1.27	1.26	10, α-cellulose
4	1.23	1.24	1.24	11, carbon

### A.3. Analytical Conditions Used On the GC

Samples of toluene collected in ethanol were analyzed by using capillary gas chromatograph (HP 5890 Series II) with flame ionization detector (FID). The temperature program and the operating conditions of the chromatogram were as follows:

Detector type	: Flame Ionization Detector (FID)
Detector temperature	: 250°C
Inlet type	: Split
Split ratio	: 1/250
Inlet temperature	: 250°C
Injection volume	: 1 μl
Column type	: Innowax (crosslinked polyethylene glycol), 25m×0.20mm×0.25μm film thickness
Carrier gas	: N <sub>2</sub>
Carrier gas flow rate	: 0.4 cm <sup>3</sup> /min
Oven temperature program	: The oven temperature was 35°C and the oven was kept at this constant temperature for 10 minutes. Total analysis time was 10 minutes.

#### A.4. Experimental Results of Toluene/CO<sub>2</sub> Binary System

The experimental set-up designed for studying the fractionation of origanum oil via supercritical CO<sub>2</sub> was first tested with the toluene/CO<sub>2</sub> binary mixture. The main objective in these trials was to compare available literature data with experimental measurements. The experimental program given in section A.2 was followed, and the results proved that both the experimental set-up and procedure could be accepted as working satisfactorily.

Regarding toluene/CO<sub>2</sub> equilibrium-phase composition data (Ng and Robinson, 1978), all saturation and adsorption/desorption experiments were performed at 40°C/10.0 MPa conditions, at which this binary mixture exists in the single-phase region. Single-phase criteria was a necessary condition in all the runs, because in this region toluene was completely miscible in CO<sub>2</sub>. Therefore, moles toluene collected at the end of each experiment would directly correspond to the feed mixture composition. Hence, as the feed mixture composition was varied by adjusting toluene flow rate at the HPLC pump (keeping CO<sub>2</sub> flow rate constant), moles of toluene collected in the sample collector changed in the same mode. Although it was not necessary to reach equilibrium in the experiments done, the equilibrium-phase composition data was useful as a starting point.

Saturation runs, in which the aim was to obtain a constant composition mixture of toluene in supercritical CO<sub>2</sub>, were first carried out at 0.05 ml/min toluene flow rate mixed with supercritical CO<sub>2</sub> at 40°C/10.0 MPa. As illustrated in Figure A.4.1, for approximately 50 minutes, the residence time, toluene was not identified in the samples taken from the cold trap. Then, toluene concentration started to increase and after 90 minutes, a linear change in moles toluene collected per time was observed. This shows that a saturated mixture of toluene and supercritical CO<sub>2</sub> was obtained after 90 minutes and the composition of this mixture could be calculated from the slope of the straight line. Throughout the experiment, toluene was introduced to the system at a rate of 0.05 ml/min, which is equal to 0.0004705 moles toluene per minute, as calculated below. As seen in Figure A.4.1, theoretical and experimental slope values were in good agreement, which proves that all toluene pumped was completely miscible in CO<sub>2</sub>. Hence, it was accepted that toluene/CO<sub>2</sub>

mixture with a composition of about 97.5% CO<sub>2</sub> was in the single-phase region at 40°C/10.0 MPa conditions.

$$0.05 \frac{\text{ml toluene}}{\text{min}} * 0.867 \frac{\text{g toluene}}{\text{cm}^3} / 92.14 \frac{\text{g toluene}}{\text{mole}} = 0.0004705 \frac{\text{mole toluene}}{\text{min}} \quad (\text{A.1})$$

If toluene flow rate is raised to 0.1 ml/min, which means increasing toluene mole fraction in the feed mixture, then the slope of moles toluene versus time graph will also be doubled provided the mixture is still in the single-phase region. Likewise, if toluene flow rate is decreased to 0.025 ml/min, then the slope of moles toluene versus time graph will be halved provided the mixture is still in the single-phase region.

In order to establish the validity of the above arguments, the saturation experiments were continued at the same operating conditions (40°C/10.0 MPa), but with 0.1 ml/min toluene flow rate while keeping CO<sub>2</sub> flow rate constant. In this case, the experimental slope, calculated from the slope of the straight line for moles toluene versus time graph (as shown in Figure A.4.2) and the theoretical slope, as calculated below, differed from each other by 95 per cent.

$$0.1 \frac{\text{ml toluene}}{\text{min}} * 0.867 \frac{\text{g toluene}}{\text{cm}^3} / 92.14 \frac{\text{g toluene}}{\text{mole}} = 0.0009410 \frac{\text{mole toluene}}{\text{min}} \quad (\text{A.2})$$

According to the above discussion, increasing toluene flow rate should also have increased the experimental slope value. But unlikely, when Figures A.4.1 and A.4.2 were compared, there was a remarkable difference both in the slopes and in the number of moles of toluene collected at the end of each saturation experiment; the number of moles of toluene collected at the end of 0.1 ml/min run were much lower than those in the 0.05 ml/min run. This shows that toluene/CO<sub>2</sub> mixture falls into the two-phase region once

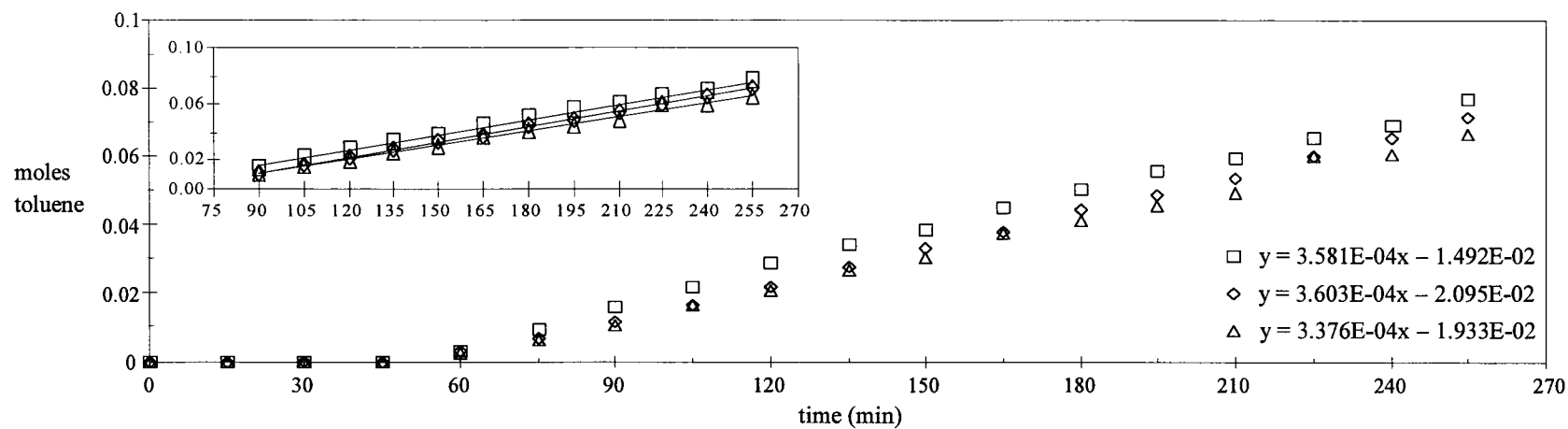


FIGURE A.4.1. Saturation experiments for toluene (0.05 ml/min) in dense CO<sub>2</sub> at 40°C/10.0 MPa (□, △, ◇: replicate runs).

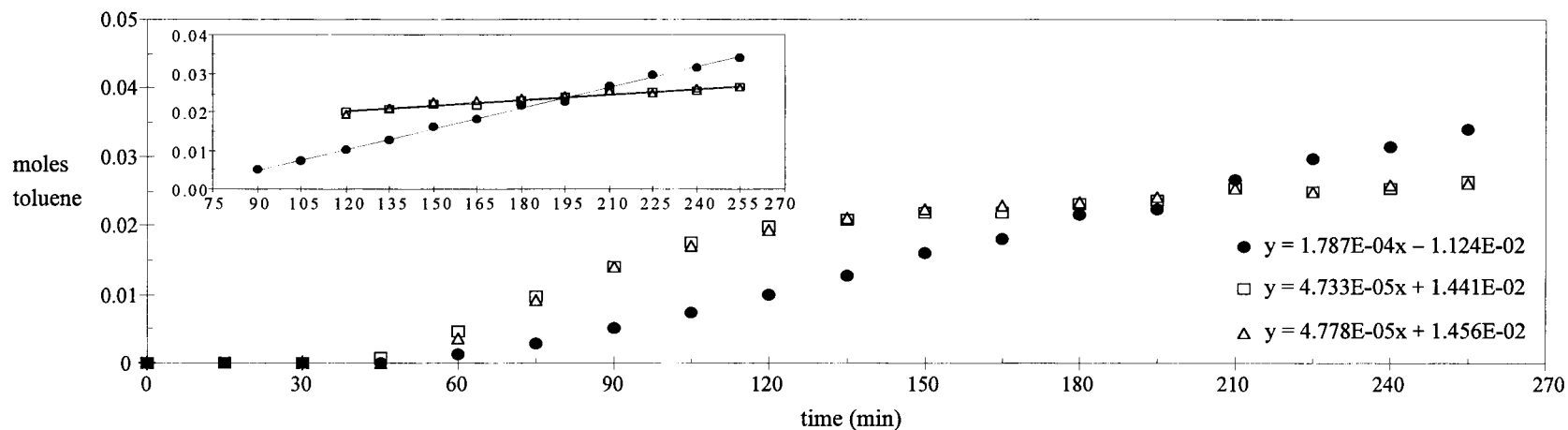


FIGURE A.4.2. Saturation runs for toluene in dense CO<sub>2</sub> at 40°C/10.0 MPa (□, △:0.01 ml/min, ●:0.025 ml/min).

toluene mole fraction in the feed mixture was increased, although temperature and pressure were kept constant. In the two-phase region, in the dense-gas phase, some toluene is dissolved in supercritical CO<sub>2</sub>, but a liquid-toluene phase is also present, which interferes with the amount of toluene dissolved in the dense-gas phase.

Finally, toluene flow rate was decreased to 0.025 ml/min (keeping CO<sub>2</sub> flow rate constant) to see the effect of feed composition on the phase behavior of the toluene/CO<sub>2</sub> binary system at 40°C/10.0 MPa. The theoretical slope, as calculated below, was in good agreement with the experimental one and this proves that toluene was completely miscible in CO<sub>2</sub> at these conditions. As illustrated in Figure A.4.2, it is obvious that as toluene flow rate was halved (from 0.05 ml/min to 0.025 ml/min), the experimental slope value was also halved. This shows that in both experiments, toluene/CO<sub>2</sub> binary system is in the single-phase region at 40°C/10.0 MPa conditions.

$$0.025 \frac{\text{ml toluene}}{\text{min}} * 0.867 \frac{\text{g toluene}}{\text{cm}^3} / 92.14 \frac{\text{g toluene}}{\text{mole}} = 0.0002352 \frac{\text{mole toluene}}{\text{min}} \quad (\text{A.3})$$

Therefore, regarding the pressure-equilibrium phase diagram of toluene-CO<sub>2</sub> binary system (presented in Figure A.4.3), not only temperature and pressure but also mole fraction of CO<sub>2</sub> in the feed is an important variable in determining the phase behavior of the mixture. In the first case corresponding to 0.05 ml/min toluene flow rate, point A, must be just on the edge of the two-phase envelope, as seen in Figure A.4.3. As toluene flow rate is increased from 0.05 ml/min to 0.1 ml/min, point B, (keeping CO<sub>2</sub> flow rate almost constant), i.e., once toluene mole fraction in the feed mixture is increased, the binary mixture falls into the two-phase region although CO<sub>2</sub> mole fraction in the feed mixture does not change much, as seen in Table A.4.1. Similarly, as toluene flow rate is decreased from 0.05 ml/min to 0.025 ml/min, point C, the binary mixture remains in the single-phase region. In order to see the effect of pressure on the phase behavior of the binary mixture, it was planned to increase the pressure from 10.0 to 14.0 MPa, keeping toluene flow rate at 0.025 ml/min and all other variables constant. As shown in Table A.4.1, although the mixture

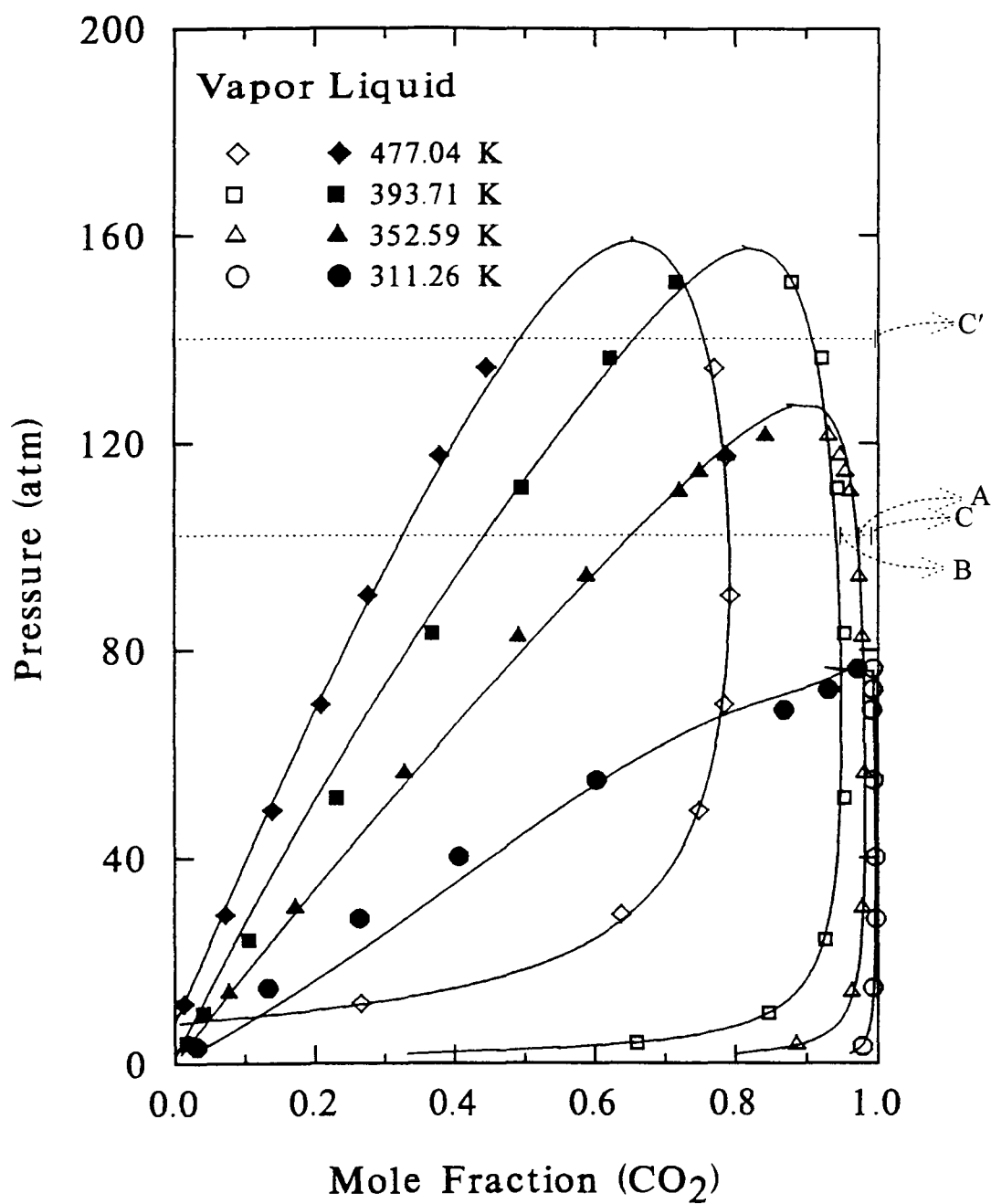


FIGURE A.4.3. Pressure-equilibrium phase composition diagram for the toluene/CO<sub>2</sub> binary system (Turgay, 1995).

composition shifts towards the right (point C') the effect can hardly be detected experimentally since a 40 per cent increase in pressure results only in an infinitesimal change in CO<sub>2</sub> mole fraction.

TABLE A.4.1. Equilibrium phase composition of toluene/CO<sub>2</sub> system at 40°C.

Position	Pressure (MPa)	Toluene flow rate (ml/min)	CO <sub>2</sub> flow rate (cm <sup>3</sup> /min)	CO <sub>2</sub> mole fraction
point A	10.0	0.05	1.30	0.97558
point B	10.0	0.10	1.30	0.95233
point C	10.0	0.025	1.30	0.98764
point C'	14.0	0.025	1.30	0.98974

After solubility experiments were completed, then adsorption/desorption behavior of this binary mixture onto  $\alpha$ -cellulose was investigated at 40°C/10.0MPa conditions and at 0.05 ml/min toluene flow rate, as presented in Table A.2.2. All these experiments were performed in three steps: (i) a constant composition mixture of toluene in supercritical CO<sub>2</sub> was obtained (ii) this feed mixture was allowed to enter the adsorber (iii) pure supercritical CO<sub>2</sub> was used to desorb the adsorbed toluene from the sorbent. At the beginning of the adsorption process, moles of toluene collected in the sample collector remained constant for some time as the toluene/CO<sub>2</sub> mixture entered the adsorber, and then started to increase. Adsorption experiments were ended when the exit concentration reached the inlet concentration. As the amount of adsorbent ( $\alpha$ -cellulose) increased, the adsorptive capacity was expected to increase. Unfortunately, the amount of toluene adsorbed on  $\alpha$ -cellulose was almost negligible in all runs showing that toluene was not selectively adsorbed on  $\alpha$ -cellulose, as seen in Figure A.4.4. This indicated that  $\alpha$ -cellulose acted as an inert packing.

Adsorption/desorption experiments were then continued using activated carbon as the adsorbent. Only one run (saturation, adsorption and desorption in series) was conducted at 40°C/10.0 MPa conditions and at 0.05 ml/min toluene flow rate. In this run, as seen in Figure A.4.5, at the beginning of the adsorption process, the number of moles of toluene remained constant for 60 minutes and then started to increase reaching the inlet

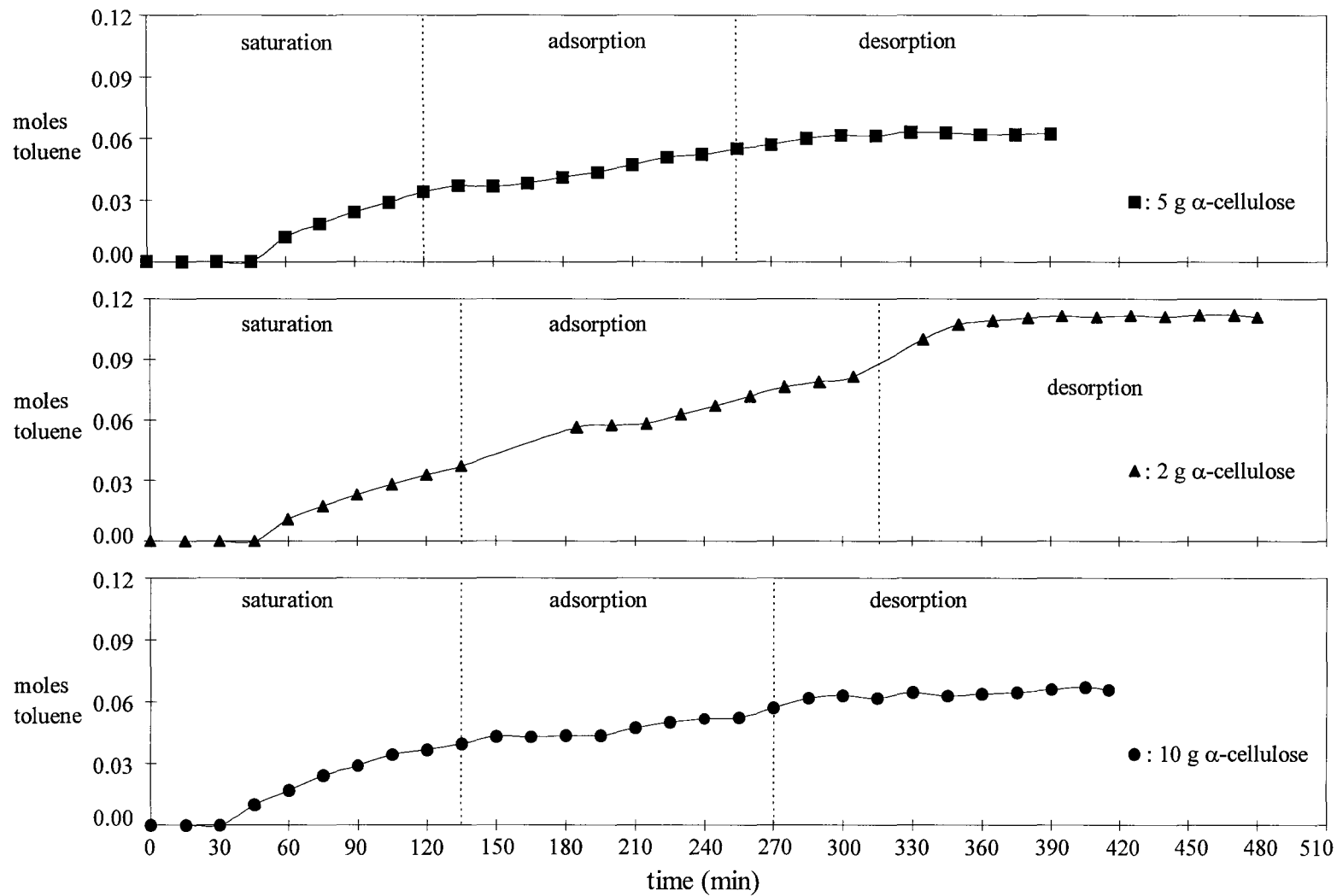


FIGURE A.4.4. The adsorption/desorption behavior of toluene/CO<sub>2</sub> mixture on  $\alpha$ -cellulose at 40°C/10.0 MPa.

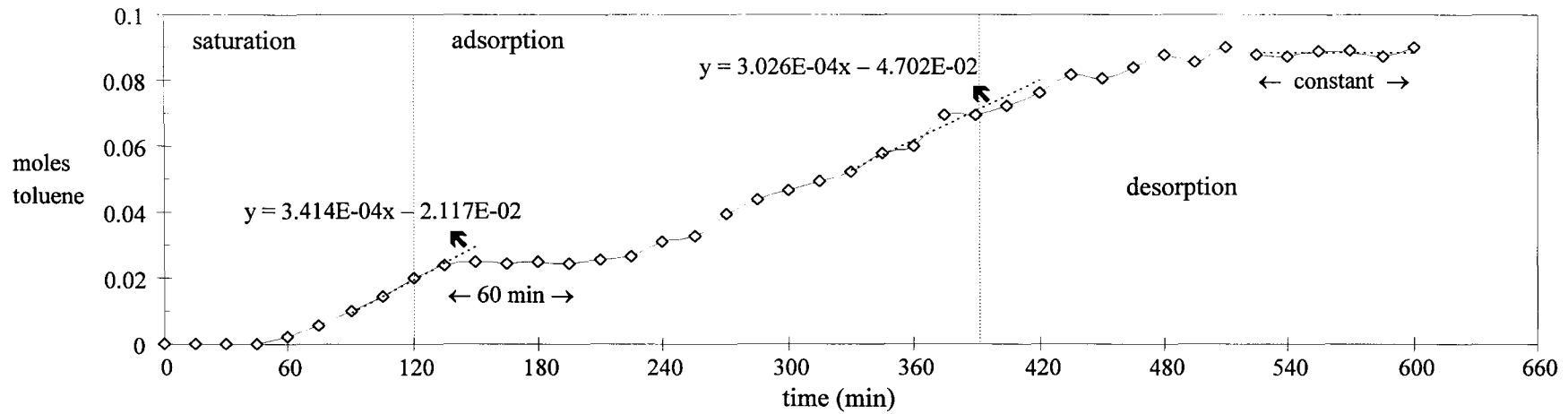


FIGURE A.4.5. The adsorption/desorption behavior of toluene/CO<sub>2</sub> mixture on activated carbon at 40°C/10.0 MPa.

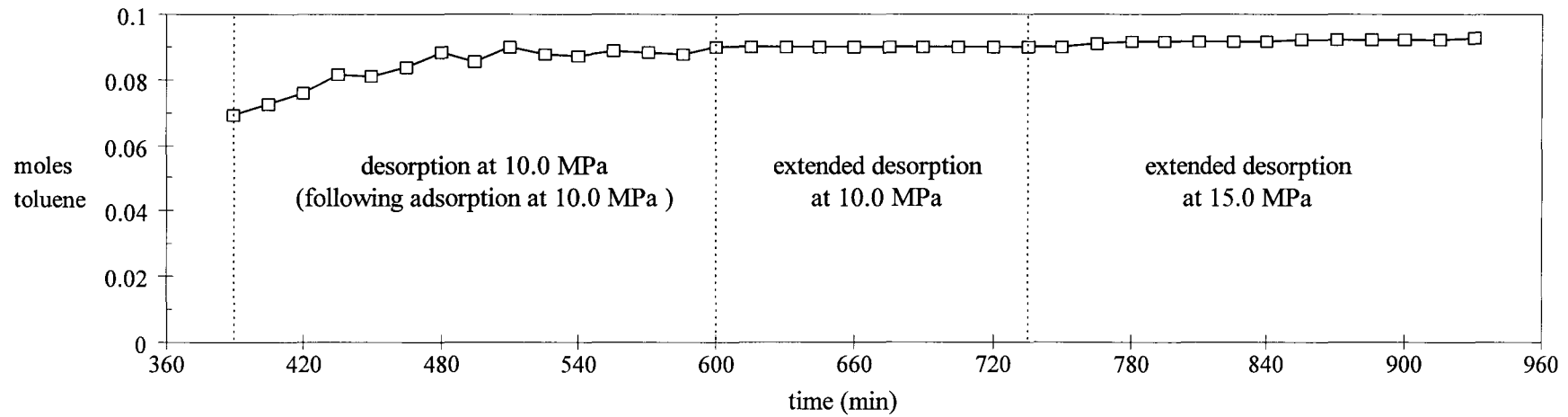


FIGURE A.4.6. Effect of pressure on the desorption from carbon (at 40°C) previously loaded with toluene/CO<sub>2</sub> mixture.

concentration, i.e., the slopes of the saturation and adsorption curves became almost identical. The number of moles of toluene adsorbed were calculated by integrating the area above the adsorption curve, and the number of moles of toluene desorbed were calculated by integrating the area under the desorption curve. Calculations showed that it was not possible to desorb (0.017 moles of toluene desorbed) all toluene adsorbed on the activated carbon (0.040 moles toluene). This showed that some adsorbed toluene was still present on the activated carbon (0.023 moles of toluene had been adsorbed on the carbon).

Finally, with the activated carbon used in the experiment described above, an extended desorption run was performed: at 10.0 MPa for 120 minutes, then at 15.0 MPa for 180 minutes. As seen in Figure A.4.6, experimental results show that it was not possible to desorb any toluene at 10.0 MPa, but once pressure was increased to 15.0 MPa, the amount of toluene desorbed started to increase at a very slow rate. An increase in pressure affected a recovery in the amount of toluene adsorbed by 12.5 per cent, but still all the toluene adsorbed was not desorbed. Further increase in the pressure might have resulted in a larger amount of toluene recovered. As a conclusion, the desorption step should be performed at a higher pressure than adsorption in order to be able to desorb all the adsorbed material from the adsorbent.

Following the adsorption/desorption experiments, another run named as “blank run” was performed using only pure CO<sub>2</sub> to confirm the validity of the following assumptions. After the supercritical CO<sub>2</sub> stream saturated with toluene was flashed to atmospheric pressure through the heated metering valve, all the precipitated toluene was assumed to be trapped in the sample collector containing ethanol (as explained in section A.1). Moreover, the volume of ethanol in the sample collector was assumed to be remaining constant, i.e., 300 ml ethanol, at all times during a run. The expanded-CO<sub>2</sub> gas leaving the sample collector was also presumed to be free of both toluene and ethanol. A predetermined concentration of toluene/ethanol mixture was prepared in the sample collector regarding the maximum attainable number of moles of toluene collected during an adsorption run. Pure CO<sub>2</sub> (at the same flow rate as in all other runs) was continuously passed through the system as if a saturation run was performed (toluene was not introduced to the system) and at 15 minute intervals samples were taken from the sample collector to be directly analyzed by

GC. As depicted in Figure A.4.7, moles of toluene collected in the sample collector were almost constant with respect to time. The results were within the experimental error limits, and therefore it could be concluded that neither toluene nor alcohol loss was detectable.

Based on the information/experience gained with the toluene/CO<sub>2</sub> system, the experimental set-up (Figure A.1) constructed was slightly changed prior to the fractionation of origanum oil via supercritical CO<sub>2</sub>. The main modification was made in the way the adsorption process was conducted. Throughout experiments performed with the toluene/CO<sub>2</sub> system, once a constant composition feed mixture was reached, the adsorption experiment was started by allowing this mixture to enter the adsorber. Considering Figure A.4.5, it seems that the residence time during the saturation and adsorption experiments is very similar. This behavior can be explained as follows: The delayed appearance of toluene in the sample collector may be due to the adsorption phenomena taking place on the activated carbon. This argument could be proved by decreasing the amount of sorbent, which in turn would affect the breakthrough time of toluene (it should be less than 60 minutes). On the other hand, the delayed appearance of toluene points out that maybe an adsorption process was not really taking place, but instead the toluene/CO<sub>2</sub> stream was simply diffusing (traveling) along the adsorber. Although all the connecting lines and the adsorber were filled with pure CO<sub>2</sub> before toluene flow was started during the saturation run (to prevent the sudden pressure-drop while switching from saturation to adsorption procedure), toluene/CO<sub>2</sub> mixture once out of the saturator would force out (push) the pure CO<sub>2</sub> present in the connecting lines and adsorber. This would take some time until the toluene/CO<sub>2</sub> feed mixture thoroughly filled the adsorber and got into contact with the adsorbent for the adsorption process to begin. Therefore, to eliminate this uncertainty, both saturation and adsorption experiments were decided to be performed in the same manner. Accordingly, during the saturation (extraction) experiment, the origanum-oil/CO<sub>2</sub> mixture was allowed to enter the adsorber filled with glass beads and during the adsorption run, the adsorber was to be filled with the adsorbent. Runs with origanum oil were performed in that manner and the entrance of the origanum oil feed was shifted towards column R4, as presented in Figure 4.2.1.

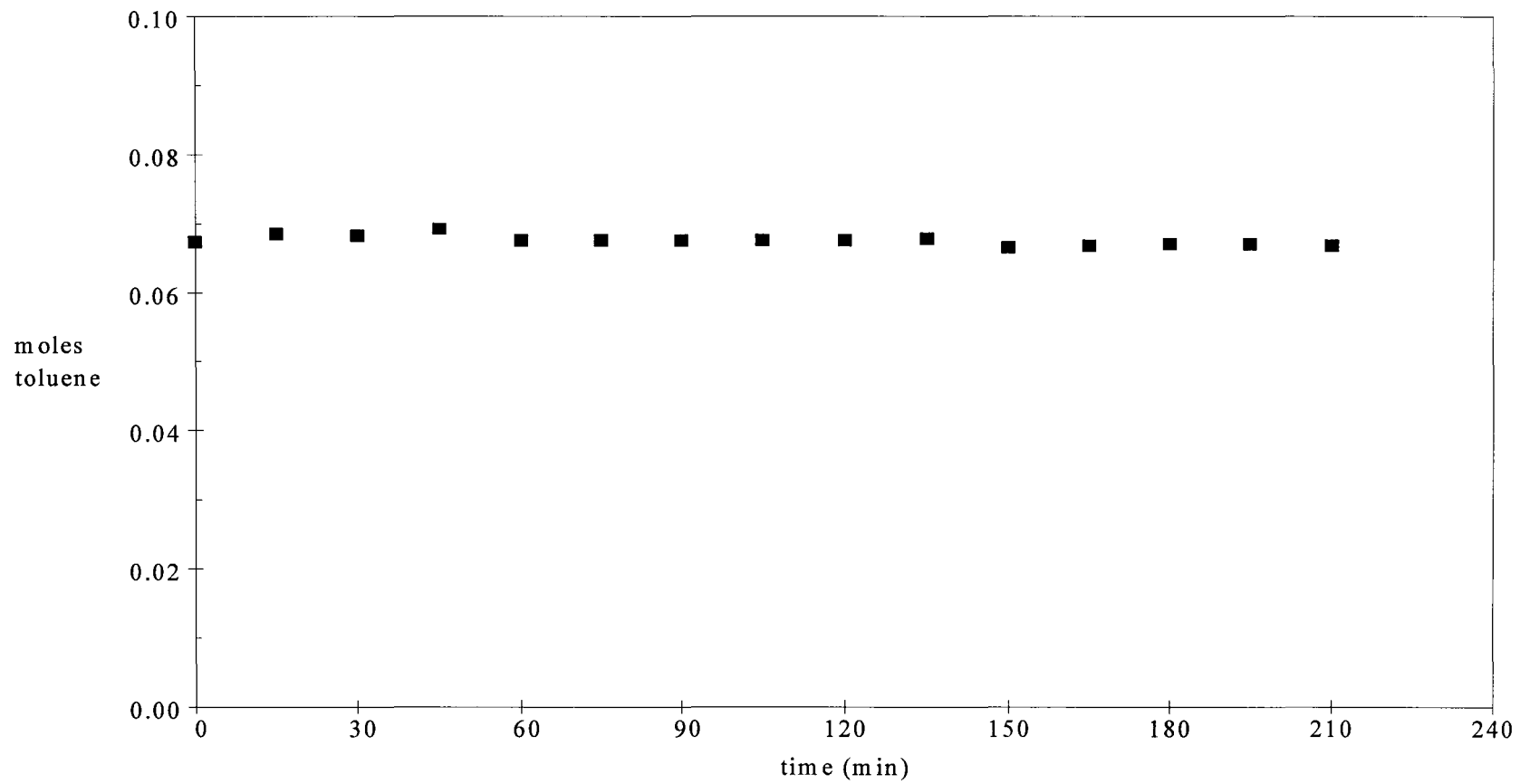


FIGURE A.4.7. Moles toluene collected during blank run.

## APPENDIX B: ANALYTICAL CONDITIONS USED ON THE GC/MS

The analyses of the oil samples and the identification of the components were performed by using capillary gas chromatograph (HP 5890 Series II) with a mass selective detector (HP 5971). The computer software, HP Chemstation, was used for the analysis, integration, normalization and identification of peaks. The operating conditions used for the analyses are listed below:

Detector type	: Mass Selective Detector (MSD)
Detector temperature	: 250°C
Inlet type	: Split
Split ratio	: 1/100
Inlet temperature	: 250°C
Injection volume	: 1µl
Column type	: Innowax (crosslinked polyethylene glycol), 60m×0.25mm×0.25µm film thickness
Carrier gas	: He
Carrier gas flow rate	: 1 cm <sup>3</sup> /min
Oven temperature program	: The oven temperature program consists of three ramps. The initial oven temperature was 70°C (the oven was kept at this temperature for 8 minutes). The final oven temperature was 240°C, and total analysis time was 45 minutes.

TABLE B.1. Temperature program of the analyses at GC/MS.

	Rate (°C/min)	Temperature (°C)	Time (min)
Level 1	8.00	130	1.00
Level 2	3.00	190	1.00
Level 3	8.00	240	1.25

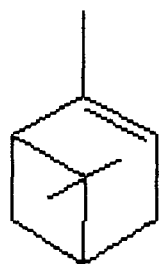
## **APPENDIX C**

### **Properties and Structures of Origanum-oil Components**

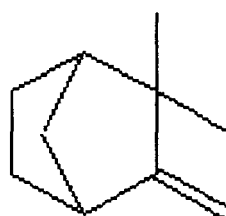
TABLE C.1. Physical and chemical properties of origanum-oil components.

Component	Formula and Molecular Weight	Boiling Point (°C) at 760 mmHg	Density (g/cm <sup>3</sup> ) at 20°C	Solubility		
				water	alcohol	ether
$\alpha$ -pinene	C <sub>10</sub> H <sub>16</sub> 136.24	156.2	0.857	insoluble	$\infty$	$\infty$
camphene	C <sub>10</sub> H <sub>16</sub> 136.24	159-160	0.870	insoluble	-	-
myrcene	C <sub>10</sub> H <sub>16</sub> 136.24	167	0.801	insoluble	soluble	soluble
$\alpha$ -terpinene	C <sub>10</sub> H <sub>16</sub> 136.24	173-175	0.837	insoluble	$\infty$	$\infty$
$\beta$ -phellandrene	C <sub>10</sub> H <sub>16</sub> 136.24	171-172	0.852	-	-	-
1,8 cineole	C <sub>10</sub> H <sub>18</sub> O 154.26	176.4	0.922	insoluble	soluble	-
$\gamma$ -terpinene	C <sub>10</sub> H <sub>16</sub> 136.24	183	0.849	insoluble	$\infty$	$\infty$
p-cymene	C <sub>10</sub> H <sub>14</sub> 134.22	177	0.857	insoluble	$\infty$	$\infty$
linalool	C <sub>10</sub> H <sub>18</sub> O 154.26	199	0.868	slightly	$\infty$	$\infty$
terpinen-4-ol	C <sub>10</sub> H <sub>18</sub> O 154.26	209-212	0.933	-	-	-
caryophyllene	C <sub>15</sub> H <sub>24</sub> 204.36	256	0.907	insoluble	soluble	-
borneol	C <sub>10</sub> H <sub>18</sub> O 154.26	210	-	insoluble	-	-
thymol	C <sub>10</sub> H <sub>14</sub> O 150.22	233	0.965	slightly	soluble	soluble
carvacrol	C <sub>10</sub> H <sub>14</sub> O 150.22	237.7	0.977	slightly	soluble	soluble

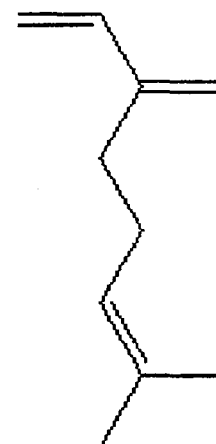
The molecular structures and CAS numbers (in brackets) of the key components of origanum oil (*Origanum Munituflorum*) are given below.



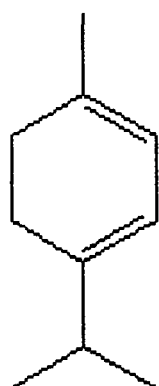
$\alpha$ -pinene  
( $C_{10}H_{16}$ )  
[80-56-8]



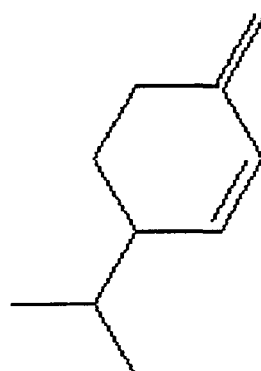
camphene  
( $C_{10}H_{16}$ )  
[79-92-5]



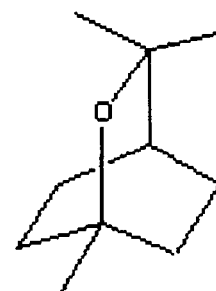
myrcene  
( $C_{10}H_{16}$ )  
[123-35-3]



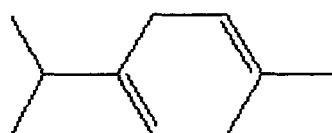
$\alpha$ -terpinene  
( $C_{10}H_{16}$ )  
[99-86-5]



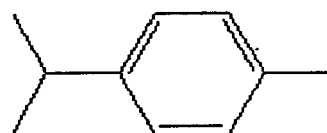
$\beta$ -phellandrene  
( $C_{10}H_{16}$ )  
[555-10-2]



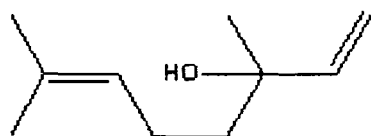
1,8 cineole  
( $C_{10}H_{18}O$ )  
[470-82-6]



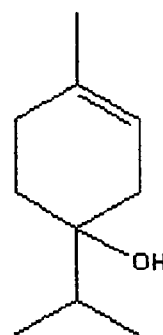
$\gamma$ -terpinene  
( $C_{10}H_{16}$ )  
[99-85-4]



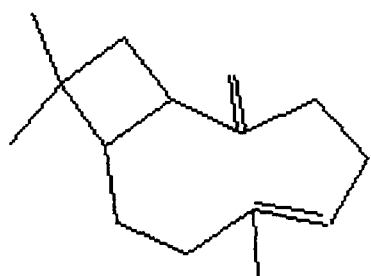
p-cymene  
( $C_{10}H_{14}$ )  
[99-87-6]



**linalool**  
(C<sub>10</sub>H<sub>18</sub>O)  
[78-70-6]



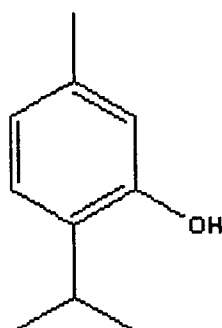
**terpinen-4-ol**  
(C<sub>10</sub>H<sub>18</sub>O)  
[562-74-3]



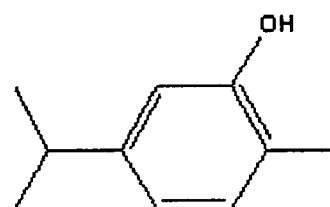
**t-caryophyllene**  
(C<sub>15</sub>H<sub>24</sub>)  
[87-44-5]



**borneol**  
(C<sub>10</sub>H<sub>18</sub>O)  
[507-70-0]



**thymol**  
(C<sub>10</sub>H<sub>14</sub>O)  
[89-83-8]



**carvacrol**  
(C<sub>10</sub>H<sub>14</sub>O)  
[499-75-2]

## **APPENDIX D**

**Relative-distribution Ratios of the Key Components in Origanum Oil  
Calculated for Each Experiment Performed**

TABLE D.1. Relative-distribution ratios of organum-oil components in extraction experiment at 40°C/7.5 MPa.

Component→ Time (min)↓	α-pinene	camphene	myrcene	α-terpinene	PC1	γ-terpinene	p-cymene	linalool	PC2	borneol	thymol	carvacrol
30	3.120	2.525	2.469	2.495	0.785	1.929	2.328	0.113	0.188	0.000	0.000	0.166
60	3.023	2.448	2.346	2.410	0.785	1.905	2.241	0.113	0.239	0.071	0.000	0.213
90	2.412	2.066	2.160	2.326	0.960	1.817	2.001	0.226	0.393	0.106	0.122	0.354
120	2.091	1.836	1.914	2.072	0.873	1.674	1.821	0.283	0.462	0.142	0.122	0.493
150	-	-	-	-	-	-	-	-	-	-	-	-
180	1.705	1.530	1.605	1.776	0.873	1.419	1.472	0.396	0.667	0.284	0.365	0.714
210	1.737	1.530	1.605	1.734	0.960	1.363	1.396	0.452	0.718	0.319	0.365	0.745
240	-	-	-	-	-	-	-	-	-	-	-	-
270	1.640	1.454	1.481	1.607	0.873	1.267	1.298	0.509	0.787	0.390	0.487	0.809
300	1.383	1.224	1.358	1.480	0.873	1.196	1.205	0.622	0.906	0.496	0.609	0.872
330	1.480	1.301	1.420	1.522	0.960	1.211	1.216	0.622	0.906	0.496	0.609	0.847
360	1.480	1.301	1.420	1.522	0.960	1.172	1.140	0.678	0.975	0.567	0.731	0.867
390	-	-	-	-	-	-	-	-	-	-	-	-
420	1.544	1.377	1.481	1.564	1.047	1.172	1.118	0.735	1.009	0.638	0.731	0.857
450	-	-	-	-	-	-	-	-	-	-	-	-
480	1.480	1.301	1.358	1.480	0.960	1.140	1.101	0.735	1.009	0.638	0.731	0.884
510	1.383	1.224	1.358	1.480	1.047	1.108	1.052	0.791	1.094	0.709	0.853	0.900
540	-	-	-	-	-	-	-	-	-	-	-	-
570	1.480	1.301	1.358	1.480	1.047	1.116	1.058	0.791	1.094	0.709	0.853	0.886
600	-	-	-	-	-	-	-	-	-	-	-	-
630	1.512	1.377	1.420	1.522	1.047	1.100	1.020	0.848	1.129	0.780	0.974	0.888
660	-	-	-	-	-	-	-	-	-	-	-	-
690	-	-	-	-	-	-	-	-	-	-	-	-
720	1.447	1.301	1.358	1.480	1.047	1.084	0.998	0.904	1.180	0.815	0.974	0.898
750	-	-	-	-	-	-	-	-	-	-	-	-
780	1.576	1.454	1.481	1.607	1.222	1.108	0.998	0.961	1.197	0.886	1.096	0.857
810	1.480	1.377	1.481	1.522	1.134	1.092	1.003	0.961	1.214	0.851	1.096	0.874
840	1.480	1.377	1.420	1.522	1.134	1.084	0.976	0.904	1.214	0.886	1.096	0.888

TABLE D.2. Relative-distribution ratios of origanum-oil components in extraction experiment at 40°C/10.0 MPa.

Component→ Time (min)↓	$\alpha$ -pinene	camphene	myrcene	$\alpha$ -terpinene	PC1	$\gamma$ -terpinene	p-cymene	linalool	PC2	borneol	thymol	carvacrol
30	0.000	0.000	0.000	0.000	0.000	0.000	0.000	0.000	0.000	0.000	0.000	0.000
60	0.000	0.000	0.000	0.000	0.000	2.056	2.525	0.000	0.000	0.000	0.000	0.563
90	0.000	0.000	0.000	0.000	0.000	2.072	2.541	0.000	0.000	0.000	0.000	0.567
120	1.480	0.000	1.296	1.607	0.000	1.769	1.990	0.000	0.000	0.000	0.000	0.638
150	-	-	-	-	-	-	-	-	-	-	-	-
180	1.866	1.760	1.852	1.818	0.785	1.363	1.505	0.113	0.274	0.106	0.000	0.764
210	1.351	1.148	1.296	1.353	0.698	1.291	1.341	0.226	0.393	0.213	0.244	0.909
240	-	-	-	-	-	-	-	-	-	-	-	-
270	0.965	0.842	0.926	1.015	0.611	0.893	0.889	0.509	0.701	0.638	0.487	1.172
300	-	-	-	-	-	-	-	-	-	-	-	-
330	0.933	0.842	0.926	0.930	0.698	0.821	0.818	0.565	0.718	0.815	0.609	1.207
360	-	-	-	-	-	-	-	-	-	-	-	-
390	0.965	0.842	0.926	0.973	0.785	0.821	0.818	0.565	0.735	0.851	0.609	1.194
420	-	-	-	-	-	-	-	-	-	-	-	-
450	0.901	0.842	0.926	0.973	0.785	0.789	0.769	0.622	0.821	0.993	0.853	1.203
480	0.901	0.765	0.926	0.930	0.785	0.773	0.758	0.622	0.855	1.063	0.974	1.203
510	0.933	0.842	0.926	0.973	0.785	0.773	0.752	0.678	0.906	1.099	0.974	1.188
540	0.868	0.765	0.926	0.973	0.873	0.749	0.725	0.735	0.906	1.170	0.974	1.203

TABLE D.3. Relative-distribution ratios of origanum-oil components in adsorption experiment at 40°C/7.5 MPa using two grams activated carbon.

Component→ Time (min)↓	$\alpha$ -pinene	camphene	myrcene	$\alpha$ -terpinene	PC1	$\gamma$ -terpinene	p-cymene	linalool	PC2	borneol	thymol	carvacrol
30	0.000	0.000	0.000	0.000	0.000	0.000	0.000	0.000	0.000	0.000	0.000	0.000
60	5.082	3.596	1.481	1.776	0.000	1.530	2.519	0.000	0.000	0.000	0.000	0.000
90	4.503	3.596	1.667	1.945	0.000	1.530	2.432	0.000	0.000	0.000	0.000	0.209
120	-	-	-	-	-	-	-	-	-	-	-	-
150	3.281	2.754	1.914	2.156	0.698	1.634	2.317	0.170	0.205	0.000	0.000	0.263
180	-	-	-	-	-	-	-	-	-	-	-	-
210	-	-	-	-	-	-	-	-	-	-	-	-
240	2.541	2.142	1.914	2.156	0.873	1.658	2.083	0.283	0.381	0.106	0.000	0.371
270	-	-	-	-	-	-	-	-	-	-	-	-
300	1.930	1.760	1.790	2.030	0.960	1.586	1.865	0.447	0.534	0.177	0.122	0.503
330	-	-	-	-	-	-	-	-	-	-	-	-
360	1.962	1.760	1.790	1.945	1.047	1.498	1.690	0.514	0.636	0.213	0.244	0.573
390	-	-	-	-	-	-	-	-	-	-	-	-
420	1.833	1.607	1.667	1.818	0.960	1.403	1.570	0.554	0.701	0.276	0.244	0.654
450	-	-	-	-	-	-	-	-	-	-	-	-
480	1.512	1.377	1.543	1.691	0.960	1.331	1.467	0.667	0.821	0.340	0.365	0.725
510	-	-	-	-	-	-	-	-	-	-	-	-
540	1.737	1.530	1.543	1.704	0.960	1.283	1.401	0.627	0.805	0.358	0.365	0.747

TABLE D.4. Relative-distribution ratios of origanum-oil components in adsorption experiment at 40°C/7.5 MPa using eight grams activated carbon.

Component→ Time (min)↓	α-pinene	camphene	myrcene	α-terpinene	PC1	γ-terpinene	p-cymene	linalool	PC2	borneol	thymol	carvacrol
30	0.000	0.000	0.000	0.000	0.000	0.000	0.000	0.000	0.000	0.000	0.000	0.000
60	0.000	0.000	0.000	0.000	0.000	0.000	0.000	0.000	0.000	0.000	0.000	0.000
90	0.000	0.000	0.000	0.000	0.000	0.000	0.000	0.000	0.000	0.000	0.000	0.000
120	-	-	-	-	-	-	-	-	-	-	-	-
150	-	-	-	-	-	-	-	-	-	-	-	-
180	0.000	0.000	0.000	0.000	0.000	0.000	0.000	0.000	0.000	0.000	0.000	0.000
210	0.000	0.000	0.000	0.000	0.000	0.000	5.453	0.000	0.000	0.000	0.000	0.000
240	-	-	-	-	-	-	-	-	-	-	-	-
270	16.340	0.000	0.000	0.000	0.000	0.000	2.683	0.000	0.000	0.000	0.000	0.000
300	-	-	-	-	-	-	-	-	-	-	-	-
330	11.032	6.656	0.000	0.000	0.000	0.972	2.443	0.000	0.000	0.000	0.000	0.000
360	10.228	6.886	0.000	0.000	0.000	1.004	2.541	0.000	0.000	0.000	0.000	0.000
390	-	-	-	-	-	-	-	-	-	-	-	-
420	8.266	7.345	0.000	1.438	0.000	1.219	2.508	0.000	0.000	0.000	0.000	0.000
450	-	-	-	-	-	-	-	-	-	-	-	-
480	6.851	6.274	1.728	1.649	0.000	1.323	2.574	0.000	0.000	0.000	0.000	0.000
510	-	-	-	-	-	-	-	-	-	-	-	-
540	6.336	5.356	1.975	1.734	0.524	1.419	2.568	0.000	0.000	0.000	0.000	0.012
570	-	-	-	-	-	-	-	-	-	-	-	-
600	5.693	4.973	2.037	2.199	0.698	1.538	2.535	0.000	0.000	0.000	0.000	0.014
630	-	-	-	-	-	-	-	-	-	-	-	-
660	5.275	4.820	2.160	2.283	0.873	1.666	2.454	0.113	0.017	0.000	0.000	0.027
690	-	-	-	-	-	-	-	-	-	-	-	-
720	5.018	4.514	2.346	2.368	1.134	1.737	2.377	0.170	0.034	0.000	0.000	0.039
750	-	-	-	-	-	-	-	-	-	-	-	-
780	4.600	4.361	2.593	2.537	1.222	1.865	2.257	0.226	0.085	0.000	0.000	0.056
810	4.214	4.208	2.840	2.579	1.309	1.865	2.241	0.283	0.120	0.035	0.000	0.070
840	4.149	4.132	2.840	2.664	1.309	1.873	2.176	0.339	0.154	0.071	0.000	0.087

TABLE D.5. Relative-distribution ratios of organum-oil components in adsorption experiment at 40°C/7.5 MPa using eight grams activated carbon (replicate exp.).

Component→ Time (min)↓	α-pinene	camphene	myrcene	α-terpinene	PC1	γ-terpinene	p-cymene	linalool	PC2	borneol	thymol	carvacrol
30	0.000	0.000	0.000	0.000	0.000	0.000	0.000	0.000	0.000	0.000	0.000	0.000
60	0.000	0.000	0.000	0.000	0.000	0.000	0.000	0.000	0.000	0.000	0.000	0.000
90	-	-	-	-	-	-	-	-	-	-	-	-
120	0.000	0.000	0.000	0.000	0.000	0.000	0.000	0.000	0.000	0.000	0.000	0.000
150	-	-	-	-	-	-	-	-	-	-	-	-
180	0.000	0.000	0.000	0.000	0.000	0.000	0.000	0.000	0.000	0.000	0.000	0.000
210	-	-	-	-	-	-	-	-	-	-	-	-
240	-	-	-	-	-	-	-	-	-	-	-	-
270	15.375	0.000	0.000	0.000	0.000	0.000	2.846	0.000	0.000	0.000	0.000	0.000
300	-	-	-	-	-	-	-	-	-	-	-	-
330	9.810	6.427	0.000	0.000	0.000	1.092	2.585	0.000	0.000	0.000	0.000	0.000
360	9.167	6.886	0.000	0.000	0.000	1.188	2.595	0.000	0.000	0.000	0.000	0.000
390	-	-	-	-	-	-	-	-	-	-	-	-
420	8.138	7.039	0.000	1.480	0.000	1.307	2.486	0.000	0.000	0.000	0.000	0.000
450	-	-	-	-	-	-	-	-	-	-	-	-
480	6.690	6.809	1.852	1.691	0.000	1.371	2.514	0.000	0.000	0.000	0.000	0.000
510	-	-	-	-	-	-	-	-	-	-	-	-
540	6.562	5.662	2.099	1.945	0.436	1.466	2.437	0.000	0.000	0.000	0.000	0.014
570	-	-	-	-	-	-	-	-	-	-	-	-
600	5.790	5.203	2.160	2.114	0.611	1.594	2.454	0.000	0.000	0.000	0.000	0.021
630	5.436	4.973	2.284	2.241	0.873	1.626	2.432	0.000	0.000	0.000	0.000	0.031
660	5.243	4.591	2.346	2.368	0.960	1.690	2.388	0.057	0.034	0.000	0.000	0.039
690	-	-	-	-	-	-	-	-	-	-	-	-
720	4.986	4.132	2.469	2.537	1.222	1.729	2.328	0.170	0.068	0.000	0.000	0.056
750	-	-	-	-	-	-	-	-	-	-	-	-
780	4.535	4.055	2.654	2.706	1.309	1.785	2.241	0.283	0.137	0.000	0.000	0.075
810	4.439	3.979	2.778	2.748	1.396	1.793	2.192	0.339	0.154	0.035	0.000	0.083
840	4.407	4.055	2.840	2.748	1.396	1.785	2.165	0.396	0.171	0.071	0.000	0.087

TABLE D.6. Relative-distribution ratios of organum-oil components in adsorption experiment at 40°C/7.5 MPa using eight grams activated carbon (replicate exp.).

Component→ Time (min)↓	α-pinene	camphene	myrcene	α-terpinene	PC1	γ-terpinene	p-cymene	linalool	PC2	borneol	thymol	carvacrol
30	0.000	0.000	0.000	0.000	0.000	0.000	0.000	0.000	0.000	0.000	0.000	0.000
60	0.000	0.000	0.000	0.000	0.000	0.000	0.000	0.000	0.000	0.000	0.000	0.000
90	0.000	0.000	0.000	0.000	0.000	0.000	0.000	0.000	0.000	0.000	0.000	0.000
120	0.000	0.000	0.000	0.000	0.000	0.000	0.000	0.000	0.000	0.000	0.000	0.000
150	-	-	-	-	-	-	-	-	-	-	-	-
180	0.000	0.000	0.000	0.000	0.000	0.000	0.000	0.000	0.000	0.000	0.000	0.000
210	0.000	0.000	0.000	0.000	0.000	0.000	5.453	0.000	0.000	0.000	0.000	0.000
240	-	-	-	-	-	-	-	-	-	-	-	-
270	15.729	0.000	0.000	0.000	0.000	0.000	2.786	0.000	0.000	0.000	0.000	0.000
300	12.641	0.000	0.000	0.000	0.000	1.084	2.568	0.000	0.000	0.000	0.000	0.000
330	11.451	6.503	0.000	0.000	0.000	1.012	2.356	0.000	0.000	0.000	0.000	0.000
360	-	-	-	-	-	-	-	-	-	-	-	-
390	9.199	7.345	0.000	1.184	0.000	1.132	2.443	0.000	0.000	0.000	0.000	0.000
420	9.070	7.269	0.000	1.268	0.000	1.108	2.475	0.000	0.000	0.000	0.000	0.000
450	-	-	-	-	-	-	-	-	-	-	-	-
480	7.108	6.350	1.605	1.691	0.000	1.299	2.546	0.000	0.000	0.000	0.000	0.000
510	-	-	-	-	-	-	-	-	-	-	-	-
540	6.176	5.509	1.914	2.030	0.436	1.435	2.541	0.000	0.000	0.000	0.000	0.012
570	-	-	-	-	-	-	-	-	-	-	-	-
600	5.468	5.050	2.284	2.368	0.698	1.610	2.465	0.000	0.000	0.000	0.000	0.019
630	-	-	-	-	-	-	-	-	-	-	-	-
660	4.503	4.361	2.531	2.579	0.960	1.753	2.443	0.170	0.051	0.000	0.000	0.033
690	-	-	-	-	-	-	-	-	-	-	-	-
720	4.214	3.979	2.716	2.706	1.134	1.833	2.366	0.226	0.085	0.000	0.000	0.048
750	-	-	-	-	-	-	-	-	-	-	-	-
780	3.956	3.826	2.963	2.833	1.309	1.905	2.236	0.339	0.154	0.000	0.000	0.068
810	3.699	3.520	2.963	2.875	1.396	1.913	2.197	0.396	0.188	0.071	0.000	0.091
840	3.699	3.596	3.086	2.918	1.396	1.913	2.137	0.452	0.205	0.106	0.000	0.099

TABLE D.7. Normalized area counts (%) of origanum-oil components in desorption experiment at 40°C/14.5 MPa.

Component → Time (min) ↓	$\alpha$ -pinene	camphene	myrcene	$\alpha$ -terpinene	PC1	$\gamma$ -terpinene	p-cymene	MT	linalool	PC2	borneol	thymol	carvacrol	NMT
30	1.40	0.80	2.20	3.90	0.90	7.20	78.60	95.00	0.00	0.00	0.00	0.00	4.90	4.90
60	1.10	0.80	2.60	4.20	1.50	7.70	71.50	89.40	0.30	0.90	0.30	0.00	9.10	10.60
90	1.10	0.70	2.60	4.10	1.70	7.50	67.50	85.20	0.40	1.30	0.40	0.00	12.70	14.80
120	1.00	0.70	2.60	4.00	1.80	7.30	62.70	80.10	0.50	1.80	0.60	0.00	17.00	19.90
150	0.80	0.60	2.40	3.70	1.70	6.90	59.20	75.30	0.60	2.10	0.70	0.00	21.30	24.70
180	-	-	-	-	-	-	-	-	-	-	-	-	-	-
210	0.70	0.50	1.90	2.90	1.50	5.30	44.20	57.00	0.80	2.80	1.30	0.10	38.10	43.10
240	-	-	-	-	-	-	-	-	-	-	-	-	-	-
270	-	-	-	-	-	-	-	-	-	-	-	-	-	-
300	0.50	0.30	1.40	2.00	1.20	3.80	31.40	40.60	0.90	3.30	1.80	0.20	53.10	59.30
330	-	-	-	-	-	-	-	-	-	-	-	-	-	-
360	-	-	-	-	-	-	-	-	-	-	-	-	-	-
390	0.40	0.30	1.20	1.70	1.10	3.30	26.80	34.80	1.00	3.70	2.10	0.30	58.10	65.20
420	0.40	0.30	1.20	1.70	1.10	3.20	26.10	34.00	1.10	3.90	2.30	0.30	58.40	66.00
450	-	-	-	-	-	-	-	-	-	-	-	-	-	-
480	0.30	0.20	1.10	1.60	1.00	2.90	24.00	31.10	1.10	4.00	2.40	0.40	61.10	69.00
510	-	-	-	-	-	-	-	-	-	-	-	-	-	-
540	0.40	0.30	1.10	1.60	1.00	3.00	23.80	31.20	1.10	4.20	2.50	0.40	60.70	68.90
570	-	-	-	-	-	-	-	-	-	-	-	-	-	-
600	0.40	0.30	1.10	1.60	1.00	2.90	23.00	30.30	1.10	4.30	2.50	0.40	61.40	69.70
630	0.30	0.20	1.00	1.50	1.00	2.70	22.10	28.80	1.00	4.10	2.40	0.40	63.20	71.10
660	-	-	-	-	-	-	-	-	-	-	-	-	-	-
690	0.30	0.30	1.10	1.60	1.00	2.90	22.30	29.50	1.10	4.40	2.50	0.40	62.10	70.50
ethanol-extracted activated-carbon residue	0.00	0.00	0.00	0.00	0.10	0.00	0.80	0.90	0.50	4.10	1.60	1.20	91.70	99.10

TABLE D.8. Relative-distribution ratios of organum-oil components in desorption experiment at 40°C/14.5 MPa.

Component→ Time (min)↓	α-pinene	camphene	myrcene	α-terpinene	PC1	γ-terpinene	p-cymene	linalool	PC2	borneol	thymol	carvacrol
30	0.450	0.612	1.358	1.649	0.785	0.574	4.286	0.000	0.000	0.000	0.000	0.101
60	0.354	0.612	1.605	1.776	1.309	0.614	3.899	0.170	0.154	0.106	0.000	0.188
90	0.354	0.536	1.605	1.734	1.483	0.598	3.680	0.226	0.222	0.142	0.000	0.263
120	0.322	0.536	1.605	1.691	1.571	0.582	3.419	0.283	0.308	0.213	0.000	0.352
150	0.257	0.459	1.481	1.564	1.483	0.550	3.228	0.339	0.359	0.248	0.000	0.441
180	-	-	-	-	-	-	-	-	-	-	-	-
210	0.225	0.383	1.173	1.226	1.309	0.422	2.410	0.452	0.479	0.461	0.122	0.789
240	-	-	-	-	-	-	-	-	-	-	-	-
270	-	-	-	-	-	-	-	-	-	-	-	-
300	0.161	0.230	0.864	0.846	1.047	0.303	1.712	0.509	0.564	0.638	0.244	1.099
330	-	-	-	-	-	-	-	-	-	-	-	-
360	-	-	-	-	-	-	-	-	-	-	-	-
390	0.129	0.230	0.741	0.719	0.960	0.263	1.461	0.565	0.633	0.744	0.365	1.203
420	0.129	0.230	0.741	0.719	0.960	0.255	1.423	0.622	0.667	0.815	0.365	1.209
450	-	-	-	-	-	-	-	-	-	-	-	-
480	0.096	0.153	0.679	0.677	0.873	0.231	1.309	0.622	0.684	0.851	0.487	1.265
510	-	-	-	-	-	-	-	-	-	-	-	-
540	0.129	0.230	0.679	0.677	0.873	0.239	1.298	0.622	0.718	0.886	0.487	1.257
570	-	-	-	-	-	-	-	-	-	-	-	-
600	0.129	0.230	0.679	0.677	0.873	0.231	1.254	0.622	0.735	0.886	0.487	1.271
630	0.096	0.153	0.617	0.634	0.873	0.215	1.205	0.565	0.701	0.851	0.487	1.308
660	-	-	-	-	-	-	-	-	-	-	-	-
690	0.096	0.230	0.679	0.677	0.873	0.231	1.216	0.622	0.752	0.886	0.487	1.286

TABLE D.9. Relative-distribution ratios of origanum-oil components in desorption experiment at 40°C with step-wise pressure increase from 8.0 to 14.5 MPa.

Component→ Time (min)↓	P (MPa)	α-pinene	camphene	myrcene	α-terpinene	PC1	γ-terpinene	p-cymene	linalool	PC2	borneol	thymol	carvacrol
30	8.0	0.611	0.765	2.346	2.156	0.000	1.761	3.430	0.000	0.000	0.000	0.000	0.066
60	8.0	0.579	0.765	2.346	2.199	0.960	1.777	3.146	0.283	0.154	0.000	0.000	0.118
90	8.0	0.482	0.689	2.346	2.199	1.222	1.769	2.901	0.452	0.325	0.000	0.000	0.188
120	8.0	0.450	0.689	2.284	2.156	1.396	1.729	2.688	0.565	0.479	0.000	0.000	0.259
150	8.0	-	-	-	-	-	-	-	-	-	-	-	-
180	8.0	0.418	0.612	2.222	2.114	1.571	1.666	2.481	0.735	0.547	0.142	0.000	0.335
210	8.0	-	-	-	-	-	-	-	-	-	-	-	-
240	8.0	0.354	0.536	2.099	1.987	1.658	1.562	2.317	0.848	0.667	0.213	0.000	0.418
270	14.5	-	-	-	-	-	-	-	-	-	-	-	-
300	14.5	0.322	0.536	2.099	1.903	1.658	1.514	2.176	0.848	0.735	0.248	0.000	0.478
330	14.5	-	-	-	-	-	-	-	-	-	-	-	-
360	14.5	0.257	0.383	1.667	1.522	1.571	1.219	1.728	0.961	0.923	0.390	0.000	0.731
390	14.5	0.225	0.306	1.358	1.226	1.483	1.068	1.418	1.018	1.026	0.532	0.244	0.892
420	14.5	-	-	-	-	-	-	-	-	-	-	-	-
450	14.5	-	-	-	-	-	-	-	-	-	-	-	-
480	14.5	0.193	0.306	1.296	1.184	1.396	0.893	1.232	1.131	1.180	0.744	0.365	0.979
510	14.5	-	-	-	-	-	-	-	-	-	-	-	-
540	14.5	0.193	0.306	1.296	1.142	1.396	0.885	1.227	1.074	1.197	0.709	0.365	0.990
570	14.5	-	-	-	-	-	-	-	-	-	-	-	-
600	14.5	0.193	0.306	1.235	1.057	1.396	0.845	1.183	1.131	1.214	0.744	0.365	1.016
630	14.5	0.193	0.306	1.235	1.057	1.396	0.845	1.194	1.074	1.180	0.709	0.365	1.021
660	14.5	0.193	0.306	1.235	1.057	1.396	0.845	1.189	1.074	1.197	0.744	0.365	1.021
690	14.5	0.193	0.306	1.173	1.015	1.396	0.837	1.189	1.074	1.197	0.744	0.365	1.023

TABLE D.10. Relative-distribution ratios of origanum-oil components in desorption experiment at 40°C with step-wise pressure increase from 8.0 to 14.5 MPa (replicate exp.).

Component→ Time (min)↓	P (MPa)	α-pinene	camphene	myrcene	α-terpinene	PC1	γ-terpinene	p-cymene	linalool	PC2	borneol	thymol	carvacrol
30	8.0	0.675	0.842	2.469	2.241	0.000	1.801	3.391	0.000	0.000	0.000	0.000	0.056
60	8.0	0.643	0.842	2.469	2.156	1.047	1.817	3.179	0.339	0.068	0.000	0.000	0.093
90	8.0	0.515	0.765	2.407	2.114	1.309	1.769	3.015	0.509	0.291	0.000	0.000	0.143
120	8.0	0.482	0.765	2.346	2.114	1.396	1.674	2.644	0.565	0.359	0.000	0.000	0.302
150	8.0	-	-	-	-	-	-	-	-	-	-	-	-
180	8.0	-	-	-	-	-	-	-	-	-	-	-	-
210	8.0	0.354	0.689	2.222	2.030	1.483	1.634	2.475	0.735	0.530	0.142	0.000	0.356
240	8.0	0.322	0.612	2.160	1.987	1.571	1.538	2.383	0.806	0.564	0.177	0.000	0.414
270	14.5	-	-	-	-	-	-	-	-	-	-	-	-
300	14.5	0.322	0.612	2.160	1.945	1.571	1.514	2.181	0.791	0.684	0.284	0.000	0.478
330	14.5	-	-	-	-	-	-	-	-	-	-	-	-
360	14.5	0.289	0.459	1.728	1.607	1.483	1.267	1.679	0.904	0.855	0.425	0.000	0.739
390	14.5	0.257	0.306	1.420	1.311	1.396	1.108	1.499	0.961	0.940	0.567	0.122	0.859
420	14.5	-	-	-	-	-	-	-	-	-	-	-	-
450	14.5	0.193	0.230	1.358	1.226	1.396	1.052	1.379	1.018	1.043	0.638	0.244	0.911
480	14.5	0.161	0.230	1.358	1.099	1.309	0.996	1.396	1.074	1.129	0.674	0.365	0.913
510	14.5	-	-	-	-	-	-	-	-	-	-	-	-
540	14.5	0.161	0.230	1.296	1.057	1.309	0.972	1.336	1.074	1.231	0.744	0.487	0.927
570	14.5	0.161	0.230	1.235	1.015	1.309	0.948	1.309	1.131	1.231	0.744	0.487	0.946
600	14.5	-	-	-	-	-	-	-	-	-	-	-	-
630	14.5	0.161	0.230	1.173	0.930	1.309	0.940	1.216	1.131	1.248	0.780	0.487	0.985
660	14.5	0.161	0.230	1.173	0.930	1.309	0.925	1.227	1.074	1.248	0.780	0.487	0.987
690	14.5	0.161	0.230	1.173	0.930	1.309	0.925	1.232	1.074	1.248	0.780	0.487	0.987

TABLE D.11. Relative-distribution ratios of origanum-oil components in adsorption experiment at 40°C/7.5 MPa using eight grams silica gel.

Component→ Time (min)↓	α-pinene	camphene	myrcene	α-terpinene	PC1	γ-terpinene	p-cymene	linalool	PC2	borneol	thymol	carvacrol
30	6.208	3.443	2.037	2.452	0.000	1.506	2.623	0.000	0.000	0.000	0.000	0.000
60	-	-	-	-	-	-	-	-	-	-	-	-
90	2.573	2.219	2.346	2.664	0.698	2.208	2.732	0.000	0.051	0.000	0.000	0.000
120	2.573	2.219	2.284	2.622	0.698	2.232	2.683	0.000	0.188	0.000	0.000	0.000
150	-	-	-	-	-	-	-	-	-	-	-	-
180	2.509	2.219	2.346	2.748	1.047	2.200	2.421	0.113	0.513	0.000	0.000	0.054
210	-	-	-	-	-	-	-	-	-	-	-	-
240	-	-	-	-	-	-	-	-	-	-	-	-
270	-	-	-	-	-	-	-	-	-	-	-	-
300	1.962	1.760	1.975	2.326	1.047	1.881	1.974	0.396	0.804	0.000	0.122	0.339
330	2.026	1.760	1.914	2.241	1.047	1.825	1.936	0.396	0.769	0.000	0.122	0.375
360	-	-	-	-	-	-	-	-	-	-	-	-
390	1.866	1.683	1.790	2.114	1.047	1.690	1.745	0.452	0.855	0.071	0.244	0.486
420	-	-	-	-	-	-	-	-	-	-	-	-
450	1.737	1.607	1.728	2.030	1.047	1.602	1.598	0.565	0.923	0.106	0.365	0.565
480	-	-	-	-	-	-	-	-	-	-	-	-
510	1.737	1.530	1.667	1.945	1.047	1.498	1.516	0.565	0.940	0.142	0.365	0.627
540	-	-	-	-	-	-	-	-	-	-	-	-
570	1.673	1.530	1.605	1.903	1.047	1.474	1.439	0.622	0.992	0.213	0.365	0.658
600	1.608	1.454	1.605	1.903	1.047	1.443	1.401	0.678	1.043	0.248	0.487	0.675
630	1.640	1.454	1.543	1.776	1.047	1.379	1.369	0.622	0.975	0.248	0.487	0.722

TABLE D.12. Relative-distribution ratios of organum-oil components in adsorption experiment at 40°C/7.5 MPa using 15 grams silica gel.

Component→ Time (min)↓	α-pinene	camphene	myrcene	α-terpinene	PC1	γ-terpinene	p-cymene	linalool	PC2	borneol	thymol	carvacrol
30	11.451	4.897	2.158	1.945	0.000	1.172	2.110	0.000	0.000	0.000	0.000	0.000
60	3.184	2.372	2.469	2.495	0.524	2.263	2.617	0.000	0.000	0.000	0.000	0.000
90	2.573	2.142	2.469	2.495	0.698	2.463	2.595	0.000	0.000	0.000	0.000	0.000
120	2.605	2.142	2.531	2.537	0.698	2.511	2.546	0.000	0.000	0.000	0.000	0.000
150	-	-	-	-	-	-	-	-	-	-	-	-
180	2.509	2.066	2.469	2.579	0.785	2.447	2.459	0.000	0.359	0.000	0.000	0.012
210	-	-	-	-	-	-	-	-	-	-	-	-
240	2.509	2.142	2.531	2.622	0.960	2.399	2.334	0.000	0.616	0.000	0.000	0.029
270	-	-	-	-	-	-	-	-	-	-	-	-
300	2.412	2.066	2.531	2.664	1.222	2.295	2.116	0.283	0.821	0.000	0.000	0.106
330	-	-	-	-	-	-	-	-	-	-	-	-
360	-	-	-	-	-	-	-	-	-	-	-	-
390	2.284	1.913	2.222	2.326	1.222	2.024	1.865	0.42	0.872	0.000	0.000	0.298
420	-	-	-	-	-	-	-	-	-	-	-	-
450	2.187	1.913	2.099	2.241	1.222	1.881	1.701	0.509	0.889	0.000	0.122	0.410
480	-	-	-	-	-	-	-	-	-	-	-	-
510	1.962	1.683	1.975	2.072	1.222	1.761	1.570	0.622	0.940	0.035	0.244	0.507
540	1.962	1.760	1.975	2.072	1.222	1.737	1.538	0.622	0.923	0.071	0.244	0.522
570	1.898	1.683	1.975	2.072	1.222	1.682	1.461	0.678	0.975	0.106	0.244	0.559
600	1.801	1.607	1.914	1.945	1.222	1.610	1.401	0.735	0.992	0.142	0.365	0.611
630	1.898	1.683	1.975	2.030	1.222	1.626	1.390	0.735	0.992	0.142	0.365	0.594

TABLE D.13. Relative-distribution ratios of organum-oil components in desorption experiment at 40°C/14.5 MPa using eight grams silica gel.

Component→ Time (min)↓	α-pinene	camphene	myrcene	α-terpinene	PC1	γ-terpinene	p-cymene	linalool	PC2	borneol	thymol	carvacrol
30	0.064	0.000	0.123	0.338	0.349	0.263	0.267	0.396	0.616	0.532	0.609	1.735
60	0.064	0.077	0.123	0.254	0.436	0.183	0.180	0.509	0.718	0.851	0.853	1.764
90	0.064	0.077	0.123	0.254	0.524	0.183	0.180	0.565	0.769	0.993	0.974	1.733
120	-	-	-	-	-	-	-	-	-	-	-	-
150	-	-	-	-	-	-	-	-	-	-	-	-
180	0.064	0.077	0.062	0.211	0.436	0.159	0.158	0.509	0.752	1.028	0.974	1.745
210	-	-	-	-	-	-	-	-	-	-	-	-
240	0.064	0.077	0.062	0.211	0.436	0.151	0.153	0.509	0.735	0.993	0.974	1.764
270	0.032	0.077	0.062	0.211	0.436	0.167	0.164	0.565	0.787	1.099	1.096	1.739
300	-	-	-	-	-	-	-	-	-	-	-	-
330	0.064	0.077	0.062	0.211	0.436	0.159	0.158	0.509	0.769	1.063	0.974	1.749
360	-	-	-	-	-	-	-	-	-	-	-	-
390	0.064	0.077	0.062	0.254	0.524	0.167	0.164	0.565	0.821	1.170	1.096	1.724
420	-	-	-	-	-	-	-	-	-	-	-	-
450	0.032	0.077	0.062	0.211	0.436	0.159	0.153	0.565	0.769	1.099	1.096	1.749
480	-	-	-	-	-	-	-	-	-	-	-	-
510	0.064	0.077	0.062	0.211	0.436	0.167	0.164	0.565	0.769	1.099	1.096	1.739
540	0.032	0.077	0.062	0.211	0.436	0.151	0.153	0.565	0.787	1.134	1.096	1.745
570	0.032	0.077	0.062	0.211	0.436	0.151	0.153	0.565	0.787	1.134	1.096	1.745

TABLE D.14. Relative-distribution ratios of origanum-oil components in desorption experiment at 40°C/14.5 MPa using 15 grams silica gel.

Component→ Time (min)↓	α-pinene	camphene	myrcene	α-terpinene	PC1	γ-terpinene	p-cymene	linalool	PC2	borneol	thymol	carvacrol
30	0.096	0.077	0.185	0.381	0.524	0.311	0.245	0.848	1.094	0.851	0.853	1.611
60	0.096	0.077	0.185	0.381	0.611	0.303	0.240	0.904	1.111	0.957	0.974	1.611
90	0.096	0.077	0.185	0.381	0.611	0.311	0.251	0.904	1.111	0.993	0.974	1.604
120	0.064	0.077	0.185	0.381	0.611	0.295	0.234	0.961	1.129	1.028	0.974	1.613
150	-	-	-	-	-	-	-	-	-	-	-	-
180	0.096	0.077	0.185	0.381	0.611	0.287	0.234	0.904	1.094	0.993	0.974	1.619
210	-	-	-	-	-	-	-	-	-	-	-	-
240	0.096	0.077	0.185	0.381	0.611	0.303	0.245	0.961	1.146	1.028	0.974	1.600
270	-	-	-	-	-	-	-	-	-	-	-	-
300	0.096	0.077	0.185	0.381	0.698	0.319	0.251	0.904	1.146	1.063	0.974	1.590
330	-	-	-	-	-	-	-	-	-	-	-	-
360	-	-	-	-	-	-	-	-	-	-	-	-
390	0.064	0.077	0.185	0.381	0.611	0.295	0.240	0.904	1.129	1.063	0.974	1.606
420	-	-	-	-	-	-	-	-	-	-	-	-
450	0.064	0.077	0.123	0.338	0.611	0.279	0.229	0.904	1.094	1.028	0.974	1.627
480	-	-	-	-	-	-	-	-	-	-	-	-
510	0.096	0.077	0.185	0.381	0.611	0.295	0.240	0.848	1.026	0.993	0.974	1.631
540	0.064	0.077	0.185	0.338	0.611	0.279	0.229	0.904	1.077	1.063	0.974	1.625
570	0.064	0.077	0.185	0.381	0.611	0.287	0.234	0.904	1.111	1.099	0.974	1.611
600	0.064	0.077	0.185	0.338	0.611	0.279	0.229	0.904	1.111	1.099	0.974	1.615
630	0.064	0.077	0.185	0.338	0.611	0.287	0.229	0.904	1.111	1.099	0.974	1.615

TABLE D.15. Relative-distribution ratios of organum-oil components in adsorption experiment at 40°C/10.0 MPa using eight grams activated carbon.

Component→ Time (min)↓	α-pinene	camphene	myrcene	α-terpinene	PC1	γ-terpinene	p-cymene	linalool	PC2	borneol	thymol	carvacrol
30	0.000	0.000	0.000	0.000	0.000	0.000	0.000	0.000	0.000	0.000	0.000	0.000
60	0.000	0.000	0.000	0.000	0.000	0.000	0.000	0.000	0.000	0.000	0.000	0.000
90	0.000	0.000	0.000	0.000	0.000	0.000	0.000	0.000	0.000	0.000	0.000	0.000
120	0.000	0.000	0.000	0.000	0.000	0.000	0.000	0.000	0.000	0.000	0.000	0.000
150	0.000	0.000	0.000	0.000	0.000	0.000	5.453	0.000	0.000	0.000	0.000	0.000
180	8.266	0.000	0.000	0.000	0.000	1.419	3.081	0.000	0.000	0.000	0.000	0.000
210	-	-	-	-	-	-	-	-	-	-	-	-
240	6.497	4.897	0.000	0.000	0.000	1.060	2.874	0.000	0.000	0.000	0.000	0.153
270	-	-	-	-	-	-	-	-	-	-	-	-
300	4.953	4.591	0.926	1.142	0.000	1.084	2.770	0.000	0.000	0.000	0.000	0.209
330	-	-	-	-	-	-	-	-	-	-	-	-
360	3.409	3.290	1.173	1.438	1.047	1.219	2.726	0.396	0.137	0.354	0.000	0.221
390	-	-	-	-	-	-	-	-	-	-	-	-
420	-	-	-	-	-	-	-	-	-	-	-	-
450	2.219	2.066	1.667	1.776	1.396	1.371	2.383	0.678	0.342	0.496	0.000	0.344
480	-	-	-	-	-	-	-	-	-	-	-	-
510	1.930	1.760	1.667	1.734	1.396	1.307	2.050	0.735	0.479	0.532	0.000	0.489
540	-	-	-	-	-	-	-	-	-	-	-	-
570	-	-	-	-	-	-	-	-	-	-	-	-
600	1.480	1.377	1.358	1.480	1.309	1.068	1.489	0.904	0.821	0.815	0.244	0.762
630	-	-	-	-	-	-	-	-	-	-	-	-
660	1.287	1.224	1.235	1.268	1.222	0.925	1.227	0.961	0.940	0.957	0.487	0.903
690	-	-	-	-	-	-	-	-	-	-	-	-
720	1.190	1.148	1.173	1.226	1.222	0.861	1.112	1.018	1.009	1.063	0.609	0.958
750	-	-	-	-	-	-	-	-	-	-	-	-
780	1.126	1.071	1.111	1.142	1.134	0.821	1.031	1.018	1.094	1.170	0.731	0.992
810	1.126	1.071	1.173	1.184	1.222	0.837	1.009	1.074	1.094	1.241	0.731	0.983
840	1.061	0.995	1.111	1.142	1.222	0.805	0.976	1.131	1.129	1.276	0.853	1.008

TABLE D.16. Relative-distribution ratios of organum-oil components in desorption experiment at 40°C/14.5 MPa using eight grams activated carbon.

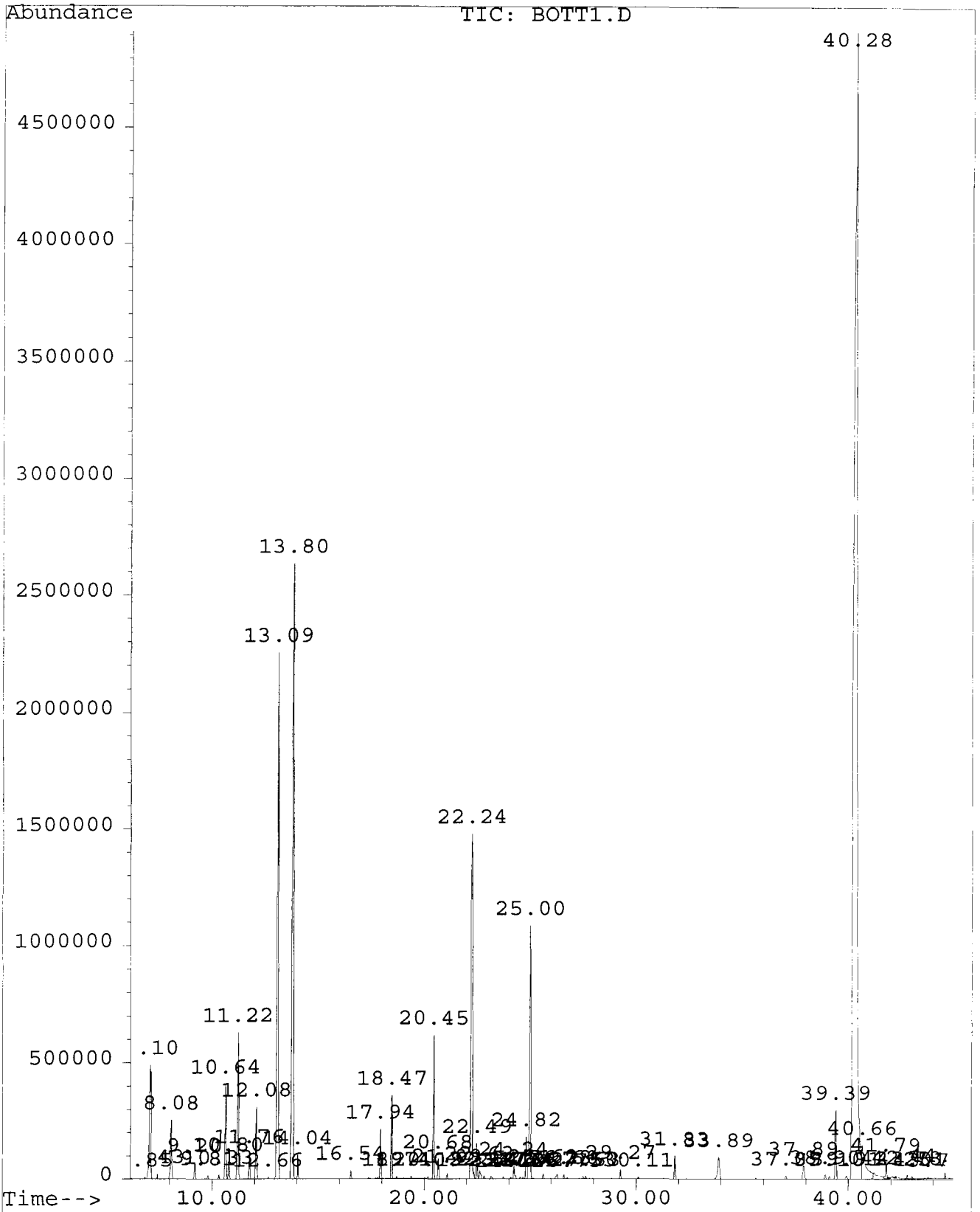
Component→ Time (min)↓	$\alpha$ -pinene	camphene	myrcene	$\alpha$ -terpinene	PC1	$\gamma$ -terpinene	p-cymene	linalool	PC2	borneol	thymol	carvacrol
30	0.547	0.000	0.926	0.507	1.222	0.000	3.266	0.000	0.000	0.000	0.000	0.712
60	0.354	0.000	0.741	0.296	1.134	0.048	2.137	0.283	0.376	0.319	0.000	1.087
90	0.193	0.000	0.370	0.169	0.785	0.048	1.161	0.339	0.513	0.496	0.244	1.457
120	-	-	-	-	-	-	-	-	-	-	-	-
150	0.129	0.153	0.309	0.127	0.698	0.032	0.840	0.396	0.598	0.709	0.487	1.559
180	0.096	0.077	0.247	0.127	0.611	0.032	0.752	0.396	0.633	0.744	0.487	1.596
210	-	-	-	-	-	-	-	-	-	-	-	-
240	0.096	0.077	0.247	0.127	0.611	0.032	0.671	0.452	0.701	0.851	0.609	1.608
270	-	-	-	-	-	-	-	-	-	-	-	-
300	0.096	0.077	0.247	0.085	0.611	0.016	0.611	0.452	0.718	0.886	0.731	1.633
330	-	-	-	-	-	-	-	-	-	-	-	-
360	0.096	0.077	0.247	0.085	0.611	0.016	0.578	0.452	0.752	0.922	0.731	1.635
390	-	-	-	-	-	-	-	-	-	-	-	-
420	0.064	0.077	0.185	0.085	0.611	0.016	0.534	0.452	0.787	0.957	0.853	1.650
450	-	-	-	-	-	-	-	-	-	-	-	-
480	0.064	0.077	0.185	0.085	0.524	0.016	0.518	0.452	0.804	0.993	0.853	1.652
510	0.064	0.077	0.185	0.085	0.524	0.016	0.507	0.452	0.821	0.993	0.853	1.658
540	0.064	0.077	0.185	0.085	0.524	0.016	0.502	0.452	0.804	0.957	0.853	1.658

## **APPENDIX E**

**Chromatogram and the GC/MS Results of the Original Origanum Oil**

File : C:\HPCHEM\1\DATA\ORIGINAL\BOTT1.D  
Operator :  
Acquired : 14 Aug 98 10:15 am using AcqMethod SEYDA  
Instrument : 5971 - on  
Sample Name:  
Misc Info :  
Vial Number: 1

196



## Area Percent Report -- Sorted by Signal

## Information from Data File:

File : C:\HPCHEM\1\DATA\ORIGINAL\BOTT1.D  
 Operator :  
 Acquired : 14 Aug 98 10:15 am using AcqMethod SEYDA  
 Sample Name: original origanum oil  
 Misc Info :  
 Vial Number: 1  
 CurrentMeth: C:\HPCHEM\1\METHODS\SEYDA.M

Retention Time	Area	Area %	Ratio %	
Total Ion Chromatogram				
6.846	311134	0.027	0.061	
7.096	32794904	2.828	6.436	$\alpha$ -pinene
7.433	519876	0.045	0.102	
8.083	13786729	1.189	2.706	camphene
9.198	2839228	0.245	0.557	
9.811	589457	0.051	0.116	
10.325	717021	0.062	0.141	
10.643	17088371	1.474	3.354	myrcene
10.800	2746454	0.237	0.539	
11.224	24946912	2.151	4.896	$\alpha$ -terpinene
11.762	3952517	0.341	0.776	
12.080	12088440	1.042	2.372	PC1
12.657	266725	0.023	0.052	
13.091	132350487	11.413	25.973	$\gamma$ -terpinene
13.798	193457236	16.682	37.966	p-cymene
14.043	2781244	0.240	0.546	
16.543	985724	0.085	0.193	
17.944	6411029	0.553	1.258	
18.469	10516274	0.907	2.064	
18.708	359500	0.031	0.071	
19.396	429080	0.037	0.084	
20.188	417483	0.036	0.082	
20.450	18660079	1.609	3.662	linalool
20.678	3233518	0.279	0.635	
21.090	730596	0.063	0.143	
22.236	61686909	5.319	12.106	PC2
22.492	5058165	0.436	0.993	
22.630	2029433	0.175	0.398	
22.835	487064	0.042	0.096	
23.166	626225	0.054	0.123	
23.731	324709	0.028	0.064	
24.095	336306	0.029	0.066	
24.241	2551287	0.220	0.501	
24.537	301516	0.026	0.059	

24.660	278322	0.024	0.055	
24.823	7247974	0.625	1.422	
25.001	29756972	2.566	5.840	borneol
25.617	858160	0.074	0.168	
26.278	1206063	0.104	0.237	
26.602	718999	0.062	0.141	
26.754	208742	0.018	0.041	
27.503	521854	0.045	0.102	
27.629	440677	0.038	0.086	
29.269	1368417	0.118	0.269	
30.106	405887	0.035	0.080	
31.827	3977688	0.343	0.781	
33.894	6992845	0.603	1.372	
37.053	637822	0.055	0.125	
37.889	3386253	0.292	0.665	
38.900	962531	0.083	0.189	
39.101	475467	0.041	0.093	
39.391	8660218	0.747	1.700	thymol
39.905	846563	0.073	0.166	
40.279	509560452	43.940	100.000	carvacrol
40.662	18983893	1.637	3.726	
41.787	3026754	0.261	0.594	
42.247	487064	0.042	0.096	
42.780	614628	0.053	0.121	
43.014	487064	0.042	0.096	
43.781	533451	0.046	0.105	
44.580	649418	0.056	0.127	

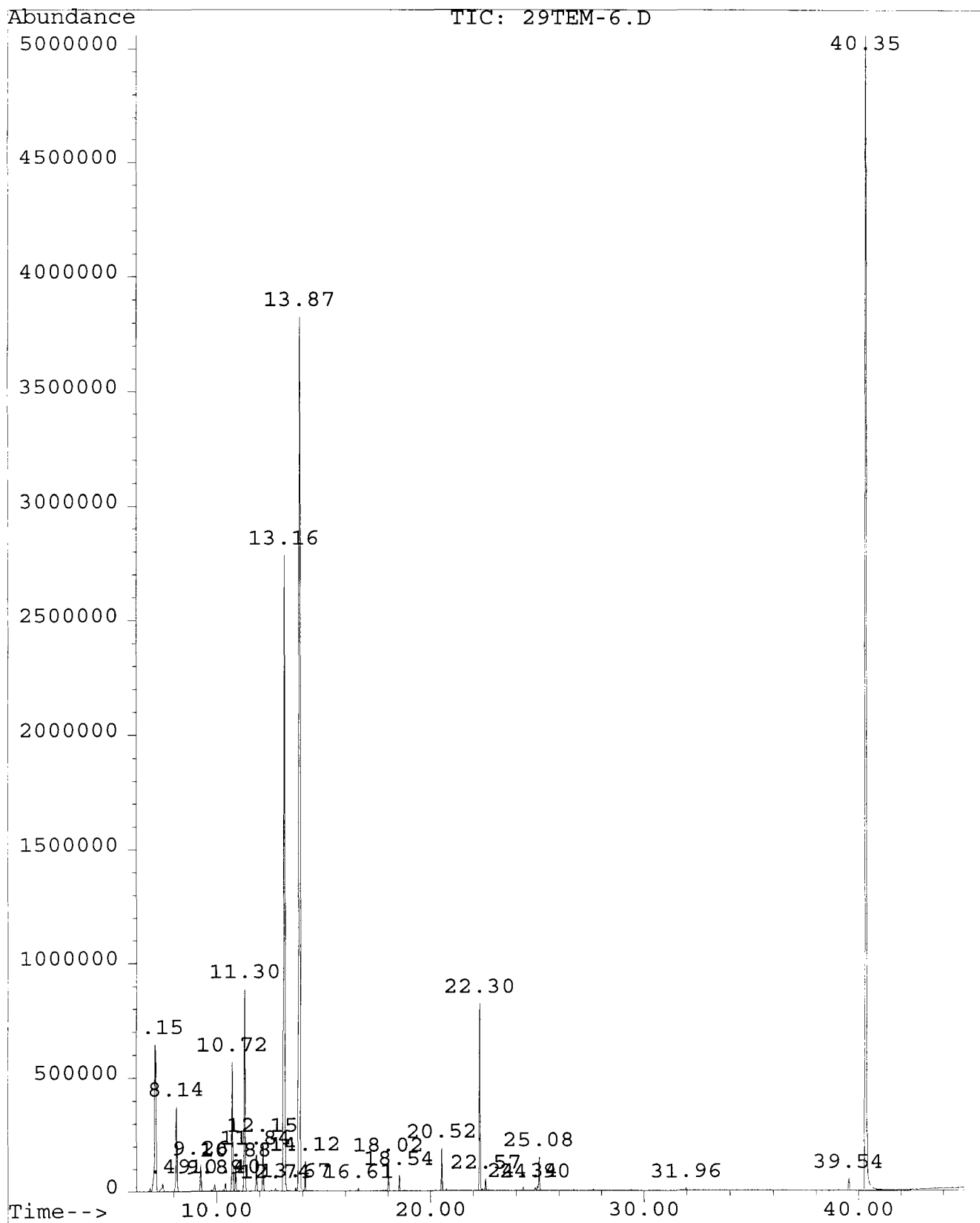
---

Wed May 19 21:15:16 1999

## **APPENDIX F**

**Chromatogram and the GC/MS Results of the Samples Collected at Different Time Intervals during Supercritical-CO<sub>2</sub> Extraction at 40°C/7.5 MPa**

File : C:\HPCHEM\1\DATA\CARBON\TEM29\29TEM-6.D  
Operator :  
Acquired : 29 Jul 97 1:10 pm using AcqMethod SEYDA  
Instrument : 5971 - on  
Sample Name:  
Misc Info :  
Vial Number: 1



## Area Percent Report -- Sorted by Signal

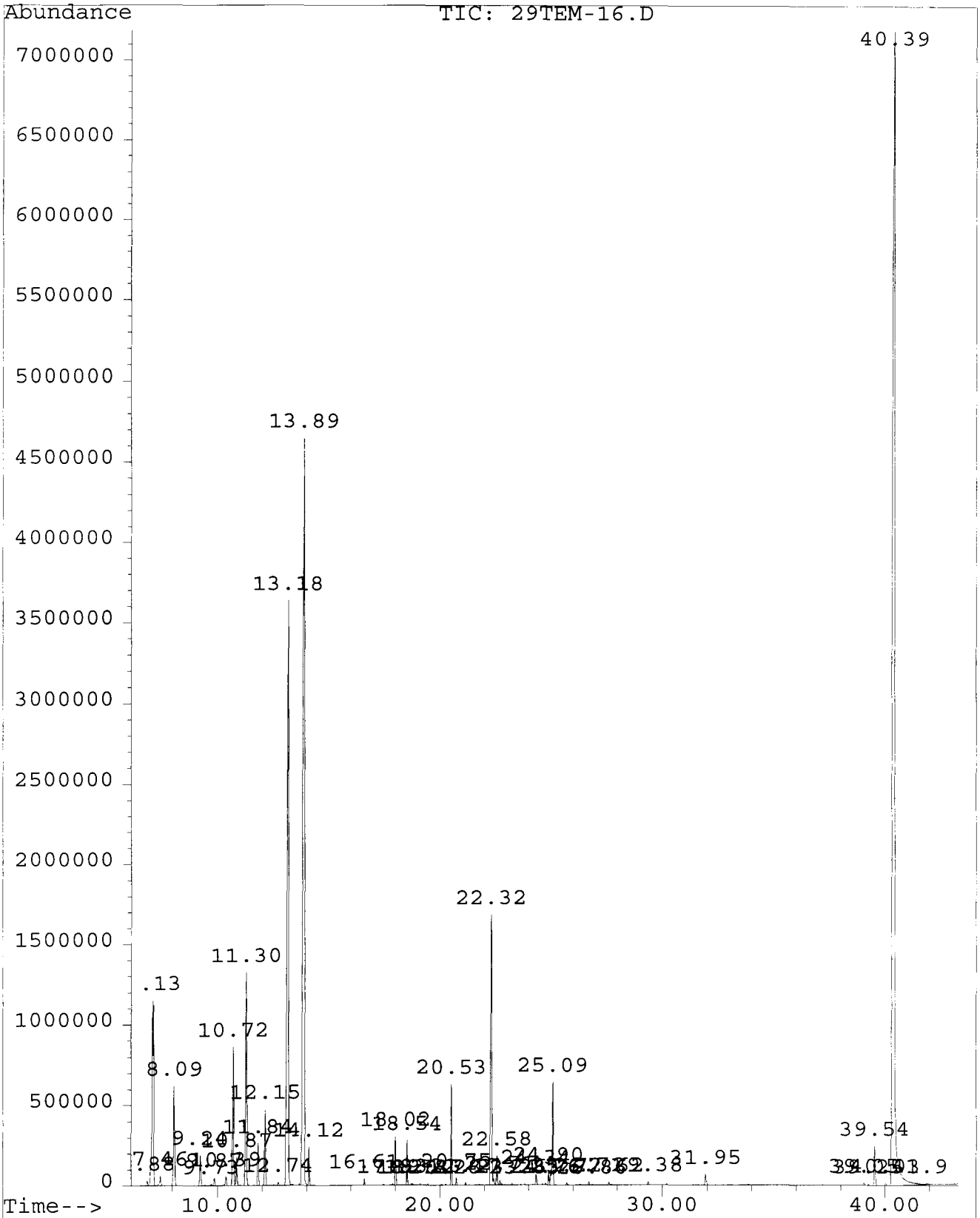
## Information from Data File:

File : C:\HPCHEM\1\DATA\CARBON\TEM29\29TEM-6.D  
 Operator :  
 Acquired : 29 Jul 97 1:10 pm using AcqMethod SEYDA  
 Sample Name: time = 180 min.  
 Misc Info :  
 Vial Number: 1  
 CurrentMeth: C:\HPCHEM\1\METHODS\SEYDA.M

Retention Time	Area	Area %	Ratio %	
Total Ion Chromatogram				
7.150	33338670	5.095	15.424	$\alpha$ -pinene
7.489	1958233	0.299	0.906	
8.144	12329447	1.884	5.704	camphene
9.264	3573056	0.546	1.653	
9.887	1191543	0.182	0.551	
10.400	1347681	0.206	0.623	
10.723	16392395	2.505	7.584	myrcene
10.876	3243863	0.496	1.501	
11.302	26042026	3.980	12.048	$\alpha$ -terpinene
11.840	4671151	0.714	2.161	
12.147	6463860	0.988	2.990	PC1
12.739	432623	0.066	0.200	
13.161	111561200	17.051	51.613	$\gamma$ -terpinene
13.672	295376	0.045	0.137	
13.875	169372606	25.886	78.359	p-cymene
14.121	3079130	0.471	1.425	
16.613	255235	0.039	0.118	
18.017	3088748	0.472	1.429	
18.537	1579587	0.241	0.731	
20.525	4684832	0.716	2.167	linalool
22.304	24376067	3.726	11.277	PC2
22.567	1320067	0.202	0.611	
24.336	378059	0.058	0.175	
24.897	342439	0.052	0.158	
25.081	4870008	0.744	2.253	borneol
31.956	322752	0.049	0.149	
39.544	1634973	0.250	0.756	thymol
40.349	216148344	33.035	100.000	carvacrol

Tue May 18 17:38:42 1999

File : C:\HPCHEM\1\DATA\CARBON\TEM29\29TEM-16.D  
 Operator :  
 Acquired : 29 Jul 97 5:37 pm using AcqMethod SEYDA  
 Instrument : 5971 - on  
 Sample Name :  
 Misc Info :  
 Vial Number: 1



## Area Percent Report -- Sorted by Signal

## Information from Data File:

File : C:\HPCHEM\1\DATA\CARBON\TEM29\29TEM-16.D  
 Operator :  
 Acquired : 29 Jul 97 5:37 pm using AcqMethod SEYDA  
 Sample Name: time = 480 min.  
 Misc Info :  
 Vial Number: 1  
 CurrentMeth: C:\HPCHEM\1\METHODS\SEYDA.M

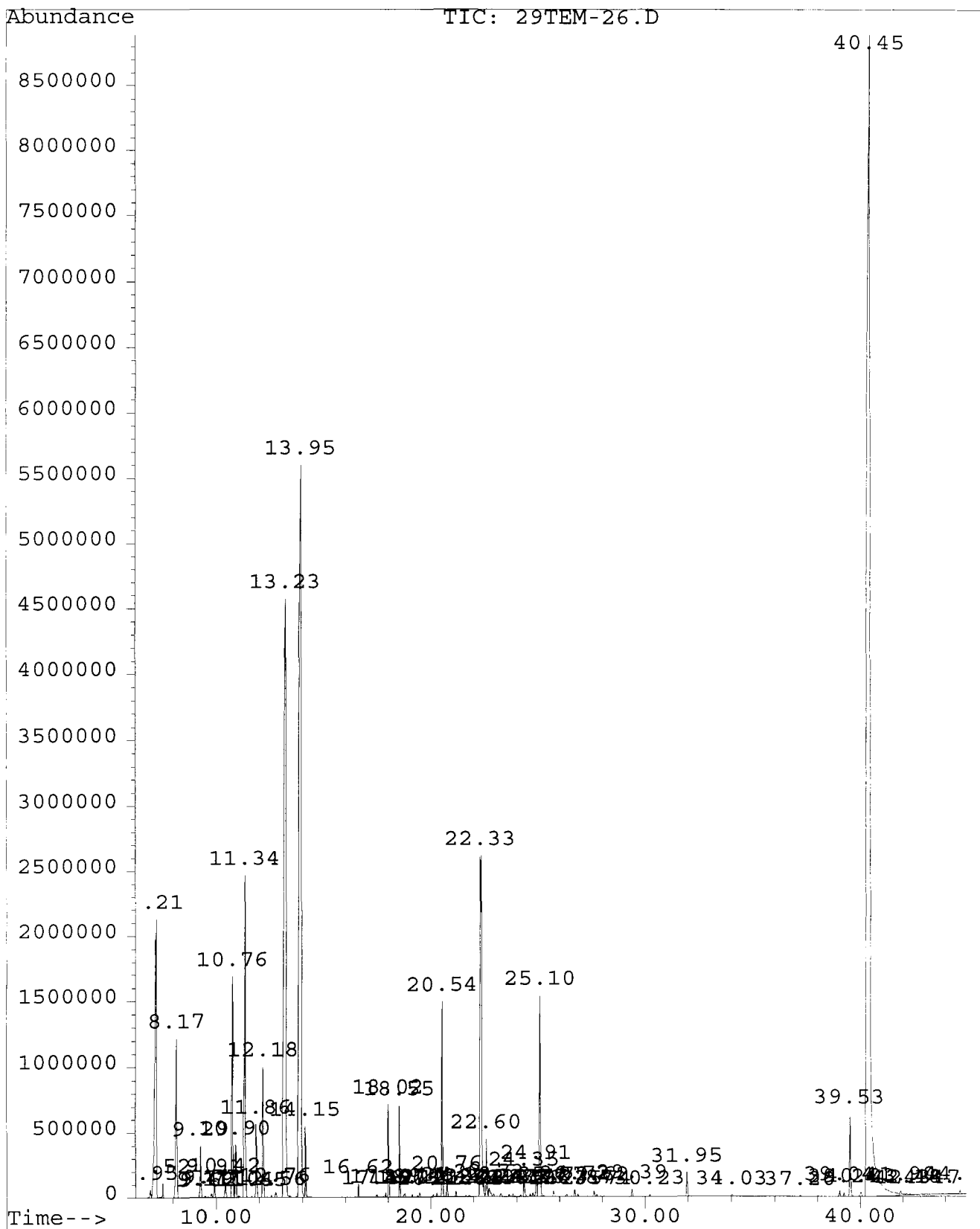
Retention Time	Area	Area %	Ratio %	
Total Ion Chromatogram				
6.877	943825	0.070	0.174	
7.132	58813685	4.383	10.840	$\alpha$ -pinene
7.465	2384301	0.178	0.439	
8.095	21981134	1.638	4.051	camphene
9.243	6429791	0.479	1.185	
9.729	401298	0.030	0.074	
9.874	1763288	0.131	0.325	
10.392	2145543	0.160	0.395	
10.721	28280872	2.108	5.212	myrcene
10.872	5513653	0.411	1.016	
11.302	44643770	3.327	8.228	$\alpha$ -terpinene
11.837	8333829	0.621	1.536	
12.148	14400874	1.073	2.654	PC1
12.740	700685	0.052	0.129	
13.176	181613764	13.534	33.473	$\gamma$ -terpinene
13.890	256844544	19.141	47.338	p-cymene
14.123	5795399	0.432	1.068	
16.611	982246	0.073	0.181	
17.881	245765	0.018	0.045	
18.017	7698619	0.574	1.419	
18.537	6592939	0.491	1.215	
18.784	428745	0.032	0.079	
19.125	246482	0.018	0.045	
19.473	258463	0.019	0.048	
20.275	286944	0.021	0.053	
20.528	16163811	1.205	2.979	linalool
20.750	1267783	0.094	0.234	
21.168	370255	0.028	0.068	
22.324	75307283	5.612	13.880	PC2
22.576	5208580	0.388	0.960	
22.714	994199	0.074	0.183	
23.256	259592	0.019	0.048	
23.826	230241	0.017	0.042	
24.338	2025847	0.151	0.373	

24.760	255881	0.019	0.047	
24.901	2483148	0.185	0.458	
25.087	22616591	1.685	4.168	borneol
25.717	485881	0.036	0.090	
26.712	564646	0.042	0.104	
26.859	199843	0.015	0.037	
27.620	535795	0.040	0.099	
29.384	585451	0.044	0.108	
31.952	2385203	0.178	0.440	
39.053	435565	0.032	0.080	
39.253	261233	0.019	0.048	
39.537	7952390	0.593	1.466	thymol
40.027	511195	0.038	0.094	
40.393	542575979	40.434	100.000	carvacrol
41.901	469134	0.035	0.086	

---

Tue May 18 17:49:17 1999

File : C:\HPCHEM\1\DATA\CARBON\TEM29\29TEM-26.D  
Operator :  
Acquired : 29 Jul 97 10:04 pm using AcqMethod SEYDA  
Instrument : 5971 - on  
Sample Name :  
Misc Info :  
Vial Number: 1



## Area Percent Report -- Sorted by Signal

## Information from Data File:

File : C:\HPCHEM\1\DATA\CARBON\TEM29\29TEM-26.D  
 Operator :  
 Acquired : 29 Jul 97 10:04 pm using AcqMethod SEYDA  
 Sample Name: time = 780 min.  
 Misc Info :  
 Vial Number: 1  
 CurrentMeth: C:\HPCHEM\1\METHODS\SEYDA.M

Retention Time	Area	Area %	Ratio %	
Total Ion Chromatogram				
6.946	2137682	0.084	0.220	
7.205	113966921	4.504	11.756	$\alpha$ -pinene
7.525	3288171	0.130	0.339	
8.170	44417890	1.755	4.582	camphene
9.289	13392972	0.529	1.381	
9.487	330336	0.013	0.034	
9.620	204062	0.008	0.021	
9.765	983252	0.039	0.101	
9.909	3790260	0.150	0.391	
10.424	4353101	0.172	0.449	
10.759	57156256	2.259	5.896	myrcene
10.904	11761537	0.465	1.213	
11.036	591889	0.023	0.061	
11.340	87945288	3.476	9.071	$\alpha$ -terpinene
11.651	333378	0.013	0.034	
11.865	17750890	0.702	1.831	
12.178	32101336	1.269	3.311	PC1
12.557	467801	0.018	0.048	
12.764	1686743	0.067	0.174	
13.230	325823715	12.877	33.608	$\gamma$ -terpinene
13.945	427851837	16.909	44.132	p-cymene
14.150	12935873	0.511	1.334	
16.617	2478954	0.098	0.256	
17.487	764953	0.030	0.079	
17.888	767709	0.030	0.079	
18.023	18513100	0.732	1.910	
18.547	17750800	0.702	1.831	
18.785	1361842	0.054	0.140	
19.132	606390	0.024	0.063	
19.479	1393707	0.055	0.144	
20.111	815324	0.032	0.084	
20.279	954401	0.038	0.098	
20.540	39878786	1.576	4.113	linalool
20.757	4080000	0.161	0.421	

21.176	1216457	0.048	0.125	
21.641	420851	0.017	0.043	
21.783	541405	0.021	0.056	
22.335	164644994	6.507	16.983	PC2
22.598	12914257	0.510	1.332	
22.726	3731136	0.147	0.385	
22.924	843818	0.033	0.087	
23.266	1053708	0.042	0.109	
23.647	700572	0.028	0.072	
23.833	784233	0.031	0.081	
24.188	583890	0.023	0.060	
24.347	5547341	0.219	0.572	
24.634	616901	0.024	0.064	
24.767	922981	0.036	0.095	
24.915	7162677	0.283	0.739	
25.102	57737123	2.282	5.956	borneol
25.722	1829972	0.072	0.189	
26.353	951904	0.038	0.098	
26.719	1681536	0.066	0.173	
26.866	606653	0.024	0.063	
27.617	1582453	0.063	0.163	
27.741	598934	0.024	0.062	
29.387	2016690	0.080	0.208	
30.228	653405	0.026	0.067	
31.952	6689081	0.264	0.690	
34.030	555216	0.022	0.057	
37.203	378453	0.015	0.039	
39.041	1395805	0.055	0.144	
39.240	835407	0.033	0.086	
39.528	20710844	0.818	2.136	thymol
40.032	1529772	0.060	0.158	
40.448	969475148	38.314	100.000	carvacrol
41.896	2421095	0.096	0.250	
42.178	879966	0.035	0.091	
42.335	626505	0.025	0.065	
43.727	813382	0.032	0.084	
44.199	792622	0.031	0.082	
44.683	1257710	0.050	0.130	

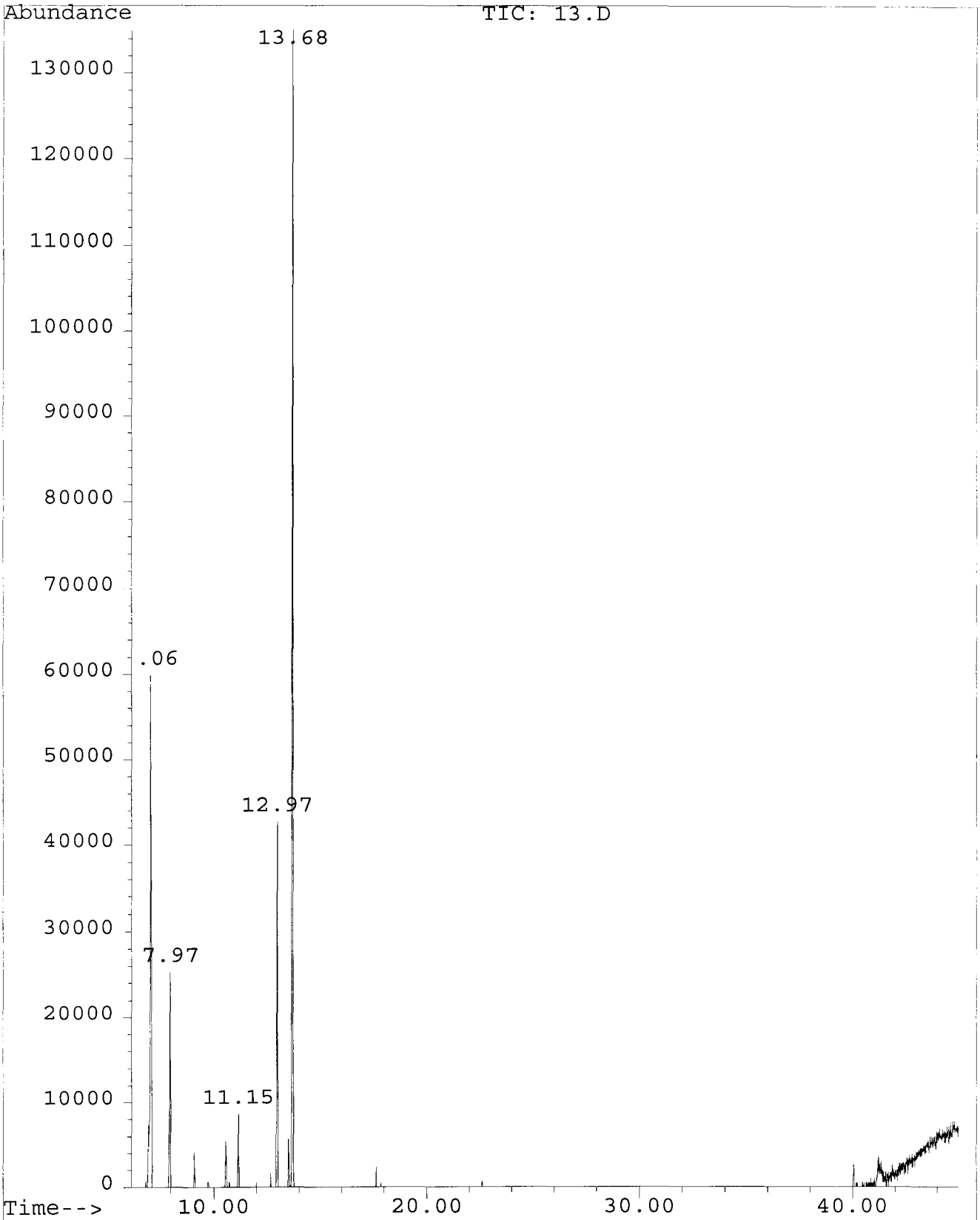
---

Tue May 18 18:01:03 1999

## **APPENDIX G**

**Chromatogram and the GC/MS Results of the Samples Collected at Different Time Intervals during Supercritical-CO<sub>2</sub> Adsorption (Following Dense-Gas Extraction) at 40°C/7.5 MPa on Eight Grams Activated Carbon**

File : C:\HPCHEM\1\DATA\CARBON\EKM27\13.D  
Operator :  
Acquired : 27 Oct 98 5:37 pm using AcqMethod SEYDA  
Instrument : 5971 - on  
Sample Name :  
Misc Info :  
Vial Number: 1



## Area Percent Report -- Sorted by Signal

---

Information from Data File:

File : C:\HPCHEM\1\DATA\CARBON\EKM27\13.D  
Operator :  
Acquired : 27 Oct 98 5:37 pm using AcqMethod SEYDA  
Sample Name: time = 390 min.  
Misc Info :  
Vial Number: 1  
CurrentMeth: C:\HPCHEM\1\METHODS\SEYDA.M

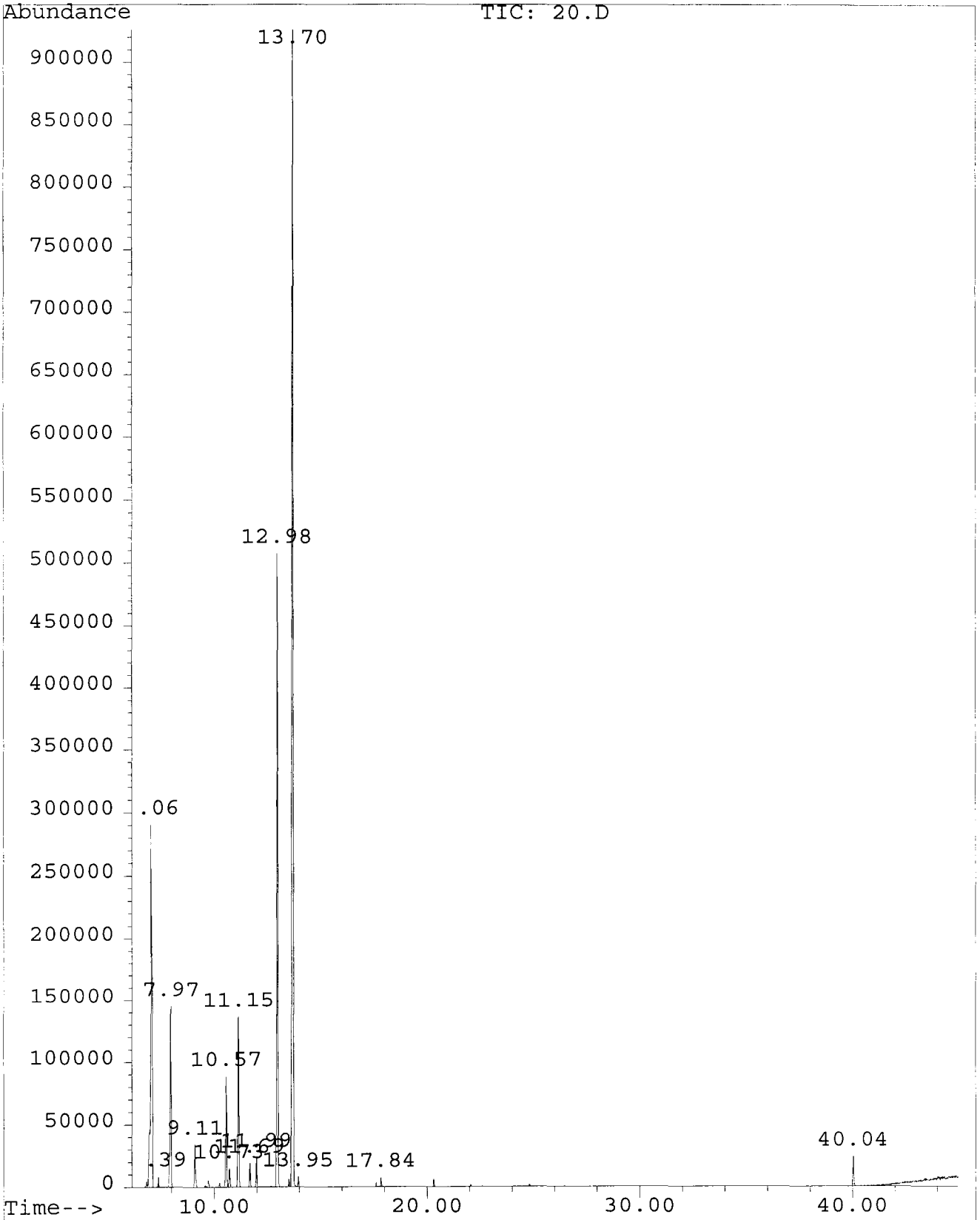
---

Retention Time	Area	Area %	Ratio %	
<hr/> Total Ion Chromatogram				
7.059	2374580	28.677	64.078	$\alpha$ -pinene
7.968	791633	9.560	21.362	camphene
11.151	234395	2.831	6.325	$\alpha$ -terpinene
12.971	1174076	14.179	31.682	$\gamma$ -terpinene
13.683	3705777	44.753	100.000	p-cymene

---

Tue May 18 18:20:52 1999

File : C:\HPCHEM\1\DATA\CARBON\EKM27\20.D  
Operator :  
Acquired : 27 Oct 98 9:08 pm using AcqMethod SEYDA  
Instrument : 5971 - on  
Sample Name:  
Misc Info :  
Vial Number: 1



## Area Percent Report -- Sorted by Signal

## Information from Data File:

File : C:\HPCHEM\1\DATA\CARBON\EKM27\20.D  
Operator :  
Acquired : 27 Oct 98 9:08 pm using AcqMethod SEYDA  
Sample Name: time = 600 min.  
Misc Info :  
Vial Number: 1  
CurrentMeth: C:\HPCHEM\1\METHODS\SEYDA.M

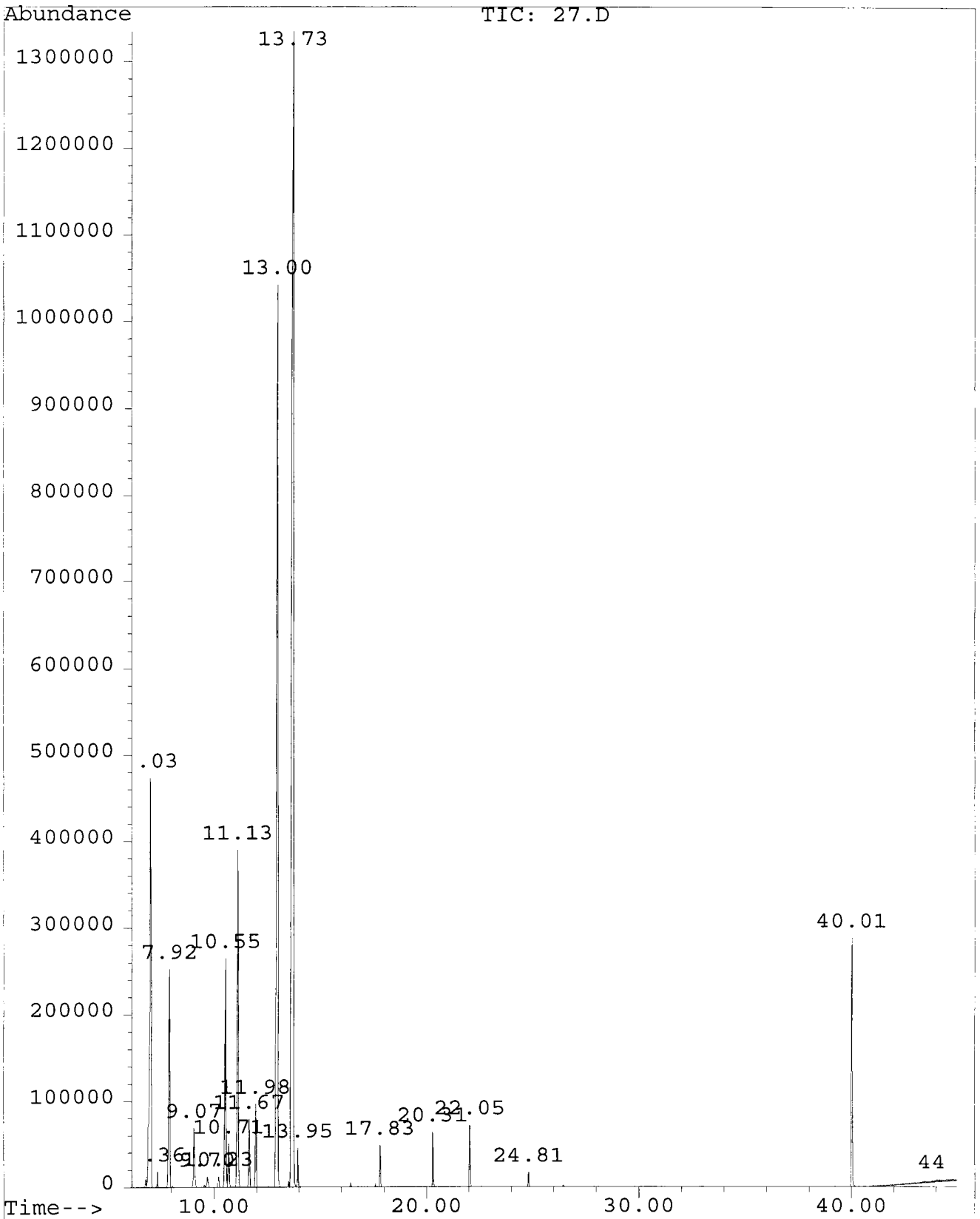
---

Retention Time	Area	Area %	Ratio %	
<hr/> Total Ion Chromatogram				
7.065	13514691	16.433	37.577	$\alpha$ -pinene
7.393	142359	0.173	0.396	
7.970	5223039	6.351	14.523	camphene
9.108	1101844	1.340	3.064	
10.569	2945960	3.582	8.191	myrcene
10.726	523145	0.636	1.455	
11.146	4432057	5.389	12.323	$\alpha$ -terpinene
11.687	551459	0.671	1.533	
11.992	653117	0.794	1.816	PC1
12.979	16074601	19.546	44.695	$\gamma$ -terpinene
13.703	35964882	43.732	100.000	p-cymene
13.955	165572	0.201	0.460	
17.843	231795	0.282	0.645	
40.040	714758	0.869	1.987	carvacrol

---

Tue May 18 18:25:31 1999

File : C:\HPCHEM\1\DATA\CARBON\EKM27\27.D  
Operator :  
Acquired : 28 Oct 98 12:28 pm using AcqMethod SEYDA  
Instrument : 5971 - on  
Sample Name :  
Misc Info :  
Vial Number: 1



## Area Percent Report -- Sorted by Signal

## Information from Data File:

File : C:\HPCHEM\1\DATA\CARBON\EKM27\27.D  
 Operator :  
 Acquired : 28 Oct 98 12:28 pm using AcqMethod SEYDA  
 Sample Name: time = 810 min.  
 Misc Info :  
 Vial Number: 1  
 CurrentMeth: C:\HPCHEM\1\METHODS\SEYDA.M

Retention Time	Area	Area %	Ratio %	
Total Ion Chromatogram				
7.034	23420502	10.866	28.539	$\alpha$ -pinene
7.358	393013	0.182	0.479	
7.923	9468034	4.393	11.537	camphene
9.075	2366357	1.098	2.883	
9.702	511435	0.237	0.623	
10.229	504145	0.234	0.614	
10.555	9841369	4.566	11.992	myrcene
10.708	1810837	0.840	2.207	
11.135	13765352	6.386	16.774	$\alpha$ -terpinene
11.670	2499173	1.159	3.045	
11.977	3168710	1.470	3.861	PC1
12.996	48935600	22.703	59.630	$\gamma$ -terpinene
13.728	82065953	38.074	100.000	p-cymene
13.949	1070293	0.497	1.304	
17.830	1156428	0.537	1.409	
20.312	1604690	0.744	1.955	linalool
22.051	2244997	1.042	2.736	PC2
24.813	494382	0.229	0.602	borneol
40.013	8860509	4.111	10.797	carvacrol
44.815	1363952	0.633	1.662	

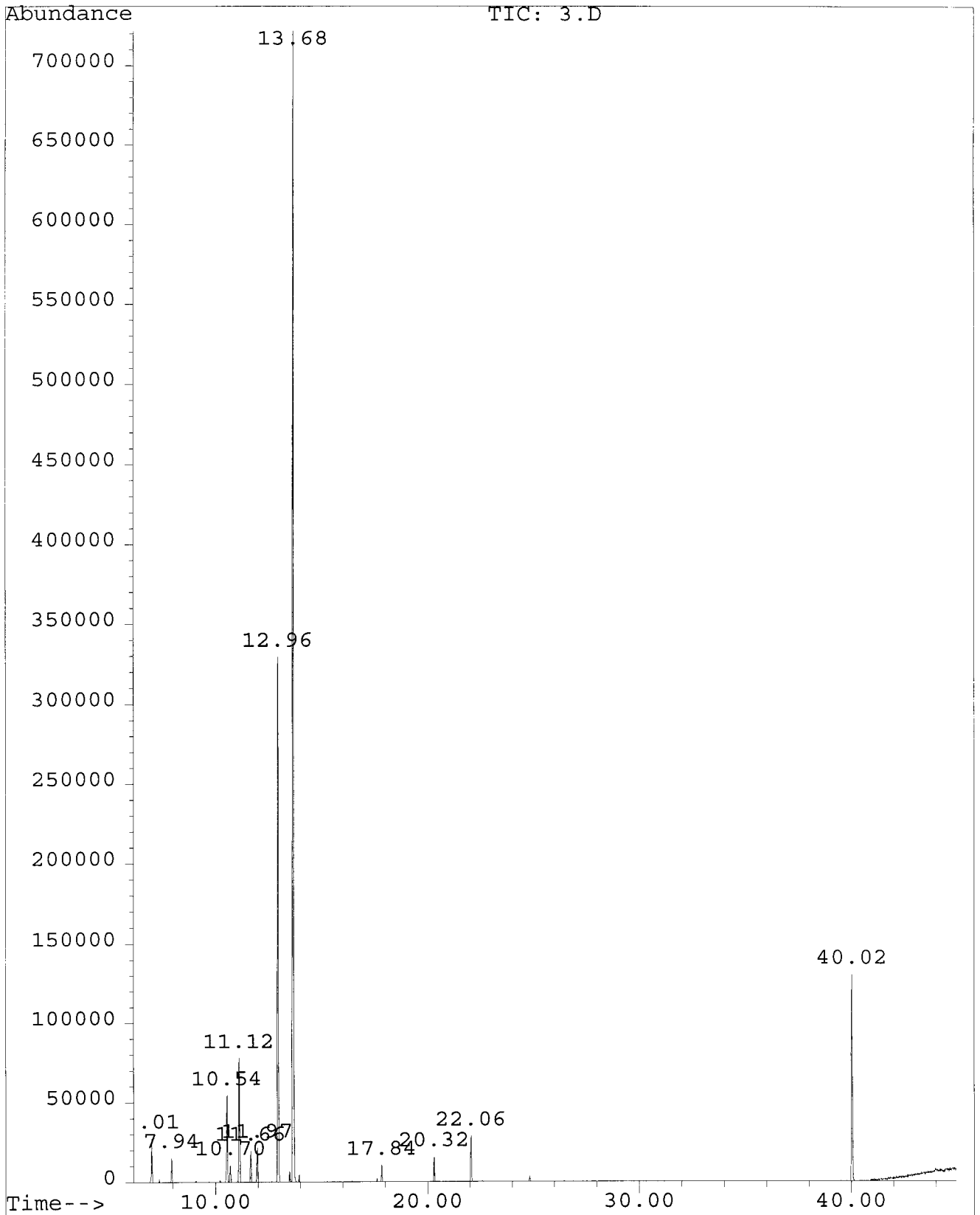
Tue May 18 18:31:08 1999

## **APPENDIX H**

**Chromatogram and the GC/MS Results of the Samples Collected at Different Time Intervals during Supercritical-CO<sub>2</sub> Desorption from Eight Grams Activated Carbon at 40°C using the Step-wise Pressure Increase Method**

File : C:\HPCHEM\1\DATA\CARBON\EKM29\3.D  
Operator :  
Acquired : 29 Oct 98 12:10 pm using AcqMethod SEYDA  
Instrument : 5971 - on  
Sample Name:  
Misc Info :  
Vial Number: 1

216



## Area Percent Report -- Sorted by Signal

## Information from Data File:

File : C:\HPCHEM\1\DATA\CARBON\EKM29\3.D  
Operator :  
Acquired : 29 Oct 98 12:10 pm using AcqMethod SEYDA  
Sample Name: time = 90 min.  
Misc Info :  
Vial Number: 1  
CurrentMeth: C:\HPCHEM\1\METHODS\SEYDA.M

---

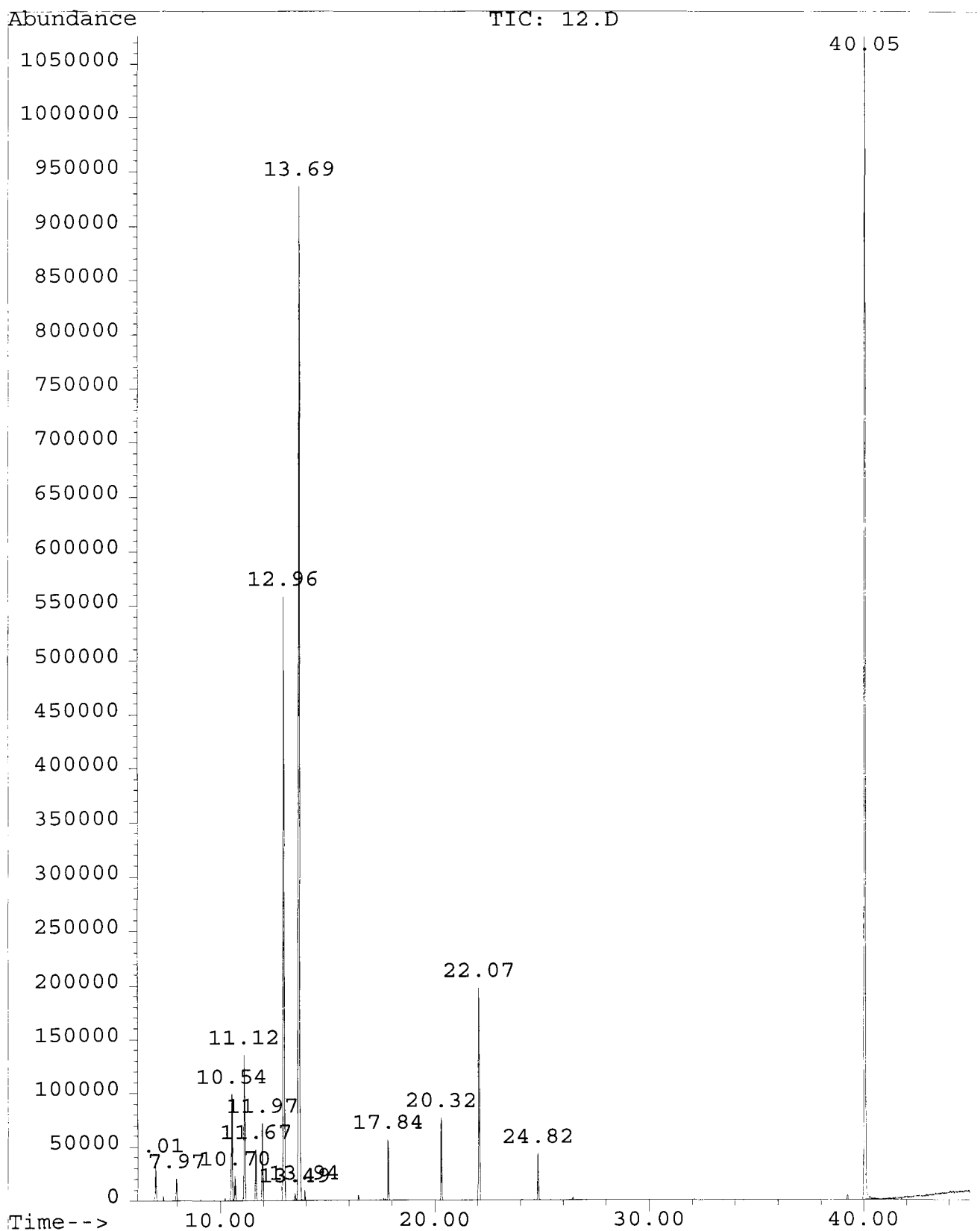
Retention Time	Area	Area %	Ratio %	
<hr/> Total Ion Chromatogram				
7.006	669045	1.480	2.856	$\alpha$ -pinene
7.941	403069	0.891	1.720	camphene
10.545	1682683	3.721	7.182	myrcene
10.701	336320	0.744	1.436	
11.121	2310532	5.110	9.862	$\alpha$ -terpinene
11.665	540858	1.196	2.309	
11.970	601190	1.329	2.566	PC1
12.955	9792673	21.656	41.799	$\gamma$ -terpinene
13.676	23428249	51.809	100.000	p-cymene
17.838	284671	0.630	1.215	
20.320	362976	0.803	1.549	linalool
22.057	817236	1.807	3.488	PC2
40.024	3990564	8.825	17.033	carvacrol

---

Tue May 18 18:44:34 1999

File : C:\HPCHEM\1\DATA\CARBON\EKM29\12.D  
Operator :  
Acquired : 29 Oct 98 4:02 pm using AcqMethod SEYDA  
Instrument : 5971 - on  
Sample Name:  
Misc Info :  
Vial Number: 1

218



## Area Percent Report -- Sorted by Signal

## Information from Data File:

File : C:\HPCHEM\1\DATA\CARBON\EKM29\12.D  
Operator :  
Acquired : 29 Oct 98 4:02 pm using AcqMethod SEYDA  
Sample Name: time = 360 min.  
Misc Info :  
Vial Number: 1  
CurrentMeth: C:\HPCHEM\1\METHODS\SEYDA.M

---

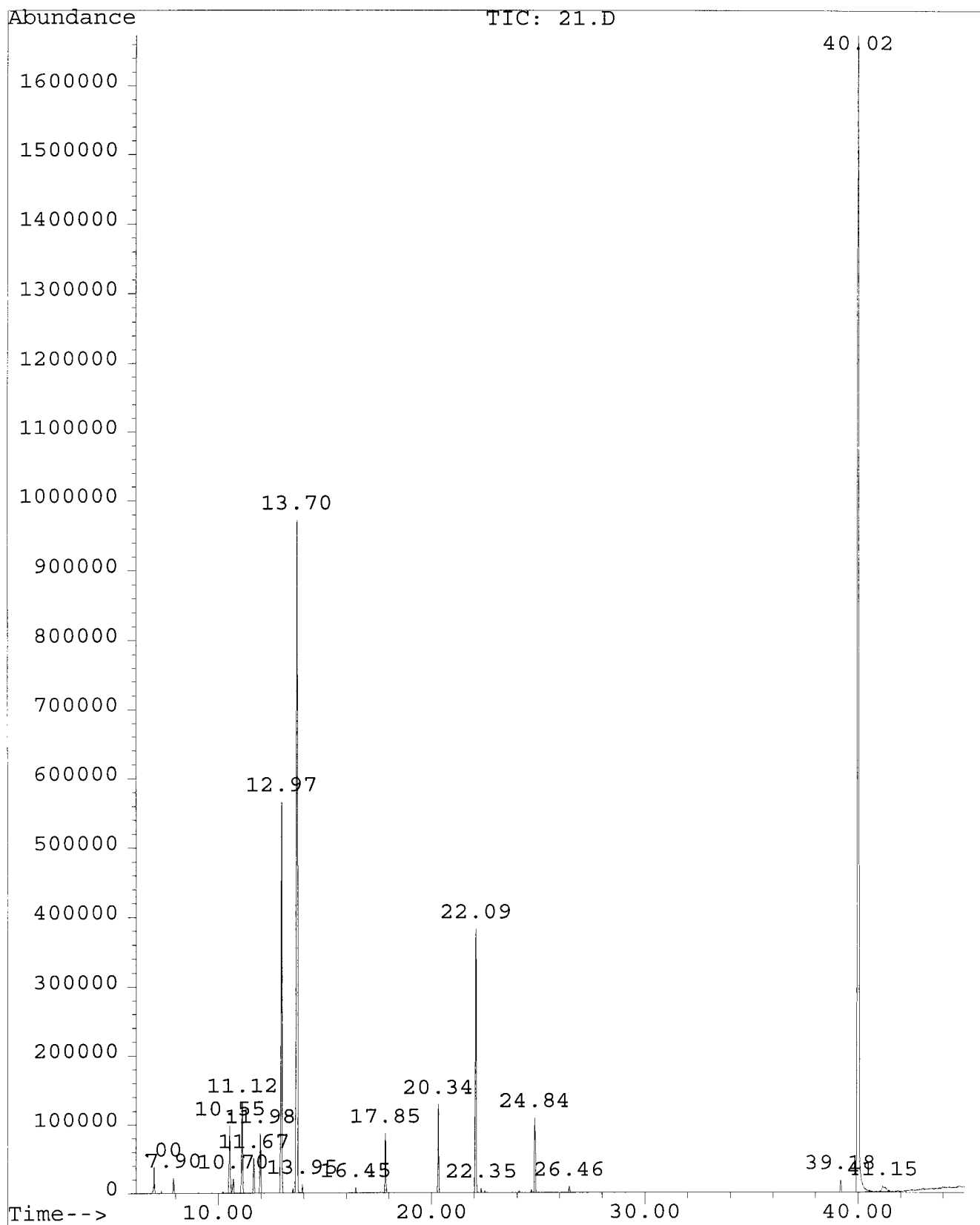
Retention Time	Area	Area %	Ratio %	
<hr/> Total Ion Chromatogram				
7.010	944285	0.800	2.342	$\alpha$ -pinene
7.974	569186	0.482	1.412	camphene
10.545	3122463	2.644	7.745	myrcene
10.701	669968	0.567	1.662	
11.122	4161526	3.524	10.323	$\alpha$ -terpinene
11.665	1381490	1.170	3.427	
11.972	2103557	1.781	5.218	PC1
12.962	17463601	14.788	43.319	$\gamma$ -terpinene
13.494	139101	0.118	0.345	
13.687	36275124	30.718	89.981	p-cymene
13.940	227847	0.193	0.565	
17.837	1323675	1.121	3.283	
20.321	1976595	1.674	4.903	linalool
22.068	6159077	5.215	15.278	PC2
24.824	1260459	1.067	3.127	borneol
40.053	40314172	34.138	100.000	carvacrol

---

Tue May 18 18:50:59 1999

File : C:\HPCHEM\1\DATA\CARBON\EKM29\21.D  
Operator :  
Acquired : 4 Nov 98 12:22 pm using AcqMethod SEYDA  
Instrument : 5971 - on  
Sample Name:  
Misc Info :  
Vial Number: 1

220



## Area Percent Report -- Sorted by Signal

## Information from Data File:

File : C:\HPCHEM\1\DATA\CARBON\EKM29\21.D  
 Operator :  
 Acquired : 29 Oct 98 12:22 pm using AcqMethod SEYDA  
 Sample Name: time = 630 min.  
 Misc Info :  
 Vial Number: 1  
 CurrentMeth: C:\HPCHEM\1\METHODS\SEYDA.M

Retention Time	Area	Area %	Ratio %	
Total Ion Chromatogram				
6.999	1030854	0.570	1.203	$\alpha$ -pinene
7.904	657814	0.364	0.768	camphene
10.546	3553729	1.966	4.148	myrcene
10.703	765659	0.424	0.894	
11.124	4436982	2.455	5.179	$\alpha$ -terpinene
11.668	1559635	0.863	1.820	
11.979	2707869	1.498	3.161	PC1
12.968	18508448	10.241	21.603	$\gamma$ -terpinene
13.695	38237289	21.158	44.631	p-cymene
13.948	262738	0.145	0.307	
16.451	179432	0.099	0.209	
17.847	2126908	1.177	2.483	
20.336	3342717	1.850	3.902	linalool
22.090	12105866	6.699	14.130	PC2
22.346	140111	0.078	0.164	
24.842	3462175	1.916	4.041	borneol
26.460	293891	0.163	0.343	
39.178	580427	0.321	0.677	thymol
40.016	85674124	47.406	100.000	carvacrol
41.155	1096011	0.606	1.279	

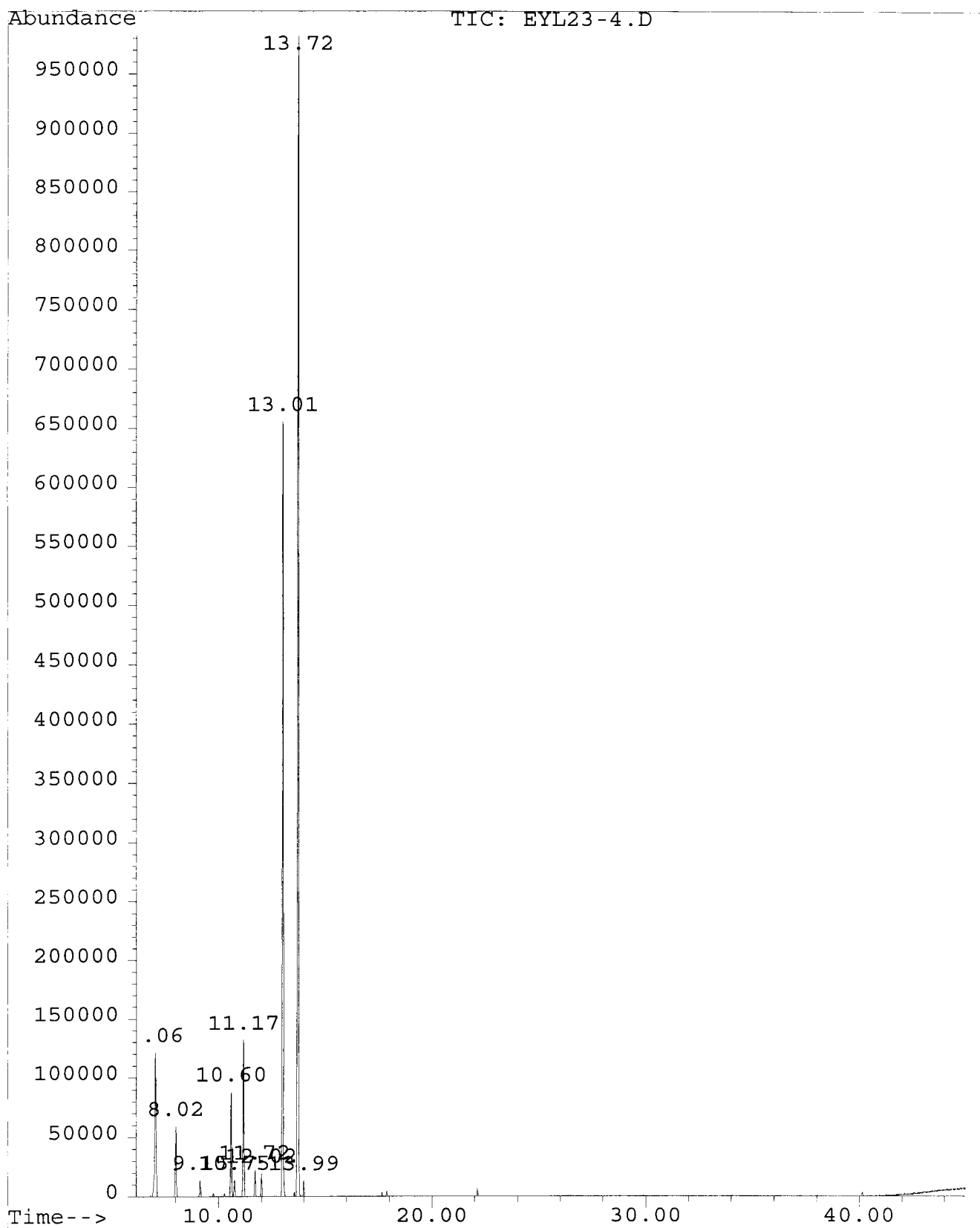
Tue May 18 18:58:24 1999

## **APPENDIX I**

**Chromatogram and the GC/MS Results of the Samples Collected at Different Time Intervals during Supercritical-CO<sub>2</sub> Adsorption (Following Dense-Gas Extraction) at 40°C/7.5 MPa on 15 Grams Silica Gel**

File : C:\HPCHEM\1\DATA\SILICA\EYL23\EYL23-4.D  
Operator :  
Acquired : 23 Sep 98 4:29 pm using AcqMethod SEYDA  
Instrument : 5971 - on  
Sample Name:  
Misc Info :  
Vial Number: 1

223



## Area Percent Report -- Sorted by Signal

## Information from Data File:

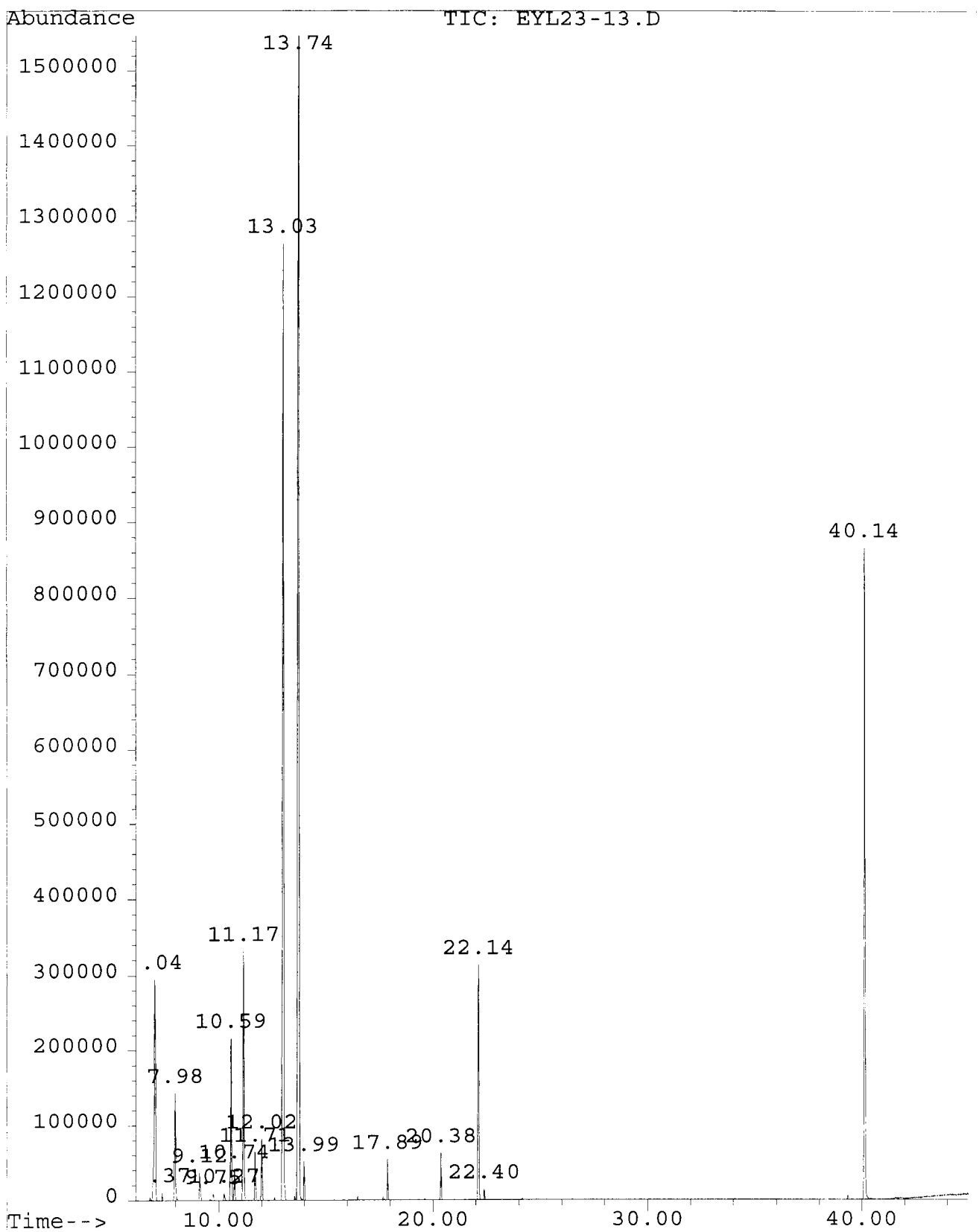
File : C:\HPCHEM\1\DATA\SILICA\EYL23\EYL23-4.D  
 Operator :  
 Acquired : 23 Sep 98 4:29 pm using AcqMethod SEYDA  
 Sample Name: time = 120 min.  
 Misc Info :  
 Vial Number: 1  
 CurrentMeth: C:\HPCHEM\1\METHODS\SEYDA.M

Retention Time	Area	Area %	Ratio %	
Total Ion Chromatogram				
7.057	5331431	7.879	17.323	$\alpha$ -pinene
8.017	1829205	2.703	5.944	camphene
9.145	412702	0.610	1.341	
10.596	2666952	3.942	8.666	myrcene
10.754	450823	0.666	1.465	
11.174	3980963	5.884	12.935	$\alpha$ -terpinene
11.717	627317	0.927	2.038	
12.017	529148	0.782	1.719	PC1
13.013	20726077	30.632	67.345	$\gamma$ -terpinene
13.724	30775882	45.484	100.000	p-cymene
13.992	332074	0.491	1.079	

Tue May 18 16:18:29 1999

File : C:\HPCHEM\1\DATA\SILICA\EYL23\EYL23-13.D  
Operator :  
Acquired : 23 Sep 98 6:16 pm using AcqMethod SEYDA  
Instrument : 5971 - on  
Sample Name:  
Misc Info :  
Vial Number: 1

225



## Area Percent Report -- Sorted by Signal

## Information from Data File:

File : C:\HPCHEM\1\DATA\SILICA\EYL23\EYL23-13.D  
Operator :  
Acquired : 23 Sep 98 6:16 pm using AcqMethod SEYDA  
Sample Name: time = 390 min.  
Misc Info :  
Vial Number: 1  
CurrentMeth: C:\HPCHEM\1\METHODS\SEYDA.M

---

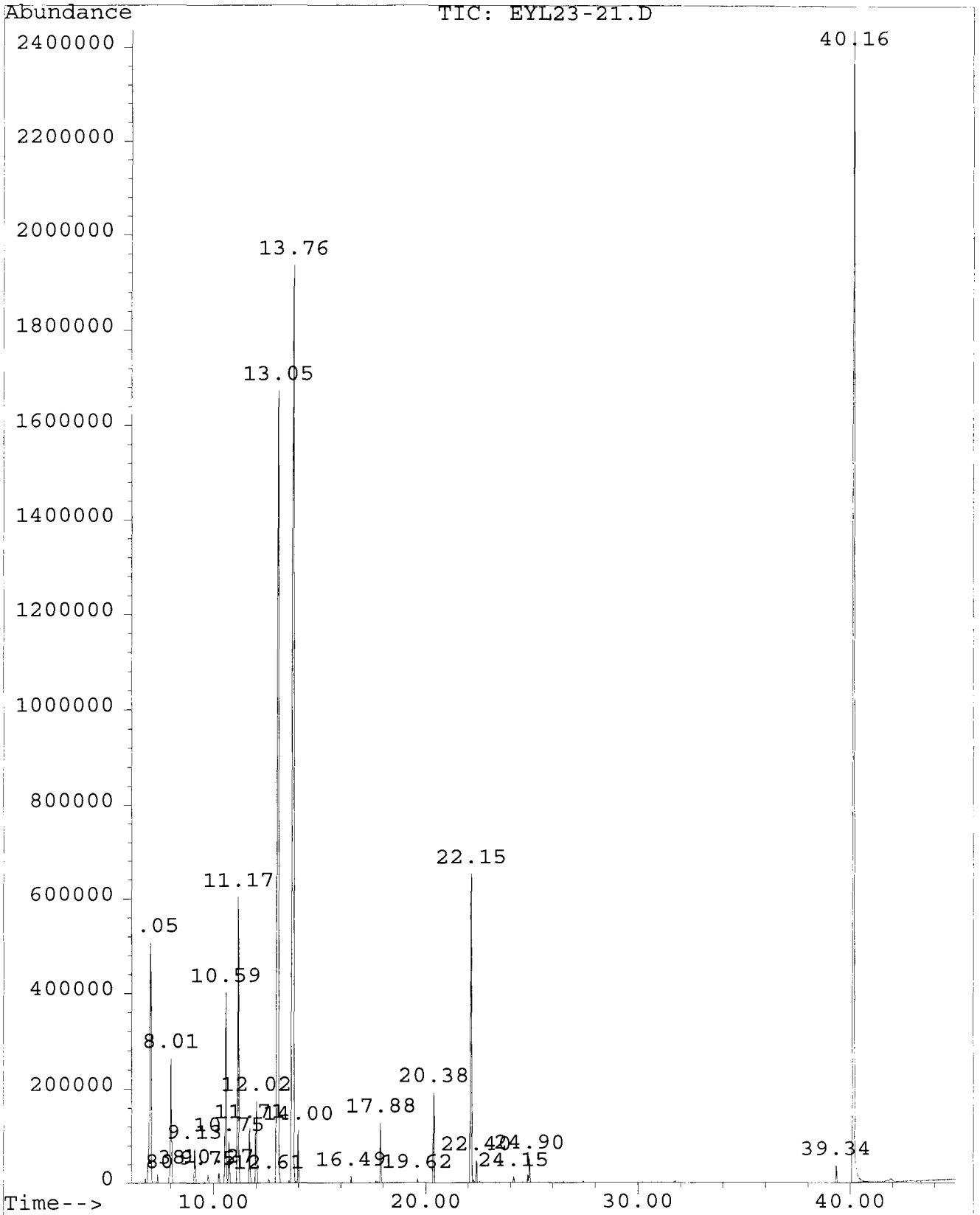
Retention Time	Area	Area %	Ratio %	
<hr/> Total Ion Chromatogram				
7.037	13833137	6.771	20.652	$\alpha$ -pinene
7.372	191725	0.094	0.286	
7.981	4917298	2.407	7.341	camphene
9.123	1304226	0.638	1.947	
9.749	310147	0.152	0.463	
10.266	298623	0.146	0.446	
10.587	7101005	3.476	10.601	myrcene
10.744	1382118	0.676	2.063	
11.167	10837340	5.304	16.179	$\alpha$ -terpinene
11.707	1938703	0.949	2.894	
12.016	2685818	1.315	4.010	PC1
13.029	49789067	24.370	74.331	$\gamma$ -terpinene
13.741	66983330	32.786	100.000	p-cymene
13.990	1276309	0.625	1.905	
17.888	1367912	0.670	2.042	
20.381	1583085	0.775	2.363	linalool
22.137	9920464	4.856	14.810	PC2
22.402	353933	0.173	0.528	
40.137	28232255	13.819	42.148	carvacrol

---

Tue May 18 16:36:51 1999

File : C:\HPCHEM\1\DATA\SILICA\EYL23\EYL23-21.D  
Operator :  
Acquired : 24 Sep 98 12:57 pm using AcqMethod SEYDA  
Instrument : 5971 - on  
Sample Name:  
Misc Info :  
Vial Number: 1

227



## Area Percent Report -- Sorted by Signal

## Information from Data File:

File : C:\HPCHEM\1\DATA\SILICA\EYL23\EYL23-21.D  
 Operator :  
 Acquired : 24 Sep 98 12:57 pm using AcqMethod SEYDA  
 Sample Name: time = 630 min.  
 Misc Info :  
 Vial Number: 1  
 CurrentMeth: C:\HPCHEM\1\METHODS\SEYDA.M

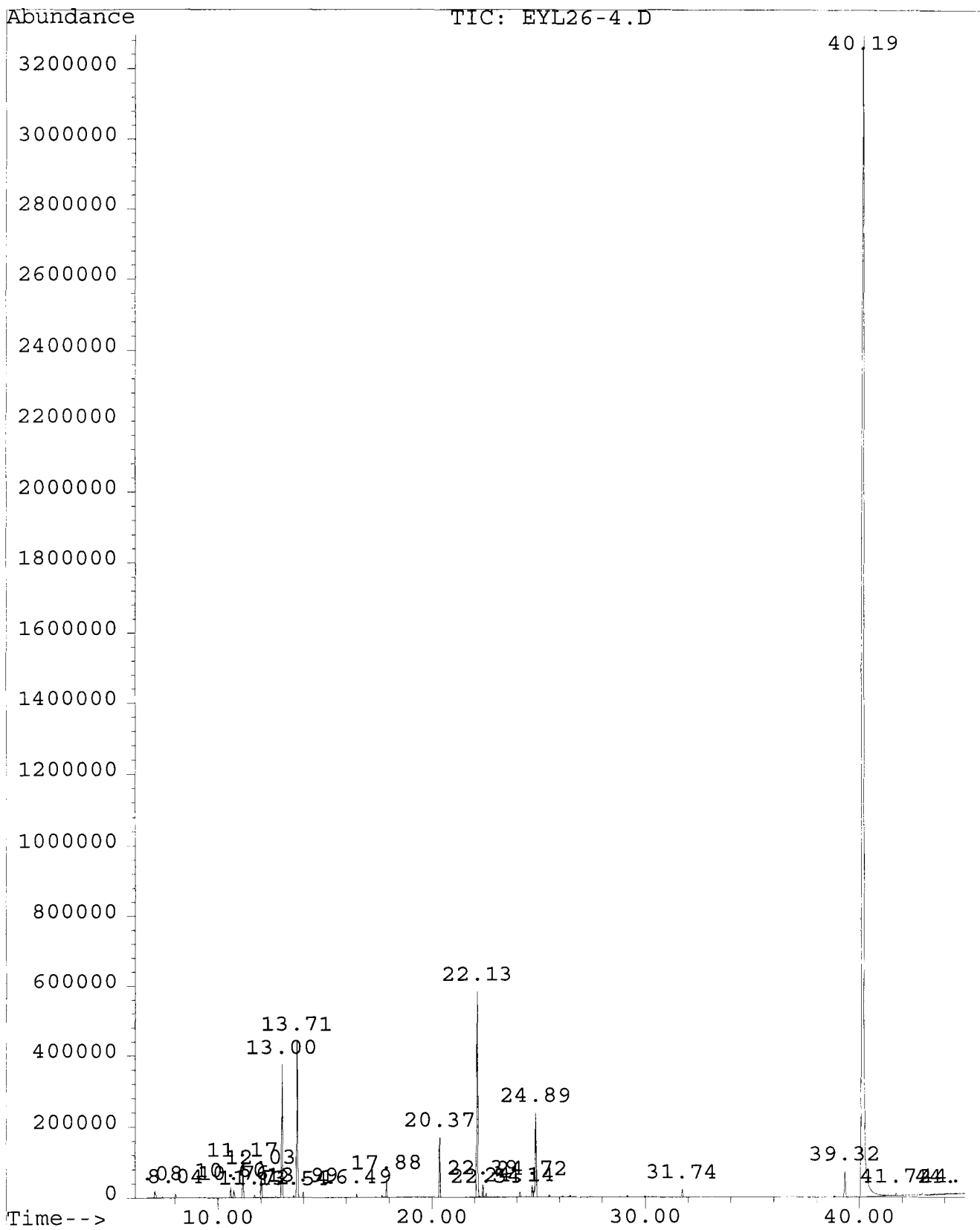
Retention Time	Area	Area %	Ratio %	
Total Ion Chromatogram				
6.799	273713	0.063	0.229	
7.046	24604657	5.635	20.556	$\alpha$ -pinene
7.378	374786	0.086	0.313	
8.007	9264729	2.122	7.740	camphene
9.132	2648383	0.607	2.213	
9.752	626683	0.144	0.524	
10.269	699203	0.160	0.584	
10.593	13314554	3.049	11.124	myrcene
10.745	2849562	0.653	2.381	
11.174	20069392	4.596	16.767	$\alpha$ -terpinene
11.710	3819674	0.875	3.191	
12.021	6019933	1.379	5.029	PC1
12.609	257702	0.059	0.215	
13.051	85231774	19.520	71.206	$\gamma$ -terpinene
13.764	106381987	24.364	88.876	p-cymene
13.995	2642216	0.605	2.207	
16.490	332924	0.076	0.278	
17.884	3295853	0.755	2.754	
19.622	198510	0.045	0.166	
20.379	5275675	1.208	4.408	linalool
22.145	24063424	5.511	20.104	PC2
22.402	1294577	0.296	1.082	
24.150	341893	0.078	0.286	
24.898	1869870	0.428	1.562	borneol
39.338	1183799	0.271	0.989	thymol
40.164	119696802	27.414	100.000	carvacrol

Tue May 18 16:44:35 1999

## **APPENDIX J**

**Chromatogram and the GC/MS Results of the Samples Collected at Different Time  
Intervals during Supercritical-CO<sub>2</sub> Desorption from 15 Grams Silica Gel  
at 40°C/14.5 MPa**

File : C:\HPCHEM\1\DATA\SILICA\EYL26\EYL26-4.D  
Operator :  
Acquired : 26 Sep 98 1:26 pm using AcqMethod SEYDA  
Instrument : 5971 - on  
Sample Name:  
Misc Info :  
Vial Number: 1



## Area Percent Report -- Sorted by Signal

## Information from Data File:

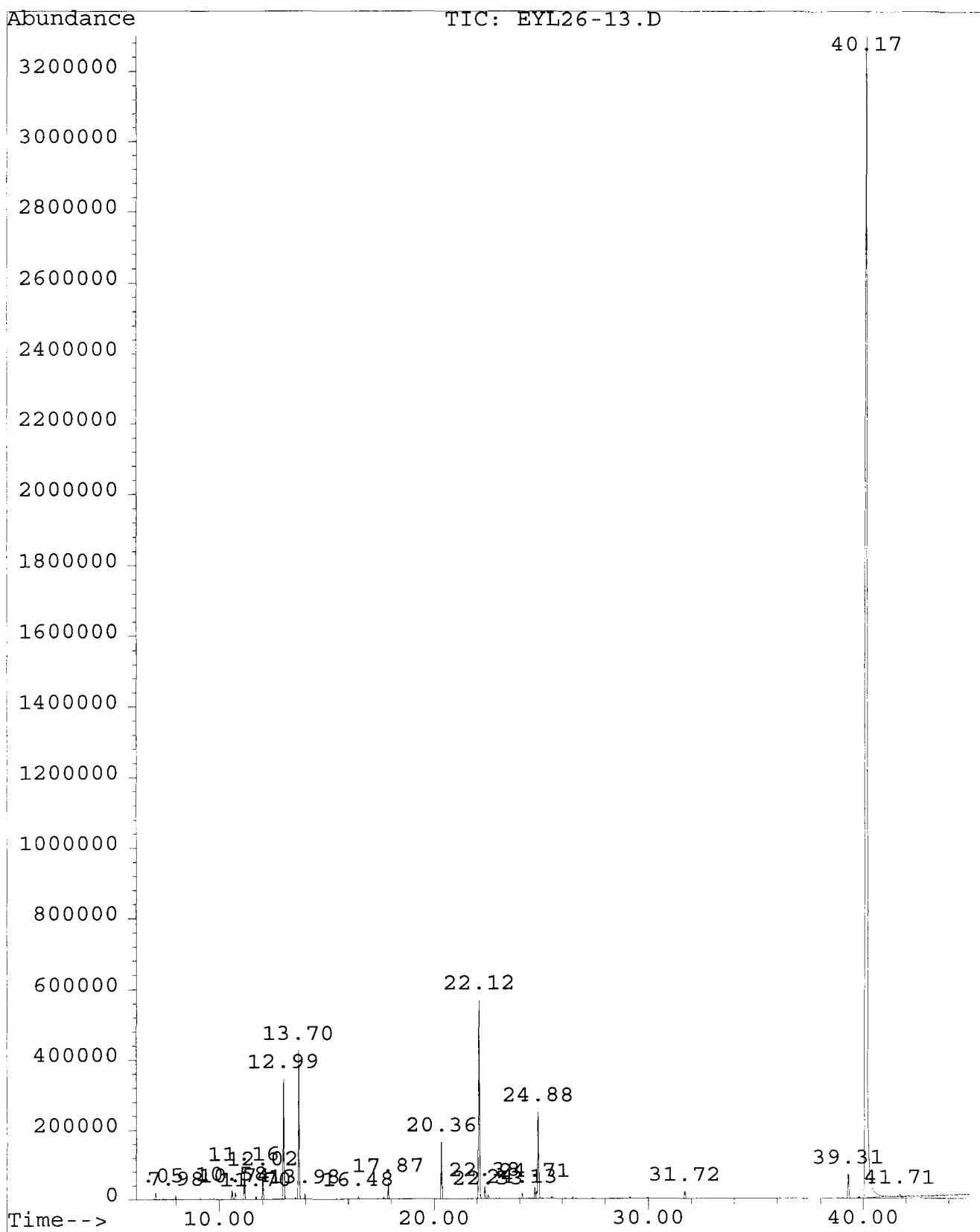
File : C:\HPCHEM\1\DATA\SILICA\EYL26\EYL26-4.D  
 Operator :  
 Acquired : 26 Sep 98 1:26 pm using AcqMethod SEYDA  
 Sample Name: time =120 min.  
 Misc Info :  
 Vial Number: 1  
 CurrentMeth: C:\HPCHEM\1\METHODS\SEYDA.M

Retention Time	Area	Area %	Ratio %	
Total Ion Chromatogram				
7.075	709825	0.238	0.314	$\alpha$ -pinene
8.037	307746	0.103	0.136	camphene
10.599	819313	0.274	0.362	myrcene
10.758	711167	0.238	0.314	
11.174	2547437	0.853	1.126	$\alpha$ -terpinene
11.718	236852	0.079	0.105	
12.028	1992100	0.667	0.881	PC1
13.001	10681100	3.578	4.723	$\gamma$ -terpinene
13.542	155358	0.052	0.069	
13.708	12510933	4.191	5.532	p-cymene
13.987	453054	0.152	0.200	
16.488	217406	0.073	0.096	
17.884	1199921	0.402	0.531	
20.373	4883981	1.636	2.160	linalool
22.133	19135847	6.411	8.462	PC2
22.393	1001844	0.336	0.443	
22.544	330367	0.111	0.146	
24.143	421465	0.141	0.186	
24.721	1086857	0.364	0.481	
24.893	8292581	2.778	3.667	borneol
31.736	704717	0.236	0.312	
39.321	2439010	0.817	1.079	thymol
40.188	226138814	75.758	100.000	carvacrol
41.721	286296	0.096	0.127	
44.301	968668	0.325	0.428	
44.532	267164	0.090	0.118	

Tue May 18 17:02:37 1999

File : C:\HPCHEM\1\DATA\SILICA\EYL26\EYL26-13.D  
Operator :  
Acquired : 26 Sep 98 4:54 pm using AcqMethod SEYDA  
Instrument : 5971 - on  
Sample Name:  
Misc Info :  
Vial Number: 1

232



## Area Percent Report -- Sorted by Signal

## Information from Data File:

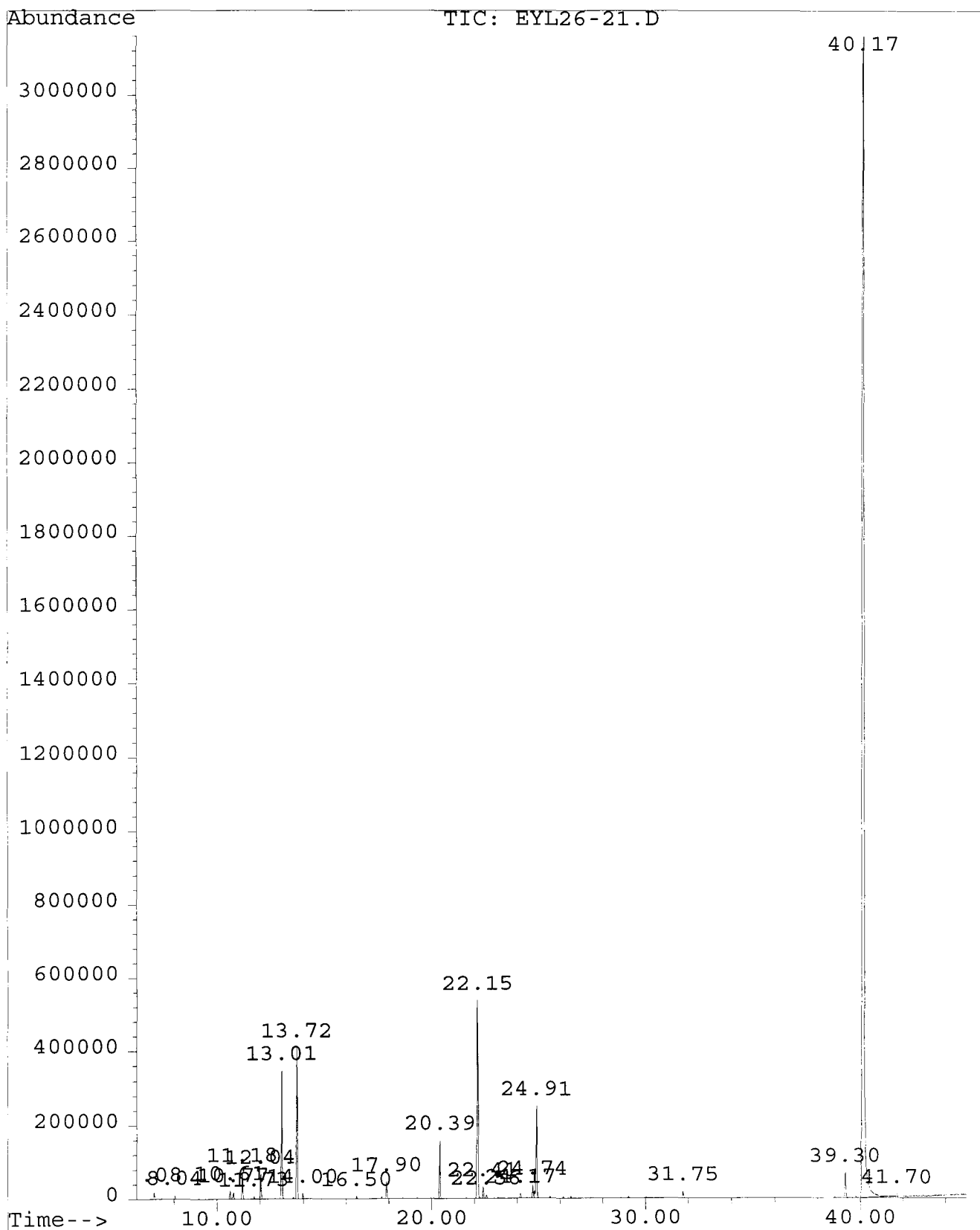
File : C:\HPCHEM\1\DATA\SILICA\EYL26\EYL26-13.D  
 Operator :  
 Acquired : 26 Sep 98 4:54 pm using AcqMethod SEYDA  
 Sample Name: time = 390 min.  
 Misc Info :  
 Vial Number: 1  
 CurrentMeth: C:\HPCHEM\1\METHODS\SEYDA.M

Retention Time	Area	Area %	Ratio %	
Total Ion Chromatogram				
7.053	663374	0.232	0.306	$\alpha$ -pinene
7.984	275940	0.096	0.127	camphene
10.585	798499	0.279	0.368	myrcene
10.744	668749	0.234	0.308	
11.162	2426184	0.848	1.118	$\alpha$ -terpinene
11.704	221368	0.077	0.102	
12.018	2020404	0.706	0.931	PC1
12.990	10331010	3.611	4.760	$\gamma$ -terpinene
13.698	12171340	4.254	5.608	p-cymene
13.977	423549	0.148	0.195	
16.479	240733	0.084	0.111	
17.873	1263813	0.442	0.582	
20.362	4494713	1.571	2.071	linalool
22.120	18532742	6.477	8.539	PC2
22.380	992922	0.347	0.458	
22.530	280147	0.098	0.129	
24.130	366023	0.128	0.169	
24.707	1002362	0.350	0.462	
24.879	8468495	2.960	3.902	borneol
31.718	721486	0.252	0.332	
39.306	2335806	0.816	1.076	thymol
40.171	217026064	75.854	100.000	carvacrol
41.713	384964	0.135	0.177	

Tue May 18 17:09:33 1999

File : C:\HPCHEM\1\DATA\SILICA\EYL26\EYL26-21.D  
Operator :  
Acquired : 28 Sep 98 1:25 pm using AcqMethod SEYDA  
Instrument : 5971 - on  
Sample Name :  
Misc Info :  
Vial Number: 1

234



## Area Percent Report -- Sorted by Signal

## Information from Data File:

File : C:\HPCHEM\1\DATA\SILICA\EYL26\EYL26-21.D  
 Operator :  
 Acquired : 28 Sep 98 1:25 pm using AcqMethod SEYDA  
 Sample Name: time = 630 min.  
 Misc Info :  
 Vial Number: 1  
 CurrentMeth: C:\HPCHEM\1\METHODS\SEYDA.M

Retention Time	Area	Area %	Ratio %	
Total Ion Chromatogram				
7.083	633988	0.226	0.297	$\alpha$ -pinene
8.039	275146	0.098	0.129	camphene
10.608	718933	0.256	0.336	myrcene
10.768	620018	0.221	0.290	
11.185	2298465	0.820	1.076	$\alpha$ -terpinene
11.728	228610	0.082	0.107	
12.040	1988622	0.709	0.931	PC1
13.010	9922404	3.539	4.643	$\gamma$ -terpinene
13.718	11618484	4.143	5.437	p-cymene
13.997	365740	0.130	0.171	
16.499	231392	0.083	0.108	
17.897	1203335	0.429	0.563	
20.389	4375512	1.560	2.047	linalool
22.150	17768966	6.337	8.315	PC2
22.412	864956	0.308	0.405	
22.564	326062	0.116	0.153	
24.166	362665	0.129	0.170	
24.742	1090006	0.389	0.510	
24.915	8581904	3.061	4.016	borneol
31.750	671378	0.239	0.314	
39.304	2208810	0.788	1.034	thymol
40.166	213708249	76.214	100.000	carvacrol
41.704	341954	0.122	0.160	

Tue May 18 17:19:52 1999

## REFERENCES

Adams, R.P., *Identification of Essential Oil Components by Gas Chromatography/Mass Spectroscopy*, Illinois: Allured Publishing, 1995.

Akman, U., "Simultaneous Extraction and Sorption Under Supercritical Conditions," Ph.D. Dissertation, University of South Florida, 1991.

Barth, D., D. Chouchi, G. Della Porta, E. Reverchon and M. Perrut, "Desorption of Lemon Peel Oil by Supercritical Carbon Dioxide: Deterpenation and Psoralens Elimination," *Journal of Supercritical Fluids*, Vol. 7, pp. 177-183, 1994.

Brandani, V., G. Del Re, G. Di Giacomo and V. Mucciante, "Phase Equilibria of Essential Oil Components and Supercritical Carbon Dioxide," *Fluid Phase Equilibria*, Vol. 59, pp. 135-145, 1990.

Brogie, H., "CO<sub>2</sub> as a Solvent: Its Properties and Applications," *Chemistry and Industry*, Vol. 19, pp. 385-396, 1982.

Chouchi, D., D. Barth, E. Reverchon and G. Della Porta, "Supercritical CO<sub>2</sub> Desorption of Bergamot Peel Oil," *Industrial and Engineering Chemistry Research*, Vol. 34, pp. 4508-4513, 1995.

Coppella, S.J. and P. Barton, "Supercritical Carbon Dioxide Extraction of Lemon Oil," in T.G. Squires and M.E. Paulaitis (Eds.), *Supercritical Fluids: Chemical Engineering Principles and Applications*, pp. 202-212, Washington, DC: American Chemical Society Press, 1987.

Cully, J., E. Schutz and H.-R. Vollbrecht, European Patent No. A 0 363 971, 1990.

Della Porta, G., E. Reverchon, D. Chouchi and D. Barth, "Mandarin and Lime Peel Oil Processing by Supercritical CO<sub>2</sub> Desorption: Deterpenation and High Molecular Weight Compounds Elimination," *Journal of Essential Oil Research*, Vol. 9, pp. 515-522, 1997.

Di Giacomo, G., V. Brandani, G. Del Re and V. Mucciante, "Solubility of Essential Oil Components in Compressed Supercritical Carbon Dioxide," *Fluid Phase Equilibria*, Vol. 52, pp. 405-411, 1989.

Dugo, P., L. Mondello, K. Bartle, A. Clifford, D. Breen and G. Dugo, "Deterpenation of Sweet Orange and Lemon Essential Oils with Supercritical Carbon Dioxide Using Silica Gel as an Adsorbent," *Flavour Fragrances Journal*, Vol. 10, pp. 51-58, 1995.

Guenther, E., *The Essential Oils*, 6th ed., New York: Van Nostrand Company, 1952.

Kander, R.G. and M.E. Paulaitis, "The Adsorption of Phenol from Dense Carbon Dioxide onto Activated Carbon," in R.D. Gray and P. Davidson (Eds.), *Chemical Engineering and Supercritical Conditions*, pp. 461-476, Ann Arbor: Ann Arbor Science, 1983.

Memory, J., *Food Flavoring Composition, Manufacture, and Use*, 2nd ed., Westport: The Avi Publishing Company, 1968.

McHugh, M.A. and V.J. Krukonis, *Supercritical Fluid Extraction Principles and Practice*, Stoneham: Butterworth Publishers, 1986.

Ng, H.-J. and D.B. Robinson, "Equilibrium Phase Properties of Toluene-Carbon Dioxide System," *Journal of Chemical and Engineering Data*, Vol.23, pp. 325-327, 1978.

Nilsson, W.B., E.J. Gauglitz, J.K. Hudson, V.F. Stout and J. Spinelli, "Fractionation of Menhaden Oil Ethyl Esters Using Supercritical Fluid CO<sub>2</sub>," *Journal of American Oil Chemists Society*, Vol. 65, pp. 109-117, 1988.

Özer, E.Ö., S. Platin, U. Akman and Ö. Hortaçsu, "Supercritical Carbon Dioxide Extraction of Spearmint Oil from Mint-Plant Leaves," *The Canadian Journal of Chemical Engineering*, Vol. 74, pp. 920-928, 1996.

Platin, S., E.Ö. Özer, U. Akman and Ö. Hortaçsu, "Equilibrium Distributions of Key Components of Spearmint Oil in Sub/Supercritical Carbon Dioxide," *Journal of the American Oil Chemists' Society*, Vol. 71, pp. 833-837, 1994.

Reverchon, E., "Fractional Separation of SCF Extracts from Marjoram Leaves: Mass Transfer and Optimization," *The Journal of Supercritical Fluids*, Vol. 5, pp. 256-261, 1992.

Reverchon, E. and G. Iacuzio, "Supercritical Desorption of Bergamot Peel Oil from Silica Gel – Experiments and Mathematical Modelling," *Chemical Engineering Science*, Vol. 52, pp. 3553-3559, 1997.

Rizvi, S.H.H., J.A. Daniels, A.L. Benado and J.A. Zollweg, "Supercritical Fluid Extraction: Operating Principles and Food Applications," *Food Technology*, Vol. 40, pp. 57-64, 1986.

Ruthven, D.M., *Principles of Adsorption and Adsorption Processes*, New York: John Wiley & Sons, 1984.

Sato, M., M. Goto and T. Hirose, "Fractional Extraction with Supercritical Carbon Dioxide for the Removal of Terpenes from Citrus Oil," *Industrial and Engineering Chemistry Research*, Vol. 34, pp. 3941-3946, 1995.

Sato, M., M. Goto and T. Hirose, "Supercritical Fluid Extraction on Semibatch Mode for the Removal of Terpene in Citrus Oil," *Industrial and Engineering Chemistry Research*, Vol. 35, pp. 1906-1911, 1996.

Sato, M., M. Goto, N. Kunishima, A. Kodama and T. Hirose, "Pressure Swing Adsorption Process in Supercritical Carbon Dioxide for the Fractionation of Citrus Oil," *Proceedings of*

*the 4<sup>th</sup> International Symposium on Supercritical Fluids*, Sendai- Japan, May 11-14, Vol. B, pp. 629-632, Sendai, Tohoku University Press, 1997.

Sato, M., M. Kondo, M. Goto, A. Kodama and T. Hirose, "Fractionation of Citrus Oil by Supercritical Countercurrent Extractor with Side-stream Withdrawal," *Journal of Supercritical Fluids*, Vol. 13, pp. 311-317, 1998.

Schulz, K., E.E. Martinelli and G. A. Mansoori, "Supercritical Fluid Extraction and Retrograde Condensation (SFE/RC) Applications in Biotechnology," in B. Thomas and F.E. James (Eds.), *Supercritical Fluid Technology: Reviews in Modern Theory and Applications*, pp. 451-479, Florida: CRC Press, 1991.

Stahl, E. and D. Gerard, "Solubility Behavior and Fractionation of Essential Oils in Dense Carbon Dioxide," *Perfumer and Flavorist*, Vol. 10, pp. 29-37, 1985.

Stahl, E., K.W. Quirin and D. Gerard, *Dense Gases for Extraction and Refining*, Translation from the German Edition by M.R.F. Ashworth, Berlin: Springer-Verlag, 1988.

Subra, P., A. Vega-Bancel and E. Reverchon, "Breakthrough Curves and Adsorption Isotherms of Terpene Mixtures in Supercritical Carbon Dioxide," *Journal of Supercritical Fluids*, Vol. 12, pp. 43-57, 1998.

Suzuki, Y., M. Konno, K. Arai and S. Saito, "Fractionation of Mono-Esters Derived from Fish Oil Using Supercritical Fluid Extraction Tower," *Kagaku Kogaku Ronbunshu*, Vol. 15, pp. 439-445, 1989.

Temelli, F., C.S. Chen and R.J. Braddock, "Supercritical Fluid Extraction in Citrus Oil Processing," *Food Technology*, Vol. 42, pp. 145-150, 1988.

Turgay, B., "Modeling of Equilibrium Sorption and Fixed-Bed Desorption for Benzene and Toluene at Supercritical Conditions," MS. Thesis, Boğaziçi University, 1995.

Westwood, S.A., *Supercritical Fluid Fractionation and its Use in Chromatographic Sample Preparation*, Florida: CRC Press, 1993.

Yang, R.T., *Gas Separation by Adsorption Processes*, Stoneham: Butterworth Publishers, 1987.

Ziegler, M., H. Brandauer, E. Ziegler and G. Ziegler, "A Different Aging Model for Orange Oil: Deterioration Products," *The Journal of Essential Oil Research*, Vol. 3, pp. 209-215, 1991.